RADIOLOGY AND ONCOLOGY

Special section

8th Alpe Adria Medical Physics Meeting

Guest Editors: **Božidar Casar** and **Dietmar Georg**

vol.52 no.3

september 2018

NOVO

CABOMETYX®
(kabozantinib) tablete
60 mg | 40 mg | 20 mg

CABOMETYX® pomembno izboljša PFS, OS in ORR v drugi liniji zdravljenja napredovalega karcinoma ledvičnih celic[1]

- PFS[2]
- OS[2]
- ORR[2]

RAZŠIRITEV INDIKACIJE:

Sedaj tudi za zdravljenje napredovalega karcinoma ledvičnih celic (KLC) pri predhodno nezdravljnenih odraslih bolnikih s srednje ugodnim ali slabim prognostičnim obetom.[2]

ORR: objektivna stopnja odziva; OS: celokupno preživetje; PFS: preživetje brez napredovanja bolezni

Referenci:
1. Choueiri TK, Escudier B, Powles T, *et al*. Cabozantinib versus everolimus in advanced renal cell carcinoma (METEOR): final results from a randomised, open-label, phase 3 trial. The Lancet Oncology. 2016;17(7):917-27.
2. Povzetek glavnih značilnosti zdravila Cabometyx.

Skrajšan povzetek glavnih značilnosti zdravila

CABOMETYX 20 mg filmsko obložene tablete
CABOMETYX 40 mg filmsko obložene tablete
CABOMETYX 60 mg filmsko obložene tablete
(kabozantinib)

TERAPEVTSKE INDIKACIJE Zdravljenje napredovalega karcinoma ledvičnih celic (KLC) pri predhodno nezdravljenih odraslih bolnikih s srednje ugodnim ali slabim prognostičnim obetom ter pri odraslih bolnikih po predhodnem zdravljenju, usmerjenem v vaskularni endotelijski rastni faktor (VEGF). **ODMERJANJE IN NAČIN UPORABE** Priporočeni odmerek je 60 mg enkrat na dan. Zdravljenje je treba nadaljevati tako dolgo, dokler bolnik več nima kliničnih koristi od terapije ali do pojava nesprejemljive toksičnosti. Pri sumu na neželene reakcije na zdravilo bo morda treba zdravljenje začasno prekiniti in/ali zmanjšati odmerek. Če je treba odmerek zmanjšati, se priporoča zmanjšanje na 40 mg na dan in nato na 20 mg na dan. Prekinitev odmerka se priporoča pri obravnavi toksičnosti 3. ali višje stopnje po CTCAE (*common terminology criteria for adverse events*) ali nevzdržni toksičnosti 2. stopnje. Zmanjšanje odmerka se priporoča za dogodke, ki bi lahko čez čas postali resni ali nevzdržni. V primeru pojava neželenih učinkov 1. in 2. stopnje, ki jih bolnik prenaša in jih je možno enostavno obravnavati, prilagoditev odmerjanja običajno ni potrebna. Treba je razmisliti o dodatni podporni oskrbi. V primeru pojava neželenih učinkov 2. stopnje, ki jih bolnik ne prenaša in jih ni mogoče obravnavati z zmanjšanjem odmerka ali podporno oskrbo, je treba zdravljenje prekiniti, dokler neželeni učinki ne izzvenijo do ≤ 1. stopnje, uvesti podporno oskrbo in razmisliti o ponovni uvedbi zdravljenja z zmanjšanim odmerkom. V primeru pojava neželenih učinkov 3. stopnje je treba zdravljenje prekiniti, dokler neželeni učinki ne izzvenijo do ≤ 1. stopnje, uvesti podporno oskrbo in ponovno uvesti zdravljenje z zmanjšanim odmerkom. V primeru pojava neželenih učinkov 4. stopnje je treba zdravljenje prekiniti, uvesti ustrezno zdravniško oskrbo, in če neželeni učinki izzvenijo do ≤ 1. stopnje, ponovno uvesti zdravljenje z zmanjšanim odmerkom. Če neželeni učinki ne izzvenijo, je treba trajno prenehati z uporabo zdravila. Pri bolnikih z blago ali zmerno ledvično okvaro je treba kabozantinib uporabljati previdno. Uporaba se ne priporoča pri bolnikih s hudo ledvično okvaro. Pri bolnikih z blago ali zmerno jetrno okvaro je priporočeni odmerek kabozantiniba 40 mg enkrat na dan. Pri teh bolnikih je treba spremljati neželene dogodke in po potrebi razmisliti o prilagoditvi odmerka ali prekinitvi dajanja. Uporaba se ne priporoča pri bolnikih s hudo jetrno okvaro. Način uporabe: Tablete je treba pogoltniti cele in jih ni dovoljeno drobiti. Bolnikom je treba naročiti, naj vsaj 2 uri pred uporabo zdravila in 1 uro po tem ničesar ne jedo. **KONTRAINDIKACIJE** Preobčutljivost na učinkovino ali katero koli pomožno snov. **POSEBNA OPOZORILA IN PREVIDNOSTNI UKREPI** Večina dogodkov se lahko pojavi zgodaj v teku zdravljenja, zato mora zdravnik bolnika v prvih 8 tednih zdravljenja skrbno spremljati, da oceni, ali je treba odmerek prilagoditi. Dogodki, ki se običajno pojavijo zgodaj, vključujejo hipokalciemijo, hipokaliemijo, trombocitopenijo, hipertenzijo, sindrom palmarno-plantarne eritrodisestezije (PPES), proteinurijo in gastrointestinalne dogodke (bolečine v trebuhu, vnetje sluznice, zaprtje, driska, bruhanje). Bolnike, ki imajo vnetno bolezen črevesja (npr. Crohnovo bolezen, ulcerozni kolitis, peritonitis, divertikulitis ali apendicitis), ki imajo tumorsko infiltracijo prebavil ali so imeli pred posegom na prebavilih zaplete (zlasti v povezavi z zapoznelim ali nepopolnim celjenjem), je treba pred uvedbo zdravljenja skrbno oceniti, nato pa natančno spremljati za pojav simptomov perforacij in fistul, vključno z abscesi in sepso. Trajna ali ponavljajoča se driska med zdravljenjem je lahko dejavnik tveganja za nastanek analne fistule. Uporabo kabozantiniba je treba pri bolnikih, pri katerih se pojavi gastrointestinalna perforacija ali fistula, ki je ni možno ustrezno obravnavati, prekiniti. Kabozantinib je treba uporabljati previdno pri bolnikih, pri katerih obstaja tveganje za pojav venske trombembolije, vključno s pljučno embolijo, in arterijske trombembolije ali imajo te dogodke v anamnezi. Z uporabo je treba prenehati pri bolnikih, pri katerih se razvije akutni miokardni infarkt ali drugi klinično pomembni znaki zapletov arterijske trombembolije. Kabozantiniba se ne sme dajati bolnikom, ki hudo krvavijo, ali pri katerih obstaja tveganje za hudo krvavitev. Zdravljenje s kabozantinibom je treba ustaviti vsaj 28 dni pred načrtovanim kirurškim posegom, vključno z zobozdravstvenim, če je mogoče. Kabozantinib je treba ukiniti pri bolnikih z zapleti s celjenjem rane, zaradi katerih je potrebna zdravniška pomoč. Pred uvedbo kabozantiniba je treba dobro obvladati krvni tlak. Med zdravljenjem je treba vse bolnike spremljati za pojav hipertenzije in jih po potrebi zdraviti s standardnimi antihipertenzivi. V primeru trdovratne hipertenzije, kljub uporabi antihipertenzivov, je treba odmerek kabozantiniba zmanjšati. Z uporabo je treba prenehati, če je hipertenzija resna ali trdovratna kljub zdravljenju z antihipertenzivi in zmanjšanemu odmerku kabozantiniba. V primeru hipertenzijske krize je treba zdravljenje prekiniti. Pri resni PPES je treba razmisliti o prekinitvi zdravljenja. Nadaljevanje zdravljenja naj se začne z nižjim odmerkom, ko se PPES umiri do 1. stopnje. V času zdravljenja je treba redno spremljati beljakovine v urinu. Pri bolnikih, pri katerih se razvije nefrotični sindrom, je treba z uporabo kabozantiniba prenehati. Pri uporabi kabozantiniba so opazili sindrom reverzibilne posteriorne levkoencefalopatije (RPLS), znan tudi kot sindrom posteriorne reverzibilne encefalopatije (PRES). Na ta sindrom je treba pomisliti pri vseh bolnikih s številnimi prisotnimi simptomi, vključno z epileptičnimi napadi, glavobolom, motnjami vida, zmedenostjo ali spremenjenim mentalnim delovanjem. Pri bolnikih z RPLS je treba zdravljenje prekiniti. Kabozantinib je treba uporabljati previdno pri bolnikih s podaljšanjem intervala QT v anamnezi, pri bolnikih, ki jemljejo antiaritmike, in pri bolnikih z relevantno obstoječo boleznijo srca, bradikardijo ali elektrolitskimi motnjami. Bolniki z redko dedno intoleranco za galaktozo, laponsko obliko zmanjšane aktivnosti laktaze ali malabsorpcijo glukoze/galaktoze ne smejo jemati tega zdravila. Plodnost, nosečnost in dojenje: Ženskam v rodni dobi je treba svetovati, da v času zdravljenja s kabozantinibom ne smejo zanositi. Zanositev morajo preprečiti tudi ženske partnerice moških bolnikov, ki uporabljajo kabozantinib. Med zdravljenjem in še vsaj 4 mesece po končanju terapije morajo tako bolniki in bolnice kot tudi njihovi partnerji uporabljati zanesljiv način kontracepcije. Kabozantiniba se ne sme uporabljati med nosečnostjo, razen če zdravljenje ni nujno potrebno zaradi kliničnega stanja ženske. Matere med zdravljenjem s kabozantinibom in še 4 mesece po končanju terapije ne smejo dojiti. Zdravljenje s kabozantinibom lahko predstavlja tveganje za plodnost pri moških in ženskah. **INTERAKCIJE** Kabozantinib je substrat za CYP3A4. Pri sočasni uporabi močnih zaviralcev CYP3A4 (npr. ritonavirja, itrakonazola, eritromicina, klaritromicina, soka grenivke) je potrebna previdnost. Kroničnі sočasni uporabi močnih induktorjev CYP3A4 (npr. fenitoina, karbamazepina, rifampicina, fenobarbitala ali pripravkov zeliščnega izvora iz šentjanževke) se je treba izogibati. Razmisliti je treba o sočasni uporabi alternativnih zdravil, ki CYP3A4 ne inducirajo in ne zavirajo ali pa inducirajo in zavirajo le neznatno. Pri sočasni uporabi zaviralcev MRP2 (npr. ciklosporin, efavirenz, emtricitabin) je potrebna previdnost, saj lahko povzročijo povečanje koncentracij kabozantiniba v plazmi. Učinka kabozantiniba na farmakokinetiko kontraceptivnih steroidov niso preučili, vendar pa se priporoča dodatna kontracepcijska metoda (pregradna metoda). Zaradi visoke stopnje vezave kabozantiniba na plazemske beljakovine je možna interakcija z varfarinom v obliki izpodrivanja s plazemskih beljakovin, zato je treba spremljati vrednosti INR. Kabozantinib morda lahko poveča koncentracije sočasno uporabljenih substratov P-gp v plazmi. Osebe je treba opozoriti na uporabo substratov P-gp (npr. feksofenadina, aliskirena, ambrisentana, dabigatran eteksilata, digoksina, kolhicina, maraviroka, posakonazola, ranolazina, saksagliptina, sitagliptina, talinolola, tolvaptana) sočasno s kabozantinibom. **NEŽELENI UČINKI** Za popolno informacijo o neželenih učinkih, prosimo, preberite celoten povzetek glavnih značilnosti zdravila Cabometyx. Najpogostejši resni neželeni učinki zdravila so hipertenzija, driska, PPES, pljučna embolija, utrujenost in hipomagneziemija. Najpogostejši neželeni učinki katere koli stopnje (ki so se pojavili pri vsaj 25 % bolnikov) so bili driska, hipertenzija, utrujenost, zvišanje vrednosti AST, zvišanje vrednosti ALT, navzea, zmanjšanje apetita, PPES, disgevzija, zmanjšanje števila trombocitov, stomatitis, anemija, bruhanje, zmanjšanje telesne mase, dispepsija in konstipacija. O hipertenziji so pogosteje poročali pri predhodno nezdravljeni populaciji bolnikov s KLC (67 %), v primerjavi z bolniki s KLC po predhodnem zdravljenju, usmerjenem v VEGF (37 %). *Zelo pogosti (≥ 1/10):* anemija, limfopenija, nevtropenija, trombocitopenija, hipotiroidizem, dehidracija, zmanjšan apetit, hiperglikemija, hipoglikemija, hipofosfatemija, hipoalbuminemija, hipomagneziemija, hiponatriemija, hipokaliemija, hiperkaliemija, hipokalciemija, hiperbilirubinemija, periferna senzorična nevropatija, disgevzija, glavobol, omotica, hipertenzija, disfonija, dispneja, kašelj, driska, navzea, bruhanje, stomatitis, konstipacija, bolečine v trebuhu, dispepsija, bolečina v ustih, suha usta, PPES, akneiformni dermatitis, izpuščaj, makulopapulozni izpuščaj, suha koža, alopecija, sprememba barve las oz. dlak, bolečine v okončinah, mišični spazmi, artralgija, proteinurija, utrujenost, vnetje sluznice, astenija, zmanjšanje telesne mase, zvišanje vrednosti ALT, AST in ALP v serumu, zvišanje vrednosti bilirubina v krvi, zvišanje vrednosti kreatinina, zvišanje vrednosti trigliceridov, zmanjšanje števila belih krvnih celic, povečana vrednost GGT, povečana vrednost amilaze, povečana vrednost holesterola v krvi, povečana vrednost lipaze. *Pogosti (≥ 1/100, < 1/10):* absces, tinitus, pljučna embolija, pankreatitis, bolečina zgornjega dela trebuha, gastroezofagealna refluksna bolezen, hemoroidi, pruritus, periferni edem, zapleti z ranami. *Občasni (≥ 1/1.000, < 1/100):* konvulzije, analna fistula, holestatični hepatitis, osteonekroza čeljusti. **Vrsta ovojnine in vsebina:** Plastenka vsebuje 30 filmsko obloženih tablet. **Režim izdaje:** Rp/Spec. **Imetnik dovoljenja za promet z zdravilom:** Ipsen Pharma, 65 quai Georges Gorse, 92100 Boulogne-Billancourt, Francija
Pred predpisovanjem, prosimo, preberite celoten povzetek glavnih značilnosti zdravila!
CAB-052018

▼Za to zdravilo se izvaja dodatno spremljanje varnosti. Tako bodo hitreje na voljo nove informacije o njegovi varnosti. Zdravstvene delavce naprošamo, da poročajo o katerem koli domnevnem neželenem učinku zdravila.

IPSEN
Innovation for patient care

SAMO ZA STROKOVNO JAVNOST

CAB0718-06, julij 2018

PharmaSwiss
Choose More Life

Odgovoren za trženje v Sloveniji:
PharmaSwiss d.o.o., Brodišče 32, 1236 Trzin
telefon: +386 1 236 47 00, faks: +386 1 283 38 10

RADIOLOGY AND ONCOLOGY

September 2018
Vol. 52 No. 3
Pages 233-352
ISSN 1318-2099
UDC 616-006
CODEN: RONCEM

Publisher
Association of Radiology and Oncology

Affiliated with
Slovenian Medical Association – Slovenian Association of Radiology, Nuclear Medicine Society,
Slovenian Society for Radiotherapy and Oncology, and Slovenian Cancer Society
Croatian Medical Association – Croatian Society of Radiology
Societas Radiologorum Hungarorum
Friuli-Venezia Giulia regional groups of S.I.R.M.
Italian Society of Medical Radiology

Aims and scope
Radiology and Oncology is a journal devoted to publication of original contributions in diagnostic and interventional radiology, computerized tomography, ultrasound, magnetic resonance, nuclear medicine, radiotherapy, clinical and experimental oncology, radiobiology, radiophysics and radiation protection.

Editorial office

Radiology and Oncology
Zaloška cesta 2
P. O. Box 2217
SI-1000 Ljubljana
Slovenia
Phone: +386 1 5879 369
Phone/Fax: +386 1 5879 434
E-mail: gsersa@onko-i.si

Reader for English
Vida Kološa

Secretary
Mira Klemenčič
Zvezdana Vukmirović

Design
Monika Fink-Serša, Samo Rovan, Ivana Ljubanović

Layout
Matjaž Lužar

Printed by
Tiskarna Ozimek, Slovenia

Published quarterly in 400 copies

Beneficiary name: DRUŠTVO RADIOLOGIJE IN ONKOLOGIJE
Zaloška cesta 2
1000 Ljubljana
Slovenia

Beneficiary bank account number: SI56 02010-0090006751
IBAN: SI56 0201 0009 0006 751
Our bank name: Nova Ljubljanska banka, d.d.,
Ljubljana, Trg republike 2,
1520 Ljubljana; Slovenia

SWIFT: LJBASI2X

Subscription fee for institutions EUR 100, individuals EUR 50

The publication of this journal is subsidized by the Slovenian Research Agency.

Indexed and abstracted by:

- *Baidu Scholar*
- *Case*
- *Chemical Abstracts Service (CAS) - CAplus*
- *Chemical Abstracts Service (CAS) - SciFinder*
- *Clarivate Analytics - Journal Citation Reports/Science Edition*
- *Clarivate Analytics - Science Citation Index Expanded*
- *Clarivate Analytics - Web of Science*
- *CNKI Scholar (China National Knowledge Infrastructure)*
- *CNPIEC*
- *Dimensions*
- *DOAJ (Directory of Open Access Journals)*
- *EBSCO (relevant databases)*
- *EBSCO Discovery Service*
- *Elsevier - Embase*
- *Elsevier - Reaxys*
- *Elsevier - SCOPUS*
- *Genamics JournalSeek*
- *Google Scholar*
- *Japan Science and Technology Agency (JST)*
- *J-Gate*
- *JournalGuide*
- *JournalTOCs*
- *KESLI-NDSL (Korean National Discovery for Science Leaders)*
- *Meta*
- *Microsoft Academic*
- *Naviga (Softweco)*
- *Primo Central (ExLibris)*
- *ProQuest (relevant databases)*
- *Publons*
- *PubMed*
- *PubsHub*
- *ReadCube*
- *SCImago (SJR)*
- *Sherpa/RoMEO*
- *Summon (Serials Solutions/ProQuest)*
- *TDNet*
- *Ulrich's Periodicals Directory/ulrichsweb*
- *WanFang Data*
- *WorldCat (OCLC)*

This journal is printed on acid- free paper

On the web: ISSN 1581-3207
https://content.sciendo.com/raon
http://www.radioloncol.com

contents

radiophysics

Selected papers from: The 8th Alpe Adria Medical Physics Meeting in Novi Sad, Serbia, 25th - 27th May 2017 guest editors Božidar Casar and Dietmar Georg

review

Breast size impact on adjuvant radiotherapy adverse effects and dose parameters in treatment planning

Ivica Ratosa[1], Aljasa Jenko[2], Irena Oblak[1]

[1] Division of Radiotherapy, Institute of Oncology Ljubljana, Ljubljana, Slovenia
[2] Division of Radiotherapy, Department of Medical Physics, Institute of Oncology Ljubljana, Ljubljana, Slovenia

Radiol Oncol 2018; 52(3): 233-244.

Received 30 March 2018
Approved 12 June 2018

Corresponding author: Assist. Prof. Irena Oblak, M.D., Ph.D., Institute of Oncology Ljubljana, Zaloška cesta 2, 1000 Ljubljana, Slovenia. Phone: +386 1 5879 661; Fax: +386 1 5879 304; E-mail: ioblak@onko-i.si

Disclosure: No potential conflicts of interest were disclosed.

Background. Breast radiotherapy is an established adjuvant treatment after breast conserving surgery. One of the important individual factors affecting the final cosmetic outcome after radiation is breast size. The purpose of this review is to summarise the clinical toxicity profile of adjuvant radiotherapy in women with breasts of various sizes, and to evaluate the treatment planning studies comparing target coverage and dose to thoracic organs at risk in relation to breast size.

Conclusions. Inhomogeneity and excessive radiation dose (hot spots) in the planning of target volume as well as large volume of the breast *per se*, all contribute to a higher rate of acute adverse events and suboptimal final cosmetic outcome in adjuvant breast cancer radiotherapy, regardless of the fractionation schedule. Improved homogeneity leads to a lower rate of ≥ grade 2 toxicity and can be achieved with three-dimensional conformal or modulated radiotherapy techniques. There may be an association between body habitus (higher body mass index, bigger breast size, pendulous breast, and large chest wall separation) and a higher mean dose to the ipsilateral lung and whole heart. A combination of the technical innovations (*i.e.* the breath-hold technique, prone position with or without holding breath, lateral decubitus position, and thermoplastic bra), dose prescription (*i.e.* moderate hypofractionation), and irradiated volume (*i.e.* partial breast irradiation) should be tailored to every single patient in clinical practice to mitigate the risk of radiation adverse effects.

Keywords: breast cancer, breast size, radiation side effects, organs at risk, treatment planning

Introduction

With the ageing population and screening programs adopted worldwide, both the incidence and prevalence of breast cancer (BC) are projected to increase over the next decades. Since radiotherapy is one of the key modalities in BC treatment, the absolute number of new BC patients in need of external beam radiotherapy is expected to increase in the immediate future in nearly all European countries.[1]

Breast conserving surgery in combination with adjuvant radiotherapy has become the standard of care in BC management.[2,3] Large retrospective population-based studies nowadays show that breast conserving therapy (BCT) may have an even better outcome in terms of BC-specific and overall survival compared to mastectomy.[4] BCT, when compared to more radical surgery, has a positive impact on the patient's quality of life many years after treatment, especially in terms of body image, sexual activity, and better physical and role functioning.[5]

Clinicians and researches alike are paying particular attention to reducing acute and late treatment toxicities in a growing number of BC survivors.[6] Acute skin toxicity is very common and

ranges from mild erythema to moist or dry skin desquamation, with the peak reaction occurring one to two weeks post treatment.[7,8] Late skin reactions include skin fibrosis, skin dyspigmentation, and telangiectasia. Acute heart or lung toxicities are rarely seen in BC adjuvant radiation treatment, but late sequelae may be life threatening, with acute coronary event and lung cancer being two possible complications.[9]

Advances in BC radiotherapy – among them being moderate hypofractionation schedule (HF), intensity modulated radiotherapy (IMRT), and prone or lateral decubitus position – have all the potential to reduce the rates of acute and long-term radiotherapy-related side effects of BCT.[6,7,10-14] The observed normal tissue toxicity rates and breast cosmetic outcome depend on treatment and patient-related factors such as the type and number of surgical procedures, systemic treatment, breast size and shape, race, age, comorbidities, smoking, individual sensitivity to ionizing radiation, choice of fractionation and radiation dose, skin bolus, inter-fraction time interval, volume irradiated, and radiotherapy delivery modality.[15] It is a widely accepted fact that patient-related factors, such as higher body mass index (BMI) and larger breasts[7,10,16] increase the risk of ≥ grade 2 (G2) dermatitis, regardless of the fractionation regimen.[11,17]

We conducted a review to summarise the clinical toxicity profile of adjuvant radiotherapy in women with breasts of various sizes, and to assess the dosimetric studies of different treatment planning techniques which compared the target coverage (also related to breast size) and dose to thoracic organs at risk with a focus to cardiac subvolumes.

Materials and methods

Literature search and selection criteria

A comprehensive literature search for clinical and dosimetric findings was carried out using PubMed/Medline from January 1990, with 30 September 2017 being the last search date. Only English literature was considered, using the following key words: "breast cancer" and "radiotherapy". Subheadings were searched with "organ size", "3D-conformal radiotherapy (3D-CRT)", "intensity modulated radiotherapy (IMRT)", "hybrid-IMRT", and "volumetric-modulated arc therapy (VMAT)", "organs at risk", "treatment planning", "Heart/radiation effects", "Coronary Vessels/radiation effects", and "dosimetric comparison". Additional relevant references were found in reference lists published with the articles. Clinical studies were selected independently of the number of the patients included. We also searched for treatment planning studies with at least 2 different treatment modalities (*i.e.* 3D-CRT, IMRT (multi-beam and tangential), hybrid-IMRT, and volumetric modulated arc therapy (VMAT) for left-sided breast cancer).

All selected articles were reviewed in full-text versions and were further divided into clinical or treatment planning articles. In clinical studies, we searched for acute skin toxicity, heart and lung toxicity, secondary malignancy risk, and for possible strategies to modify the toxicity, again taking into account the different breast size categories. Treatment planning studies were reviewed in detail and selected only if the delineated organs at risk included at least one additional heart substructure, namely coronary arteries or cardiac chambers.

Results

The aim of the literature search was to select all clinical and treatment planning studies of adjuvant breast radiotherapy, taking into account the different breast size categories. The search retrieved 6074 articles, 5980 of which were excluded from the review because the content of the article did not match the search criteria, the content was irrelevant to the review topic, or the records were duplicated. Ultimately, 94 articles were found relevant to this study.

Definition of small, medium, and large breast volume

Clinical studies do not define different breast sizes uniformly. Some of the studies differentiate between breast volumes using measures such as clothing and bra size, where a cup size ≥ D categorises woman as having large breasts.[7,18] In a study by Pignol *et al.*, breast size was defined as follows: small (USA bra sizes 32A/B, 34A/B, and 36A), medium (USA bra sizes 32C, 34C, 36B/C, and 38A/B/C), or large (all other).[7] Some studies use the distance between the edges of the lateral and medial fields, where a breast separation of approximately 18 and 25 cm constitutes medium and larger breast sizes, respectively.[19] Modern three-dimensional treatment planning allows for the target volume to be measured, and clinical target volumes (CTV) of ≥ 1.600 cm^3, 975–1.600 cm^3, and ≤ 500–975 cm^3 have been defined as large, medium, and small breasts, respectively.[20,21] One study described a standard-

ised and reproducible protocol to measure breast size (the thickness of left and right axillary fat and nipple-to-pectoral muscle distance), finding that anthropometric measurements correlate with the risk of skin toxicity.[16]

Acute toxicity

Randomised clinical trials and retrospective clinical data from standard tangential two-dimensional radiotherapy with wedges (2D-RT) *vs.* IMRT show an improvement in planning target volume homogeneity and conformity with IMRT, which may have a clinically significant benefit in reducing the rates of acute dermatitis, moist desquamation, pruritus, palpable breast fibrosis, and acute and chronic oedema in women with all breast sizes.[7,10,22-25] A detailed investigation about the IMRT technique across the studies revealed different planning approaches. IMRT was partly defined as a manual forward-planned technique (F-IMRT)[7,10,22,23,25-27] and partly as an inverse algorithm[7,23], hybrid IMRT (H-IMRT)[28], and typically used physical compensators and step-and-shoot multi-leaf collimator (MLC) fields[7,10,22,23,25,26] or enhanced dynamic wedges and dynamic MLCs.[29] A systematic review and meta-analysis of side effects associated with the use of IMRT in adjuvant BC treatment can be found elsewhere.[30]

In 2008, Pignol *et al.* reported a correlation of increased moist desquamation anywhere in the breast with BMI, increasing breast separation, smaller *vs.* larger breast sizes, and with a higher relative volume of the breast receiving > 105–115 % of the prescribed dose.[7] In a multivariate analysis, IMRT was associated with a decreased risk of moist desquamation (odds ratio, OR, 0.418, p = 0.0034) while breast size (per 100 cm^3) (OR 1.23, p < 0.0001) was associated with an increased risk.[7] Moist desquamation was also correlated with a reduction in the global health status scale (p = 0.0019), ≥ G2 pain score, and with an increase in the breast symptoms scale (p = 0.0028).[7] G2–4 acute pain was not statistically different between IMRT or conventional radiotherapy arms at the end of the radiation treatment, nor was the data on chronic pain in 241 patients available after 9.8 years of follow-up (OR = 0.74, range 0.432–1.271).[7,31]

Six other clinical studies reported a comparison of the clinically adverse events in regard to the three groups of breast sizes. Four compared 2D-RT *vs.* IMRT[7,10,23,25,27] in the supine position, one study compared 3D-CRT *vs.* IMRT in the prone position[28], and one study compared conventional (CF) *vs.* HF in the prone or supine position (Table 1).[32] The percentages of patients experiencing ≥ G2 acute breast toxicity categorised in groups of small, medium, or large-sized are presented separately in Figure 1.

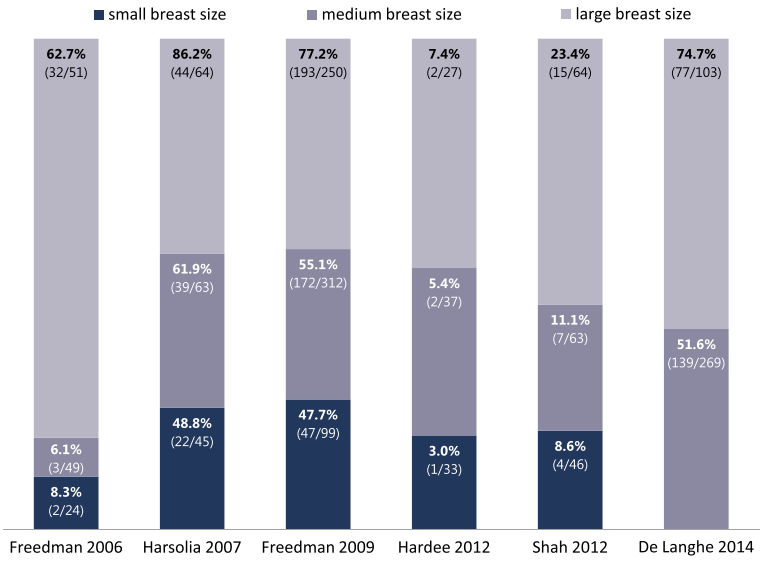

FIGURE 1. Percentage of patients experiencing ≥ G2 acute breast toxicity, categorised in groups of small, medium, or large-sized breasts as reported in selected studies. The numbers displayed in parentheses are the absolute numbers of patients experiencing toxicity and absolute numbers of patients in a group. De Langhe *et al.* grouped small and medium-sized breasts in one category.

Harsolia *et al.* found a correlation between ≥ G2 dermatitis, the development of chronic hyperpigmentation, and breast oedema with a larger than average breast size.[25] Interestingly, no ≥ G3 toxicity was reported in smaller breast volumes in either treatment modality (2D-RT *vs.* IMRT). In comparison with 2D-RT, IMRT improved the rates of ≥ G2 acute oedema (36 % *vs.* 0 %, p < 0.001), ≥ G2 chronic oedema (30 % *vs.* 3 %, p = 0.007), and ≥ G2 hyperpigmentation (41 % *vs.* 3 %, p = 0.001) regardless of the breast volume. No statistically significant difference was observed in acute or chronic rates of ≥ G2 acute dermatitis, pain, chronic hyperpigmentation, or breast induration.[25]

Increased rates of acute dermatitis, acute and chronic oedema, and chronic hyperpigmentation, irrespective of the treatment technique (prone *vs.* supine) or fractionation (CF *vs.* HF), were noted in large-breasted patients (volume > 1.600 cm^3) by Shah *et al.*, when compared to patients with a smaller breast size. In large-breasted patients, IMRT was superior to the 2D-RT technique in reducing the rates of ≥ G2 acute dermatitis (0 % *vs.* 19 %, p = 0.02) and oedema (7 % *vs.* 24 %, p = 0.06).[23]

TABLE 1. Selected studies evaluating IMRT versus 2D-RT or 3D-CRT. Patients were further stratified by small, medium or large-sized breasts

Study	Number of patients	Type of study	Technique	Total dose and Fractionation CF/HF	Breast size (median breast volume)cm^3	Scoring system	G1 or G2 (%) (whole group)	G2 or G3 (%) (whole group)	G3 or G4 (%) (whole group)	General comments
Freedman 2006[27]	131	Case-control retrospective study	F-IMRT 2D-RT	46–50 Gy in 23–25 fractions + boost 10-16 Gy	Breast size was grouped as small (34 A,B; 36 A), medium (34 C; 36 B,C; 38A,B,C), or large (any D or size ≥ 40)	CTCAE v. 3.0	30 (IMRT) 28 (2D-RT)	70 (IMRT) 72 (2D-RT)	0 (IMRT) 0 (2D-RT)	IMRT is associated with a decrease in severity of acute desquamation compared with a matched control group treated with conventional radiation therapy.
Harsolia, 2007[25]	172	Retrospective study	F-IMRT 2D-RT	CF median dose 45 Gy + 16 Gy boost	1.326 (IMRT) 1.489 (2D-RT) Breast volume divided into groups: 1.000 cm^3 (small), 1.000–1.599 cm^3 (medium), 1.600 cm^3 (large)	NCI CTC v. 2.0	41 (IMRT) 85 (2D-RT)		1 (IMRT) 6 (2D-RT)	Lower rates of ≥ G2 toxicity with IMRT regardless of breast size. ≥ G2 clinical toxicities associated with larger irradiated breast sizes, on average (<1.000 cm^3; vs. >1.600 cm^3) No G3 acute toxicity with breast volume (<1.000 cm3) and 3% G3 skin reaction in patients with breast volumes 1.600 cm^3.
Freedman 2009[10]	804	Retrospective study	F-IMRT 2D-RT	46–50 Gy in 23–25 fractions + boost 10–18 Gy	Bra size, (at least 63% with small and medium sizes) Small (32; 34A,B; 36A), Medium (34C; 36B,C;38A,B,C); Large (any D or size 40+)	CTCAE v. 3.0		52 (IMRT) 75 (2D-RT)		More large-breasted patients in IMRT group. IMRT reduces the incidence of ≥ G2 dermatitis in women of all breast sizes.
Shah 2012[23]	335	Prospective study	IMRT 2D-RT IMRT: HF -inversely planned IMRT CF - forward planned IMRT	Median dose 45 Gy + boost 16 Gy or 42.56 Gy without a boost	1.378 for the whole group Breast volume divided into groups: 1.000 cm^3 (small), 1.000-1.599 cm^3 (medium), 1.600 cm^3 (large)	CTCAE v. 3.0		1 (CF-IMRT) 23 (HF-IMRT) 12 (2D-RT)		IMRT is associated with reduced toxicities compared with 2D radiotherapy. In large-breasted patients, CF-IMRT was associated with reduced acute toxicities, while HF-IMRT was not.
Hardee 2012[28]	97	Prospective study	H-IMRT 3D-CRT IMRT: hybrid IMRT using a mixture of 3D tangent fields and dynamic multileaf collimator (MLC) IMRT fields in a 2:1 ratio	46 Gy in 23 fractions + 14-Gy boost or 42.72 Gy in 16 fractions; all in prone position	Breast size was classified as small (A cup, <750 cm^3), medium (B-C cups, 750–1.499 cm^3), and large (D cup or larger,≥ 1,500 cm^3)	RTOG		5.1% ≥ G2		Hypofractionated breast radiotherapy is well tolerated when treating patients in the prone position, even among those with large breast volumes. Breast IMRT significantly improves dosimetry but yields only a modest but confirmed benefit in terms of toxicities.
De Langhe 2014[32]	377	Prospective study	Prone or supine position with INV-IMRT or prone with F-IMRT or prone position with DIBH (n = 22) or supine F-IMRT ± DIBH	40.05 Gy in 15 fractions + boost 10 Gy in 4 fractions (90–75% of patients) or 50 Gy in 25 fractions for 65% of patients with bra cup size ≥ D	Breast size was classified A, B, C and ≥ D cup	CTCAE v. 3.0		57.3 (≥ G2)		CF, supine IMRT, concomitant hormone treatment, high BMI, large breast, smoking during treatment, and genetic variation (in MLH1 rs1800734): all were associated with ≥ G2 toxicity.

2D-RT = standard 2D wedged plan; CTCAE v. 3.0 = common terminology criteria for adverse events for acute radiation dermatitis, version 3.0; CF = conventional fractionation; HF = hypofractionation; DIBH = deep inspiration breath hold; F-IMRT = forward planned intensity modulated radiotherapy; H-IMRT = hybrid intensity modulated radiotherapy; NCI CTC v. 2.0 = National Cancer Institute common toxicity criteria; version 2.0; RTOG = Radiation Therapy Oncology Group criteria

Acute skin toxicity, especially moist desquamation, is associated with late complications of radiotherapy, namely telangiectasia and late subcutaneous fibrosis, as shown in a ten-year update of a Canadian breast IMRT trial and other studies.[31,33] Five-year results of simple IMRT (F-IMRT) support the use of BC adjuvant radiotherapy technique that improves homogeneity: the benefit of IMRT was confirmed in a multivariate analysis for both overall cosmesis ($p = 0.038$) and skin telangiectasia ($p = 0.031$), although there was no difference in breast shrinkage, breast oedema, tumour bed induration, or pigmentation.[24]

Hypofractionation

Moderate HF schedule is an established adjuvant treatment in lymph node-negative BC after breast conserving surgery with no differences in disease-related outcomes and with a favourable toxicity profile.[34-37] Moreover, shorter treatment schedules are a cost-effective approach for both the patient and healthcare providers.[38] The advantages of a hypofractionated schedule over conventional fractionation, *e.g.* convenience, a less acute pain, fatigue, and dermatitis, were recently confirmed with prospectively collected physician-assessed data and patient-reported outcome measures in a large comparative analysis by Jagsi *et al.*[37] In this multicentre cohort, the mean breast volume, BMI, and separation distance were slightly smaller in the hypofractionated group: 1270 *vs.* 980 cm^3, 23 *vs.* 21.9 cm, and 30.8 *vs.* 28.7, respectively.[37]

A higher daily fraction size (> 1.8–2.0 Gy) and hot spots (> V105 %) may contribute to so-called 'triple trouble' or an unequal distribution of the biological effective dose (BED), although the risk is probably insignificant.[39,40] To avoid any of the possible complications (greater fibrosis or late normal tissue effects) with HF, it is generally recommended to limit the volume of hot spots and not to exceed 107 % of the prescribed dose.[40] Some authors suggest that patients with a large breast size that precludes achieving the maximum dose of > 107 % should be offered a dose/fractionation that is biologically less intense, for example 45 Gy in 25 daily fractions at 1.8 Gy daily with an addition of a boost dose.[41]

Similarly as with the CF schedule, high BMI, an increasing PTV volume with a cut off value as small as 500 cm^3[32,35,42], and excessive radiation dose in the target volume (*i.e.* V107–110 %) contribute to increased acute skin toxicity.[17,42] When CF was compared to HF, the CF schedule was a predictive factor for increased ≥ G2 toxicity.[17,32,35] One study reported no differences in acute skin toxicity when HF was compared to CF in similar groups of large-breasted women (volume > 1.500 cm^3), BMI > 30, or breast separation > 25 cm. Breast volume was the only patient factor significantly associated with moist desquamation in a multivariable analysis ($p = 0.01$). A very large breast volume (> 2.500 cm^3) had a higher rate of focal moist desquamation (40.7 %) compared to breast volume < 2.500 cm^3 (11.1 %) ($p = 0.002$).[11] In a randomised clinical trial by Shaitelman *et al.*, where three-quarters of patients were overweight or obese and half of the patients had a Dmax of 107 % or higher, the authors have confirmed the administration of the HF schedule in regard to acute toxic effects to be safe.[36]

Lung and heart toxicity

The dose-volume predictors for acute and late radiation-induced toxicities are established for the lung and heart as a whole structure.[43-45] Recent studies have evaluated the dose to the whole heart and the proportional increase in cardiac events after BC radiotherapy. An estimated linear increase of 7.4 % and 4.1 % was found per every Gy mean dose to the whole heart for major coronary events and cardiac mortality, respectively.[9,45] A systematic literature review on modern radiation doses to heart and lung in BC radiotherapy showed an estimated absolute 30-year risk for cardiac mortality of 1 % for smokers and 0.3 % for non-smokers.[9] Patient-related factors (age and smoking), systemic therapy, the fractionation schedule (total dose and daily fraction), and dose-volume parameters of radiation treatment plan such as mean dose to the whole lung and V20, all constitute risk factors for pneumonitis and lung fibrosis.[15,43]

In a recent retrospective clinical study of 4688 WBRT-treated BC patients, it was reported that larger breast separation (> 22 cm) was one of the factors significantly increasing the mean heart dose (MHD) for CF by 1.5 % per 1 cm and in HF by 1.7 % per every 1 cm increase, respectively.[46] It has been demonstrated that the dose to the heart can be significantly reduced in both CF and HF by means of breathing adaptation and prone positioning.[13,46]

Hannan *et al.* found that increasing breast size results in increased mean and maximum point heart doses.[13] PTV, BMI, or age were generally unrelated to ipsilateral lung dose. The lung dose decreased markedly in the prone compared to supine position for the whole group of patients. Large-breasted prone-treated patients received a higher ipsilateral lung D5 (greatest dose delivered to

5 cm^3) compared to small-breasted prone-treated patients (PTV < 1000 cm^3), but without significant differences in V5 or V20.[13] Breast shape (*i.e.* pendulous breasts) can contribute to a higher maximum heart dose as well.[47] One small dosimetric study in free-breathing supine-position radiation therapy did not find a correlation of increasing breast separation with higher heart doses, but instead found a correlation with an increased dose to the ipsilateral lung (parameters V5 Gy, V10 Gy and V20 Gy), with the greatest increase noted in breast separation between 25 and 27 cm.[48] By contrast, Hardee *et al.* found an opposite association between breast size and lung dosimetric parameters in the prone position (in-field lung volume, V5, and Dmax). All parameters decreased as breast size increased.[28]

Secondary malignancy risk

In BC radiotherapy, differences in body habitus may influence doses to organs at risk, but it is not known if small differences in radiation exposure at the time of the first radiation course significantly influence the risk of a secondary non-breast cancer. Compared to the general population, BC patients have an increased risk of secondary non-breast cancers, five or more years after BC diagnosis with and without radiation therapy (RR 1.12; 95 % confidence interval [CI] 1.06–1.19).[49] But probably less than 3.5 % of secondary malignancies in BC survivors are attributable to radiation therapy.[50] The total dose of radiation, premenopausal age (< 40–45 years) and the irradiated volume of normal tissue all increase the risk for secondary lung, oesophageal, or thyroid cancer, and secondary sarcomas.[49,51] The risk of lung cancer increases with the mean dose to the whole lung.[52] A systematic review of modern radiation doses to the lung in BC radiotherapy showed an estimated absolute 30-year risk for lung cancer of 4 % for long-term continuing smokers and 0.3 % for non-smokers.[9]

The radiation dose to the lung increases with lymph node irradiation and the use of IMRT techniques, and decreases with breathing adaptations and prone/lateral decubitus positioning.[52] Younger women (< 40 years of age) with an absorbed radiation dose > 1.0 Gy to the contralateral breast have an elevated long-term risk of developing a second primary contralateral BC.[52]

A study by Bhatnagar *et al.* suggests that the size of the primary irradiated breast significantly affects the scatter dose to the contralateral breast but not the ipsilateral lung or heart when using IMRT for breast irradiation. The mean volume of the primary irradiated breast in the study was 1167.9 cm^3.[53] However, Jin *et al.* found that in the population of women with smaller breasts (360.8 ± 149.1 cm^3), the size of the treated breast does not significantly increase the dose to the contra-lateral breast with 2D-RT, 3D-CRT with 3–5 subfields, or tangential IMRT techniques.[54]

Strategies to modify acute toxicity and dose to organs at risk

Different strategies in BC radiotherapy exist to lower the dose to organs at risk. Approaches could be further divided according to patient or breast positioning modification, breathing adaptation, and treatment volume reduction.

Patient positioning modification

The prone positioning setup demonstrated to be an excellent strategy to spare the ipsilateral lung in 100 % and heart dose in 85–87 % of the patients, independently of their BMI or breast size[12,55–58], but a particular benefit was observed in large-breasted women (CTV > 1000 cm^3).[12,13,57] Similar findings were confirmed in a study by Formenti *et al.* but, in this study, the prone treatment position did not necessarily spare the heart in patients with breast volumes smaller than 750 cm^3.[57] On the other hand, one study reported having achieved similar heart doses for prone and supine 3D-CRT WBRT in women with large breast volumes (the average treated volume was 1804 cm^3 in right-sided breasts and 1500 cm^3 in left-sided breasts). They also noted a significantly higher incidental dose to the LADCA in the prone position with left-sided BC.[59]

3D-CRT lateral isocentric decubitus position was recently described as a treatment planning solution. Long-term toxicity results were published by the Institut Curie group.[14,60] Women with a median BMI of 26.3 were treated with different types of fractionation. Acute dermatitis of any grade was present in 93 % of the patients and G3 dermatitis in only 2.8 %. In a 1-year follow-up, 94.1 % of cases had no skin reaction, making this technique feasible with excellent toxicity rates, but the results need to be confirmed with a longer follow-up. In a multivariate analysis, the cup size and the fractionation had a significant influence on acute dermatitis.[14]

Breathing adaptation

The deep inspiration breath-hold (DIBH) technique helps to minimise the "trade-off" between

the target and OAR, a compromise often required, and is less resource-intensive than the IMRT technique. It reduces the low-dose irradiation to the heart, left anterior descending coronary artery (LADCA), and lung, ultimately benefiting women of all breast sizes.[61] DIBH can be accurately clinically implemented with an acceptable reproducibility and stability in both supine and prone position.[61,62] In a group of women with a volume of the treated breast > 750 cm^3, supine voluntary DIBH enabled a cardiac sparing and reproducibility superior to that of free-breathing prone position.[63]

Partial breast irradiation

Another strategy to lower the absorbed radiation dose to the heart is partial breast irradiation. Patients may benefit in terms of lower mean whole heart doses with moderate HF using 3D-CRT and the accelerated partial breast irradiation technique (APBI) with an external beam or interstitial brahcytherapy.[64-67] Meszaros *et al.* demonstrated the reproducibility of image-guidance intensity modulated APBI and feasibility in terms of acute toxicity and the cosmetic outcome with a median follow up of 3.2 years. In a study, 55 % of the patients had cup size C and 21 % cup size ≥ D.[67] Investigators emphasised the necessity of image guidance prior to each radiation fraction to reduce the CTV to PTV margins.[67]

Breast tissue modification

A thermoplastic bra which helps to raise the lateral breast border is also an option to lower the dose to thoracic organs in BC radiotherapy. Piroth *et al.* demonstrated an excellent reduction in radiation exposure to the heart (mean dose reduction by ≈ 23 %) and ipsilateral lung (mean dose reduction by ≈ 30 % and V20 by 39.5 %) without additional skin toxicity in women of all breast sizes (clinical target volume ranging from 283.1 to 1581.6 cm^3).[68]

Treatment planning studies

Many different treatment planning options are available in the modern treatment era: 3D-CRT with or without wedged filters, forward-planned IMRT (F-IMRT), inverse-planned IMRT (INV-IMRT), Helical Tomotherapy (HT), VMAT, and hybrid techniques (H-IMRT). The recommended first choice for WBRT varies across numerous treatment planning studies comparing different modalities (*i.e.* 3D-CRT *vs.* IMRT *vs.* VMAT) and usually depends on the available equipment, technical innovations, irradiated volume, treatment planning system with dose calculation algorithm, and skills of the planner.

There are numerous publications comparing the dosimetric parameters of radiotherapy plans, mostly for patients with left-sided early BC. Some of them have been summarised in a review of treatment planning options by Balaji *et al.* where most authors favoured hybrid planning techniques (3D CRT + IMRT/VMAT) while weighing the target coverage *vs.* dose to the organs at risk.[69] While INV-IMRT is not routinely recommended after breast-only radiation, the use of advanced techniques is increasing in challenging anatomy cases (up to 9.4 % of all BC patients treated with radiotherapy).[70] The majority of techniques can be combined with DIBH and/or the prone position. The role of the VMAT technique in clinical practice is still not known precisely and the technique itself is not routinely recommended. The dosimetric data, although promising, need to be validated from a clinical point of view.[71] The VMAT technique is sometimes the first choice in complex anatomy cases (including large breasts, bilateral BC adjuvant radiotherapy, pectus excavatum, etc.).[71] HT (TomoDirect) can be delivered in a 3D-CRT or IMRT modality in whole-breast adjuvant BC radiotherapy. Both HT modalities have a good PTV coverage and dose homogeneity, but some caution is needed as the dose to ipsilateral lung and heart can be significantly high with the 3D-CRT modality in specific patient anatomic situations. Authors have proposed that simple anatomic measures like maximal heart distance can be helpful in selecting the appropriate treatment strategy.[72]

For the purpose of this review, we have evaluated the treatment planning studies which included at least coronary arteries or cardiac chambers as organs at risk. Overall, we have found eight treatment planning studies comparing radiotherapy plans in free-breathing CTs.[54,73-79] The studies indicate an improved dose homogeneity with the IMRT[54,73,75,78,79] or VMAT[73,74] techniques regardless of the PTV volume, but the number of CT study sets compared was relatively low (10–20). The sizes of the target volumes reported by investigators comparing treatment planning approaches were dissimilar, ranging from 296 cm^3 (mean value) to 1160 cm^3 (median value).[74,79] A study by Tan *et al.* found additional heart subvolumes (left ventricle or LV and anterior myocardial territory or AMT) to be helpful in the IMRT plan optimization process, although there have been no reports available so

far for the dose–volume constraints in these two OARs.[75]

Besides the heart as a whole structure, authors typically delineated LADCA[73,74,76-78], LV[75,76,78,79], right ventricle (RV)[76,78], left atrium (LA)[76,78], right atrium (RA)[76,78], great vessels[78], and AMT.[54,74,75] The delineation of heart substructures was not uniformly defined or was rarely guided by written instructions, making it difficult to compare the presented studies.[54,74,75]

Discussion

Growing clinical data on BC adjuvant radiotherapy suggest that a smaller PTV and/or the use of the IMRT technique may be associated with a decreased rates of acute breast toxicity. Most studies evaluated women with small or medium-sized breasts, so maybe all of the results are not directly applicable in large-breasted woman. The clinical studies which reported a comparison of the clinical adverse events in regard to the three categories of breast sizes mostly used the CTCAE v.3.0 scoring system.[7,10,23,25,27,28] The rates of ≥ G2 toxicity for the whole group of patients from selected studies used in Figure 1 ranged from 5.1 % to 70 %. The percentage of patients with ≥ G2 toxicity was the highest in the subcategory of large-breasted patients in all the studies, ranging from 7.4 % to 86.2 %.[10,23,27,32] The differences in adverse event reporting could at least partly be attributed to different scoring systems, *i.e.* the subjective scoring by investigators and different planning techniques.

Moderately hypofractionated schedules proved superiority over CF and conformal radiation therapy (3D-CRT or F-IMRT) over 2D-RT in terms of acute and late adverse effects in early BC WBRT.[7,12,22,24,26,34,37] Clinical reports are confirming the long-term safety and feasibility of moderately hypofractionated schedules also in women with large breasts.[11,17,32,36,38,42,80,81] Most of the investigators attributed higher toxicity rates in BC radiotherapy to dose inhomogeneity and a higher percentage of hot spots, irrespective of breast volume.[7,12,17,31] V105–107 % of the prescribed dose (PD) was significantly related to increased desquamation, dermatitis, oedema, and pain[12]; and V105 % PD[82,83] or V110 % PD[83] to long-term breast pain. Significant reductions in hot spots can be achieved with 3D-CRT or F-IMRT treatment plans, also in patients with large/pendulous breasts (PTV >1000 cm^3).[20,26,28,84] An improvement in dose homogeneity was achieved with IMRT, and correlated with less acute toxicity rates in a study by Mulliez *et al.*[85]

However, some of the studies show that large breast volume seems to be a risk factor for acute or late adverse events independently of dose inhomogeneity and regardless of the conformal radiotherapy technique (3D-CRT *vs.* IMRT) or fractionation schedule.[11,24,86] A retrospective analysis of selected patients from UK FAST hypofractionation (3D-CRT) trial found that breast size and dosimetric parameters are significantly associated with late effects in a univariate analysis where breast size was the only remaining independent significant risk factor for change in breast appearance when included in a multiple regression model together with other prognostic factors.[86] Investigators failed to correlate the breast composition (breast tissue distribution and scar tissue presence) with late adverse effects, with the exception of seroma.[87] Combining all data, there is no reason to withhold the hypofractionation schedule in large-breasted women.

The data published support the hypothesis that every Gy of increase in the whole lung mean dose increases the risk for second lung cancer.[9] In the long run, as far as the sub-population of continuing smokers is concerned, the second lung cancer risk is even greater and the benefits of adjuvant radiotherapy in early BC may be reduced to the point where long-term risks outweigh the benefits of adjuvant radiotherapy.[9] At the same time smokers, portend lifelong cardiac mortality risks and smoking during BC radiotherapy significantly increase the risk of acute ≥ G2 dermatitis.[32,52] Smoking cessation counselling may be provided to modify acute and late toxicity risks. Breathing-adapted radiotherapy in the prone or supine position in women with all breast sizes, and prone or lateral setup in medium or large-breasted patients (approximately ≥ 1000 cm^3) have been shown to decrease the whole lung and heart dose parameters.[12,13,52,57,88]

In terms of the heart as an organ at risk, ideally, all treatment planning comparisons of WBRT in patients with left-sided BC should be done in DIBH. Treatment planning or retrospective dose evaluation studies often only include the heart as a whole structure, without separately delineated heart subvolumes, although the dose distribution in the heart itself in BC adjuvant radiotherapy is usually not homogeneous.[89] In some patients, the dose to the LADCA can be significantly higher in the prone (without breath-hold) compared to the supine setup, which could also be attributed to the differences in contouring and treatment tech-

niques.[59] The routine use of delineation guidelines for thoracic organs at risk and dose reporting with clinical correlation could help us further understand normal tissue complication probability models, especially in the least known dose-response relationships, *i.e.* for coronary arteries and cardiac chambers. Using individual 3D-CRT planning data, one study independently validated the mean heart dose-based normal tissue complication probability (NTCP) model (published by Darby *et al.* in 2013[45]) for acute coronary events within 9 years after adjuvant radiotherapy. Investigators found an increase of 16.5 % in the cumulative incidence of acute coronary events per every Gy increase of the mean heart dose. One step further was made in understanding the radiation tolerance for particular cardiac segments, as there are no current models for dose-response relationships. The study found a significant prognostic importance of the left ventricle V5 Gy dose relationship with an acute coronary event.[44,90]

Treatment planning studies usually compare a limited number of CT study sets and it is not known if small improvement in dosimetric metrics would translate into clinically meaningful lower rates of adverse events for the larger population. For example, one treatment planning study in the modern treatment era reported very little difference in dosimetric parameters between patients of different breast size regardless of the modality (static HT, IMRT, and 3D-CRT).[21] Expected absolute differences in the rates of clinical adverse events (3D-CRT *vs.* other highly conformal techniques) are likely negligible. HT, INV-IMRT, and VMAT may all increase the mean and maximum dose to contralateral breast, and mean dose to the heart and ipsilateral lung compared to F-IMRT or 3D CRT, although doses to organs at risk may also depend on the patient's anatomy or positioning.[52,73,75,91]

In order to de-escalate radiotherapy, selected patients will be treated routinely with the moderate HF or accelerated partial breast irradiation techniques (treating only the tumour bed with a safety margin) in the near future, as emerging data confirm a similar 5-year cumulative incidence of loco-regional and distant relapse compared to WBRT.[38,92,93] In a 5-year assessment, patients treated with partial radiotherapy approaches self-reported less moderate or marked skin ($p = 0.051$) or overall breast appearance change ($p < 0.0001$) compared to the WBRT group.[88] APBI using interstitial brachytherapy was able to significantly reduce acute G3 skin toxicity (7 % in WBRT group *vs.* 0.2 %; $p < 0.0001$).[94] Simple F-IMRT techniques using shortened tangential fields and interstitial brachytherapy APBI were able to minimise the dose to the heart and lung.[66,92] A higher APBI-PTV/breast volume ratio most probably contributes to adverse acute and poor final cosmetic results.[67] Further clinical trials with longer follow-ups are needed in partial breast radiotherapy, especially in large-breasted woman, to confirm the clinical relevance.

Conclusions

One of the important individual factors affecting the final cosmetic outcome of radiation therapy treatment is the size of the treated PTV. It seems that beside the target volume, inhomogeneity, and a higher percentage of the excessive radiation dose, bigger breast size itself is an independent risk factor for acute adverse effects regardless of the fractionation regimen or dose inhomogeneity, although the lower the excessive radiation dose, the lower the risk of ≥ G2 toxicity. While weighing the risk of BC relapse *vs.* acute or late treatment toxicity, an appropriate postoperative radiotherapy technique (3D-CRT *vs.* modulated approaches), patient setup (prone *vs.* supine with or without a breath hold), and volume irradiated (*i.e.* candidates for partial breast irradiation) should be optimally selected and tailored to the patient's anatomy (including BMI, breast separation, or cup size), age, and tumour characteristics. A personalised approach is therefore needed in every single patient, with the patient's social, economic, or psychological issues to be taken into account.

References

1. Borras JM, Lievens Y, Barton M, Corral J, Ferlay J, Bray F, et al. How many new cancer patients in Europe will require radiotherapy by 2025? An ESTRO-HERO analysis. *Radiother Oncol* 2016; **119:** 5-11. doi: 10.1016/j.radonc.2016.02.016
2. Fisher B, Anderson S, Bryant J, Margolese RG, Deutsch M, Fisher ER, et al. Twenty-year follow-up of a randomized trial comparing total mastectomy, lumpectomy, and lumpectomy plus irradiation for the treatment of invasive breast cancer. *N Engl J Med* 2002; **347:** 1233-41. doi: 10.1056/NEJMoa022152
3. Veronesi U, Cascinelli N, Mariani L, Greco M, Saccozzi R, Luini A, et al. Twenty-year follow-up of a randomized study comparing breast-conserving surgery with radical mastectomy for early breast cancer. *N Engl J Med* 2002; **347:** 1227-32. doi: 10.1056/NEJMoa020989
4. Gentilini OD, Cardoso M-J, Poortmans P. Less is more. Breast conservation might be even better than mastectomy in early breast cancer patients. *Breast* 2017; **35:** 32-3. doi: 10.1016/j.breast.2017.06.004
5. Arndt V, Stegmaier C, Ziegler H, Brenner H. Quality of life over 5 years in women with breast cancer after breast-conserving therapy versus mastectomy: a population-based study. *J Cancer Res Clin Oncol* 2008; **134:** 1311-8. doi: 10.1007/s00432-008-0418-y

6. Berry S. Advances in breast bancer radiotherapy and the impact on quality of life. *J Cancer Biol Res* 2014; **2:** 1041.

7. Pignol J-P, Olivotto I, Rakovitch E, Gardner S, Sixel K, Beckham W, et al. A multicenter randomized trial of breast intensity-modulated radiation therapy to reduce acute radiation dermatitis. *J Clin Oncol* 2008; **26:** 2085-92. doi: 10.1200/JCO.2007.15.2488

8. Pignol J-P, Vu TTT, Mitera G, Bosnic S, Verkooijen HM, Truong P. Prospective evaluation of severe skin toxicity and pain during postmastectomy radiation therapy. *Int J Radiat Oncol* 2015; **91:** 157-64. doi: 10.1016/j.ijrobp.2014.09.022

9. Taylor C, Correa C, Duane FK, Aznar MC, Anderson SJ, Bergh J, et al. Estimating the risks of breast cancer radiotherapy: evidence from modern radiation doses to the lungs and heart and from previous randomized trials. *J Clin Oncol* 2017; **35:** 1641-9. doi: 10.1200/JCO.2016.72.0722

10. Freedman GM, Li T, Nicolaou N, Chen Y, Ma CC-M, Anderson PR. Breast intensity-modulated radiation therapy reduces time spent with acute dermatitis for women of all breast sizes during radiation. *Int J Radiat Oncol* 2009; **74:** 689-94. doi: 10.1016/j.ijrobp.2008.08.071

11. Corbin KS, Dorn PL, Jain SK, Al-Hallaq HA, Hasan Y, Chmura SJ. Hypofractionated radiotherapy does not increase acute toxicity in large-breasted women: results from a prospectively collected series. *Am J Clin Oncol* 2014; **37:** 322-6. doi: 10.1097/COC.0b013e31827b45b7

12. Mulliez T, Veldeman L, van Greveling A, Speleers B, Sadeghi S, Berwouts D, et al. Hypofractionated whole breast irradiation for patients with large breasts: a randomized trial comparing prone and supine positions. *Radiother Oncol* 2013; **108:** 203-8. doi: 10.1016/j.radonc.2013.08.040

13. Hannan R, Thompson RF, Chen Y, Bernstein K, Kabarriti R, Skinner W, et al. Hypofractionated Whole-Breast Radiation Therapy: Does Breast Size Matter? *Int J Radiat Oncol* 2012; **84:** 894-901. doi: 10.1016/j.ijrobp.2012.01.093

14. Bronsart E, Dureau S, Xu HP, Bazire L, Chilles A, Costa E, et al. Whole breast radiotherapy in the lateral isocentric lateral decubitus position: Long-term efficacy and toxicity results. *Radiother Oncol* 2017; **124:** 214-9. doi: 10.1016/j.radonc.2017.07.001

15. Meattini I, Guenzi M, Fozza A, Vidali C, Rovea P, Meacci F, et al. Overview on cardiac, pulmonary and cutaneous toxicity in patients treated with adjuvant radiotherapy for breast cancer. *Breast Cancer* 2016; **24:** 52-62. doi: 10.1007/s12282-016-0694-3

16. Méry B, Vallard A, Trone J-C, Pacaut C, Guy J-B, Espenel S, et al. Correlation between anthropometric parameters and acute skin toxicity in breast cancer radiotherapy patients: a pilot assessment study. *Br J Radiol* 2015; **88:** 20150414. doi: 10.1259/bjr.20150414

17. Tortorelli G, Di Murro L, Barbarino R, Cicchetti S, di Cristino D, Falco MD, et al. Standard or hypofractionated radiotherapy in the postoperative treatment of breast cancer: a retrospective analysis of acute skin toxicity and dose inhomogeneities. *BMC Cancer* 2013; **13:** 230. doi: 10.1186/1471-2407-13-230

18. Dundas KL, Atyeo J, Cox J. What is a large breast? Measuring and categorizing breast size for tangential breast radiation therapy. *Australas Radiol* 2007; **51:** 589-93. doi: 10.1111/j.1440-1673.2007.01898.x

19. Back M, Guerrieri M, Wratten C, Steigler A. Impact of radiation therapy on acute toxicity in breast conservation therapy for early breast cancer. *Clin Oncol (R Coll Radiol)* 2004; **16:** 12-6. doi: 10.1016/j.clon.2003.08.005

20. Vicini FA, Sharpe M, Kestin L, Martinez A, Mitchell CK, Wallace MF, et al. Optimizing breast cancer treatment efficacy with intensity-modulated radiotherapy. *Int J Radiat Oncol Biol Phys* 2002; **54:** 1336-44. doi: 10.1016/S0360-3016(02)03746-X

21. Michalski A, Atyeo J, Cox J, Rinks M, Morgia M, Lamoury G. A dosimetric comparison of 3D-CRT, IMRT, and static tomotherapy with an SIB for large and small breast volumes. *Med Dosim* 2014; **39:** 163-8. doi: 10.1016/j.meddos.2013.12.003

22. Donovan E, Bleakley N, Denholm E, Evans P, Gothard L, Hanson J, et al. Randomised trial of standard 2D radiotherapy (RT) versus intensity modulated radiotherapy (IMRT) in patients prescribed breast radiotherapy. *Radiother Oncol* 2007; **82:** 254-64. doi: 10.1016/j.radonc.2006.12.008

23. Shah C, Wobb J, Grills I, Wallace M, Mitchell C, Vicini FA. Use of intensity modulated radiation therapy to reduce acute and chronic toxicities of breast cancer patients treated with traditional and accelerated whole breast irradiation. *Pract Radiat Oncol* 2012; **2:** e45–51. doi: 10.1016/j.prro.2012.01.008

24. Mukesh MB, Barnett GC, Wilkinson JS, Moody AM, Wilson C, Dorling L, et al. Randomized controlled trial of intensity-modulated radiotherapy for early breast cancer: 5-year results confirm superior overall cosmesis. *J Clin Oncol* 2013; **31:** 4488-95. doi: 10.1200/JCO.2013.49.7842

25. Harsolia A, Kestin L, Grills I, Wallace M, Jolly S, Jones C, et al. Intensity-modulated radiotherapy results in significant decrease in clinical toxicities compared with conventional wedge-based breast radiotherapy. *Int J Radiat Oncol Biol Phys* 2007; **68:** 1375-80. doi: 10.1016/j.ijrobp.2007.02.044

26. Barnett GC, Wilkinson J, Moody AM, Wilson CB, Sharma R, Klager S, et al. A randomised controlled trial of forward-planned radiotherapy (IMRT) for early breast cancer: baseline characteristics and dosimetry results. *Radiother Oncol* 2009; **92:** 34-41. doi: 10.1016/j.radonc.2009.03.003

27. Freedman GM, Anderson PR, Li J, Eisenberg DF, Hanlon AL, Wang L, et al. Intensity Modulated Radiation Therapy (IMRT) Decreases Acute Skin Toxicity for Women Receiving Radiation for Breast Cancer. *Am J Clin Oncol* 2006; **29:** 66-70. doi: 10.1097/01.coc.0000197661.09628.03

28. Hardee ME, Raza S, Becker SJ, Jozsef G, Lymberis SC, Hochman T, et al. Prone hypofractionated whole-breast radiotherapy without a boost to the tumor bed: comparable toxicity of IMRT versus a 3D conformal technique. *Int J Radiat Oncol* 2012; **82:** e415-23. doi: 10.1016/j.ijrobp.2011.06.1950

29. McDonald MW, Godette KD, Butker EK, Davis LW, Johnstone PAS. Long-term outcomes of IMRT for breast cancer: a single-institution cohort analysis. *Int J Radiat Oncol Biol Phys* 2008; **72:** 1031-40. doi: 10.1016/j.ijrobp.2008.02.053

30. Jensen KE, Soril LJJ, Stelfox HT, Clement FM, Lin Y, Marshall DA. Side effects associated with the use of intensity-modulated radiation therapy in breast cancer patients undergoing adjuvant radiation therapy: a systematic review and meta-analysis. *J Med Imaging Radiat Sci* 2017; **48:** 402-13. doi: 10.1016/j.jmir.2017.09.002

31. Pignol J-P, Truong P, Rakovitch E, Sattler MG, Whelan TJ, Olivotto IA. Ten years results of the Canadian breast intensity modulated radiation therapy (IMRT) randomized controlled trial. *Radiother Oncol* 2016; **121:** 414-9. doi: 10.1016/j.radonc.2016.08.021

32. De Langhe S, Mulliez T, Veldeman L, Remouchamps V, van Greveling A, Gilsoul M, et al. Factors modifying the risk for developing acute skin toxicity after whole-breast intensity modulated radiotherapy. *BMC Cancer* 2014; **14:** 711. doi: 10.1186/1471-2407-14-711

33. Lilla C, Ambrosone CB, Kropp S, Helmbold I, Schmezer P, von Fournier D, et al. Predictive factors for late normal tissue complications following radiotherapy for breast cancer. *Breast Cancer Res Treat* 2007; **106:** 143-50. doi: 10.1007/s10549-006-9480-9

34. Haviland JS, Owen JR, Dewar JA, Agrawal RK, Barrett J, Barrett-Lee PJ, et al. The UK Standardisation of breast radiotherapy (START) trials of radiotherapy hypofractionation for treatment of early breast cancer: 10-year follow-up results of two randomised controlled trials. *Lancet Oncol* 2013; **14:** 1086-94. doi: 10.1016/S1470-2045(13)70386-3

35. De Felice F, Ranalli T, Musio D, Lisi R, Rea F, Caiazzo R, et al. Relation between hypofractionated radiotherapy, toxicity and outcome in early breast cancer. *Breast J* 2017; **23:** 563-8. doi: 10.1111/tbj.12792

36. Shaitelman SF, Schlembach PJ, Arzu I, Ballo M, Bloom ES, Buchholz D, et al. Acute and short-term toxic effects of conventionally fractionated vs hypofractionated whole-breast irradiation: a randomized clinical trial. *JAMA Oncol* 2015; **1:** 931-41. doi: 10.1001/jamaoncol.2015.2666

37. Jagsi R, Griffith KA, Boike TP, Walker E, Nurushev T, Grills IS, et al. Differences in the acute toxic effects of breast radiotherapy by fractionation schedule: comparative analysis of physician-assessed and patient-reported outcomes in a large multicenter cohort. *JAMA Oncol* 2015; **1:** 918-30. doi: 10.1001/jamaoncol.2015.2590

38. Franco P, Iorio GC, Bartoncini S, Airoldi M, De Sanctis C, Castellano I, et al. De-escalation of breast radiotherapy after conserving surgery in low-risk early breast cancer patients. *Med Oncol* 2018; **35:** 62. doi: 10.1007/s12032-018-1121-8

39. Jones B, Dale RG, Deehan C, Hopkins KI, Morgan DA. The role of biologically effective dose (BED) in clinical oncology. *Clin Oncol (R Coll Radiol)* 2001; **13:** 71-81. doi: 10.1053/clon.2001.9221

40. Yarnold J, Somaiah N, Bliss JM. Hypofractionated radiotherapy in early breast cancer: Clinical, dosimetric and radio-genomic issues. *Breast* 2015; **24 (Suppl 2):** S108-13. doi: 10.1016/j.breast.2015.07.025

41. Koulis TA, Phan T, Olivotto IA. Hypofractionated whole breast radiotherapy: current perspectives. *Breast Cancer (Dove Med Press)* 2015; **7:** 363-70. doi: 10.2147/BCTT.S81710

42. Lazzari G, Terlizzi A, Della Vittoria Scarpati G, Perri F, De Chiara V, Turi B, et al. Predictive parameters in hypofractionated whole-breast 3D conformal radiotherapy according to the Ontario Canadian trial. *Onco Targets Ther* 2017; **10:** 1835-42. doi: 10.2147/OTT.S127833

43. Marks LB, Bentzen SM, Deasy JO, Kong F-MS, Bradley JD, Vogelius IS, et al. Radiation dose-volume effects in the lung. *Int J Radiat Oncol Biol Phys* 2010; **76:** S70-6. doi: 10.1016/j.ijrobp.2009.06.091

44. Gagliardi G, Constine LS, Moiseenko V, Correa C, Pierce LJ, Allen AM, et al. Radiation dose-volume effects in the heart. *Int J Radiat Oncol Biol Phys* 2010; **76:** S77-85. doi: 10.1016/j.ijrobp.2009.04.093

45. Darby SC, Ewertz M, Hall P. Ischemic heart disease after breast cancer radiotherapy. *N Engl J Med* 2013; **368:** 2527. doi: 10.1056/NEJMc1304601

46. Pierce LJ, Feng M, Griffith KA, Jagsi R, Boike T, Dryden D, et al. Recent time trends and predictors of heart dose from breast radiation therapy in a large quality consortium of radiation oncology practices. *Int J Radiat Oncol* 2017; **99:** 1154-61. doi: 10.1016/j.ijrobp.2017.07.022

47. Guan H, Dong YL, Ding LJ, Zhang ZC, Huang W, Liu CX, et al. Morphological factors and cardiac doses in whole breast radiation for left-sided breast cancer. *Asian Pac J Cancer Prev* 2015; **16:** 2889-94. doi: 10.7314/APJCP.2015.16.7.2889

48. Wernicke Ag, Heineman T, Sabbas A, Delamerced M, Chiu Y, Smith M, et al. Impact of a large breast separation on radiation dose delivery to the ipsilateral lung as result of respiratory motion quantified using free breathing and 4D CT-based planning in patients with locally advanced breast cancers: a potential for adverse clinical implications. *J Cancer Res Ther* 2013; **9:** 154. doi: 10.4103/0973-1482.110368

49. Grantzau T, Overgaard J. Risk of second non-breast cancer after radiotherapy for breast cancer: a systematic review and meta-analysis of 762,468 patients. *Radiother Oncol* 2015; **114:** 56-65. doi: 10.1016/j.radonc.2014.10.004

50. Burt LM, Ying J, Poppe MM, Suneja G, Gaffney DK. Risk of secondary malignancies after radiation therapy for breast cancer: comprehensive results. *Breast* 2017; **35:** 122-9. doi: 10.1016/j.breast.2017.07.004

51. Stovall M, Smith SA, Langholz BM, Boice JD, Shore RE, Andersson M, et al. Dose to the contralateral breast from radiotherapy and risk of second primary breast cancer in the WECARE study. *Int J Radiat Oncol* 2008; **72:** 1021-30. doi: 10.1016/j.ijrobp.2008.02.040

52. Aznar MC, Duane FK, Darby SC, Wang Z, Taylor CW. Exposure of the lungs in breast cancer radiotherapy: a systematic review of lung doses published 2010–2015. *Radiother Oncol* 2018; **126:** 148-54. doi: 10.1016/j.radonc.2017.11.022

53. Bhatnagar AK, Heron DE, Deutsch M, Brandner E, Wu A, Kalnicki S. Does breast size affect the scatter dose to the ipsilateral lung, heart, or contralateral breast in primary breast irradiation using intensity-modulated radiation therapy (IMRT)? *Am J Clin Oncol* 2006; **29:** 80-4. doi: 10.1097/01.coc.0000198743.80991.15

54. Jin G-H, Chen L-X, Deng X-W, Liu X-W, Huang Y, Huang X-B. A comparative dosimetric study for treating left-sided breast cancer for small breast size using five different radiotherapy techniques: conventional tangential field, filed-in-filed, tangential-IMRT, multi-beam IMRT and VMAT. *Radiat Oncol* 2013; **8:** 89. doi: 10.1186/1748-717X-8-89

55. Osa E-OO, DeWyngaert K, Roses D, Speyer J, Guth A, Axelrod D, et al. Prone Breast Intensity Modulated Radiation Therapy: 5-Year Results. *Int J Radiat Oncol* 2014; **89:** 899-906. doi: 10.1016/j.ijrobp.2014.03.036

56. Ramella S, Trodella L, Ippolito E, Fiore M, Cellini F, Stimato G, et al. Whole-breast irradiation: a subgroup analysis of criteria to stratify for prone position treatment. *Med Dosim* 2012; **37:** 186-91. doi: 10.1016/j.meddos.2011.06.010

57. Lymberis SC, deWyngaert JK, Parhar P, Chhabra AM, Fenton-Kerimian M, Chang J, et al. Prospective assessment of optimal individual position (prone versus supine) for breast radiotherapy: volumetric and dosimetric correlations in 100 patients. *Int J Radiat Oncol* 2012; **84:** 902-9. doi: 10.1016/j.ijrobp.2012.01.040

58. Fan L-L, Luo Y-K, Xu J-H, He L, Wang J, Du X. A dosimetry study precisely outlining the heart substructure of left breast cancer patients using intensity-modulated radiation therapy. *J Appl Clin Med Phys* 2014; **15:** 4624. doi: 10.1120/jacmp.v15i5.4624

59. Würschmidt F, Stoltenberg S, Kretschmer M, Petersen C. Incidental dose to coronary arteries is higher in prone than in supine whole breast irradiation. *Strahlenther Onkol* 2014; **190:** 563-8. doi: 10.1007/s00066-014-0606-4

60. Kirova YM, Hijal T, Campana F, Fournier-Bidoz N, Stilhart A, Dendale R, et al. Whole breast radiotherapy in the lateral decubitus position: a dosimetric and clinical solution to decrease the doses to the organs at risk (OAR). *Radiother Oncol* 2014; **110:** 477-81. doi: 10.1016/j.radonc.2013.10.038

61. Bartlett FR, Colgan RM, Donovan EM, Carr K, Landeg S, Clements N, et al. Voluntary breath-hold technique for reducing heart dose in left breast radiotherapy. *J Vis Exp* 2014; **89**. doi: 10.3791/51578

62. Mulliez T, Veldeman L, Vercauteren T, De Gersem W, Speleers B, Van Greveling A, et al. Reproducibility of deep inspiration breath hold for prone left-sided whole breast irradiation. *Radiat Oncol* 2015; **10:** 9. doi: 10.1186/s13014-014-0313-4

63. Bartlett FR, Colgan RM, Donovan EM, McNair HA, Carr K, Evans PM, et al. The UK HeartSpare Study (tage IB): randomised comparison of a voluntary breath-hold technique and prone radiotherapy after breast conserving surgery. *Radiother Oncol* 2015; **114:** 66-72. doi: 10.1016/j.radonc.2014.11.018

64. Merino Lara TR, Fleury E, Mashouf S, Helou J, McCann C, Ruschin M, et al. Measurement of mean cardiac dose for various breast irradiation techniques and corresponding risk of major cardiovascular event. *Front Oncol* 2014; **4:** 284. doi: 10.3389/fonc.2014.00284

65. Moran JM, Ben-David MA, Marsh RB, Balter JM, Griffith KA, Hayman JA, et al. Accelerated partial breast irradiation: what is dosimetric effect of advanced technology approaches? *Int J Radiat Oncol* 2009; **75:** 294-301. doi: 10.1016/j.ijrobp.2009.03.043

66. Lettmaier S, Kreppner S, Lotter M, Walser M, Ott OJ, Fietkau R, et al. Radiation exposure of the heart, lung and skin by radiation therapy for breast cancer: a dosimetric comparison between partial breast irradiation using multicatheter brachytherapy and whole breast teletherapy. *Radiother Oncol* 2011; **100:** 189-94. doi: 10.1016/j.radonc.2010.07.011

67. Mészáros N, Major T, Stelczer G, Zaka Z, Mózsa E, Pukancsik D, et al. Implementation of image-guided intensity-modulated accelerated partial breast irradiation: three-year results of a phase II clinical study. *Strahlenther Onkol* 2017; **193:** 70-9. doi: 10.1007/s00066-016-1074-9

68. Piroth MD, Petz D, Pinkawa M, Holy R, Eble MJ. Usefulness of a thermoplastic breast bra for breast cancer radiotherapy. *Strahlenther Onkol* 2016; **192:** 609-16. doi: 10.1007/s00066-016-0981-0

69. Balaji K, Subramanian B, Yadav P, Anu Radha C, Ramasubramanian V. Radiation therapy for breast cancer: literature review. *Med Dosim* 2016; **41:** 253-7. doi: 10.1016/j.meddos.2016.06.005

70. Arsene-Henry A, Fourquet A, Kirova YM. Evolution of radiation techniques in the treatment of breast cancer (BC) patients: from 3D conformal radiotherapy (3D CRT) to intensity-modulated RT (IMRT) using helical tomotherapy (HT). *Radiother Oncol* 2017; **124:** 333-4. doi: 10.1016/j.radonc.2017.07.002

71. Cozzi L, Lohr F, Fogliata A, Franceschini D, De Rose F, Filippi AR, et al. Critical appraisal of the role of volumetric modulated arc therapy in the radiation therapy management of breast cancer. *Radiat Oncol* 2017; **12:** 1-12. doi: 10.1186/s13014-017-0935-4

72. Borca VC, Franco P, Catuzzo P, Migliaccio F, Zenone F, Aimonetto S, et al. Does TomoDirect 3DCRT represent a suitable option for post-operative whole breast irradiation? A hypothesis-generating pilot study. *Radiat Oncol* 2012; **7:** 211. doi: 10.1186/1748-717X-7-211

73. Virén T, Heikkilä J, Myllyoja K, Koskela K, Lahtinen T, Seppälä J. Tangential volumetric modulated arc therapy technique for left-sided breast cancer radiotherapy. *Radiat Oncol* 2015; **10:** 79. doi: 10.1186/s13014-015-0392-x

74. Zhao H, He M, Cheng G, Han D, Wu N, Shi D, et al. A comparative dosimetric study of left sided breast cancer after breast-conserving surgery treated with VMAT and IMRT. *Radiat Oncol* 2015; **10:** 231. doi: 10.1186/s13014-015-0531-4

75. Tan W, Wang X, Qiu D, Liu D, Jia S, Zeng F, et al. Dosimetric comparison of intensity-modulated radiotherapy plans, with or without anterior myocardial territory and left ventricle as organs at risk, in early-stage left-sided breast cancer patients. *Int J Radiat Oncol Biol Phys* 2011; **81:** 1544-51. doi: 10.1016/j.ijrobp.2010.09.028

76. Zhang L, Mei X, Chen X, Hu W, Hu S, Zhang Y, et al. Estimating cardiac substructures exposure from diverse radiotherapy techniques in treating left-sided breast cancer. *Medicine (Baltimore)* 2015; **94:** e847. doi: 10.1097/MD.0000000000000847

77. Haciislamoglu E, Colak F, Canyilmaz E, Dirican B, Gurdalli S, Yilmaz AH, et al. Dosimetric comparison of left-sided whole-breast irradiation with 3DCRT, forward-planned IMRT, inverse-planned IMRT, helical tomotherapy, and volumetric arc therapy. *Phys Medica* 2015; **31:** 360-7. doi: 10.1016/j.ejmp.2015.02.005

78. Baycan D, Karacetin D, Balkanay AY, Barut Y. Field-in-field IMRT versus 3D-CRT of the breast. Cardiac vessels, ipsilateral lung, and contralateral breast absorbed doses in patients with left-sided lumpectomy: a dosimetric comparison. *Jpn J Radiol* 2012; **30:** 819-23. doi: 10.1007/s11604-012-0126-z

79. Lohr F, El-Haddad M, Dobler B, Grau R, Wertz H-J, Kraus-Tiefenbacher U, et al. Potential effect of robust and simple IMRT approach for left-sided breast cancer on cardiac mortality. *Int J Radiat Oncol Biol Phys* 2009; **74:** 73-80. doi: 10.1016/j.ijrobp.2008.07.018

80. Rudat V, Nour A, Ghaida SA, Alaradi A. Impact of hypofractionation and tangential beam IMRT on the acute skin reaction in adjuvant breast cancer radiotherapy. *Radiat Oncol* 2016; **11:** 100. doi: 10.1186/s13014-016-0674-y

81. Ciammella P, Podgornii A, Galeandro M, Micera R, Ramundo D, Palmieri T, et al. Toxicity and cosmetic outcome of hypofractionated whole-breast radiotherapy: predictive clinical and dosimetric factors. *Radiat Oncol* 2014; **9:** 97. doi: 10.1186/1748-717X-9-97

82. Lee E, Takita C, Wright JL, Reis IM, Zhao W, Nelson OL, et al. Characterization of risk factors for adjuvant radiotherapy-associated pain in a tri-racial/ethnic breast cancer population. *Pain* 2016; **157:** 1122-31. doi: 10.1097/j.pain.0000000000000489

83. Mak KS, Chen Y-H, Catalano PJ, Punglia RS, Wong JS, Truong L, et al. Dosimetric inhomogeneity predicts for long-term breast pain after breast-conserving therapy. *Int J Radiat Oncol Biol Phys* 2014; **93:** 1087-95. doi: 10.1016/j.ijrobp.2014.05.021

84. Stimato G, Ippolito E, Silipigni S, Venanzio C Di, Rinaldi CG, Gaudino D, et al. A new three-dimensional conformal radiotherapy (3DCRT) technique for large breast and/or high body mass index patients: evaluation of a novel fields assessment aimed to reduce extra–target-tissue irradiation. *Br J Radiol* 2016; **89:** 20160039. doi: 10.1259/bjr.20160039

85. Mulliez T, Speleers B, Madani I, De Gersem W, Veldeman L, De Neve W. Whole breast radiotherapy in prone and supine position: is there a place for multi-beam IMRT? *Radiat Oncol* 2013; **8:** 151. doi: 10.1186/1748-717X-8-151

86. Goldsmith C, Haviland J, Tsang Y, Sydenham M, Yarnold J. Large breast size as a risk factor for late adverse effects of breast radiotherapy: is residual dose inhomogeneity, despite 3D treatment planning and delivery, the main explanation? *Radiother Oncol* 2011; **100:** 236-40. doi: 10.1016/j.radonc.2010.12.012

87. Juneja P, Bonora M, Haviland JS, Harris E, Evans P, Somaiah N. Does breast composition influence late adverse effects in breast radiotherapy? *Breast* 2016; **26:** 25-30. doi: 10.1016/j.breast.2015.12.004

88. Kirby AM, Evans PM, Donovan EM, Convery HM, Haviland JS, Yarnold JR. Prone versus supine positioning for whole and partial-breast radiotherapy: a comparison of non-target tissue dosimetry. *Radiother Oncol* 2010; **96:** 178-84. doi: 10.1016/j.radonc.2010.05.014

89. Aznar MC, Korreman S-S, Pedersen AN, Persson GF, Josipovic M, Specht L. Evaluation of dose to cardiac structures during breast irradiation. *Br J Radiol* 2011; **84:** 743-6. doi: 10.1259/bjr/12497075

90. van den Bogaard VAB, Ta BDP, van der Schaaf A, Bouma AB, Middag AMH, Bantema-Joppe EJ, et al. Validation and modification of a prediction model for acute cardiac events in patients with breast cancer treated with radiotherapy based on three-dimensional dose distributions to cardiac substructures. *J Clin Oncol* 2017; **35:** 1171-8. doi: 10.1200/JCO.2016.69.8480

91. Haciislamoglu E, Colak F, Canyilmaz E, Zengin AY, Yilmaz AH, Yoney A, et al. The choice of multi-beam IMRT for whole breast radiotherapy in early-stage right breast cancer. *Springerplus* 2016; **5:** 688. doi: 10.1186/s40064-016-2314-2

92. Coles CE, Griffin CL, Kirby AM, Titley J, Agrawal RK, Alhasso A, et al. Partial-breast radiotherapy after breast conservation surgery for patients with early breast cancer (UK IMPORT LOW trial): 5-year results from a multicentre, randomised, controlled, phase 3, non-inferiority trial. *Lancet* 2017; **390:** 1048-60. doi: 10.1016/S0140-6736(17)31145-5

93. Strnad V, Ott OJ, Hildebrandt G, Kauer-Dorner D, Knauerhase H, Major T, et al. 5-year results of accelerated partial breast irradiation using sole interstitial multicatheter brachytherapy versus whole-breast irradiation with boost after breast-conserving surgery for low-risk invasive and in-situ carcinoma of the female breast: a randomised, phase 3, non-inferiority trial. *Lancet* 2016; **387:** 229-38. doi: 10.1016/S0140-6736(15)00471-7

94. Ott OJ, Strnad V, Hildebrandt G, Kauer-Dorner D, Knauerhase H, Major T, et al. GEC-ESTRO multicenter phase 3-trial: Accelerated partial breast irradiation with interstitial multicatheter brachytherapy versus external beam whole breast irradiation: Early toxicity and patient compliance. *Radiother Oncol* 2016; **120:** 119-23. doi: 10.1016/j.radonc.2016.06.0

research article

Dynamics of CT visible pleural effusion in patients with pulmonary infarction

Igor Kocijancic[1], Jernej Vidmar[1,2], Marko Kastelic[3]

[1] Institute of Radiology, University Medical Centre Ljubljana, Ljubljana, Slovenia
[2] Institute of Physiology, Faculty of Medicine, University of Ljubljana, Slovenia
[3] Department of Radiology, General Hospital Celje, Celje, Slovenia

Radiol Oncol 2018; 52(3): 245-249.

Received 08 August 2018
Accepted 17 August 2018

Correspondence to: Marko Kastelic, M.D., Department of Radiology, General Hospital Celje, Oblakova 5, 3000 Celje, Slovenia.
Phone: ++386 31 685 135; E-mail: marko.kastelic@gmail.com, or marko.kastelic@sb-celje.si

Disclosure: No potential conflict of interest were disclosed.

Background. Pleural effusion remains largely unexplored in patients with pulmonary embolism and concurrent pulmonary infarction. The aim of the study was to investigate the relationship between the size of pulmonary infarction and pleural effusion as well as the time course of pleural effusion in patients with pulmonary infarction.

Patients and methods. Data from 103 patients with pulmonary infarction was retrospectively analysed along with patient comorbidities, size of pulmonary infarction, presence and size of pleural effusion with the time between the onset of clinical symptoms of pulmonary infarction and CT study.

Results. Assessment of possible correlations between the size of pulmonary infarction and age revealed a significant negative correlation. There was a highly significant difference ($p = 0.005$) in the mean size of pulmonary infarction in patients with effusion (34.5 cm^3) compared to those without it (14.3 cm^3), but the size of the effusion had no correlation with the size of pulmonary infarction. The size of the effusion peaked between 4^{th}–5^{th} day after the onset of clinical symptoms of pulmonary infarction. In the first 5 days after the onset of clinical symptoms of pulmonary infarction a significant correlation was found between the size of the effusion and time with approximation of 1.3 mm/12 h.

Conclusions. The data shows that patients with a pleural effusion are more likely to have a larger pulmonary infarction than those without it. If present, the effusion can be expected to increase in a relatively slow linear fashion in the first 5 days after the onset of clinical symptoms of pulmonary infarction.

Key words: pulmonary infarction; pleural effusion; pulmonary embolism; CTA of pulmonary arteries

Introduction

Pleural effusion is a known and well described occurrence in the setting of an acute pulmonary embolism and infarction.[1,2] In patients with acute pulmonary embolism, it has been proven to be a factor of poor prognosis and has been correlated with higher mortality.[3,4] Size-wise, it has been shown to peak 3 days after and resolve within 7–10 days of acute pulmonary embolism.[5]

However, focusing solely on patients with pulmonary infarction, the topic of pleural effusion remains largely unexplored in the literature published in the last 20 years (PubMed search term "pulmonary infarction pleural effusion" yields no relevant results). The aim of this study is therefore (1) to investigate the relationship between the volume of pulmonary infarction and pleural effusion and (2) to investigate the relationship between the amount of CT visible pleural effusion and its change in size with regards to time after the clinical onset of symptoms of pulmonary infarction.

Patients and methods

Patient selection and image analysis

The study is a part of an ongoing project at University Medical Centre Ljubljana and was approved by the National Medical Ethics Committee

of Slovenia (No. 0120-509/2017/6, 18th May 2018). Data has been retrospectively evaluated from CT pulmonary angiography (CT-PA) of 103 patients in University Medical Centre in Ljubljana in the period of 15th April 2017 – 30th June 2018.

In our PACS archive we reviewed all CT-PA studies in the aforementioned period and included the patients with CT signs of pulmonary embolism and pulmonary infarction. We recorded: demographic data, comorbidities, location and size of the pulmonary infarction, presence, location and size of pleural effusion and time between the onset of clinical symptoms (pleuritic pain, haemoptysis) and the time at which CT-PA was performed.[6] The size of the effusion was expressed as a fluid layer, measured in its thickest part, perpendicular to the thoracic wall[7], as shown in Figure 1. Pulmonary infarction was defined as pleural based pulmonary consolidation without contrast enhancement.[8,9] The volume of pulmonary infarction was measured using Aquarius iNtuition version 4.4.6 (TeraRecon, USA) by manually drawing regions of interest (ROIs) around the infarcted area (Figure 1). All the measurements were independently performed by two experienced radiologists.

TABLE 1. Demographic data and comorbidities. (*) Multiple linear regression was performed to test for correlation. P-values are shown

Gender	**N**	**(%)**			
Male	37	(38.9 %)			
Female	58	(61.6 %)			
Age					
Mean (SD)	61.3	(± 19.5)			
Pleural effusion	**N**	**(%)**			
Present	57	(60 %)			
Not present	38	(40 %)			
			Correlation(*) with		
Comorbidities	**N**	**(%)**	**PI size**	**Ef. size**	**Presence of ef.**
Reduced mobility	38	(40 %)	0.6	0.5	0.7
Previous PE	8	(8.4 %)	0.7	0.2	0.9
Oral contraceptives	7	(7.4 %)	0.5	0.4	0.2
Known malignancy	6	(6.3 %)	0.09	0.2	0.3
Proven GVT	6	(6.3 %)	0.9	0.7	0.1
Congestive heart failure	5	(5.3 %)	0.5	0.3	0.7
COPD	4	(4.2 %)	0.5	0.9	0.07
Number of comorbidities present in a patient	**N**	**(%)**			
No comorbidities	37	(38.9 %)			
1	51	(53.7 %)			
2	5	(5.3 %)			
3	2	(2.1 %)			

Ef. = effusion; PE = pulmonary embolism; PI = pulmonary infarction

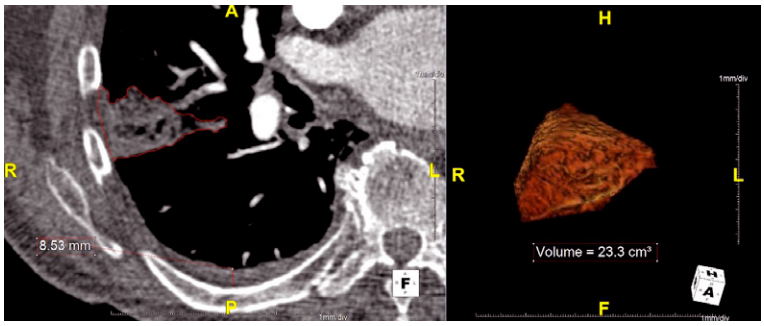

FIGURE 1. Measurements of pulmonary infarction volume and effusion layer size. Left: ROI around infarcted area and pleural effusion layer thickness measurement. Right: 3D visualization of the infarcted area.

Statistical analysis

Multiple linear regression, independent samples t-test and bivariate correlation (i.e. Pearson correlation coefficient) were used as appropriate. Statistical significance was set at the p-value of 0.05. All the statistics were performed using IBM SPSS Statistics version 22 (IBM, USA).

Results

Study population characteristics

Of the 103 patients, 8 were excluded due to: (1) previous pleural effusion and (2) CT imaging more than 10 days after the onset of symptoms in order to avoid effusions of other aetiologies, such as hemothorax and infection.[5,10] The study thus included 95 patients. Most of the patients (53.7%) had at least one comorbidity at the time of the pulmonary infarction, with reduced mobility being the most common (40%, Table 1). Patients with reduced mobility included post-operative patients, patients after cerebrovascular insult, patients with casts and other similar causes.

Pulmonary infarction size

The average size of the pulmonary infarction was 26.8 ± 40.9 cm^3. There was a weak, but statistically significant negative correlation between age and the size of the pulmonary infarction, with older patients having smaller pulmonary infarctions ($r = -0.21$; $p < 0.05$; Figure 2). There was no significant correlation between the presences of different comorbidities with the size of pulmonary infarction (Table 1).

TABLE 2. Mean pulmonary infarction size in patients with and without pleural effusion

Pleural effusion	Mean PI size
Not present	14.3 cm^3 (± 17.8 cm^3)
Present	34.5 cm^3 (± 50.5 cm^3)

PI = pulmonary infarction

Pulmonary effusion presence and size

Pleural effusion was present in 57 patients (60 %) with an average thickness of 10.6 ± 8.5 mm. We found a highly statistically significant difference in size of the pulmonary infarction in patients with and without effusion, with effusions being present in patients with larger infarctions (p = 0.005; Table 2). No significant correlation was found between different comorbidities and the presence of the effusion (Table 1). In the group of patients with pleural effusion, there was no significant correlation between the size of the pulmonary infarction and the layer thickness of the effusion (r = 0.12; p = 0.4) or the presence of comorbidities and the layer thickness of the effusion (Table 1).

Time course of a pleural effusion in patients with pulmonary infarction

In patients with a pleural effusion the layer thickness of the effusion peaked between the 4th and the 5th day after the onset of symptoms (Figure 3). In the first five days, we established a highly statistically significant positive correlation between the layer thickness of the effusion and time (r = 0.45; p = 0.001). Using a linear trend line fit, the resulting linear function was y = 5.7 + 0.1·x, where y is the effusion layer thickness in mm and x is time elapsed since the onset of symptoms in hours. Between the 5th and the 10th day, we found a negative correlation between the size of the effusion and time, but it was not statistically significant (r = - 0.4; p = 0.3).

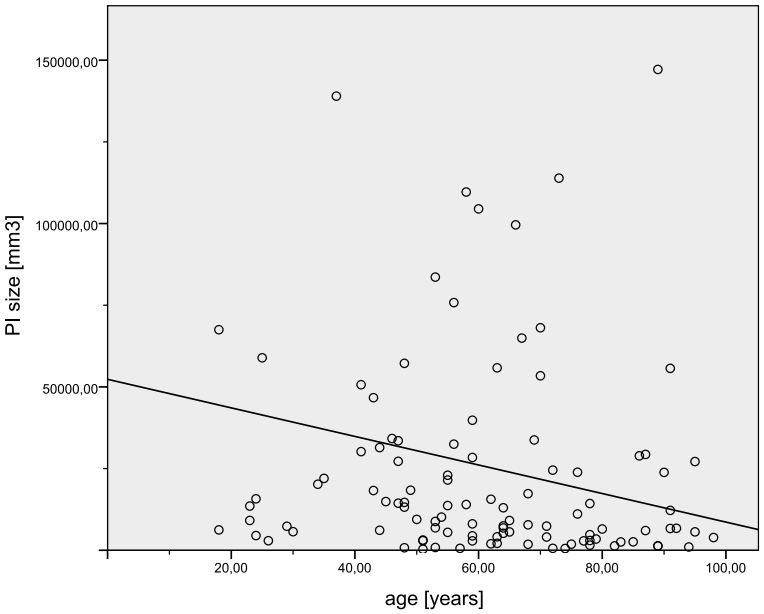

FIGURE 2. Size of the pulmonary infarction (in mm^3) in relation to patients' age (in years).

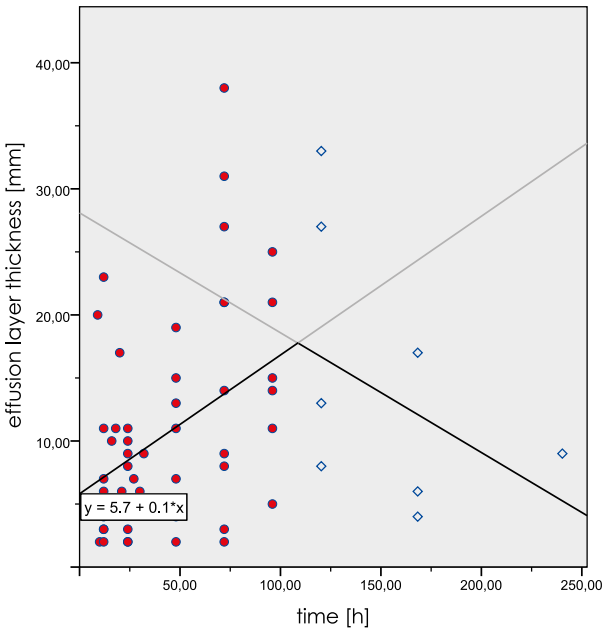

FIGURE 3. Thickness of the pleural effusion layer (in mm) in relation to time since the onset of symptoms (in hours).

Discussion

One of our main findings was that the size of the pulmonary infarction was significantly smaller in older patients. This seems to be complementary to previous studies, which report significantly lower prevalence of pulmonary infarction in the elderly.[8,11,12] One of the probable mechanisms for this could be that in elderly patients with chronic cardiopulmonary disease regional hypoxia promotes collateral pulmonary angiogenesis, thus protecting the pulmonary parenchyma from infarction.[11] Another possible mechanism, which could also interfere, is that the dilatation and extension of the bronchial circulation in patients with chronic lung diseases decreases flow dynamics through the established pulmonary circulation.[8] Both of these hy-

potheses could reasonably be applied to our results as well.

The effusion layer present in patients with pulmonary infarction was generally relatively small (10.6 mm on average), which is in agreement with previous studies.[1,3,4,10,13] However, while there was no correlation between pulmonary infarction size and effusion layer thickness, larger pulmonary infarctions seem more likely to be associated with an accompanying effusion than the smaller ones, which is in contrast to the previously published data.[2] Our findings seem to be in agreement with proposed pathophysiological mechanisms, which suggest that the dynamics of pleural effusions are influenced by numerous, possibly alternating factors. Several mechanisms have been proposed by which pleural effusion develops in patients with pulmonary infarction. The first one is an increase of the capillary permeability in the lungs secondary to the release of inflammatory mediators.[10,14] This mechanism could explain the correlation between larger pulmonary infarctions and the presence of pleural effusion. Larger volume of infarcted tissue results in the release of greater quantities of inflammatory mediators, which efficiently promote the development of the effusion. On the other hand, this hypothesis would also suggest that the size of the effusion layer could possibly correlate with the size of the pulmonary infarction, which we found not to be the case. The additional mechanism which could alter the pleural effusion dynamics in patients with pulmonary embolism and pulmonary infarction is the increase of hydrostatic pressure in systemic veins and capillaries in the parietal pleura as a result of impaired blood flow. The increased pressure in systemic veins could impair lymphatic drainage and therefore promote pleural fluid formation.[14] Therefore, one of the plausible explanations for relatively small or no pleural effusion in our study is that in the cases with relatively small pulmonary infarction pre-existent modifications in the bronchial circulation could have been present with already reduced pulmonary blood flow. Small flow dynamics could have consequently caused only relatively small increments in hydrostatic pressure with little or no pleural effusion.

In the cases of CT visible pleural effusion, the layer of effusion is more likely to increase in thickness with time in the first five days after the onset of pulmonary infarction. Using the fitted linear function, according to which the layer of pleural effusion would increase by about 1.3 mm every 12 h, one can predict the possible peak size of the effusion after the initial CT imaging. An assessment of the peak of pleural effusion seems to be useful, since a major increase in the effusion size has already been shown to be a worrisome feature, indicating complications and possibly prompting diagnostic thoracentesis in patients with pulmonary embolism.[10] Our data also suggests that if the patient has a concurrent pulmonary infarction, the increase in size is not necessarily a sign of complications as long as it follows the expected trend line in the first five days. In any case, further investigation is needed, especially in light of our findings, which contradict previous studies.[2]

The major limitation of our study was the inability to differentiate between the area of true infarction (i.e. necrotic tissue) and the area of haemorrhage following pulmonary embolism, because both present as an area of unenhanced consolidation on a CT scan. We categorized these entities as pulmonary infarction in both cases, which probably resulted in overestimating the size of the true pulmonary infarction in our study.[9] However, this has been suggested to be clinically less important as the entire volume of the consolidation (i.e. true infarction with surrounding haemorrhage) represents tissue with severely decreased, non-functional ventilation/perfusion (V/P) ratio. Due to radiation constraints we only analysed CT scans of multiple patients at different time points. In an ideal case, the dynamics of the effusion layer size would be measured in the same patient at different times and then the results could be averaged. Therefore, a reasonable continuation of this CT study would be to monitor pleural effusion dynamics in patients with CT confirmed pulmonary infarction by using complementary imaging modalities. One of the limitations of our study is also the relatively small sample size, especially with regards to the patients imaged later than 5 days after the onset of symptoms. One could expect a reduction of size of the effusion in this group; however, a considerably larger number of subjects is needed, preferably in a multicentre study.

Conclusions

With increasing patient age, the size of pulmonary infarction gets smaller. Pleural effusion is more likely to occur in patients with larger pulmonary infarction, however the size of the effusion does not necessarily correlate with the size of the pulmonary infarction. Our data suggests that if an effusion in a patient with pulmonary infarction is present, an increase in the effusion in the first five

days is not necessarily a sign of complication, as long as it follows the expected trend line with an increase of about 1.3 mm in layer thickness every 12 h.

References

1. Choi SH, Cha S-I, Shin K-M, Lim J-K, Yoo S-S, Lee S-Y, et al. Clinical relevance of pleural effusion in patients with pulmonary embolism. *Respiration* 2017; **93:** 271-8. doi: 10.1159/000457132
2. Porcel JM, Madroñero AB, Pardina M, Vives M, Esquerda A, Light RW. Analysis of pleural effusions in acute pulmonary embolism: radiological and pleural fluid data from 230 patients. *Respirology* 2007; **12:** 234-9. doi: 10.1111/j.1440-1843.2006.01026.x
3. Zhou X, Zhang Z, Zhai Z, Zhang Y, Miao R, Yang Y, et al. Pleural effusions as a predictive parameter for poor prognosis for patients with acute pulmonary thromboembolism. *J Thromb Thrombolysis* 2016; **42:** 432-40. doi: 10.1007/s11239-016-1371-2
4. Kiris T, Yazıcı S, Koc A, Köprülü C, Ilke Akyildiz Z, Karaca M, et al. Prognostic impact of pleural effusion in acute pulmonary embolism. *Acta Radiol* 2017; **58:** 816-24. doi: 10.1177/0284185116675655
5. Findik S. Pleural effusion in pulmonary embolism. *Curr Opin Pulm Med* 2012; **18:** 347-54. doi: 10.1097/MCP.0b013e32835395d5
6. Tapson VF. Pulmonary infarction: a disease of the (mostly) young. *Respirology* 2018 Jul 16. [Epub ahead of print]. doi: 10.1111/resp.13366
7. Hazlinger M, Ctvrtlik F, Langova K, Herman M. Quantification of pleural effusion on CT by simple measurement. *Biomed Pap* 2014; **158:** 107-11. doi: 10.5507/bp.2012.042
8. Miniati M. Pulmonary infarction: an often unrecognized clinical rntity. *Semin Thromb Hemost* 2016; **42:** 865-9. doi: 10.1055/s-0036-1592310
9. He H, Stein MW, Zalta B, Haramati LB. Pulmonary infarction: spectrum of findings on multidetector helical CT. *J Thorac Imaging* 2006; **21:** 1-7. doi: 10.1097/01.rti.0000187433.06762.fb
10. Light R. Pleural effusion in pulmonary embolism. *Semin Respir Crit Care Med* 2010; **31:** 716-22. doi: 10.1055/s-0030-1269832
11. Islam M, Filopei J, Frank M, Ramesh N, Verzosa S, Ehrlich M, et al. Pulmonary infarction secondary to pulmonary embolism: an evolving paradigm. *Respirology* 2018 Mar 25. [Epub ahead of print]. doi: 10.1111/resp.13299
12. Kirchner J, Obermann A, Stückradt S, Tüshaus C, Goltz J, Liermann D, et al. Lung infarction following pulmonary embolism: a comparative study on clinical conditions and CT findings to identify predisposing factors. *Rofo* 2015; **187:** 440-4. doi: 10.1055/s-0034-1399006
13. Shi HZ, Teng LL, Wang XJ, Wang Z, Xu LL, Zhai ZG, et al. Incidence of pleural effusion in patients with pulmonary embolism. *Chin Med J (Engl)* 2015; **128:** 1032-6. doi: 10.4103/0366-6999.155073
14. Agarwal R, Singh N, Gupta D. Pleural effusions associated with pulmonary thromboembolism: a systematic review. *Indian J Chest Dis* 2009; **51:** 159-64.

research article

Three-dimensional ultrasound evaluation of tongue posture and its impact on articulation disorders in preschool children with anterior open bite

Sanda Lah Kravanja[1], Irena Hocevar-Boltezar[2], Maja Marolt Music[3,4], Ana Jarc[2], Ivan Verdenik[5], Maja Ovsenik[6]

[1] Dental Centre Dr Lah Kravanja, Bovec, Slovenia
[2] Department of Otorhinolaryngology and Head & Neck Surgery, University Medical Centre Ljubljana, Ljubljana, Slovenia
[3] Department of Radiology, Institute of Oncology Ljubljana, Ljubljana, Slovenia
[4] Faculty of Medicine, University of Ljubljana, Ljubljana, Slovenia
[5] Department of Obstetrics and Gynecology, University Medical Centre Ljubljana, Ljubljana, Slovenia
[6] Department of Orthodontics and Dentofacial Orthopedics, Faculty of Medicine, University of Ljubljana, Ljubljana, Slovenia

Radiol Oncol 2018; 52(3): 250-256.

Received 7 July 2018
Accepted 13 July 2018

Correspondence to: Prof. Maja Ovsenik, D.M.D., Ph.D., Department of Orthodontics and Dentofacial Orthopaedics, Faculty of Medicine, University of Ljubljana, Vrazov trg 2, SI-1000 Ljubljana, Slovenia. E-mail: maja.ovsenik@mf.uni-lj.si

Disclosure: No potential conflicts of interest were disclosed.

Background. Tongue posture plays an important role in the etiology of anterior open bite (AOB) and articulation disorders, and is crucial for AOB treatment planning and posttreatment stability. Clinical assessment of tongue posture in children is unreliable due to anatomical limitations. The aim of the study was to present functional diagnostics using three-dimensional ultrasound (3DUS) assessment of resting tongue posture in comparison to clinical assessment, and the associations between the improper tongue posture, otorhinolaryngological characteristics, and articulation disorders in preschool children with AOB.

Patients and methods. A cross-sectional study included 446 children, aged 3–7 years, 236 boys and 210 girls, examined by an orthodontist to detect the prevalence of AOB. The AOB was present in 32 children. The control group consisted of 43 children randomly selected from the participants with normocclusion. An orthodontist, an ear, nose and throat (ENT) specialist and a speech therapist assessed orofacial and ENT conditions, oral habits, and articulation disorders in the AOB group and control group. Tongue posture was also assessed by an experienced radiologist, using 3DUS. The 3DUS assessment of tongue posture was compared to the clinical assessment of orthodontist and ENT specialist.

Results. The prevalence of AOB was 7.2%. The AOB group and the control group significantly differed regarding improper tongue posture ($p < 0.001$), and articulation disorders ($p < 0.001$). In children without articulation disorders from both groups, the improper tongue posture occured less frequently than in children with articulation disorders ($p < 0.001$). After age adjustment, a statistical regression model showed that the children with the improper tongue posture had higher odds ratios for the presence of AOB (OR 14.63; $p < 0.001$) than the others. When articulation disorders were included in the model, these odds ratios for the AOB became insignificant ($p = 0.177$). There was a strong association between the improper tongue posture and articulation disorders ($p = 0.002$). The 3DUS detected the highest number of children with improper resting tongue posture, though there was no significant difference between the 3DUS and clinical assessments done by orthodontist and ENT specialist.

Conclusions. The 3DUS has proved to be an objective, non-invasive, radiation free method for the assessment of tongue posture and could become an important tool in functional diagnostics and early rehabilitation in preschool children with speech irregularities and irregular tongue posture and malocclusion in order to enable optimal conditions for articulation development.

Key words: anterior open bite; tongue posture; three-dimensional ultrasound; prevalence; clinical evaluation; oral habits; articulation disorder

Introduction

Anterior open bite (AOB) is defined as the absence of contact of the anterior teeth when the posterior teeth are in contact.[1-3] It was established that heredity and several other factors (thumb and/or finger sucking, lip and tongue posture habits, impaired nasal breathing, and true skeletal growth abnormalities) play an important role in the etiology of this type of malocclusion.[4-7] The intrinsic vertical gap can cause difficulties in biting and chewing, affects the articulation and has unfavorable aesthetic and psychological consequences. Since 80% of specific speech movements are made in the anterior part of the mouth, it is not surprising that a relationship between articulation defects and malocclusion has long been assumed to exist.[8] Among great diversity of malocclusions, AOB is the most common malocclusion associated with articulation disorders.[9,10]

The tongue is a muscular, largely movable organ in the oral cavity, important for many oral and oropharyngeal functions. The tongue resting posture is believed to be even more important for the morphology of the growing jaws and the occlusion of the teeth than the tongue function during swallowing or speaking.[8] Specifically, the total time of swallowing and speaking is too short to affect the equilibrium of the forces acting on the teeth and the growth of jaws. The resting tongue with its tone and pressure on the adjacent structures represents one of the most important long-acting forces in the orofacial region. It has a great impact on the dentoalveolar development, dental occlusion, orofacial functions, the need for orthodontic treatment, and the posttreatment stability of the dental occlusion.[3,10] An incorrect tongue posture has long been reported as a primary etiologic factor in the development of malocclusion, including AOB and articulation disorders.[9,11]

The clinical evaluation of the tongue resting posture is routinely performed during clinical examination by ear, nose and throat (ENT) specialists and maxillofacial surgeons treating patients with clefts or orthognatic problems as well as by the orthodontists. However, clinical assessment of the tongue posture at rest without influencing and disturbing its natural posture is highly subjective in small growing children due to anatomical limitations.[8] Despite its subjectivity, it remains the golden standard in clinical practise. There have been no reports in the literature on the reliability of clinical assessment of the resting tongue posture by different professionals for the same group of children.

Three-dimensional ultrasonographic (3DUS) assessment of the tongue became recently an important tool for imaging tongue size, shape and posture, recording functional tongue movements during swallowing, feeding and speech.[12-16] With the use of 3DUS the objective resting tongue posture can be displayed even in preschool children.

The aim of the study was to present functional diagnostics using 3DUS assessment of resting tongue posture in comparison to its clinical assessment, and the associations between the improper tongue posture, and AOB, orofacial, otorhinolaryngological characteristics, and articulation disorders in preschool children.

Patients and methods

The study protocol was approved by the Republic of Slovenia National Medical Ethics Committee (protocol No. 96/04/13). The parents of all included children signed an informed consent for their and their children participation in the study.

Patients

In the first part of the survey the prevalence of AOB and articulation disorders was established by a cross-sectional epidemiological study in children attending kindergartens in municipality Tolmin. In total, 446 preschool children (236 boys, 211 girls), aged 3 to 7 years, were included.

The children with AOB (AOB group) and their parents were invited to participate in the second part of the study. The control group was recruited from the rest of the examined children without AOB. Seventy children without AOB were randomely selected and invited to further participate in the study as control group.

Patient examination procedures

In the first part of the study, all children were examined by the same orthodontist (SLK) during the kindergarten visits to detect AOB and articulation disorders. The parents gave their assessment of nasal breathing, possible articulation disorders and the necessity for speech therapy in their children.

In the second part of the study, all AOB and control group children were examined at the orthodontic clinic of the Community Dental Health Centre (Tolmin, Slovenia). During the intraoral examination the dental status, functional and morphological malocclusions were registered accord-

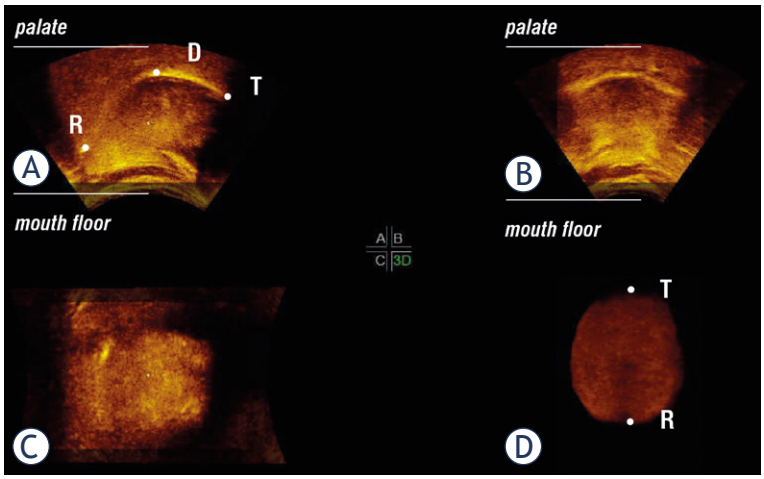

FIGURE 1. The US images of the child's resting tongue posture on the palate: sagittal view **(A)**; antero - posterior (transverse) view **(B)**; vertical view **(C)**; 3D reconstruction of the tongue showing a convexity of the tongue dorsum **(D)**.

D = Dorsum, R = Radix, T = Tip of the tongue

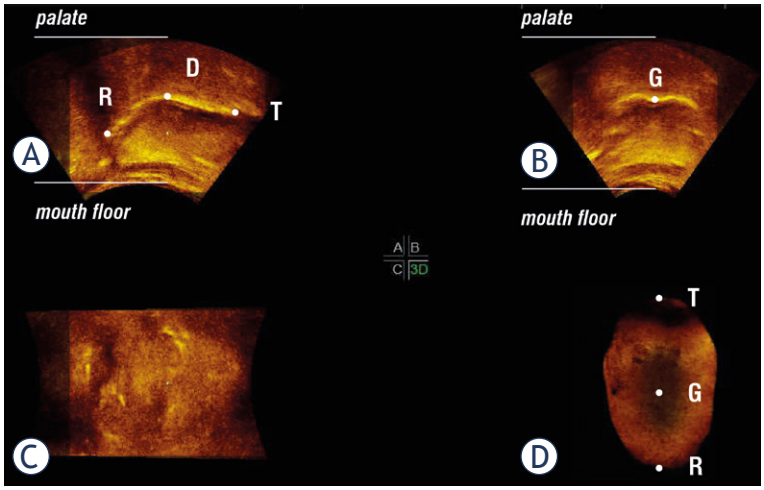

FIGURE 2. The US images of the child's resting tongue posture on the floor of the mouth: sagittal view **(A)**; anteroposterior (transverse) view **(B)**; vertical view **(C)**; 3D reconstruction of the tongue **(D)** showing a a central groove (G) on the tongue dorsum.

D = Dorsum, R = Radix, T = Tip of the tongue

ing to the method by Ovsenik *et al*.[8] Alginate impressions and wax bite registrations were obtained and dental casts were prepared in the ortholab for documentation. The tongue posture at rest was recorded.

All AOB and control group children were examined by an experienced ENT specialist (IHB) and a speech therapist (AJ). The clinical ENT examination was performed with special emphasis on the resting tongue posture. In the case of an upper respiratory infection, the child was reinvited for the examination when he/she was healthy.

The speech therapist performed a three-position test for articulation disorders and registered possible articulation disorders.

Three-dimensional US examination

The children from both groups were invited for a 3DUS examination of the tongue posture by an experienced radiologist (MMM), Institute of Oncology in Ljubljana, with the use of the ultrasound system Voluson 730 Expert (General Electrics Healthcare, Kretztechnik, Zipf Austria) with a 3D convex transducer (RAB 2–5 MHz, GEH). Each child was seated in the dental chair, head positioned in the Frankfort horizontal line, parallel to the floor, and fixed with a strap. The 3D convex tranducer was coated with an aqueous contact transmission gel and positioned on the skin of the mouth floor in the midsagittal line. Each child was asked to be relaxed and to remain still for 15 seconds; no instructions were given for the tongue posture. The recording procedure was repeated twice, using the following parameters: 55-65-degree view, mechanical index 0.8, thermical index 0.3. The acquired data were transferred to a personal computer and visualized using the 4D View software version 5.0 (General Electrics Healthcare, Waukesha, Wisconsin). Referential 3D reconstructions obtained from 10 children without malocclusion in deciduous dentition were then used to compare the tongue posture for each child according to the method presented by Volk *et al*.[17]

The correct resting tongue posture was recorded when the tip of the tongue was on the palate behind the upper incisors (Figure 1). In the improper resting tongue posture, the 3DUS displayed the tip of the tongue to be low on the mouth floor (Figure 2) according to the method by Volk *et al*.[17] The US image of the tongue on the palate showed convexity of its dorsum (Figure 1), while when on the mouth floor the tongue dorsum showed a distinctive concavity with a central groove (Figure 2).

Statistical analysis

All the collected data were analysed using the R statistical package (www.R-project.org). The data were analysed and compared using χ^2-test or Fisher's exact test, t-test or nonparametric Mann-Whitney test. The multiple logistic regression model was used for the assessments of factors possibly associated with AOB. The results of the

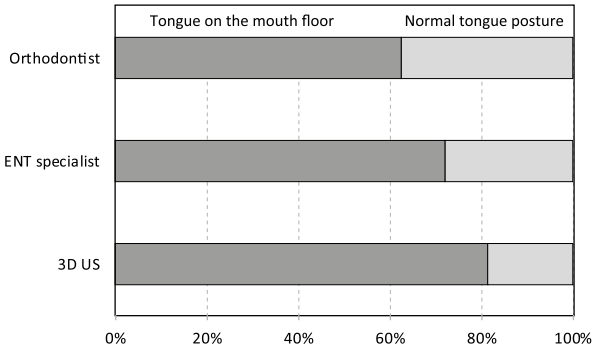

FIGURE 3. Comparison of the assessment of the resting tongue posture by the clinical orthodontic examination, clinical ENT examination, and 3DUS examination in the AOB children.

clinical assessment of the resting tongue posture performed by an orthodontist and an ENT specialist were compared with the results of US imaging using McNemar's test. The reliability of the clinical evaluation was calculated. The level of statistical significance was set at 0.05, and 95% confidence intervals were used.

Results

AOB was found in 32 subjects (7.2%). The comparison of the general data and the parents' assessment of possible child's articulation disorders for the AOB children and the rest of the pediatric population without AOB are presented in Table 1. There were significant differences between the groups in the occurrence of articulation disorders, and necessity for speech therapy.

The parents of 61.4% children out of the 70 randomly selected were willing to allow them to participate in the second part of the study. Thus, the control group consisted of 43 children.

All AOB and control group children underwent further examinations by the orthodontist, the ENT specialist, the speech therapist and the radiologist. The orthodontist found improper tongue posture on the floor of the mouth in 20 (62.5%) children from the AOB group, and in 9 (20.9%) children from the control group.

During the ENT examination, 12 AOB children and 14 control group children were found to have an upper airway infection. They were invited again for the examination three weeks later. All AOB children and only two control group children had a control ENT examination. Therefore, the findings of the ENT examination of the AOB group could only be considered for further analysis. In the AOB group, the ENT examination detected low tongue posture in 23 subjects (71.8%), incompetent lip closure in 22 subjects (68.8%), nasal breathing impairment in 19 subjects (59.4%), and hypertrofic adenoid/status post adenoidectomy in 17 subjects (53.1%).

The 3DUS assessment of the resting tongue posture showed the improper tongue posture on the mouth floor in 81.3% of the AOB children and in 25.6% of the control group children. When the results of the US-assessed tongue posture (26 children with improper posture) were compared with the ENT clinical assessment (23 subjects with improper posture) and clinical orthodontic assessment (20 children with improper posture), no significant differences were detected ($p = 0.549$ and $p = 0.180$, respectively; Figure 3).

The speech therapist and orthodontist found articulation disorders in 84.4% of AOB children and in 23.2% of control group children. In the AOB group, the most frequently detected articulation disorders were sigmatism (present in 25 children) and rhotacism (present in 16 children). Sixteen children had multiple articulation disorders. In the control group, there were 8 children with sigma-

TABLE 1. Comparison of the general data and the parents' assessment of the child's nasal breathing, the possible articulation disorders and the necessity for speech therapy between the group of children with anterior open bite (AOB) (N = 32) and the rest of the pediatric population without anterior open bite (N = 414)

Parameter	AOB (N = 32)	Without AOB (N = 414)	P
Age (years)1	4.9 (1.0)	5.0 (0.9)	0.548
Nasal breathing, day2	31 (96.9%)	348 (84.1%)	0.056
Nasal breathing, night	29 (90.6%)	350 (84.5%)	0.382
Articulation disorder (parental assessment)	27 (84.4%)	108 (26.1%)	< 0.001
Necessity for speech therapy	13 (40.6%)	99 (23.9%)	0.018

[1] For numerical variables mean and SD are given; [2] for categorical number and percentage

tism and 6 children with rhotacism; 7 children had multiple articulation disorders.

In the AOB group and control group together, there were 37 children with articulation disorders. Among them there were 31 children with resting tongue posture on the floor of the mouth. In 38 children without articulation disorders, there were only 6 children with improper resting tongue posture ($p < 0.001$).

Table 2 compares the AOB and the control group children with respect to the general data, the resting posture of the tongue and the occurrence of articulation disorders detected by orthodontist and speech therapist. There was a significant difference between the groups in age, resting tongue posture, and occurence of articulation disorders.

There was a significant difference in age between the AOB group and control group. For further analysis, age adjustment was performed. The significant variables were included into two multiple logistic regression models: model 1 (age, improper tongue posture) and model 2 (age, improper tongue posture, presence of articulation disorders). The results for model 1 showed that the improper resting tongue posture (according to the US examination) and the presence of AOB were associated. The children with the tongue posture on the floor of the mouth had higher odds ratios for the presence of AOB (OR 14.63, 95% CI 4.08–52.39, and $p < 0.001$). When articulation disorders were included (model 2), the odds ratios for the presence of AOB became insignificant for the children with improper resting tongue posture (OR 3.16, 95% CI 0.59–16.79, and $p = 0.177$). This was likely a consequence of a strong association between the tongue posture and articulation disorders. Apparently, it is the presence of articulation disorders, strongly associated with improper tongue posture, that has the most significant correlation with the presence of AOB (OR 13.79, 95% CI 2.56–74.23, and $p = 0.002$).

Discussion

Clinical examination of the tongue posture and function is an important part of functional diagnostics in orthodontics and dentofacial orthopaedics as well as in the field of ENT. However, it is difficult to get objective findings of tongue posture during clinical examination in small children because of their cooperation and anatomical characteristics of the orofacial area.[17]

According to Graber *et al*.[18] the assessment of tongue posture during clinical examination should be performed in the physiological resting position of the mandible and the examiner should slightly open the lips of the examinee to register the posture of the tongue in the oral cavity. However, even a slightest touch of the lips could represent a stimulus for the examinee to drop the tongue to the mouth floor and in the direction of the touched lips.[16,19]

Many studies investigated tongue function during swallowing and speech by using radiocinematography,[20,21] magnetic resonance,[22] and 2-dimensional ultrasonography,[19,23] while tongue posture has been evaluated by using lateral cephalograms and computed tomography.[24] The disadvantage of these diagnostic procedures is radiation exposure, which contraindicates these methods to be used in small still growing children and disables frequent repetitions of the proposed methods. Ultrasonography is a noninvasive method and is widely used in many fields in medicine, obstetrics, gynecology, perinatology, and pediatrics.[25-27] Three-dimensional ultrasonography greatly improved and nowadays permits acquisition of high resolution images. It was also used in the studies in the orofacial area (e.g. in adult patients after partial resection of the tongue).[28,29] However, data about 3D surface morphology of anatomically normal but diversely postured tongues at rest in growing children have only been performed in the field of orthodontics.[17]

TABLE 2. Comparison of the general data, ultrasound-assessed resting tongue posture, and the prevalence of articulation disorders between the anterior open bite group (N = 32) and the control group (N = 43)

Parameter	AOB group (N = 32)	Control group (N = 43)	p
Male gender[1]	17 (53%)	20 (46%)	0.571
Age (years)[2]	4.9 (1.0)	4.3 (0.3)	< 0.001
Articulation disorder (speech therapist's assessment)	27 (84%)	10 (23%)	< 0.001
Improper resting tongue posture (3DUS)	26 (81%)	11 (26%)	0.001

[1] For categorical variables number and percentage is given; [2] for numerical mean and SD. AOB = anterior open bite; 3D US = three-dimensional ultrasound

In the present study, 3D ultrasonography was used for the first time in the assessment of tongue posture in the early stage of growth and development in preschool children with articulation disorders and AOB. Furthermore, in this study the clinical assessment of the tongue posture under standard conditions was performed independently by two different specialists, the experts in functional diagnostics of the orofacial area, by the ENT specialist and by the orthodontist. Their assessments were compared to the 3DUS examination performed by an experienced radiologist. The results of all three examiners using different methods were found to be in agreement (Mc Nemar's test, $p = 0.180$ and $p = 0.549$, respectively) (Figure 3). However, the 3DUS method objectively revealed the largest number of children with low tongue posture, which proved the validity of this diagnostic tool. To the best of our knowledge, this study was the first one to evaluate the reliability between the clinical ENT and orthodontic assessment of the tongue posture, and compared to the 3DUS assessment.

With the use of 3DUS, 81.2% of the children with AOB were found to have improper tongue posture on the mouth floor, while in the control group subjects, the irregular tongue posture was registered only in 25.6% of the examined children (McNemar's test, $p < 0.001$). The interpretation of our findings confirmed that improper tongue posture on the mouth floor is prevalent in children with AOB.

Furthermore, the present study found similar results of the irregular tongue posture in control group subjects (25,6 %) without malocclussion as reported previously in the study by Volk *et al*.[17] The two studies demonstrated very clearly that 3DUS can be used for the assessment of tongue posture in growing children. The main advantage of the 3DUS method is its non-invasive character, which enabels that repetitions of the examination can frequently be performed.

The results suggested that besides the known risk factors (long bottle feeding, finger sucking) the resting tongue posture on the mouth floor is crucial for the development of AOB. The important factors for the development of AOB can be impaired nasal breathing and enlarged adenoids which were detected in almost two thirds of the AOB group. Unfortunately, a comparison with the control group was not possible because a considerable number of children from control group had upper airway infection at the time of ENT examination. The oedema of the nasal mucosa and the size of adenoids as a consequence of viral infection influenced the patency of the nose, possibility of nasal breathing, lip closure and resting posture of the tongue in the oral cavity. Therefore, the signs of the infection prevented a comparison of the AOB group and control group at the time when the ENT examination took place.

On the other hand, when we compared the data on child's nasal breathing during day according to the parents' report between the children with AOB and the other children without AOB, the difference was close to the significant values. This result suggested that the cause for improper tongue posture might be an insufficient patency of the nose in the time of jaws' development resulting in a malocclusion.

The majority of the children with AOB (84.4%) had articulation disorders in comparison to the control group children (23.2%). One of the reasons for such a high number of children with articulation disorders may be a result of individual stage of growth and development of articulation. At the age of 5-6 years late maturation articulation disorders can still be observed.[11] However, when children from both groups were observed, the children without articulation disorders had a statistically significantly lower percentage of the improper tongue posture (15.8%) than the children with articulation disorders (83.8%). This strong association between AOB, improper resting tongue posture, and articulation disorders was found to be one of the main clinically relevant results of this study. It can therefore be concluded that these factors are important risk factors for articulation disorders of the sounds performed in the anterior part of the mouth.

From this point of view, a precise functional diagnostics is very important in the assessment of early treatment needs for AOB in the deciduous dentition in order to implement interceptive and preventative actions, and to provide optimal balanced condition in the oral cavity for proper articulation development.

The 3DUS assessment of tongue posture was found to be an important and valuable tool for the objective assessment of resting tongue posture not only in the etiology of malocclusion and articulation disorders, but also to further objectify the efficiency of early orthodontic treatment, assessment of the success of treatment, and consequently to evaluate successful long-term oral rehabilitation. The main advantage of the proposed method is its non-invasive character. 3DUS proved to be the most valid and reliable method to assess improper resting tongue posture as it most objectively identified the highest number of children with improper resting posture of the tongue in the oral cavity. From

the clinician's point of view, it is also relatively simple, quick, repeatable and child-friendly method.

Conclusions

This study demonstrated that 3DUS is an objective, reliable, non-invasive, radiation free, non time-consuming, and child-friendly diagnostic tool for the assessment of tongue posture in small children. Furthermore, 3DUS identified the highest number of incorrect tongue postures, which was highly related to articulation disorders in preschool children with malocclusion. Therefore, every clinical examination of orofacial functions in preschool children should be focused on proper resting tongue posture. The child and his/her parents should get the early information about the correct resting tongue posture in the mouth. In this way, an optimal condition in the oral cavity for proper tongue maturation and articulation development can be created.

The 3DUS was found to be the most objective method to identify tongue posture in growing children and could become in the future an important tool in functional diagnostics in radiology, ENT as well as in orthodontics and dentofacial orthopedics.

Acknowledgments

The authors would like to thank Dr Alexei Zhurov and Dr Greg Huang for their valuable comments and suggestions that helped to improve this paper. This work was financially supported from the state budget by the Slovenian Research Agency [Grants: P3-0374; P3-0289; P3-0307].

References

1. Ballanti F, Franchi L, Cozza P. Transverse Dentoskeletal Features of Anterior Open Bite in the Mixed Dentition A Morphometric Study on Posteroanterior Films. *Angle Orthod* 2009; **79:** 615-20. doi: 10.2319/071808-375.1
2. Mucedero M, Fusaroli D, Franchi L, Pavoni C, Cozza P, Lione R. Long-term evaluation of rapid maxillary expansion and bite-block therapy in open bite growing subjects: A controlled clinical study. *Angle Orthod* 2018 88: 523-9. doi: 10.2319/102717-728.1
3. Proffit WR. Equilibrium theory revisited: factors influencing position of the teeth. *Angle Orthod* 1978; **48:** 175-86. doi: 10.1043/0003-3219(1978)048 < 0175:ETRFIP>2.0.CO;2
4. Greenlee GM, Huang GJ, Chen SSH, Chen JD, Koepsell T, Hujoel P. Stability of treatment for anterior open-bite malocclusion: A meta-analysis. *Am J Orthod Dentofac* 2011; **139:** 154-69. doi: 10.1016/j.ajodo.2010.10.019
5. Ngan P, Fields HW. Open bite: a review of etiology and management. *Pediatr Dent* 1997; **19:** 91-8.
6. Silvestrini-Biavati A, Salamone S, Silvestrini-Biavati F, Agostino P, Ugolini A. Anterior open-bite and sucking habits in Italian preschool children. *Eur J Paediatr Dent* 2016; **17:** 43-6.
7. Zuroff JP, Chen SH, Shapiro PA, Little RM, Joondeph DR, Huang GJ. Orthodontic treatment of anterior open-bite malocclusion: Stability 10 years postretention. *Am J Orthod Dentofac* 2010; **137:** doi: 10.1016/j.ajodo.2009.06.020
8. Ovsenik M. Incorrect orofacial functions until 5 years of age and their association with posterior crossbite. *Am J Orthod Dentofac* 2009; **136:** 375-81. doi: 10.1016/j.ajodo.2008.03.018
9. Johnson NCL, Sandy JR. Tooth position and speech - is there a relationship? *Angle Orthod* 1999; **69:** 306-10. doi: 10.1043/0003-3219(1999)069 < 0306:tpasit>2.3.co;2
10. Stahl F, Grabowski R, Gaebel M, Kundt G. Relationship between occlusal findings and orofacial myofunctional status in primary and mixed dentition - Part II: Prevalence of orofacial dysfunctions. *J Orofac Orthop* 2007; **68:** 74-90. doi: 10.1007/s00056-007-2606-9
11. Farronato G, Giannini L, Riva R, Galbiati G, Maspero C. Correlations between malocclusions and dyslalias. *Eur J Paediatr Dent* 2012; **13:** 13-8.
12. Barbič U, Verdenik I, Marolt Mušič M, Ihan Hren N. Three - dimensional ultrasound evaluation of tongue volume. *Zdrav Vest* 2016; **85:** 228-36. doi: 10.6016/ZdravVestn.1477
13. Hiiemae KM, Palmer JB. Tongue movements in feeding and speech. *Crit Rev Oral Biol Med* 2003; **14:** 413-29. doi: 14/6/413 [pii]
14. Moss JP. The use of three-dimensional imaging in orthodontics. *Eur J Orthod* 2006; **28:** 416-25. doi: 10.1093/ejo/cjl025
15. Ovsenik M, Volk J, Marolt MM. A 2D ultrasound evaluation of swallowing in children with unilateral posterior crossbite. *Eur J Orthodont* 2014; **36:** 665-71. doi: 10.1093/ejo/cjt028
16. Peng CL, Jost-Brinkmann PG, Yoshida N, Miethke RR, Lin CT. Differential diagnosis between infantile and mature swallowing with ultrasonography. *Eur J Orthodont* 2003; **25:** 451-6. doi: 10.1093/Ejo/25.5.451
17. Volk J, Kadivec M, Music MM, Ovsenik M. Three-dimensional ultrasound diagnostics of tongue posture in children with unilateral posterior crossbite. *Am J Orthod Dentofacial Orthop* 2010; **138:** 608-12. doi: 10.1016/j.ajodo.2008.12.028.
18. Graber TM, Rakosi T, Petrovic AG. *Dentofacial orthopedics with functional appliances.* St. Louis: Mosby; 1985.
19. Peng CL, Jost-Brinkmann PG, Yoshida N, Chou HH, Lin CT. Comparison of tongue functions between mature and tongue-thrust swallowing - an ultrasound investigation. *Am J Orthod Dentofac* 2004; **125:** 562-70. doi: 10.1016/j.ajodo.2003.06.003
20. Ekberg O, Hillarp B. Radiologic Evaluation of the Oral Stage of Swallowing. *Acta Radiol Diagn (Stockh)* 1986; **27:** 533-7. doi: 10.1177/028418518602700508
21. Fujiki T, Inoue M, Miyawaki S, Nagasaki T, Tanimoto K, Takano-Yamamoto T. Relationship between maxillofacial morphology and deglutitive tongue movement in patients with anterior open bite. *Am J Orthod Dentofac* 2004; **125:** 160-7. doi: 10.1016/j.ajodo.2003.03.009
22. Lauder R, Muhl ZF. Estimation of Tongue Volume from Magnetic-Resonance-Imaging. *Angle Orthod* 1991; **61:** 175-84. doi: 10.1043/0003-3219(1991)061 < 0175:eotvfm>2.0.co;2
23. Peng CL, Jost-Brinkmann PG, Miethke RR, Lin CT. Ultrasonographic measurement of tongue movement during swallowing. *J Ultras Med* 2000; **19**: 15-20.
24. Lowe AA, Fleetham JA, Adachi S, Ryan CF. Cephalometric and computed tomographic predictors of obstructive sleep-apnea severity. *Am J Orthod Dentofac* 1995; **107:** 589-95. doi: Doi 10.1016/S0889-5406(95)70101-X
25. De Candia A, Como G, Passon P, Pedace E, Bazzocchi M. Sonographic findings in glomus tympanicum tumor. *J Clin Ultrasound* 2002; **30:** 236-40. doi: 10.1002/jcu.10058
26. Pavcec Z, Zokalj I, Saghir H, Pal A, Roic G. *Doppler ultrasound in the diagnosis and follow-up of the muscle rupture and an arteriovenous fistula of the thigh in 12 year boy. Radiol Oncol* 2006; **40:** 211-5.
27. Vegar-Zubovic S, Lincender L, Dizdarevic S, Sefic I, Dalagija F. Ultrasound signs of acute appendicitis in children - clinical application. *clinical application. Radiol Oncol 2005;* **39:** 15-21+82.
28. Bressmann T, Ackloo E, Heng CL, Irish JC. Quantitative three-dimensional ultrasound imaging of partially resected tongues. *Otolaryng Head Neck* 2007; **136:** 799-805. doi: 10.1016/j.otohns.2006.11.022
29. Bressmann T, Thind P, Uy C, Bollig C, Gilbert RW, Irish JC. Quantitative three-dimensional ultrasound analysis of tongue protrusion, grooving and symmetry: Data from 12 normal speakers and a partial glossectomee. *Clin Linguist Phonet* 2005; **19:** 573-88. doi: 10.1080/02699200500113947

research article

Prevalence of papillary thyroid cancer in subacute thyroiditis patients may be higher than it is presumed: retrospective analysis of 137 patients

Nurdan Gül[1], Ayşe Kubat Üzüm[1], Özlem Soyluk Selçukbiricik[1], Gülçin Yegen[2], Refik Tanakol[1], Ferihan Aral[1]

[1] Division of Endocrinology and Metabolism, Department of Internal Medicine, Istanbul Faculty of Medicine, Istanbul University, Istanbul, Turkey

[2] Department of Pathology, Istanbul Faculty of Medicine, Istanbul University, Istanbul, Turkey

Radiol Oncol 2018; 52(3): 257-262.

Received 12 March 2018
Accepted 12 July 2018

Correspondence to: Nurdan Gül, M.D., Istanbul Faculty of Medicine, Department of Internal Medicine, Division of Endocrinology and Metabolism, 34093 Fatih, Istanbul, Turkey. Phone: +90 212 4142000/32735; Fax: +90 212 5232891; E-mail: nurdan.gul@istanbul.edu.tr

Disclosure: No potential conflicts of interest were disclosed.

Background. The association of subacute thyroiditis (SAT) and papillary thyroid carcinoma is a rare finding. In this study, we aimed to investigate the prevalence of differentiated thyroid cancer in a cohort of patients followed with the diagnosis of SAT.

Patients and methods. We retrospectively screened medical records of Endocrinology and Metabolism outpatient clinic in the past 20 years for patients with SAT. Patients with nodules and suspicious ultrasonography findings who underwent fine needle aspiration biopsy (FNAB) and operated due to malignancy risk were identified.

Results. We identified 137 (100 females, 37 males) patients with reliable records to confirm the diagnosis of SAT. The mean age of female patients was 41.1 ± 9.1 (range, 20–64) and of male patients was 43.0 ± 9.3 (range, 20–65). One or more FNAB was performed in 23 of the patients (16.8%) at the beginning and/or during the follow-up period when needed. Seven patients with suspicious FNAB findings were operated, and histopathological examination of the nodules confirmed the diagnosis of papillary thyroid carcinoma in 6 patients (4.4%).

Conclusions. Our observations suggesting a relatively higher prevalence of thyroid cancer in a small series of SAT patients warrant further studies to identify the real frequency of differentiated thyroid cancer and its association with inflammatory pathogenesis of SAT. This finding is compatible with the trend of increased thyroid cancer incidence all over the world. A repeat ultrasonography after resolution of clinical and inflammatory findings, and FNAB should be recommended to all patients with suspicious nodules.

Key words: subacute thyroiditis; thyroid nodule; thyroid cancer; ultrasonography

Introduction

Subacute thyroiditis (SAT) is a self-limited, granulomatous inflammatory disorder of the thyroid gland. The diagnosis of SAT is based on the clinical findings including fever, pain and tenderness in the thyroid gland and laboratory findings of acute phase response such as elevated C-reactive protein (CRP) and erythrocyte sedimentation rate (ESR), elevated free T4 (fT4) and decreased thyroid stimulating hormone (TSH) concentrations in serum.[1] The scintigraphy findings and/or low 24 h radioiodine uptake results are also used to confirm the diagnosis.[1]

Although it is not necessary for diagnosis of SAT, most of the patients undergo an ultrasound imaging of the thyroid gland, and the presence of typical thyroiditis findings support the diag-

nosis.[2-4] Thyroid ultrasonography is currently the most sensitive method to detect the presence of nodules in the thyroid, which is a common and usually benign disorder. Among persons without suspected thyroid disease, the frequency of thyroid nodules detected by ultrasound is ranging between 19% to 67%.[5] Ultrasonographic features of the nodules may give important clues in terms of their potential for malignancy[5,6], and about 8% to 16% of the nodules can be documented as malignant.[5]

There are very few studies reporting the prevalence of thyroid cancer in patients with SAT.[1,7-10] In addition to the findings compatible with thyroiditis, ultrasonographic examination of the patients with SAT may also reveal thyroid nodules incidentally. In some patients, pseudo-nodules seen in association with thyroiditis, which cannot be distinguished easily from malignant nodules with irregular margins; and a close follow-up in parallel with the resolution of inflammatory findings of SAT may be helpful in differential diagnosis.

In this study, we aimed to investigate the prevalence of differentiated thyroid cancer in a cohort of patients followed with the diagnosis of SAT.

Patients and methods

We retrospectively screened available medical records of Endocrinology and Metabolism outpatient clinic archive in the past 20 years for patients with SAT. To confirm the diagnosis of SAT from the charts, we re-evaluated their records for the clinical findings compatible with the diagnosis such as fever, painful or tender thyroid gland, laboratory findings of acute phase response such as elevated ESR (>20 mm/hour) and/or serum CRP levels (>5 mg/L), thyroid function tests such as elevated serum fT4 and decreased serum TSH, compatible thyroid scintigraphy findings and decreased 24 h radioiodine uptake, and when available histopathological evaluation of thyroidectomy material.

Available records of ultrasonographic findings of the patients during follow-up were evaluated, and those patients who underwent fine needle aspiration biopsy (FNAB) and operated due to malignancy risk were identified.

Haematoxylin and eosin stained sections of thyroidectomy specimens of all cases diagnosed with papillary thyroid cancer, except one case who was operated in another hospital, were re-evaluated for this study by one of the authors (GY) to confirm the diagnosis of thyroid cancer according to the WHO 2017 classification of thyroid tumors; and histopathological changes of the non-tumoral thyroid tissue were also evaluated for the subacute thyroiditis associated findings.

The study adhered to the tenets of the Declaration of Helsinki and was submitted and approved by Institution Ethical Committee. All data were recorded using a standard form.

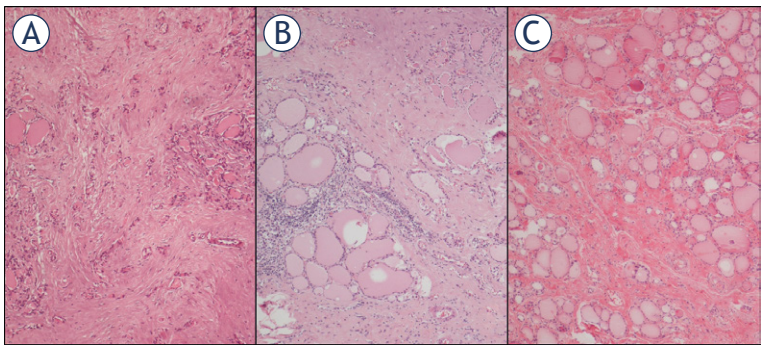

FIGURE 1. Haematoxylin and eosin stained sections of Case 4 **(A)**, Case 5 **(B)** and Case 6 **(C).** Follicular atrophy and fibrosis, fibrosis accompanied by chronic inflammatory cells and fibrosis are seen, respectively.

Results

We screened the records of the 9156 charts, which included 4757 patients with a thyroid disease, including 699 with Graves disease, 658 with Hashimoto thyroiditis and 2453 with papillary thyroid cancer. Among these 4757 patients with thyroid disease, we identified 137 (100 females, 37 males) patients with reliable records to confirm the diagnosis of SAT. The mean age of female patients was 41.1 ± 9.1 (range, 20–64) and of male patients was 43.0 ± 9.3 (range, 20–65).

One or more FNAB was performed in 23 of the patients with SAT (16.8%) at the beginning and/or during the follow-up period when needed according to the ultrasonography findings suspicious for thyroid malignancy. Because of cytological examination, 7 out of 23 patients with suspicious FNAB findings underwent thyroidectomy, and histopathological examination of the nodules confirmed the diagnosis of papillary thyroid carcinoma in 6 patients (4.4%).

In one of the operated 7 patients (54-year-old, female), diagnosis of SAT was done after the pathological evaluation of thyroidectomy material. She had been previously followed for hyperthyroidism at another center, and she was referred to our center for operation because of the nodules with suspicious ultrasonographic findings and FNAB findings, which were reported as suspicious for papillary carcinoma. Histopathological examina-

TABLE 1. Demographic characteristics and laboratory findings at disease onset of patients with subacute thyroiditis and papillary thyroid cancer

Cases	Age	Sex	FT3 (pmol/L) (3.1–6.8)	FT4 (pmol/L) (12–22)	TSH (mIU/L) (0.27–4.2)	CRP (mg/L) (0–5)	ESR (mm/h) (0–20)	*Tc 99m /RAI Uptake (%) (0.3–3 vs. 20–50)	Ultrasonography
1	42	F	NA	19.9	0.2	NA	55	Low/0.2	3.2 cm hypoechoic nodule
2	56	F	6.73	26.3	0.009	NA	34	0.06/1.35	Diffuse HEAs, 2.2 cm hypo-isoechoic nodule
3	56	F	4.5	21.1	0.68	125.0	100	0.59/NA focal hypoactivity	1.8 cm focal HEA, 0.7 cm hypoechoic nodule with microcalcification
4	51	M	NA	44.2	0.01	NA	91	Low/NA	Focal HEAs, 1.6 cm isoechoic nodule
5	52	F	7.01	24.7	0.02	15.6	60	Low/NA	2.4 cm heterogenous nodule with calcification and 1.1 cm isoechoic nodule
6	45	F	13	45	0.005	138.8	132	Low/NA	2.2 cm hypoechoic, 1.9 cm isoechoic nodules

CRP =C-reactive protein; ESR = erythrocyte sedimentation rate; F = female; FT3 = free triiodothyronine; FT4 = free thyroxine; HEA = hypoechogenic area; M = male; NA, not available; RAI = radioactive iodine; Tc 99m = Technetium-99m; TSH = thyroid-stimulating hormone

* All of the patients had Technetium-99m scintigraphy, additionally some of them had either Technetium- 99m uptake or 24-h RAI uptake.

tion revealed colloid nodules, chronic lymphocytic thyroiditis as well as findings of subacute thyroiditis including granulomatous thyroiditis. There was no evidence of malignancy, and retrospective evaluations revealed only elevated acute phase response but no clinical findings related to SAT such as neck pain or fever.

Demographic characteristics and laboratory findings of the remaining six patients with papillary thyroid carcinoma at the time of diagnosis of SAT are given in Table 1; and their presurgical ultrasonographic findings and histopathologic features are summarized in Table 2.

Three of the 137 patients with SAT and papillary thyroid cancer described a positive family history for papillary thyroid cancer. Case 3 and Case 5 were first cousins, and the elderly sister of Case 3 was also diagnosed with SAT, and her father had a history of thyroid cancer diagnosed elsewhere.

Another patient (Case 1) described a positive family history for papillary thyroid cancer in her elderly brother. She was diagnosed with acromegaly and papillary cancer during the follow-up period, about 9 years after the diagnosis of SAT. She was first operated for thyroid nodule following findings of FNAB compatible with papillary thyroid cancer. She was later operated for acromegaly by endoscopic trans-sphenoidal pituitary surgery, which resulted in remission.

In four of the patients, the tumor size was ≤1cm and the remaining two patients had multifocal thyroid cancers with only one focus >1cm (the largest tumor diameter was 1.1 cm and 1.2 cm, respectively).

Non-tumoral thyroid tissue findings were summarized in Table 2. Patients underwent thyroidectomy 35.8 ± 36.2 (range, 13–107) months after SAT diagnosis (Table 2). Re-examination of all cases except Case 2, who was operated at another center, revealed findings of focal fibrosis. Case 1 and Case 5 had additional findings of chronic inflammation. In Case 4, focal follicular atrophy was also observed. No evidence of granulomatous or acute inflammation was seen in the investigated samples.

Another patient who underwent FNAB twice was still being followed-up closely, since his first biopsy was suspicious and the second biopsy was considered as benign.

Discussion

This retrospective investigation of 137 patients with confirmed diagnosis of SAT revealed 6 patients (4.4%) with papillary thyroid carcinoma. The association of SAT and thyroid carcinoma is a very rare finding, and they were usually published as case reports.[1,7-12] The most comprehensive study on this subject is the work of Nishihara *et al.* in Japanese patients with SAT.[8] In this study, 5 papillary thyroid carcinomas were detected in 1152 cases (0.4%) of SAT. Another study conducted with data of 160 SAT patients from Olmsted County, Minnesota, USA documented no thyroid cancer.[1] In this study a subgroup of 94 patients were followed-up for 28 years, which revealed 11.4% cumulative malignancy rate, but none of them had thyroid cancers.[1]

TABLE 2. Presurgical ultrasonographic findings and histopathologic features of subacute thyroiditis patients with papillary thyroid cancer

Cases	Op. Time (mo)	Nodule size in USG (cm)*	Sonographic features of nodules	FNAB	Tumor subtype/Histology	Tumor size (cm)	Stage (8th TNM)	Treatment
1	107	0.55 and 0.50	Hypoechoic, indefinite margins	Suspicious for malignancy	Papillary-tall cell and classical Focal fibrosis	0.5 and 0.05	I	TT+RAI
2	13	2.4 and 1.0	Hypo-isoechoic, calcification	Dyskaryotic thyrocytes	Papillary-classical Chronic lymphocytic thyroiditis	1.0	I	TT+RAI
3	29	0.7	Hypoechoic, microcalcification	FLUS Suspicious for malignancy	Papillary-follicular variant Fibrosis, chronic lymphocytic thyroiditis	0.6	I	TT
4	16	1.9	Isoechoic	Suspicious for malignancy	Papillary-follicular variant Fibrosis, focal follicular atrophy	0.4	I	Lobectomy
5	13	1.1 and 0.73	Isoechoic, microcalcification	Suspicious for malignancy	Papillary-classical and follicular Fibrosis, chronic lymphocytic thyroiditis	1.1, 0.7, 0.3, 0.2	I	TT+ RAI
6	37	1.7 and 0.9	Hypoechoic and isoechoic	AUS Papillary carcinoma	Papillary-classical and follicular Fibrosis	1.2, 0.3, 0.2	I	TT+RAI

AUS = atypia of undetermined significance; FLUS = follicular lesion of undetermined significance; FNAB = fine needle aspiration biopsy; Op = operation time after the diagnosis of subacute thyroiditis in months; RAI = radioactive iodine; TT = total thyroidectomy; USG = ultrasonography

*In patients with more than two nodules, the sizes of the dominant ones are given.

Relatively high prevalence of papillary thyroid carcinoma in our study may have some explanations. First, the records of our Endocrinology and Metabolism Outpatient Clinic may have biases as a tertiary referral center which lead to the accumulation of refractory cases or of patients requiring advanced care. An important proportion of SAT patients could be managed at the general internal medicine outpatient clinic of our hospital, and 137 out of 9156 screened archive patients being followed at Endocrinology clinic may not represent the whole SAT patients.

In tertiary referral centers, the co-incidence of two or more rare conditions may be seen at higher rates than expected due to Berkson's bias. Similarly, co-incidental conditions may affect the risk of other diseases. One of our patients who underwent total thyroidectomy approximately 9 years after the diagnosis of SAT also had acromegaly and a positive family history for papillary thyroid carcinoma, which are known to be associated with increased thyroid cancer risk.[13-15]

Differences in the prevalence of papillary cancer in various populations may also contribute to the conflicting results. Epidemiological surveys from different regions of Turkey revealed a thyroid cancer incidence rate of 5.5/100,000 in healthy male population and 20.7/100,000 in healthy female population.[16] These rates are compatible with the rates of thyroid cancer reported from other countries including Japan (approximately 5/100,000 in males and 20/100,000 in females) and USA (overall 14.3/100,000, and 6.9/100,000 in males, 21.4/100,000 in females).[17,18] Therefore, it is hard to explain the results of current study with the amount of variability of papillary cancer rates in different countries.

The widespread use of imaging methods is usually considered as an important factor for the current trend all over the world documenting an increase in the incidence of thyroid cancer.[17-22] Increased use of diagnostic imaging procedures results in the identification of previously undiagnosed subclinical thyroid cancers. All our patients were operated after 2008. Therefore, closer follow-up due to another thyroid disease may result in increased diagnosis of sub-centimeter thyroid cancers, which otherwise would not be noticed.

Another explanation for the increased prevalence may be due to environmental factors such as ionizing radiation exposure, which has the strongest association with thyroid cancers. Chernobyl disaster related radioactive dispersion in 1986 affected mainly the North Eastern part of the Black Sea region of Turkey, and this exposure may have a role

on the observed findings.[23-28] Epidemiological surveys provided contradictory results regarding the effects of Chernobyl disaster in Turkey, which happened in an area more than 1500 km away from the shores of Black Sea shores. All but one of our 6 patients lived in cities around the Black Sea and their mean age was 25.2 ± 6.6 (range, 17–35) in 1986. We think that available data do not provide hard evidences associated with Chernobyl disaster for any type of cancer in Turkey within 30 years and it is not possible to draw a conclusive decision for ionizing radiation exposure as a possible etiological factor.

Other environmental factors like cigarette smoking, iodine excess, obesity and endocrine disrupting chemicals may also be associated with the increased thyroid cancer risk.[20] Mandatory iodization of household salt in Turkey after 1999 may also be speculated as an additional environmental factor.[29-31] However no comparative data could be found regarding the risk for thyroid cancer associated with increased iodine uptake following the changes in household salts.

On the other hand, inflammation is one of the most critical components affecting the cancer risk in patients with an inflammatory disorder. Increased rates of papillary cancer were reported in autoimmune thyroid disorders.[32,33] Papillary cancer rate was found 8% in patients with Graves' disease, (13% and 5.4% in those with and without a nodule, respectively) in a study from Turkey.[34] On the other hand, studies in Hashimoto thyroiditis provided conflicting results.[35,36] Within the same context, SAT may also be considered as a risk factor for the development of papillary thyroid cancer by its unique inflammatory changes within the thyroid tissue. Findings of the current study warrant further investigations to understand the dynamics of different inflammatory pathways and associated risk for thyroid cancers.

Lastly, guidelines affect the indications for FNAB in the follow-up of patients with thyroid nodules.[37-38] Two of the patients with nodules <1cm at ultrasonography were evaluated before 2015, and both had a family history for thyroid cancers in first degree relatives. FNAB investigation may not have been performed according to current guidelines since papillary microcarcinomas are considered as clinically not significant.[38] However, one of these patients had a 0.5 cm tall cell variant of papillary microcarcinoma, and this early intervention would be beneficial for her long-term survival.[39,40]

Our work has several limitations. It is a retrospective study, and it lacks some important information. Ultrasonographic examination findings were the main clues for the decision of thyroidectomy, but some of the investigations were performed by different radiologists in different hospitals before being referred to us. Since SAT is a self-limiting disorder, some of the patients lost to follow-up and had no repeated ultrasonographic examinations. However, all these limitations may only lower the possibility of diagnosed patients among this series and cannot explain the relatively higher frequency compared to the Japanese and American series of SAT patients.

Conclusions

In conclusion, our observations suggesting a relatively higher prevalence of thyroid cancer compared to healthy controls in a small series of SAT patients warrant further studies to identify the real frequency of differentiated thyroid cancer and its association with inflammatory pathogenesis of SAT. Considering the possibly increased prevalence rate of thyroid cancer in SAT patients, a repeat ultrasonography after resolution of clinical and inflammatory findings for all patients and FNAB for those with suspicious nodules should be recommended.

References

1. Fatourechi V, Aniszewski JP, Fatourechi GZ, Atkinson EJ, Jacobsen SJ. Clinical features and outcome of subacute thyroiditis in an incidence cohort: Olmsted County, Minnesota, study. *J Clin Endocrinol Metab* 2003; **88:** 2100-5. doi: 10.1210/jc.2002-021799
2. Nishihara E, Amino N, Ohye H, Ota H, Ito M, Kubota S, et al. Extent of hypoechogenic area in the thyroid is related with thyroid dysfunction after subacute thyroiditis. *J Endocrinol Invest* 2009; **32:** 33-6. doi: 10.1007/BF03345675
3. Frates MC, Marqusee E, Benson CB, Alexander EK. Subacute granulomatous (de Quervain) thyroiditis: grayscale and color Doppler sonographic characteristics. *J Ultrasound Med* 2013; **32:** 505-11. doi: 10.7863/jum.2013.32.3.505
4. Lee YJ, Kim DW. Sonographic characteristics and interval changes of subacute thyroiditis. *J Ultrasound Med* 2016; **35:** 1653-9. doi: 10.7863/ultra.15.09049
5. Burman KD, Wartofsky L. Thyroid nodules. *N Engl J Med* 2015; **373:** 2347-56. doi: 10.1056/NEJMcp1415786
6. Russ G, Bonnema SJ, Erdogan MF, Durante C, Ngu R, Leenhardt L. European Thyroid Association guidelines for ultrasound malignancy risk stratification of thyroid nodules in adults: the EU-TIRADS. *Eur Thyroid J* 2017; **6:** 225-37. doi: 10.1159/000478927
7. Lam KY, Lo CY. Papillary carcinoma with subacute thyroiditis. *Endocr Pathol* 2002; **13:** 263-5.
8. Nishihara E, Hirokawa M, Ohye H, Ito M, Kubota S, Fukata S, et al. Papillary carcinoma obscured by complication with subacute thyroiditis: sequential ultrasonographic and histopathological findings in five cases. *Thyroid* 2008; **18:** 1221-5. doi: 10.1089=thy.2008.0096

9. Choia YS, Kima BK, Kwon HJ, Lee JS, Heo JJ, Jung SB, et al. Subacute lymphocytic thyroiditis with coexisting papillary carcinoma diagnosed by immediately repeat fine needle aspiration: a case report. *J Med Cases* 2012; **3:** 308-11.
10. Valentini RB, Macedo BM, Izquierdo RF, Meyer EL. Painless thyroiditis associated to thyroid carcinoma: role of initial ultrasonography evaluation. *Arch Endocrinol Metab* 2016; **60:** 178-82. doi: 10.1590/2359-3997000000104
11. Ucan B, Delibasi T, Cakal E, Arslan MS, Bozkurt NC, Demirci T, et al. Papillary thyroid cancer case masked by subacute thyroiditis. *Arq Bras Endocrinol Metabol* 2014; **58:** 851-4. doi: 10.1590/0004-2730000003222
12. Şenel F, Karaman H, Ertan T. Co-occurrence of subacute granulomatous thyroiditis and papillary microcarcinoma. *Kulak Burun Bogaz Ihtis Derg* 2016; **26:** 248-50. doi: 10.5606/kbbihtisas.2016.36776
13. Gullu BE, Celik O, Gazioglu N, Kadioglu P. Thyroid cancer is the most common cancer associated with acromegaly. *Pituitary* 2010; **13:** 242-8. doi: 10.1007/s11102-010-0224-9
14. dos Santos MC, Nascimento GC, Nascimento AG, Carvalho VC, Lopes MH, Montenegro R, et al. Thyroid cancer in patients with acromegaly: a case-control study. *Pituitary* 2013; **16:** 109-14. doi: 10.1007/s11102-012-0383-y
15. Wolinski K, Stangierski A, Dyrda K, Nowicka K, Pelka M, Iqbal A, et al. Risk of malignant neoplasms in acromegaly: a case-control study. *J Endocrinol Invest* 2017; **40:** 319-22. doi: 10.1007/s40618-016-0565-y
16. Republic of Turkey Ministry of Health. Health Statistics Yearbook 2015 [cited 2017 Nov 15]; Available from: http://ekutuphane.sagem.gov.tr/kitaplar/health_statistics_yearbook_2015.pdf
17. Katanoda K, Hori M, Matsuda T, Shibata A, Nishino Y, Hattori M, et al. An updated report on the trends in cancer incidence and mortality in Japan, 1958-2013. *Jpn J Clin Oncol* 2015; **45:** 390-401. doi: 10.1093/jjco/hyv002
18. Davies L, Welch HG. Current thyroid cancer trends in the United States. *JAMA Otolaryngol Head Neck Surg* 2014; **140:** 317-22. doi: 10.1001/jamaoto.2014.1
19. Morris LG, Sikora AG, Tosteson TD, Davies L. The increasing incidence of thyroid cancer: the influence of access to care. *Thyroid* 2013; **23:** 885-91. doi: 10.1089/thy.2013.0045
20. Kitahara CM, Sosa JA. The changing incidence of thyroid cancer. *Nat Rev Endocrinol* 2016; **12:** 646-53. doi: 10.1038/nrendo.2016.110
21. Morris LG, Tuttle RM, Davies L. Changing trends in the incidence of thyroid cancer in the United States. *JAMA Otolaryngol Head Neck Surg* 2016; **142:** 709-11. doi: 10.1001/jamaoto.2016.0230
22. Wiltshire JJ, Drake TM, Uttley L, Balasubramanian SP. Systematic review of trends in the incidence rates of thyroid cancer. *Thyroid* 2016; **26:** 1541-52. doi: 10.1089/thy.2016.0100
23. Acar H, Cakabay B, Bayrak F, Evrenkaya T. Effects of the Chernobyl disaster on thyroid cancer incidence in Turkey after 22 years. *ISRN Surg* 2011; **2011:** 257943. doi: 10.5402/2011/257943
24. Kocakusak A. Did Chernobyl accident contribute to the rise of thyroid cancer in Turkey? *Acta Endo (Buc)* 2016, **12:** 362-67. doi: 10.4183/aeb.2016.362
25. Emral R, Baştemir M, Güllü S, Erdoğan G. Thyroid consequences of the Chernobyl nuclear power station accident on the Turkish population. *Eur J Endocrinol* 2003; **148:** 497-503.
26. Zengi A, Karadeniz M, Erdogan M, Ozgen AG, Saygili F, Yilmaz C, et al. Does Chernobyl accident have any effect on thyroid cancers in Turkey? A retrospective review of thyroid cancers from 1982 to 2006. *Endocr J* 2008; **55:** 325-30. doi: 10.1507/endocrj.K08E-007
27. Ozdemir D, Dagdelen S, Kiratli P, Tuncel M, Erbas B, Erbas T. Changing clinical characteristics of thyroid carcinoma at a single center from Turkey: before and after the Chernobyl disaster. *Minerva Endocrinol* 2012; **37:** 267-74.
28. Yildiz SY, Berkem H, Yuksel BC, Ozel H, Kendirci M, Hengirmen S. The rising trend of papillary carcinoma in thyroidectomies: 14-years of experience in a referral center of Turkey. *World J Surg Oncol* 2014; **12:** 34. doi: 10.1186/1477-7819-12-34
29. Burgess JR. Temporal trends for thyroid carcinoma in Australia: an increasing incidence of papillary thyroid carcinoma (1982–1997). *Thyroid* 2002; **12:** 141-9. doi: 10.1089/105072502753522374
30. Słowińska-Klencka D, Klencki M, Sporny S, Lewiński A. Fine-needle aspiration biopsy of the thyroid in an area of endemic goiter: influence of restored sufficient iodine supplementation on the clinical significance of cytological results. *Eur J Endocrinol* 2002; **146:** 19-26.
31. Zimmermann MB, Galetti V. Iodine intake as a risk factor for thyroid cancer: a comprehensive review of animal and human studies. *Thyroid Res* 2015; **8:** 8. doi: 10.1186/s13044-015-0020-8
32. Chen YK, Lin CL, Chang YJ, Cheng FT, Peng CL, Sung FC, et al. Cancer risk in patients with Graves' disease: a nationwide cohort study. *Thyroid* 2013; **23:** 879-84. doi: 10.1089/thy.2012.0568
33. Chen YK, Lin CL, Cheng FT, Sung FC, Kao CH. Cancer risk in patients with Hashimoto's thyroiditis: a nationwide cohort study. *Br J Cancer* 2013; **109:** 2496-501. doi: 10.1038/bjc.2013.597.
34. Tam AA, Kaya C, Kılıç FB, Ersoy R, Çakır B. Thyroid nodules and thyroid cancer in Graves' disease. *Arq Bras Endocrinol Metabol* 2014; **58:** 933-8. doi: 10.1590/0004-2730000003569
35. Gul K, Dirikoc A, Kiyak G, Ersoy PE, Ugras NS, Ersoy R, et al. The association between thyroid carcinoma and Hashimoto's thyroiditis: the ultrasonographic and histopathologic characteristics of malignant nodules. *Thyroid* 2010; **20:** 873-8. doi: 10.1089/thy.2009.0118
36. Anil C, Goksel S, Gursoy A. Hashimoto's thyroiditis is not associated with increased risk of thyroid cancer in patients with thyroid nodules: a single-center prospective study. *Thyroid* 2010; **20:** 601-6. doi: 10.1089/thy.2009.0450
37. American Thyroid Association (ATA) guidelines taskforce on thyroid nodules and differentiated thyroid cancer, Cooper DS, Doherty GM, Haugen BR, Kloos RT, Lee SL, et al. Revised American Thyroid Association management guidelines for patients with thyroid nodules and differentiated thyroid cancer. *Thyroid* 2009; **19:** 1167-214. doi: 10.1089/thy.2009.0110
38. Haugen BR, Alexander EK, Bible KC, Doherty GM, Mandel SJ, Nikiforov YE, et al. 2015 American Thyroid Association management guidelines for adult patients with thyroid nodules and differentiated thyroid cancer: the American Thyroid Association guidelines task force on thyroid nodules and differentiated thyroid cancer. *Thyroid* 2016; **26:** 1-133. doi: 10.1089/thy.2015.0020
39. Ghossein RA, Leboeuf R, Patel KN, Rivera M, Katabi N, Carlson DL, et al. Tall cell variant of papillary thyroid carcinoma without extrathyroid extension: biologic behavior and clinical implications. *Thyroid* 2007; **17:** 655-61. doi: 10.1089=thy.2007.0061.
40. Morris LG, Shaha AR, Tuttle RM, Sikora AG, Ganly I. Tall-cell variant of papillary thyroid carcinoma: a matched-pair analysis of survival. *Thyroid* 2010; **20:** 153-8. doi: 10.1089/thy.2009.0352

research article

Epidemiology of oral mucosal lesions in Slovenia

Andrej Aleksander Kansky[1], Vojko Didanovic[1], Tadej Dovsak[1], Bozana Loncar Brzak[2], Ivica Pelivan[3], Diana Terlevic[4]

[1] Department for Oral and Maxillofacial Surgery, University Medical Centre Ljubljana, Slovenia
[2] Department of Oral Medicine, School of Dental Medicine, University of Zagreb, Croatia
[3] Department of Prosthodontics, School of Dental Medicine, University of Zagreb, Croatia
[4] Private Dental Practice, Ljubljana, Slovenia

Radiol Oncol 2018; 52(3): 263-266.

Received 11 April 2018
Accepted 23 June 2018

Correspondence to: Assist. Prof. Andrej Kansky, D.M.D, Ph.D., Department for Oral and Maxillofacial Surgery, School of Dental medicine, University of Ljubljana, Slovenia. Phone: +386 31 755 326; E-mail: andrej.kansky@kclj.si

Disclosure: No potential conflicts of interest were disclosed.

Background. Among the diseases of oral mucosa, malignant tumors are the most dangerous, but not the most common lesions that might appear in the oral cavity. Since most of the studies are focused on the detection of cancer in the oral cavity, we were interested in detecting the frequency of benign changes of the oral mucosa in Slovene population. Oral mucosal lesions are important pointer of oral health and quality of life, especially in elderly. The prevalence of oral mucosal lesions, together with information on the risk habits associated with oral health, such as tobacco and alcohol use, can help in planning future oral health studies and screening programs.

Patients and methods. Survey upon oral mucosal lesions was conducted during the national project for oral cancer screening in spring 2017 in the Slovenia in which more than 50% of dentists participated and 2395 patients (904 men and 1491 women) were included.

Results. Clinical examination, which was conducted according to the WHO standards revealed that 645 patients (27%) had oral mucosal lesions. The ten most common oral lesions detected were fibroma, gingivitis, Fordyce spots, white coated tongue, cheek biting, linea alba, denture stomatitis, geographic tongue, recurrent aphthous ulcerations and lichen planus.

Conclusions. Overall, these epidemiological data suggest need for specific health policies for prevention, diagnosis and treatment of oral mucosal lesions.

Key words: oral mucosa lesions; epidemiological data

Introduction

Oral health is an important factor of individual's quality of life. Disrupted oral health negatively affects speech, chewing and swallowing and deteriorates social contacts.[1] Prevalence of oral mucosal diseases varies from 10.8%–81.3% in the general population as reported in the literature[2-5], with malignant tumors, as the most widely studied entity, representing only a minority among these lesions. These reports point out that there is a need for additional epidemiological data as percentages of various oral mucosal conditions within studies differ greatly. Also, some studies report prevalence of only few diagnoses, which does not accurately show the variability and prevalence of all lesions in the oral cavity. Prevalence of oral mucosal diseases is even greater (95–100%) in the residents within nursing homes and patients referred to the oral medicine specialists.[6,7] These differences in prevalence might be due to the geographic peculiarities, age, gender, habits, intake of medication, denture presence *etc*. It is quite obvious that oral mucosal lesions change and increase with age, however not only due to the age itself but due to the long lasting effect of bad habits (such as alcohol intake and

smoking. It is well known that oral precancerous lesions (*i.e.* lesions with higher malignant potential) are oral lichen planus, leukoplakia and erythroplakia, the latter two being dependent on alcohol and tobacco intake.[2,3] It is very important that dentists recognize these lesions, as their regular monitoring reveals their potential to become malignant lesions. The prevalence of oral mucosal lesions, together with information on the risk habits associated with oral health, such as tobacco and alcohol use, can help in planning future oral health studies and improving regional screening program. The aim of our study was to obtain additional data upon prevalence of oral mucosal lesions in Slovenia.

TABLE 1. Frequency of lesion occurrence, diagnosis and percentage of the lesion within the whole sample and within the sample with oral lesions

Frequency of occurrence	Oral lesion	Number and % within the whole sample and within the patients with oral lesions
1.	fibroma	56 (2.33%–8.7 %)
2.	gingivitis	51 (2.12%–7.90%)
3.	Fordyce spots	46 (1.92%–7.13%)
4.	white coated tongue	40 (1.67%–6.20%)
5.	cheek biting	39 (1.62%–6.04%)
6.	linea alba	38 (1.58%–5.89%)
7.	denture stomatitis	36 (1.50%–5.58%)
8.	geographic tongue	32 (1.33%–4.96%)
9.	recurrent aphthous ulceration	31 (1.29%–4.80%)
10.	fissured tongue	27 (1.12%–4.18%)
11.	traumatic ulcer	27 (1.12%–4.18%)
12.	lichen	26 (1.08%–4.03%)
13.	mucosal pigmentation	25 (1.04%–3.87%)
14.	amalgam tattoo	21 (0.87%–3.25%)
15.	vascular lesions	21 (0.87%–3.25%)
16.	hyperkeratosis	21 (0.87%–3.25%)
17.	mucocele	20 (0.83%–3.10%)
18.	haemangioma	19 (0.79%–2.94%)
19.	papilloma	18 (0.75%–2.79%)
20.	reccurrent herpes	15 (0.62%–2.32%)
21.	decubital ulcer	15 (0.62%–2.32%)
22.	leukoplakia	12 (0.50%–1.86%)
23.	papillitis lingue	10 (0.41%–1.55%)
24.	oral squamous cell carcinoma	9 (0.37%–1.39%)
25.	mucosal petechiae	7 (0.29%–1.08%)
26.	candidal infection	7 (0.29%–1.08%)
27.	leukoedema	5 (0.20%–0.77%)
28.	frictional hyperkeratosis	5 (0.20%–0.77%)
29.	teeth impressions on the mucosa	4 (0.16%–0.62%)
30.	haematoma after bite	3 (0.12%–0.46%)
31.	black hairy tongue	3 (0.12%–0.46%)
32.	angular cheilitis	2 (0.08%–0.31%)
33.	median rhomboid glossitis	2 (0.08%–0.31%)
34.	lingua accreta	2 (0.08%–0,31%)
35.	hyperplastic candidiasis	1 (0.04%–0.15%)
36.	nicotine stomatitis	1 (0.04%–0.15%)

Patients and methods

Every participant signed informed consent according to the Helsinki II. Oral mucosal alterations were recorded according to the WHO protocol-Guide to the Epidemiology and Diagnosis of Oral Mucosal Diseases and Conditions.[8] The statistical analysis was done using the SPSS software, where $p < 0.05$ was considered to be significant. Chi-square test was used to analyze the data.

Results

This study included 2395 patients (904 men and 1491 women) who attended general dental practice in Ljubljana, Slovenia.

Mean age for men was 57.94 years, median 61 years, age range 25–92 years. Mean age for women was 57.62 years, median 60 years, age range 22–92 years. Out of 2395 patients, 1755 patients were without oral mucosal changes, while 645 patients (27%) had oral mucosal lesions (Table 1). Oral lesions were equally present in both gender (males 241/904, 26.66%; females 404/1 491, 27.09%). Majority of patients in all groups (smokers, non-smokers, ex-smokers) had only one oral lesion present, as seen in Table 2. In all patients with more than one lesion in the mouth, the median number of lesions was two. Statistically significant association was found only between oral cancer and tobacco smoking ($p < 0.05$, chi-square = 40.23), while statistical analysis of our results did not reveal significant differences in the prevalence of other oral lesions between smokers and non-smokers (chi square test). The most frequent oral lesions in smokers were cheek biting and linea alba, while the most frequent oral lesion in non-smokers were Fordyce spots and fibroma. Oral squamous cell carcinoma was found in only 0.37% of the patients, representing as low as 1.39% of all the examined patients with oral lesions (Table 3).

TABLE 2. Frequency of oral lesions in non-smokers, smokers and ex-smokers

		Without oral lesions	Oral lesions present	One oral lesion	Two or more oral lesions	The most frequent oral lesion
Male (N = 904)	Non-smokers (N = 719)	531 (73.85%)	188 (26.14%)	154/188 (81.91%)	34/188 (18.08%)	Fordyce spots
	Smokers (N = 166)	117 (70.48%)	49 (29.51%)	35/49 (71.5%)	14/49 (28.5%)	cheek biting
	Ex-smokers (N = 19)	15 (78.94 %)	4 (21.05%)	4/4	-	-
Female (N = 1491)	Non-smokers (N = 1249)	914 (73.17%)	335 (26.82%)	288/335 (85.97%)	47/335 (14.02%)	fibroma
	Smokers (N = 226)	163 (72.12%)	63 (27.87%)	53/63 (84.12%)	10/63 (15.85%)	linea alba
	Ex-smokers (N = 16)	10 (62.5%)	6 (37.5%)	6/6	-	traumatic ulcer

TABLE 3. Prevalence of tobacco smoking and most frequent oral lesions, precancerous lesions (oral lichen planus and leukoplakia) and oral cancer. Ex-smokers who have stopped smoking more than 10 years ago are considered as non-smokers. Statistically significant association was found only between oral cancer and tobacco smoking ($p < 0.05$, chi-square = 40.23)

	Study group (N = 2395; %)	Cheek biting (N = 39)	Linea alba (N = 38)	Fibroma (N = 56)	Fordyce spots (N = 46)	Oral cancer (N = 9)	Oral lichen planus (N = 26)	Oral leukoplakia (N = 12)
Smokers	392; 16.37%	20; 51.28%	15; 39.47%	10; 17.86%	11; 23.91%	9**; 100%	6; 23.1%	4; 3.33%
Non-smokers	2003; 83.63%	19; 48.72%	23; 60.53%	46; 82.14%	35; 76.08%	0; 0%	20; 76.9%	8; 6.66%

Discussion

Literature data about the prevalence of oral mucosal lesions are very variable and depend on the observed diagnoses and studied population. Most of published literature observes only the prevalence of precancerous and cancerous lesions. The results of our study show that malignant (OSCC) and potentially malignant lesions of leukoplakia were more frequently diagnosed in males (OSCC - all male patients; leukoplakia - 33.3% females, 66.6% males), which is consistent with the findings from the published literature.[3] It is interesting to note that potentially malignant lesion, *i.e.* oral *lichen planus* was also more frequently diagnosed in males (58% in males compared to 42% in females, respectively). This differs from data published by Kovac-Kavcic and Skaleric[3] and Mathew *et al.*[9] who found greater oral lichen prevalence in females.

Regarding the prevalence of different oral mucosal lesions in population, several authors have reported higher prevalence than in our study.[3,5,10] According to Kovač-Kavčič *et al.*[3], 61.6% of examined patients (N = 555) had oral mucosal lesions, and the most prevalent were Fordyce spots, fissured tongue, lingual varices and recurrent herpes simplex. Campisi *et al.*[5] studied randomly selected 118 male subjects and revealed oral mucosal lesions in 81.3% of the participants. Oral mucosal lesions were coated tongue (51.4%), leukoplakia (13.8%), traumatic oral lesions in 9.2%, actinic cheilitis (4.6%) and oral squamous cell carcinoma (OSCC) in one case. Shet *et al.*[10] found that 48% of the examined patients (N = 570) had oral mucosal lesions which is higher percentage than obtained within our study. This is probably due to the fact that their sample included only geriatric patients older than 60 years, which was not the case in our study. Furthermore, the same authors[10] stated that the most common oral mucosal lesions were lingual varices (13.68%), denture induced inflammatory fibrous hyperplasia (4.21%) and squamous cell cancer (4.21%), all of them which can be seen more often in geriatric population. Our study has shown the prevalence of oral mucosal lesions of 27%. These data are comparable with our previous study[12] which included 1908 patients and where the prevalence of oral mucosal lesions was 16.8%. As seen, literature data show great variability in reported prevalence of oral lesions, depending on the sample size and observed population. When greater number of patients is included in the study, the frequency of oral lesions usually lowers.

Feng *et al.*[2] reported that the prevalence of oral diseases was 10.8% in their study (N = 11 054) which is lower than the prevalence seen in our study (27%). The same authors[2] further reported that the most common type of oral lesions were fissured tongue (3.15%), recurrent aphthous ulcers (1.48%), traumatic ulcer (1.13%) and angular cheilitis (0.86%). This is contrary to the results of our study, as our findings suggest that the five most

common oral diagnoses were fibroma, gingivitis, Fordyce spots, white coated tongue and cheek biting with higher percentages. Previously, various authors such as Chosack *et al.*[13] and Miloglu *et al.*[14] found significant coexistance of geographic and fissured tongue which was not found in our sample.

It is interesting to note that the results from this study are different from the study we performed three years ago on the Slovenian population when cheek biting was the most common lesions followed by fibroma, geographic tongue, amalgam tattoo and Fordyce spots.[12] On the other hand, among five most common oral lesions in our previous[13] and current study, three are consistent (Fordyce spots, cheek biting and fibroma). Furthermore, when our data are compared to an earlier study on Slovene population[3], it can be observed that the prevalence of smokers among the examined patients is much lower than 20 years ago (35% compared to 13.7%), while the prevalence of the oral mucosal lesions is higher (27% compared to 16.8%).

Our results have shown that oral lesions were equally present in both gender (males 241/904, 26.66%; females 404/1 491, 27.09%), unlike Pentenero *et al.*[15] who found greater prevalence of oral mucosal lesions in males. Statistical analysis of our results did not reveal significant differences in the prevalence of oral lesions between smokers and non-smokers (chi square test), except for oral cancer. The most frequent oral lesions in smokers were cheek biting and linea alba, while the most frequent oral lesion in non-smokers were Fordyce spots and fibroma.

Additionally, higher percentage of patients with oral malignancies was found within this sample (9 patients with OSCC; 0.37%) when compared to our previous[12] and also when compared to the other authors such as Triantos *et al.*[1], Feng *et al.*[2], Kovac-Kavcic and Skaleric[3], Mozafari *et al.*[6], Brailo *et al.*[7] and Cebeci *et al.*[16] This requires additional attention and highlights the need for regular oral examinations/screening, especially of the elderly population and individuals with smoking and drinking habits or in which other possible risk factor can be identified (mechanical trauma, HPV infection).

Conclusions

Our study provided information that one fourth (1/4) of the population attending general dental practice had oral mucosal alterations. Irritational, inflammatory and anatomic changes were the most common types of oral mucosal lesions. The frequency of newly diagnosed oral malignancies increased when compared with the previous results. These data provide valuable information for planning future oral health studies and strategy.

It is important to encourage people, to attend preventive medical examination by doctors and dentists. In the same time it is important to educate medical doctors and dentists, to be able to recognize suspicious oral mucosal lesions, because early treatment of oral cancer significantly improves prognosis, treatment outcomes and diminishes post treatment morbidity.

References

1. Triantos D. Intra-oral findings and general health conditions among institutionalized and non-institutionalized elderly in Greece. *J Oral Pathol Med* 2005; **34:** 577-82. doi: 10.1111/j.1600-0714.2005.00356.x
2. Feng J, Zhou Z, Shen X, Wang Y, Shi L, Wang Y, et al. Prevalence and distribution of oral mucosal lesions: a cross-sectional study in Shangai, China. *J Oral Pathol Med* 2015; **44:** 490-4. doi: 10.1111/jop.12264
3. Kovac-Kavcic M, Skaleric U. The prevalence of oral mucosal lesions in a population in Ljubljana, Slovenia. *J Oral Pathol Med* 2000; **29:** 331-5. doi: 10.1034/j.1600-0714.2000.290707.x
4. Espinoza I, Rojas R, Aranda W, Gamonal J. Prevalence of oral mucosal lesions in elderly people in Santiago, Chile. *J Oral Pathol Med* 2003; **32:** 571-5. doi: 10.1034/j.1600-0714.2003.00031.x
5. Campisi G, Margiotta V. Oral mucosal lesions and risk habits among men in an Italian study population. *J Oral Pathol Med* 2001; **30:** 22-8. doi: 10.1034/j.1600-0714.2001.300104.x
6. Mozafari PM, Dalirsani Z, Delavarian Z, Amirchaghmaghi M, Shakeri MT, Esfandyari A, et al. Prevalence of oral mucosal lesions in institutionalized elderly people in Mashhad, Northeast Iran. *Gerodontology* 2012; **29:** e930-4. doi: 10.1111/j.1741-2358.2011.00588
7. Brailo V, Boras VV, Pintar E, Juras DV, Karaman N, Rogulj AA. [Analysis of oral mucosal lesions in patients referred to oral medicine specialists]. [Croatian]. *Lijec Vjesn* 2013; **135:** 205-8.
8. Kramer IR, Pindborg JJ, Bezroukov V, Infi rri JS. Guide to epidemiology and diagnosis of oral mucosal diseases and conditions. World Health Organization. *Community Dent Oral Epidemiol* 1980; **8:** 1-26. doi: 10.1111/j.1600-0528.1980.tb01249.x
9. Mathew AL, Pai KM, Sholapurkar AA, Vengal M. The prevalence of oral mucosal lesions in patients visiting a dental school in Southern India. *Indian J Dent Res* 2008; **19:** 99-103.
10. Shet R, Shetty SR, MK, Kumar MN, Yadav RD, SS. A study to evaluate the frequency and association of various muosal conditions among geriatric patients. *J Contem Dent Pract* 2013; **14:** 904-10.
11. Axell T. A prevalence study of oral mucosal lesions in an adult Swedish population. *Thesis Odontol Revy* 1976; **27:** 1-103.
12. Terlevic Dabic D, Kansky A, Vucicevic Boras V. Prevalence of oral mucosal lesions in Slovenia. *RJPBCS* 2015; **6:** 1154-7.
13. Chosack A, Zadik D, Eidelman E. The prevalence of scrotal tongue and geographic tongue in 70359 Israeli school children. *Community Dent Oral Epidemiol* 1974; **2:** 253-7.
14. Miloglu O, Goregen M, Akgul HM, Acemoglu H. The prevalence and risk factors associated with benign migratory glossitis lesions in 7619 Turkish dental outpatients. *Oral Surg Oral Med Oral Pathol Oral Radiol Endod* 2009; **107:** e29-33. doi: 10.1016/j.tripleo.2008.10.015
15. Pentenero M, Broccoletti R, Carbone M, Conrotto D, Gandolfo S. The prevalence of oral mucosal lesions in adults from the Turin area. *Oral Dis* 2008; **14:** 356-66. doi: 10.1111/j.1601-0825.2007.01391.x
16. Cebeci AR İ, Gülşahı A, Kamburoğlu K, Orhan BK, Öztaş B. Prevalence and distribution of oral mucosal lesions in an adult Turkish population. *Med Oral Patol Oral Cir Bucal* 2009; **14:** E272-7.

research article

Induction chemotherapy, chemoradiotherapy and consolidation chemotherapy in preoperative treatment of rectal cancer - long-term results of phase II OIGIT-01 Trial

Danijela Golo[1], Jasna But-Hadzic[1], Franc Anderluh[1], Erik Brecelj[2], Ibrahim Edhemovic[2], Ana Jeromen[1], Mirko Omejc[3], Irena Oblak[1], Ajra Secerov-Ermenc[1], Vaneja Velenik[1]

[1] Department of Radiotherapy, Institute of Oncology Ljubljana; Ljubljana, Slovenia
[2] Department of Surgery, Institute of Oncology Ljubljana; Ljubljana, Slovenia
[3] Department of Surgery; University Medical Centre Ljubljana

Radiol Oncol 2018; 52(3): 267-274.

Received 1 February 2018
Accepted 2 March 2018

Correspondence to: Assoc. Prof. Vaneja Velenik, M.D., Ph.D., Institute of Oncology Ljubljana, Zaloška cesta 2, SI-1000 Ljubljana, Slovenia. Phone: +386 1 5879 297; Fax: +386 1 5879 416; E-mail: vvelenik@onko-i.si

Disclosure: No potential conflicts of interest were disclosed.

Background. The purpose of the study was to improve treatment efficacy for locally advanced rectal cancer (LARC) by shifting half of adjuvant chemotherapy preoperatively to one induction and two consolidation cycles.

Patients and methods. Between October 2011 and April 2013, 66 patients with LARC were treated with one induction chemotherapy cycle followed by chemoradiotherapy (CRT), two consolidation cycles, surgery and three adjuvant capecitabine cycles. Radiation doses were 50.4 Gy for T2-3 and 54 Gy for T4 tumours in 1.8 Gy daily fraction. The doses of concomitant and neo/adjuvant capecitabine were 825 mg/m²/12h and 1250mg/m²/12h, respectively. The primary endpoint was pathologic complete response (pCR).

Results. Forty-three (65.1%) patients were treated according to protocol. The compliance rates for induction, consolidation, and adjuvant chemotherapy were 98.5%, 93.8% and 87.3%, respectively. CRT was completed by 65/66 patients, with G ≥ 3 non-hematologic toxicity at 13.6%. The rate of pCR (17.5%) was not increased, but N and the total-down staging rates were 77.7% and 79.3%, respectively. In a median follow-up of 55 months, we recorded one local relapse (LR) (1.6%). The 5-year disease-free survival (DFS) and overall survival (OS) rates were 64.0% (95% CI 63.89–64.11) and 69.5% (95% CI 69.39–69.61), respectively.

Conclusions. In LARC preoperative treatment intensification with capecitabine before and after radiotherapy is well tolerated, with a high compliance rate and acceptable toxicity. Though it does not improve the local effect, it achieves a high LR rate, DFS, and OS.

Key words: rectal cancer; neoadjuvant chemotherapy; preoperative chemoradiotherapy; pathologic complete response, total neoadjuvant therapy

Introduction

Over the past 15 years, there have been unprecedented advances in the multimodality treatment of locally advanced rectal cancer (LARC). The shift of chemoradiotherapy (CRT) from a postoperative to a preoperative setting enabled tumour downsizing and downstaging and, consequently, increased the likelihood of microscopic complete clearance of the primary tumour (R0 resection). With a highly precise surgical technique and a total mesorectal excision, combined modality treatment resulted in an excellent local control and, as such, represents the standard of care for these pa-

tients. Still, the prognosis remains largely unsatisfactory due to a high rate of distant relapse, which is the most common cause of death.[1]

The results of two meta-analyses suggest that the pathological stage of the disease and/or the rate of tumour reduction (pathohistological tumour regression - TRG) after pre-operative treatment are predictive factors for disease-free survival. A particularly low risk of recurrence of the disease has a subgroup of patients with a complete pathohistological response (pCR).[2,3] With standard 5-FU based CRT, pCR is reported to range between 9 and 20%.[3,4] In an attempt to increase the pCR rate, many trials integrated oxaliplatin and/or molecular targeted agents into fluoropyrimidine-based preoperative CRT protocols. They achieved a high rate of pCR, but it was accompanied by higher toxicity and had no impact on survival.[5,6]

In the search for improving the rate of pCR and the control of micrometastatic disease without causing greater toxicity, the intensification of standard chemotherapy (ChT) treatment in the neoadjuvant setting, namely by integrating induction chemotherapy before CRT and consolidation ChT before the operation, represents a rational approach.

In this study, we sought to determine whether the intensification of ChT in the neoadjuvant setting was associated with an improved outcome of the disease. The primary goal was to establish the proportion of complete pathohistological response to the treatment. Secondary objectives were to evaluate the pathological downstaging rate, histopathological R0 resection rate, sphincter preservation rate, perioperative surgical complication rate, local control (LC), disease-free survival (DFS), overall survival (OS), late toxicity, and the quality of life.

In this paper, we summarize the results of the phase II trial altogether and provide 5-year follow-up data.

Patients and methods

Patients

The inclusion criteria comprised a histologically proven adenocarcinoma of the rectum, a clinical TNM stage II or III based on magnetic resonance imaging (MRI) of the pelvis, and an operable disease or disease likely to become operable after neoadjuvant therapy.[7] The extent of disease was determined according to the International Union Against Cancer (UICC) classification.[7]

Patients had to be ≥ 18 years old with a performance status 0–2 according to the World Health Organisation (WHO) scale, and had to have adequate cardiac, bone marrow, liver and renal function. All patients signed written informed consents before commencing treatment. The trial was approved by the National Medical Ethics Committee of the Republic of Slovenia (No. 163/06/11) and was registered in the ClinicalTrials.gov database (NCT01489332).

Pre-treatment evaluation

Before entering the study, the patients underwent a complete history and physical examination, full blood count, serum biochemistry profiles with liver and renal function tests, carcinoembryonic antigen (CEA), chest X-rays, ultrasonography (USG) or computed tomography (CT) of the abdomen, and colonoscopy with biopsy. Each patient underwent a magnetic resonance imaging (MRI) of the pelvis for local staging.

Study protocol

Intervention ChT included one cycle of oral capecitabine before and two cycles after CRT at a dose of 1250 mg/m²/12 hours, 14 consecutive days. The patients were irradiated with 15-MV linear accelerator photon beams, using the four-field 3-dimensional conformal technique. The total dose to the small pelvis was 45.0 Gy in 1.8 Gy daily fraction, followed by a boost to the primary tumour (1.8 Gy daily) to 5.4 Gy for T2–T3, and 9.0 Gy for T4 tumours. Oral capecitabine was administered concomitantly with radiotherapy at a dose of 825 mg/m² twice daily from the first to the last day of radiotherapy (including weekends).

Surgery was performed 2 weeks after the completion of ChT. Adjuvant ChT began 4–6 weeks after resection and comprised three cycles of oral capecitabine 1250mg/m²/12, 14 consecutive days.

Follow-up

During therapy, acute toxicity was monitored on a three-week basis for ChT and on a weekly basis for CRT. A clinical examination and complete blood count were performed. Toxic side effects were assessed according to the National Cancer Institute Common Toxicity Criteria (NCI-CTC) (version 4.0).[8]

All patients were followed up every 3 months in the first 2 years after surgery, and then every

TABLE 1. Pre-treatment patients and tumour characteristics (N = 66)

Median age (years)	60 (37-81)
Gender	
Male	42 (63.6%)
Female	24 (36.4%)
WHO performance status[7]	
0	54 (81.8%)
1	11 (16.7%)
2	1 (1.5 %)
Stage[8]	
T2	9 (13.6%)
T3	50 (75.8%)
T4	7 (10.6%)
N0	9 (13.6%)
N1	34 (51.5%)
N2	23 (34.9%)
Tumour differentiation (grade)	
Well (G1)	8 (12.1%)
Moderate (G2)	35 (53.0%)
Poorly (G3)	4 (6.0%)
Unknown or not stated (GX)	19 (28.9%)
MRF distance	
MRF+	20
MRF-	44
Median tumour distance from the anal verge (cm)	6 (0-12)

MRF distance = distance between tumour and mesorectal fascia

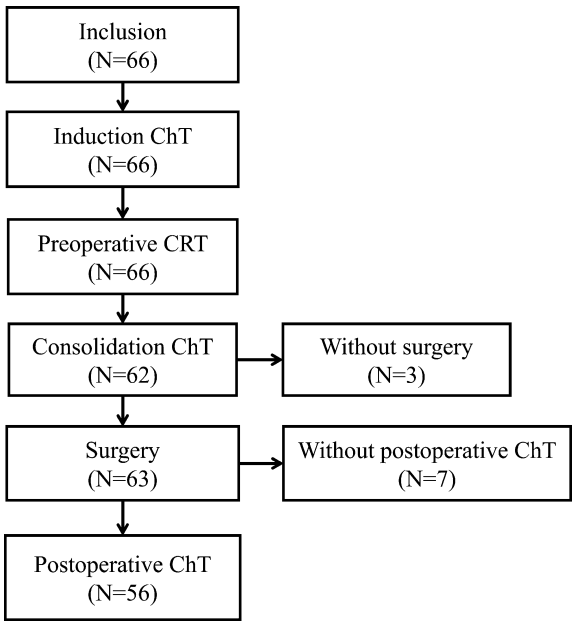

FIGURE 1. Distribution of patients through the trial.

6 months for 5 years. A clinical examination was performed and the serum scanned for CEA at each follow-up. An abdominal ultrasound was performed every 6 months, chest radiograph every 12 months, and colonoscopy annually. The terminal time for the evaluation of outcomes was 5 years. The follow-up rate was 100%.

Statistics

The sample size calculation was based on a hypothesis that the experimental treatment regime will increase the pCR rate by 14%, from our 9%[9] to 23%. To confirm the hypothesis that the pCR rate was greater than 23% with 80% power and to reject the hypothesis that the pCR rate was lower or equal to 9% with 5% significance, a sample size of 50 was required.[11,12] In case that 10% proved not to be evaluable, we planned to include 60 patients.

Statistical calculations were performed using the SPSS statistical software package, version 18 (SPSS Inc., Chicago, IL, USA). Statistical analyses were performed using the Chi-square test with Fisher's exact test. The survival rates were obtained using the Kaplan-Meier method and the significance of the difference in survival rate was determined by means of the log-rank test. P-values < 0.05 were considered statistically significant.

All time intervals were calculated from the date of operation or date of CRT completion (for non-operated patients). The end dates for time calculations were the dates of the last follow-up or death for overall survival (OS); and the dates of detected local/distant relapse, last follow-up, or death for disease-free survival (DFS). In non-operated patients, the DFS time was 0 months.

Results

Patients

Between October 2011 and April 2013, 66 patients with locally advanced rectal cancer were treated in the trial. Table 1 lists the pre-treatment patient and tumour characteristics. The median age was 60 years (range 37–81) and 42 (63.6%) patients were men. The WHO performance status was graded as 0 in 54 (81.8%) patients, as 1 in 11 (16.7%) patients, and as 2

in 1 (1.5%) patient. Fifty-seven (86.4%) patients had nodal involvement. In 31 patients (47%), the primary tumour was sited ≤ 5 cm from the anal verge, 33 (50%) tumours were located at 5–10 cm, and 2 (3%) were above 10 cm from anal verge. The flow of the patients through the trial is shown in Figure 1.

Neoadjuvant treatment

The toxic side effects of preoperative treatment are listed in Table 2. The induction cycle of capecitabine was well tolerated with no G ≥ 2 toxicity. Sixty-five (98.5%) patients completed radiotherapy according to the treatment protocol. In one patient, radiotherapy was discontinued after the TD 45 Gy due to prolonged G4 thrombocytopenia and septic shock caused by *Pseudomonas aeruginosa*. The radiotherapy treatment was completed in the median time of 39 days (range 37–53 days). The median time of radiotherapy interruption was 2 days (range 0–15 days). The median duration of ChT was 39 days (6–45 days) and the median time of ChT interruption was 0 days (0–47 days). Nine (13.8%) patients received less than 90% of the planned capecitabine dose due to G ≥ 2 (3/66; 4.5%) thrombocytopenia, G3 neutropenia and G3 diarrhoea (2/66; 3%), infection (2/66; 3%), chest pain (1/66; 1.5%) and due to protocol violation by the patient (1/66; 1.5%).

After the completion of CRT, one patient died due to pulmonary thromboembolism.

TABLE 2. Toxicity[8] of preoperative treatment (N = 66)

	Toxicity grade (N)				
	1	2	3	4	5
Haematological					
Anaemia	23	7	1	0	0
Neutropenia	4	**7**	2	0	0
Thrombocytopenia	6	1	1	1	0
Non-haematological					
Fatigue	5	0	0	/	/
Nausea/vomiting	2	2	0	/	/
Hand-foot syndrome	11	5	1		
Radiodermatitis	7	18	5		
Diarrhoea	11	3	2		
Urinary infection	6	0	0	0	0
Systemic infection	0	1	0	1	0
Proctitis	6	2	0		
Thromboembolism	2	2	0	0	1
Chest pain			1		

Consolidation chemotherapy

After CRT, ChT was administered to 93.8% patients according to protocol. The consolidation treatment was omitted due to patient refusal in one, prolonged neutropenia in the second, and thrombocytopenia in the third patient. It was discontinued after the first cycle for a patient with L1 fracture.

Surgery and perioperative toxicity

Surgery was performed in 63/66 (95.4%) patients in median 8 weeks (range 6.6–11.3) after CRT completion. One patient refused the operation, one was unfit for surgery due to low performance status (PS), and one patient died after CRT before operation. A low anterior resection was performed in 46 patients (73%) and abdominoperineal resection in 17 (27%), with hysterectomy +/- ovariectomy in three patients. During surgery, solitary hepatic metastases were discovered in two patients and a synchronous metastasectomy was performed. In all patients but one a radical resection was achieved (98.4%).

Within 30 days of the operation we recorded thirty adverse events in 24 patients. In 10 out of 63 (15.8%) patients, toxicity was graded as G ≥ 3 with postoperative wound complications, including a local infection with delayed healing (N = 7), anastomotic leakage (N = 2), intraabdominal infection (N = 4), urinary infection (N = 1), and pneumonia (N = 2). Three patients were re-operated because of acute abdomen, intraabdominal, and anastomotic bleeding. In one patient, a revision of the necrotic epidermal bound lope under general anaesthesia was performed. There was no perioperative mortality.

Adjuvant chemotherapy

Fifty-five of the 63 operated patients (87.3%) received adjuvant capecitabine treatment, two of them with oxaliplatin on account of pathological upstaging. All three cycles of the recommended dose were able to receive 94.3% of patients. No G ≥ 3 toxicity was observed. Two patients were treated with chemotherapy and targeted agents after synchronous liver metastasectomy.

Tumour response

A complete pathological response (pCR) was observed in 11/63 (17.5%) patients. In 2 patients, liver metastases were found during the operation. The

tumour, nodal and overall downstaging rates were 55.5%, 77.7%, and 79.3%, respectively. An increase in T- and/or N-stage (upstaging) was recorded in 6 patients (9.5%). The pathologic TNM stages, as assessed in histopathological examination of the resected specimens in relation to preoperative TNM status, are listed in Table 4. In 5 patients, the local pathological stage was higher than the clinical.

According to the Dworak criteria, the tumour regression grades (TRG) were TRG 4, TRG 3, TRG 2, TRG 1, and TRG 0 in 11, 7, 32, 12, and 1 patients, respectively [12].

The sphincter preservation rate for the low rectal tumours ≤ 5 cm from the anal verge was 45% (14/31).

There was no association between pCR and the stage of the disease, tumour grade, radiotherapy or ChT interruption, the total dose of radiation therapy, and time to operation from CRT completion on the Fisher's exact test.

Survival and late toxicity

The median follow-up time was 55 months (range 2–71 months). One local relapse was recorded (1/63; 1.6%) among the operated patients. The 5-year local control rate was 92.7% (95% CI 85.9–99.6). Distant metastases were noted in 14 (14/66; 21.2%) patients (three patients with liver metastases, seven with lung metastases, three with both liver and lung, and one with both lung metastases and peritoneal carcinomatosis).

As of August 2017, 20 of the 66 (20/66; 30.3%) patients had died due to: treatment complications (N = 2), disease progression (N = 14), secondary cancers (i.e. gastric cancer (N = 1), prostate cancer (N = 1), new rectal cancer (N = 1)), and non-disease or treatment-related cause (suicide (N = 1)).

The 5-year DFS rate was 64.0% (95 % CI 63.89–64.11). The median survival has not yet been reached. The 5-year OS rate was 69.5% (95% CI 69.39–69.61).

Patients with pN+ or T3–4 had a significantly worse OS and DFS (Figure 2).

Forty-three (65.1 %) of all patients in the study received all treatment according to protocol and they had significantly better OS (79.1% *vs*. 52.2%) and DFS (74.4% *vs*. 47.8%) compared to patients with less treatment with $p < 0.05$ (Table 5).

Late toxicity data was available for 57 patients. The recorded rate for G ≥ 3 toxicity was: 3.5% faecal incontinence, 1.8% stoma prolapse, 3.5% rectal anastomotic leak, 1.8% rectal stenosis, 1,8% diarrhoea, 1.8% perineal abscess, 3.5% ileus, 1.8%

TABLE 3. Toxicity[8] of postoperative treatment (N = 55)[12]

	Toxicity grade (N)				
	1	2	3	4	5
Haematological					
Anaemia	23	1			
Neutropenia		1			
Non-haematological					
Fatigue	2				
Nausea/vomiting	2	1			
Hand-foot syndrome	3	3			
Diarrhoea	1				
Urinary infection		2			
Thromboembolic event		1			

TABLE 4. Distribution of clinical and pathological stages

	pT0	pT1	pT2	pT3	pT4		pN0	pN1	pN2
cT1	-	-	-	-	-	**cN0**	7	-	-
cT2	2	-	3	4	-	**cN1**	28	4	1
cT3	8	6	16	18	1	**cN2**	17	4	2
cT4	1	-	1	1	2				

c = clinical; p = pathological

TABLE 5. Univariate analysis of overall survival (OS) and disease free survival (DFS) according to patient, disease, and treatment characteristics (N = 66)

Parameter	OS	DFS
Gender	ns	ns
Age	ns	ns
WHO PS[a]	ns	ns
Tumour location in the rectum	ns	ns
cTumour stage	ns	ns
cNodal stage	ns	ns
Type of surgery: APR vs. LAR	ns	ns
pT1-2 *vs*. pT3-4	0.005	0.002
pT0 *vs*. pT4	0.009	0.009
pN0 *vs*. pN+	0.009	0.005
TRG 3–4 *vs*. 0–2	ns	ns
pCR	ns	ns
All treatment *vs*. less treatment	0.016	0.018

APR = abdominoperineal resection; LAR = low anterior resection; ns = not specific ($p > 0.05$); p = pathologic; PS = performance status, PCR = pathologic complete response; TRG = tumour regression grade

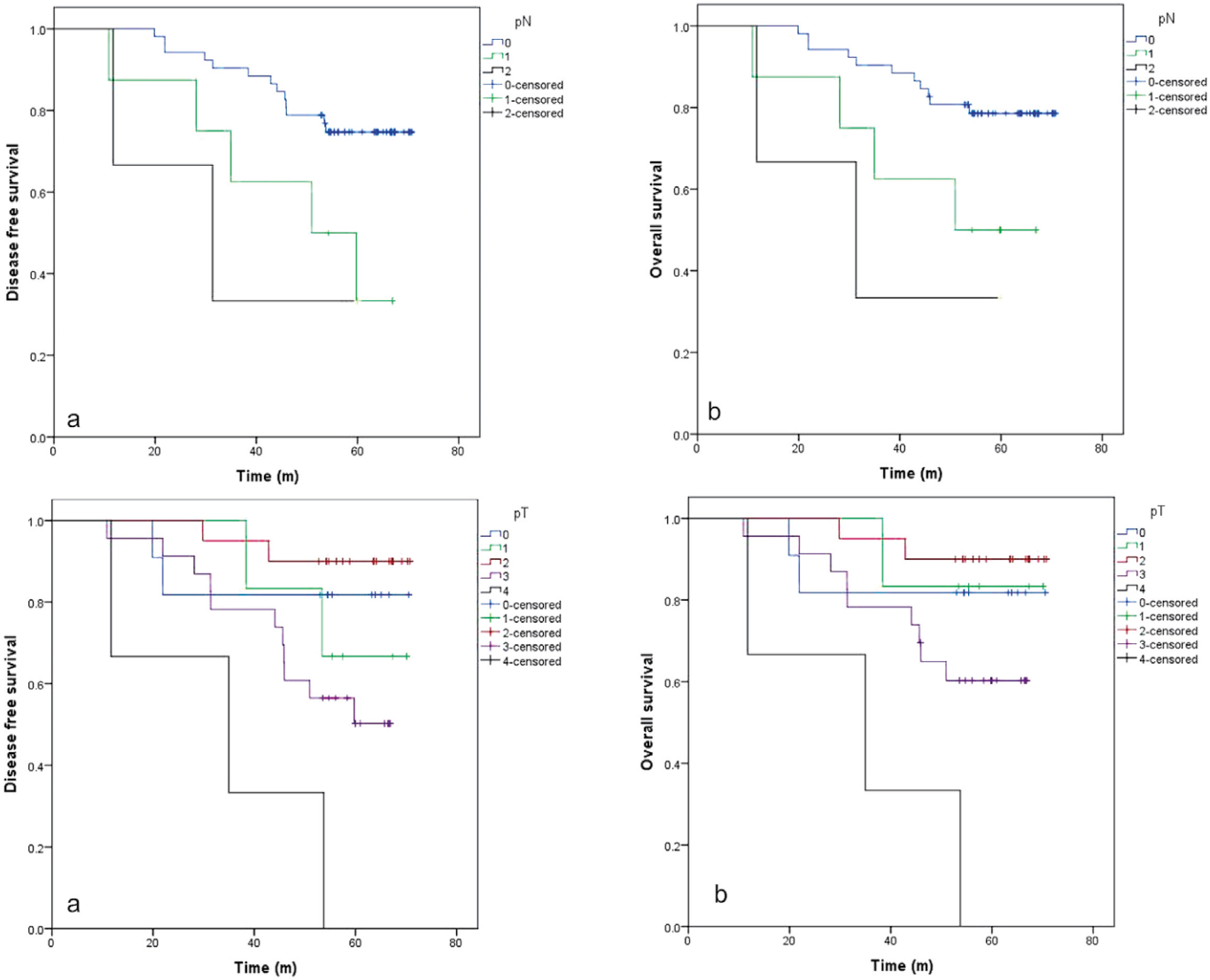

FIGURE 2. Prognostic significance of pathologic nodal stage (pN) and pathologic tumour stage (pT) in 5-year disease free survival and overall survival in rectal cancer after preoperative chemoradiotherapy and surgery. *Time (m = months)*.

myocutaneous flap defect and 3.5% urinary tract obstruction. One patient died due to colon perforation.

Discussion

Neoadjuvant treatment intensification with one-cycle induction capecitabine, standard CRT, and two-cycle consolidation capecitabine did not significantly improve the rate of pCR in LARC compared to standard CRT with capecitabine.

Additional three cycles of capecitabine prior to operation were not enough to achieve a better local effect in preoperative treatment, which is in agreement with the studies that tried to optimize the treatment of LARC with total neoadjuvant (NA) therapy. In a Spanish GCR-3 phase II trial, patients were randomized to 4 cycles of neoadjuvant CAPOX (capecitabine and oxaliplatin), followed by CRT and operation; or to second arm with CRT, operation, and 4 cycles of adjuvant (A) CAPOX.[13] The treatment was intensified with an up-front ChT in the first arm and with the addition of oxaliplatin to concomitant capecitabine in both arms. They reported pCR rates of 14% and 13% in the first and second arms, respectively. The second randomized trial with standard CRT with or without NA ChT with 5-FU/OX was closed prematurely due to the similar rates of pCR in both arms.[14] In a pooled analysis of phase II EXPERT (NA ChT CAPOX - CRT and A CAPOX) and EXPERT C (addition of

cetuximab) trials, the pooled pCR rate for 269 patients was 19%.[15-17] With only three additional cycles to CRT preoperatively with capecitabine only, we report a pCR rate of 17.5%. The negative results of our primary endpoint and the rate of pCR similar to other studies suggests that NA capecitabine does not have an additional local effect in standard CRT, nor does the second concomitant chemotherapy agent in more intensified regimes - a conclusion that is supported by a recent meta-analysis.[18]

Despite the questionable local effect of systemic neoadjuvant capecitabine, we have recorded an improvement in N downstaging rate from 52% with classical treatment[12] to 77% with experimental treatment and, consequently, improved the total downstaging rates from 50% to 79%, respectively. With potential to impact micrometastatic disease early with an up-front ChT, the regional effect can potentially contribute to an improved treatment outcome with NA ChT, since the pathologic N stage is an independent prognostic factor for the incidence of distant metastasis.[19] This observed effect addresses an additional question on the appropriateness of pCR as a primary endpoint for phase II LARC treatment optimization trials.

The expected effect of adjuvant ChT on the treatment outcome in rectal cancer is compromised by the late introduction of ChT after local treatment with CRT and surgery[20] and the treatment compliance, since less than half of the patients receive the planed dose.[21] The main findings of trials with total neoadjuvant ChT were the improved tolerance and completion rates of ChT.[13,14,17,22,23] Our results are in concordance with the reported compliance of 85–95%[13.17.23], since all the patients received an induction cycle and 93.8% received both consolidation cycles. CRT was not compromised, with 98.5% patients having completed radiotherapy according to the treatment protocol. We recorded an excellent 87% adherence to adjuvant ChT, compared to only 57% in the GCR 3 trial, probably due to the toxicity of oxaliplatin addition to the regime.[13]

The acute toxicity of our protocol treatment was acceptable. No G3/4 events were recorded during induction and adjuvant ChT. However, after CRT one patient died (G5 toxicity) because of pulmonary thromboembolism. The most frequent G3/4 toxicities during CRT were diarrhoea, radiodermatitis, and hematologic side effects. An intensified preoperative treatment regime did not affect the surgery complication rate, as is the case with standard treatment.[24] All patients but one achieved R0 resection and we report an excellent 5-year local recurrence rate of 1.6%.

Compared to our historical cohort, we achieved a similar 5y LC (92% *vs*. 87%), slightly improved 5y OS (69.5% *vs*. 61%), and improved 5y DFS of 64% compared to 52% in standard treatment.[12] The results are similar to the 5y OS 67%–77% and DFS 63%–64% results[16,25,26] from total neoadjuvant therapy trials. Similarly to other studies, we found the pathologic T and N stages to be significant prognostic factors for OS and DFS.[21,23] The OS and DFS were also significantly better in patients who received all planed therapy, compared to the patients with less treatment, signalling the importance of treatment compliance for disease outcome.

The main limitations of our study are the single-arm non-randomized design with pCR as a primary endpoint and the small sample size. The systemic treatment consisted of capecitabine, which was standard at the time but is suboptimal today.[16,25,26] Larger randomized trials are needed to evaluate the efficacy of intensified neoadjuvant treatment.

To our knowledge, this study is, beside the Italian investigation of Zampino *et al.*, the only neoadjuvant intensification study that does not influence the timing of CRT and surgery.[27] We took advantage of the waiting time in local therapy for an additional administration of three cycles of capecitabine preoperatively, without the additional intensification with a second systemic agent. Our regime was well tolerated with excellent compliance, and although we couldn't achieve a significantly higher rate of pCR, we report high 5y DFS and OS that are within range of the published results from more intensified regimes. We believe that our regime can be used to treat patients with LARC who are not suited for combination chemotherapy, namely because of good results, excellent compliance and the additional advantage of shorter treatment time.

References

1. Breugom AJ, Swets M, Bosset JF, Collette L, Sainato A, Cionini L, et al. Adjuvant chemotherapy after preoperative (chemo)radiotherapy and surgery for patients with rectal cancer: a systematic review and meta-analysis of individual patient data. *Lancet Oncol* 2015; **16:** 200-7. doi: 10.1016/S1470-2045(14)71199-4
2. Martin ST, Heneghan HM, Winter DC. Systematic review and meta-analysis of outcomes following pathological complete response to neoadjuvant chemoradiotherapy for rectal cancer. *Br J Surg* 2012; **99:** 918-28. doi: 10.1002/bjs.8702
3. Zorcolo L, Rosman AS, Restivo A, Pisano M, Nigri GR, Fancellu A, et al. Complete pathologic response after combined modality treatment for rectal cancer and long-term survival: a meta-analysis. *Ann Surg Oncol* 2012; **19:** 2822-32. doi: 10.1245/s10434-011-2209-y
4. Velenik V, Anderluh F, Oblak I, Strojan P, Zakotnik B. Capecitabine as a radiosensitizing agent in neoadjuvant treatment of locally advanced resectable rectal cancer: prospective phase II trial. *Croat Med J* 2006; **47:** 693-700.

5. Gérard JP, Azria D, Gourgou-Bourgade S, Martel-Lafay I, Hennequin C, Etienne PL, et al. Clinical outcome of the ACCORD 12/0405 PRODIGE 2 randomized trial in rectal cancer. *J Clin Oncol* 2012; **30:** 4558-65. doi: 10.1200/JCO.2012.42.8771

6. Aschele C, Cionini L, Lonardi S, Pinto C, Cordio S, Rosati G, et al. Primary tumor response to preoperative chemoradiation with or without oxaliplatin in locally advanced rectal cancer: pathologic results of the STAR-01 Randomized Phase III Trial. *J Clin Oncol* 2011; **29:** 2773-80. doi: 10.1200/JCO.2010.34.4911

7. Edge SB, Compton CC. The American Joint Committee on Cancer: the 7th edition of the AJCC cancer staging manual and the future of TNM. *Ann Surg Oncol* 2010; **17:** 1471-4. doi: 10.1245/s10434-010-0985-4

8. National Cancer Institute. Common Terminology Criteria for Adverse Events (CTCAE) Common terminology criteria for adverse events v4.0 (CTCAE). Publish 2009; 2009: 0-71. Available at https://www.eortc.be/services/doc/ctc/CTCAE_4.03_2010-06-14_QuickReference_5x7.pdf

9. Oken MM, Creech RH, Tormey DC, Horton J, Davis TE, McFadden ET, et al. Toxicity and response criteria of the Eastern Cooperative Oncology Group. *Am J Clin Oncol* 1982; **5:** 649-56.

10. Fleming TR. One-sample multiple testing procedure for phase II clinical trials. Biometrics 1982; **38:** 143-51.

11. A'Hern RP. Sample size tables for exact single-stage phase II designs. *Stat Med* 2001; **20:** 859-66. doi: 10.1002/sim.721

12. Velenik V, Oblak I, Anderluh F. Long-term results from a randomized phase II trial of neoadjuvant combined-modality therapy for locally advanced rectal cancer. Radiat Oncol 2010; **5:** 88. doi: 10.1186/1748-717X-5-88

13. Fernández-Martos C, Pericay C, Aparicio J, Salud A, Safont M, Massuti B, et al. Phase II, randomized study of concomitant chemoradiotherapy followed by surgery and adjuvant capecitabine plus oxaliplatin (CAPOX) compared with induction CAPOX followed by concomitant chemoradiotherapy and surgery in magnetic resonance imaging-defined, locally advanced rectal cancer: Grupo cancer de recto 3 study. *J Clin Oncol* 2010; **28:** 859-65. doi: 10.1200/JCO.2009.25.8541

14. Marechal R, Vos B, Polus M, Delaunoit T, Peeters M, Demetter P, et al. Short course chemotherapy followed by concomitant chemoradiotherapy and surgery in locally advanced rectal cancer: a randomized multicentric phase II study. *Ann Oncol* 2012; **23:** 1525-30. doi: 10.1093/annonc/mdr473

15. Dewdney A, Cunningham D, Tabernero J, Capdevila J, Glimelius B, Cervantes A, et al. Multicenter randomized phase II clinical trial comparing neoadjuvant oxaliplatin, capecitabine, and preoperative radiotherapy with or without cetuximab followed by total mesorectal excision in patients with high-risk rectal cancer (EXPERT-C). *J Clin Oncol* 2012; **30:** 1620-7. doi: 10.1200/JCO.2011.39.6036

16. Sclafani F, Peckitt C, Cunningham D, Tait D, Giralt J, Glimelius B, et al. Short- and long-term quality of life and bowel function in patients with MRI-defined, high-risk, locally advanced rectal cancer treated with an intensified neoadjuvant strategy in the randomized phase 2 EXPERT-C Trial. *Int J Radiat Oncol* 2015; **93:** 303-12. doi: 10.1016/j.ijrobp.2015.03.038

17. Sclafani F, Brown G, Cunningham D, Wotherspoon A, Tait D, Peckitt C, et al. PAN-EX: a pooled analysis of two trials of neoadjuvant chemotherapy followed by chemoradiotherapy in MRI-defined, locally advanced rectal cancer. *Ann Oncol* 2016; **27:** 1557-65. doi: 10.1093/annonc/mdw215

18. Teo MTW, McParland L, Appelt AL, Sebag-Montefiore D. Phase 2 neoadjuvant treatment intensification trials in rectal cancer: a systematic review. *Int J Radiat Oncol* 2018; **100:** 146-58. doi: 10.1016/j.ijrobp.2017.09.042

19. Fokas E, Liersch T, Fietkau R, Hohenberger W, Beissbarth T, Hess C, et al. Tumor regression grading after preoperative chemoradiotherapy for locally advanced rectal carcinoma revisited: updated results of the CAO/ARO/AIO-94 trial. *J Clin Oncol* 2014; **32:** 1554-62. doi: 10.1200/JCO.2013.54.3769

20. Biagi JJ, Raphael MJ, Mackillop WJ, Kong W, King WD, Booth CM. Association between time to initiation of adjuvant chemotherapy and survival in colorectal cancer. *JAMA* 2011; **305:** 2335. doi: 10.1001/jama.2011.749

21. Bosset JF, Collette L, Calais G, Mineur L, Maingon P, Radosevic-Jelic L, et al. Chemotherapy with preoperative radiotherapy in rectal cancer. N Engl J Med 2006; **355:** 1114-23. doi: 10.1056/NEJMoa060829

22. Perez K, Safran H, Sikov W, Vrees M, Klipfel A, Shah N, et al. Complete neoadjuvant treatment for rectal cancer: the Brown University Oncology Group CONTRE Study. *Am J Clin Oncol* 2017; **40:** 283-7. doi: 10.1097/COC.0000000000000149

23. Nogue M, Salud A, Vicente P, Arrivi A, Roca JM, Losa F, et al. Addition of bevacizumab to XELOX induction therapy plus concomitant capecitabine-based chemoradiotherapy in magnetic resonance imaging-defined poor-prognosis locally advanced rectal cancer: the AVACROSS Study. *Oncologist* 2011; **16:** 614-20. doi: 10.1634/theoncologist.2010-0285

24. O'Connell MJ, Colangelo LH, Beart RW, Petrelli NJ, Allegra CJ, Sharif S, et al. Capecitabine and oxaliplatin in the preoperative multimodality treatment of rectal cancer: surgical end points from National Surgical Adjuvant Breast and Bowel Project trial R-04. *J Clin Oncol* 2014; **32:** 1927-34. doi: 10.1200/JCO.2013.53.7753

25. Schou J V, Larsen FO, Rasch L, Linnemann D, Langhoff J, Høgdall E, et al. Induction chemotherapy with capecitabine and oxaliplatin followed by chemoradiotherapy before total mesorectal excision in patients with locally advanced rectal cancer. *Ann Oncol* 2012; **23:** 2627-33. doi: 10.1093/annonc/mds056

26. Fernandez-Martos C, Garcia-Albeniz X, Pericay C, Maurel J, Aparicio J, Montagut C, et al. Chemoradiation, surgery and adjuvant chemotherapy versus induction chemotherapy followed by chemoradiation and surgery: long-term results of the Spanish GCR-3 phase II randomized trial. *Ann Oncol* 2015; **26:** 1722–8. doi: 10.1093/annonc/mdv223

27. Zampino MG, Magni E, Leonardi MC, Petazzi E, Santoro L, Luca F, et al. Capecitabine initially concomitant to radiotherapy then perioperatively administered in locally advanced rectal cancer. *Int J Radiat Oncol Biol Phys* 2009; **75:** 421-7. doi: 10.1016/j.ijrobp.2008.11.002

research article

Is postmastectomy radiotherapy really needed in breast cancer patients with many positive axillary lymph nodes?

Tanja Marinko, Karmen Stanic

Department for Radiotherapy, Institute of Oncology Ljubljana, Ljubljana, Slovenia

Radiol Oncol 2018; 52(3): 275-280.

Received: 13 December 2017
Accepted: 21 December 2017

Correspondence to: Assist. Karmen Stanič, M.D., Ph.D., Institute of Oncology Ljubljana, Zaloška 2, SI-1000 Ljubljana, Slovenia.
Phone: +386 1 5879 502; Fax: +386 1 5879 400; E-mail: kstanic@onko-i.si

Disclosure: No potential conflicts of interest were disclosed.

Background. Postmastectomy radiotherapy (PMRT) improves survival by eliminating potential occult lesions in the chest wall and lymphatic drainage area. Meta-analysis has shown that PMRT reduces mortality and local recurrence of patients with node positive breast cancer, but there is no specific data about the effectiveness of PMRT in a subgroup of patients with a high number of positive axillary lymph nodes (PALN). The aim of the study was to analyse the impact of the number of PALN on local and distant metastasis occurrence, overall survival (OS) and distant metastases free survival (DMFS) in patients treated with PMRT.

Patients and methods. We reviewed medical records of 129 consecutive breast cancer patients with PALN, treated at Institute of Oncology Ljubljana with PMRT between January 2003 and December 2004. We grouped patients according to the number of PALN as follows: Group 1 (less than 15 PALN) and Group 2 with more than 15 PALN. All patients received adjuvant systemic therapy according to the clinical guidelines. We analysed number of locoregional (LR) recurrences, distant metastasis, overall survival (OS), progression free survival (PFS) and DMFS.

Results. After the median follow-up time of 11.5 years, the Kaplan-Meier survival analysis of PALN showed significantly shorter OS ($p = 0.006$), shorter PFS ($p = 0.002$) and shorter DMFS ($p < 0.001$) in the group of > 15 PALN. Only one LR was found in the group of patients with more than 15 PALN. In multivariate analysis more than 15 PALN and treatment with anthracycline chemotherapy statistically significantly influenced OS and DMFS. For PFS presence of more than 15 PALN were the only independent factor of shorter survival.

Conclusions. Patients with more than 15 PALN have shorter DMFS, PFS and OS as compared to patients with less than 15 PALN, though they receive the same LR treatment. More studies with higher number of patients included are needed to further evaluate our findings.

Key words: breast cancer; postmastectomy radiotherapy; positive axillary lymph nodes

Introduction

The aim of postmastectomy radiotherapy (PMRT) in breast cancer patients is to improve loco-regional (LR) control and survival by eliminating potential occult lesions in the chest wall and lymphatic drainage area. These benefits have been consistently reported in multiple studies.[1-3] Meta-analysis, made by Early Breast Cancer Trialists' Collaborative Group (EBCTCG), published in Lancet in 2014, has shown that PMRT reduces recurrence and breast cancer mortality in women with one to three positive lymph nodes.[4] There is almost no doubt that the group of breast cancer patients with more than 3 positive axillary lymph nodes (PALN) benefit from PMRT, but it is questionable if the benefit is the same all over the described group.[2] Currently, inadequate data exist to provide answer to this question.

According to our clinical experience, we assumed that patients with many PALN might have a greater chance of already present micrometastatic disease and therefore a greater chance for distant spread than for LR relapse. However, existing TNM classification with 10 lymph nodes as the lower limit of the group with the highest number of PALN might not correspond appropriately to or clinical experiences as it seems to be set too low.[5] Majority of breast cancer patients treated with mastectomy receive systemic therapy within the frame of radical treatment, with impact also on potential subclinical LR lesions, destroying them before they become clinically evident and symptomatic. Moreover, at the time of eventual distant spread, patients receive another line of systemic treatment, which again impact also on potential subclinical LR lesions.

Even though all patients in the studied group received the same kind of LR treatment, we anticipated that patients with many PALN would have less LR relapses than group of patients with smaller number of PALN. We also hypothesized that patients with many PALN might have shorter overall survival and distant metastasis free survival.

In addition to proven benefits, radiation therapy (RT) also has its known side effects. Those need to be over weighted with a benefit of the treatment. Among long known toxicities of RT are skin changes, secondary tumours and lately highly reported cardio-toxic effects.[6-9] In multimodality treatment specific toxicities of each treatment are potentiated, therefore benefit of RT in patients with many PALN should be addressed.

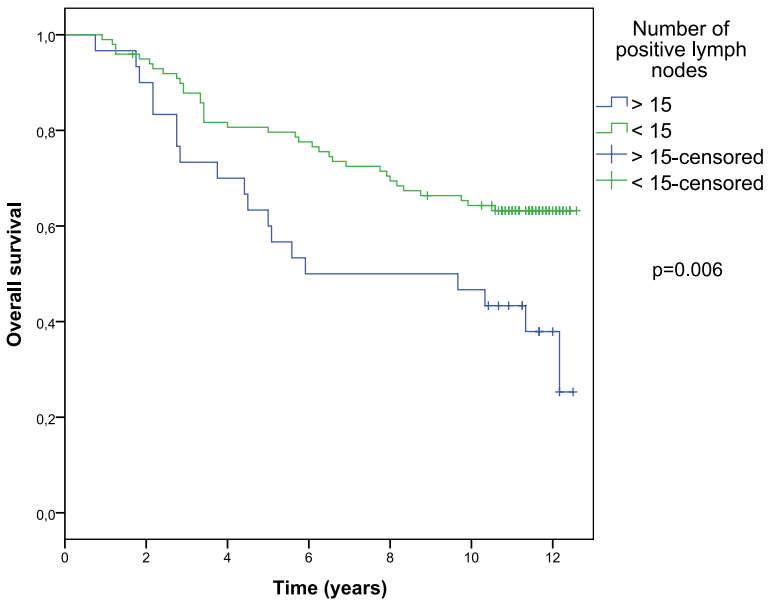

FIGURE 1. Overall survival according to number of positive axillary lymph nodes.

Patients and methods

We reviewed medical records of 129 consecutive breast cancer patients with PALN who were treated at the Institute of Oncology Ljubljana with PMRT between January 2003 and December 2004. All the patients received RT to the thoracic wall and ipsilateral periclavicular region according to clinical guidelines. External beam irradiation was delivered with photons and/or electrons with a total dose of 48 Gy–56 Gy in 5 daily fractions per week.

We grouped patients according to the number of PALN in groups with a low and that with a high number of PALN. Our clinical experiences suggest that the lower limit for N3 class in TNM classification is set too low to reliably predict a greater chance of a distant recurrence.[5]

Therefore, we performed the following grouping for local recurrence: Group 1 (1–3 PALN); Group 2 (4–15 PALN); Group 3 (more than 15 PALN). In further analysis we compared only patients with more than 15 (Group 1) to less than 15 PALN (Group 2).

All patients received adjuvant systemic therapy according to the clinical guidelines. At that time treatment with trastuzumab has not been a part of standard adjuvant treatment yet. However, HER2 was determined in all patients. Additional variables were age, tumour histology, tumour grade, tumour size, estrogen receptor (ER) status, progesterone receptor status (PR), lympho-vascular invasion, peri-neural invasion, adjuvant hormonal therapy, adjuvant chemotherapy and intrinsic subtypes. Breast cancer subtypes were defined based on 2015 St. Gallen Consensus Conference classification but without information on Ki-67, as routine testing was not available at that time, as follows: Luminal A (ER positive, HER2 negative, PR > 20% positive), luminal B (ER positive, HER2 positive or negative, PR < 20%), HER2-overexpression (HER2 positive, ER negative, PR negative), triple negative breast cancer (TNBC) or basal like (ER negative, PR negative, HER2 negative).[10]

Data was analysed with respect to overall survival (OS), progression free survival (PFS) distant metastasis free survival (DMFS) and locoregional free survival (LRFS).

Statistical analysis and ethical consideration

OS time was calculated from the date of surgery to the date of death or last follow up. PFS time was calculated from the date of surgery to the time of first progression, either locoregional or distant. LRFS was calculated from the date of surgery to the first LR progression and DMFS to the event of first distant metastasis. Kaplan-Meier methods were used to estimate survival curves. Log rank tests were used for univariate analysis to compare the survival contribution. In multivariate Cox regression only variables with $p < 0.2$ from univariate analysis were included. Data was calculated using SPSS v.20 statistical package. All p values reported were based on the two-sided hypothesis and were considered statistical significant for values < 0.05 and 95% confidence interval (CI) of hazard ratio (HR) that did not include 1.

The study has been approved by Institutional Review Board Committee and Ethics Committee and conducted in accordance with the declaration of Helsinki.

Results

The median follow-up time was 11.5 years. Patients' characteristics are presented in Table 1. Median age of breast cancer patients was 56 years and majority had invasive ductal carcinoma (80.7%). Beside to mastectomy, patients also had lymph node dissection. Mean number of examined lymph nodes was 19 (SD 8.1). With respect to breast cancer subtype Luminal A was predominant (47.3%), followed by luminal B (31%), HER2 group (12.4%) and TNBC (9.3%). HER2 positive patients were present in 28.7%. All ER positive patients (77.5%) received hormonal therapy (HT). Adjuvant chemotherapy was delivered to 83% of patients.

Kaplan-Meier survival analysis for lymph node groups with > 15 PALN (30 patients) *vs.* < 15 PALN (99 patients) showed significant difference in median OS survival. For the group with > 15 PALN was 5.9 years (SD 3.6), while for the group with < 15 PALN median time was not reached at the time of analysis ($p = 0.006$) as shown on Figure 1. The number of LR recurrences occurred as follows: 5 (17%) in group with 1–3 PALN, 4 (5.7%) in group 4–15 PALN and the lowest number was in the group with the highest number of PALN–Group 3; only 1 recurrence (3.3%). Further analysis was not performed due to low number of events. Distant me-

TABLE 1. Patients' characteristics

Patients characteristics	No patients	%
	129	100
Age (years)		
Median	56	
Q1-Q3	48-64	
Histology		
IDC	104	80.7
ILC	25	19.3
Tumour size		
T1	29	9.3
T2	79	45.7
T3	21	45.0
Histological grade		
G1	12	9.3
G2	59	45.7
G3	58	45.0
Lymphovascular invasion		
Yes	54	41.9
No	64	49.6
N/A	11	8.5
Perineural invasion		
Yes	20	15.5
No	83	64.3
N/A	26	20.2
No. of positive axillary lymph nodes (PALN)		
1-3	29	22.5
4-15	70	54.3
>15	30	23.2
No. of PALN according to N category		
N1	29	22.5
N2	47	36.5
N3	53	41.0
Estrogen receptor		
Positive	100	77.5
Negative	29	22.5
Progesteron receptor		
Positive	85	65.9
Negative	44	34.1
HER–2 overexpression		
Positive	37	28.7
Negative	92	71.3
Adjuvant hormone therapy		
Yes	101	78.3
No	28	21.7
Adjuvant chemotherapy		
Yes	108	83.7
No	21	16.3
Adjuvant chemotherapy with anthracyclines		
Yes	99	76.7
No	30	23.2
Breast cancer subtype		
Luminal A	61	47.3
Luminal B	40	31.0
Her2-overexpression	16	12.4
Triple negative breast cancer (TNBC)	12	9.3

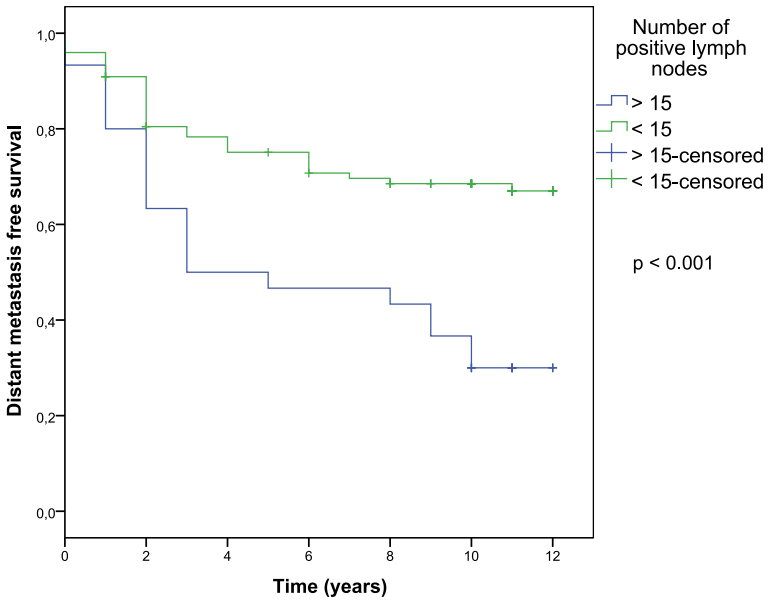

FIGURE 2. Distant metastasis free survival according to number of positive axillary lymph nodes.

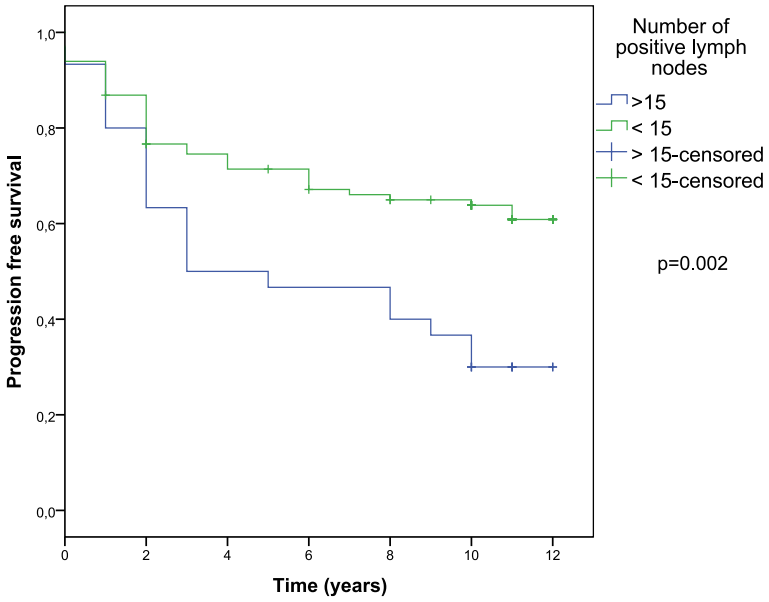

FIGURE 3. Progression free survival according to number of positive axillary lymph nodes.

tastases developed in 52 patients with no statistical difference between groups with more than 15 *vs*. less than 15 PALN (p = 0.48). Patients with the high number of PALN had significantly shorter DMFS (median 3.0 years, CI 0.1–8.3; for the group with < 15 PALN not reached; p < 0.001) and PFS (median 3.0 years, CI 0.1–7.6; for the group with < 15 PALN not reached; p < 0.002) (Figure 2, 3).

Multivariate analysis showed two variables with significant influence on OS, adjuvant chemotherapy with anthracyclines (p = 0.005, HR = 0.39, CI 0.20–0.75) and group of patients with more than 15 positive PALN (p = 0.002, HR = 2.52, CI 1.38–4.57). For PFS only more than 15 PALN showed significant influence (p = 0.003, HR = 2.24). None of the investigated factors independently influenced LRF. Adjuvant chemotherapy with anthracyclines (HR = 0.51) and more than 15 PALN (HR 3.05) were also statistically significant for DMFS. We found no significant influence of the breast cancer subtypes on any of the categories analysed.

Discussion

Patients with more than 15 PALN had shorter PFS, OS and DMFS. On the other hand, treatment with anthracyclines showed increased DMFS and OS. In our analysis only one patient experienced LR in the group with more than 15 PALN.

Published data provides evidence that the most significant prognostic factor for OS in patients with early-stage breast cancer is the presence or absence of axillary lymph node involvement. Furthermore, there is a direct relationship between the number of involved axillary nodes and the risk for distant recurrence.[11,12] More than three decades ago Fisher *et al*. reported that the 5-year OS for patients with node-negative disease was 82.8% compared with 73% for 1–3 positive nodes, 45.7% for 4–12 positive nodes, and 28.4% for ≥13 positive nodes.[13] Nowadays we use more potential systemic therapy and there are substantial improvements in OS of patients with clinically localized breast cancer.[14] But in spite of better systemic treatment, the number of PALN remains a negative prognostic factor for breast cancer patients.

The impact of local therapy on survival of patients with breast cancer has been debated for decades. In breast cancer, three theories of cancer spread in breast cancer exist.[15] More than hundred years ago dr. Wiliam Halsted believed that breast cancer begins as a strictly local disease and that tumour cells only spread haematogenously to other organs at a later stage.[16] Unfortunately, only 12% of patients treated with radical mastectomy, survived 10 years. The poor outcome with the Halstedian approach, as well as the observation that 20%–30% of node-negative patients ultimately develop metastatic disease, led to the »systemic view« theory, proposed by dr. Bernard Fisher.[17,18] He believed that breast cancer is systemic disease and if distant

metastases were destined to develop, such metastases already exist at the time of diagnosis of the breast cancer.

Neither Halstedian nor the systemic view could have explained the course of the disease for all breast cancer.[15] A third hypothesis, the "spectrum" theory, synthesized aspects of both opposing approaches. As Punglia *et al.* wrote in their article, »this theory holds that for many breast cancers there is a time when tumor cells have not metastasized to distant sites but that it is generally not known whether this time has passed at the point of diagnosis for any patient«. They also wrote that this theory acknowledges that the greater the likelihood that systemic spread has occurred at the time of diagnosis in a patient, the lower the likelihood that local therapy will influence the patient's survival.[15] The results of our analysis are in accordance with their theory showing that patients with higher number of PALN have low number of LR recurrences and greater likelihood for shorter OS.[11,12,13] With regards to the spectrum theory and explanation of Punglia *et al.*, it seems that in the subgroup of patients with many PALN local treatment has a minor impact.

Punglia *et al.* also pointed out, that contribution of improved LR control to survival depends on the effectiveness of systemic treatment.[15] Later on, Poortmans added to this factor also the component of metastatic risk of primary tumour and he concluded that with combining both components, the contribution of improved LR treatment to the final outcome can be estimated.[19] We agree that metastatic potential of different breast cancer tumours is very heterogenic, as is disease itself. It is well known that different breast cancer subtypes have different OS and in our opinion this is the component that really needs to be explored.[20] However, in our analysis we didn't show any significant difference in breast cancer subgroups regarding PALN and OS, probably due to small number of patients in each subgroup.

Based on our analysis, it seems that our results fit best to the spectrum theory. We grouped patients according to the number of PALN in groups with a low and that with a high number of PALN. Interestingly, Fisher in his article grouped patients very similar as we did.[13] It seems that if the number of PALN is very high, the chance of haematogenic relapse at distant sites is higher than the chance of lymphogenic local relapse and the time to evident haematogenic distant metastases is shorter than the time to local lymphogenic relapse which is in line with the theory of Punglia and collegues.[15] Finally, it is also in concordance with the results of our multivariate analysis, showing that adjuvant chemotherapy with antracyclines and more than 15 PALN predict for shorter DMFS.

Our study was limited with a small number of patients. According to clinical guidelines, all patients with a high number of PALN are treated with PMRT; therefore, it was not possible to compare studied patients with a cohort treated without RT. For the future, trials comparing our results with a cohort of patients treated also with adjuvant trastuzumab would be interesting. Trastuzumab, with proven important impact on overall survival, became a part of adjuvant treatment in 2005, soon after our cohort was treated.[21] We assume that it might further diminish a need for PMRT in HER2 positive breast cancer patients due to its very potent systemic effectiveness.

Conclusions

Patients with more than 15 PALN have shorter OS, PFS and DMFS compared to patients with less than 15 PALN though they receive the same LR therapy. They also have the smallest number of LR recurrences. Our results suggest that systemic treatment with anthracyclines is important component of adjuvant treatment for patients with higher number of PALN and radiation treatment might be questionable in this group, but studies with larger number of patients would be needed to answer this question.

References

1. Danish Breast Cancer Cooperative Group, Nielsen HM, Overgaard M, Grau C, Jensen AR, Overgaard J. Study of failure pattern among high-risk breast cancer patients with or without postmastectomy radiotherapy in addition to adjuvant systemic therapy: long-term results from the Danish Breast Cancer Cooperative Group DBCG 82 b and c randomized studies. *J Clin Oncol* 2006; **24:** 2268-75. doi: 10.1200/JCO.2005.02.8738
2. Clarke M, Collins R, Darby S, Davies C, Elphinstone P, Evans V, et al. Effects of radiotherapy and of differences in the extent of surgery for early breast cancer on local recurrence and 15-year survival: an overview of the randomised trials. *Lancet* 2005; **366:** 2087-106. doi: 10.1016/S0140-6736(05)67887-7
3. Ragaz J, Olivotto IA, Spinelli JJ, Phillips N, Jackson SM, Wilson KS, et al. Locoregional radiation therapy in patients with high-risk breast cancer receiving adjuvant chemotherapy: 20-year results of the British Columbia randomized trial. *J Natl Cancer Inst* 2005; **97:** 116-26. doi: 10.1093/jnci/djh297
4. EBCTCG (Early Breast Cancer Trialists' Collaborative Group). Effect of radiotherapy after mastectomy and axillary surgery on 10-year recurrence and 20-year breast cancer mortality: meta-analysis of individual patient data for 8135 women in 22 randomised trials. *Lancet* 2014; **383:** 2127-35. doi: 10.1016/S0140-6736(14)60488-8
5. Coates AS, Winer EP, Goldhirsch A, Gelber RD, Gnant M, Piccart-Gebhart M, et al. Tailoring therapies - improving the management of early breast cancer: St Gallen International Expert Consensus on the Primary Therapy of Early Breast Cancer 2015. *Ann Oncol* 2015; **26:** 1533-46. doi: 10.1093/annonc/mdv221

6. Darby SC, McGale P, Taylor CW, Peto R. Long-term mortality from heart disease and lung cancer after radiotherapy for early breast cancer: prospective cohort study of about 300,000 women in US SEER cancer registries. *Lancet Oncol* 2005; **6:** 557-65. doi: 10.1016/S1470-2045(05)70251-5

7. Darby SC, Ewertz M, McGale P, Bennet AM, Blom-Goldman U, Brønnum D, et al. Risk of ischemic heart disease in women after radiotherapy for breast cancer. *N Engl J Med* 2013; **368:** 987-98. doi: 10.1056/NEJMoa1209825

8. Marinko T, Borstnar S, Blagus R, Dolenc J, Bilban-Jakopin C. Early cardiotoxicity after adjuvant concomitant treatment with radiotherapy and trastuzumab in patients with breast cancer. *Radiol Oncol* 2018; **52:** 204-212. doi: 10.2478/raon-2018-0011

9. Sardar P, Kundu A, Chatterjee S, Nohria A, Nairooz R, Bangalore S, et al. Long-term cardiovascular mortality after radiotherapy for breast cancer: a systematic review and meta-analysis. *Clin Cardiol* 2017; **40:** 73-81. doi: 10.1002/clc.22631

10. Union Against Cancer (UICC). *TNM classification of malignant tumours.* Sobin LH, Gospodarowicz MK, Wittekind C, editors. 7th edition. Chichester, UK: Wiley-Blackwell; 2009.

11. Saez RA, McGuire WL, Clark GM. Prognostic factors in breast cancer. *Semin Surg Oncol* 1989; **5:** 102-10.

12. Nemoto T, Natarajan N, Bedwani R, Vana J, Murphy GP. Breast cancer in the medial half. Results of 1978 National Survey of the American College of Surgeons. *Cancer* 1983; **51:** 1333-8. doi: 10.1002/1097-0142(19830415)51:8<1333::AID-CNCR2820510802>3.0.CO;2-T

13. Fisher B, Bauer M, Wickerham DL, Redmond CK, Fisher ER, Cruz AB, et al. Relation of number of positive axillary nodes to the prognosis of patients with primary breast cancer. An NSABP update. *Cancer* 1983; **52:** 1551-7. doi: 10.1002/1097-0142(19831101)52:9<1551::AID-CNCR2820520902>3.0.CO;2-3

14. Early Breast Cancer Trialists' Collaborative Group (EBCTCG). Effects of chemotherapy and hormonal therapy for early breast cancer on recurrence and 15-year survival: an overview of the randomised trials. *Lancet* 2005; **365:** 1687-717. doi: 10.1016/S0140-6736(05)66544-0

15. Punglia RS, Morrow M, Winer EP, Harris JR. Local therapy and survival in breast cancer. *N Engl J Med* 2007; **356:** 2399-405. doi: 10.1056/NEJMra065241

16. Halsted WS. I. The results of radical operations for the cure of carcinoma of the breast. *Ann Surg* 1907; **46:** 1-19. doi: 10.1097/SLA.0b013e31824b7e35

17. Fisher B, Gebhardt MC. The evolution of breast cancer surgery: past, present, and future. *Semin Oncol* 1978; **5:** 385-94.

18. Cianfrocca M, Goldstein LJ. Prognostic and predictive factors in early-stage breast cancer. *Oncologist* 2004; **9:** 606-16. doi: 10.1634/theoncologist.9-6-606

19. Poortmans P. Postmastectomy radiation in breast cancer with one to three involved lymph nodes: ending the debate. *Lancet* 2014; **383:** 2104-6. doi: 10.1016/S0140-6736(14)60192-6

20. Haque R, Ahmed SA, Inzhakova G, Shi J, Avila C, Polikoff J, et al. Impact of breast cancer subtypes and treatment on survival: an analysis spanning two decades. *Cancer Epidemiol Biomarkers Prev* 2012; **21:** 1848-55. doi: 10.1158/1055-9965.EPI-12-0474

21. Cameron D, Piccart-Gebhart MJ, Gelber RD, Procter M, Goldhirsch A, de Azambuja E, et al. 11 years' follow-up of trastuzumab after adjuvant chemotherapy in HER2-positive early breast cancer: final analysis of the HERceptin Adjuvant (HERA) trial. *Lancet* 2017; **389:** 1195-205. doi: 10.1016/S0140-6736(16)32616-2

research article

Long-term survival of locally advanced stage III non-small cell lung cancer patients treated with chemoradiotherapy and perspectives for the treatment with immunotherapy

Martina Vrankar, Karmen Stanic

Institute of Oncology Ljubljana, Ljubljana, Slovenia

Radiol Oncol 2018; 52(3): 281-288.

Received: 22 November 2017
Accepted: 30 November 2017

Correspondence to: Assist. Karmen Stanič, M.D., Ph.D., Institute of Oncology Ljubljana, Zaloška 2, 1000 Ljubljana, Slovenia.
Phone: +386 1 5879 51; Fax: +386 1 5879 400; E-mail: kstanic@onko-i.si

Disclosure: No potential conflicts of interest were disclosed

Background. Standard treatment for patients with inoperable locally advanced non-small cell lung cancer (NSCLC) is concurrent chemoradiotherapy (CCRT). Five-year overall survival rates range between 15 and 25%, while long term survival data are rarely reported.

Patients and methods. A total of 102 patients with stage III NSCLC treated between September 2005 and November 2010 with induction chemotherapy and CCRT were included in this long term survival analysis. All patients were tested for PD-L1 status and expression of PD-L1 was correlated with overall survival (OS), progression free survival (PFS) and toxicities.

Results. The median OS of all patients was 24.8 months (95% CI 18.7 to 31.0) with 10 year-survival rate of 11.2%. The median OS of patients with PD-L1 expression was 12.1 months (95% CI 0.1 to 26.2), while in patients with negative or unknown PD-L1 status was significantly longer, 25.2 months (95% CI 18.9 to 31.6), p = 0.005. The median PFS of all patients was 16.4 months (95% CI 13.0 to 19.9). PFS of patients with PD-L1 expression was 10.1 months (95% CI 0.1 to 20.4) and in patients with negative or unknown PD-L1 status was 17.9 months (95% CI 14.2 to 21.7), p = 0.003.

Conclusions. 10-year overall survival of stage III NSCLC patients after CCRT is 11.2%. PFS and OS differ with regard to PD-L1 status and are significantly shorter for patients with PD-L1 expression. New treatment with check-point inhibitors combined with RT therefore seems reasonable strategy to improve these results.

Key words: locally advanced NSCLC; survival; immunotherapy; PD-L1 expression; chemoradiotherapy

Introduction

Locally advanced non-small cell lung cancer (LA-NSCLC) patients represent one third of all patients with NSCLC.[1] Approximately 70% of NSCLC patients in stage III have inoperable disease. Standard treatment for these patients is concurrent chemoradiotherapy (CCRT).[2] Five-year overall survival rates of these subgroups are ranging between 15 and 25%. Some centres have reported encouraging five-year survival results of 30% with trimodality treatment including surgery in selected patients.[3,4] Even by escalation of radiation dose and integration of molecular targeted agents the prognosis of these patients remains poor.[5] It seems that the plateau has been reached in the treatment of patients with LA-NSCLC with different schedules of radiotherapy (RT) and chemotherapy (ChT), therefore new strategies to improve survival outcomes of these patients are desperately needed.

The programmed cell death 1 (PD-1)/programmed cell death ligand 1 (PD-L1) checkpoint inhibitors demonstrated impressive activity for the treatment of metastatic NSCLC.[6-8] Several clini-

cal trials evaluating immunotherapy and RT for NSCLC have focused on patients with metastatic disease and this combination showed the synergistic therapeutic effect.[9] Recently, for the first time in LA-NSCLC, adjuvant treatment with anti PD-L1 immunotherapy after standard treatment with CCRT showed clinically significant improvement in progression-free survival. Consolidation treatment with durvalumab did not require PD-L1 testing in this study.[10]

It is unclear whether PD-L1 testing is necessary in this patients setting. However, based on several trials in metastatic patients who responded better to immunotherapy, if the expression of PD-L1 was higher, it seems reasonable to collect as many information on expression of PD-L1 as possible.

In light of this new therapeutic options we report here almost 10-year overall survival rate of a prospective phase II study in LA-NSCLC treated with induction ChT and CCRT, in whom additional PD-L1 testing was performed. We discuss the perspectives of new treatment strategies by adding immunotherapy to the standard treatment.

Patients and methods

Patients with inoperable stage III LA- NSCLC treated with combined induction ChT and CCRT were included in this analysis. All patients were without relevant contraindications and treated with curative intent.

All patients were treated with three cycles of induction ChT followed by RT concurrent with two cycles of ChT. For induction ChT we compared two different dosages and time of application for gemcitabine: the standard i.v. dose in half hour and one fifth of the standard dose in prolonged 6-hours i.v. infusion on days 1 and 8. To all patients cisplatin on day 2 was administered. All patients continued treatment within 8 days after the last cycle of ChT with RT concurrent with cisplatin and etoposide on days 1–5 and 29–33.[11] RT was administered with a linear accelerator photon beam of 5–10 MV in 2 Gy fractions to a total dose of 60–66 Gy. Three-dimensional CT-based conformal radiation therapy was used for planning for all patients and no elective nodal volumes were included. Dosimetric parameters were generated from the dose-volume histogram (DVH).

Toxicities were assessed according to Common Terminology Criteria for Adverse Events (CTCAE) version 3.0.[12] The responses were evaluated according to Response Evaluation Criteria in Solid Tumour (RECIST) criteria version 1.0.[13] After completion of the treatment, all patients were closely followed-up.

Retrospectively, PD-L1 testing was performed from archived tumour tissue samples, collected before any tumour directed treatment. Staining threshold on either tumour cells or tumour infiltrating immune cells for PD-L1 positivity was set at 5% or higher. Ventana monoclonal antibody and an automated staining platform was used as described in our previous report.[14]

All patients were fully informed and signed the informed consent to participate in the trial. The protocol was approved by the Institutional Review Board (Institute of Oncology, Ljubljana) and by the National Committee for Medical Ethics, Ministry of Health, Republic of Slovenia.

Statistical analysis

The primary endpoints of this retrospective analysis were 10-year overall survival (OS) and OS with respect to PD-L1 expression. Secondary endpoints were progression-free survival (PFS) and long term update of safety profile.

OS was calculated as the time from the start of the treatment to death from any cause. PFS was defined as the time from the beginning of treatment to disease progression or death. Censoring was defined as the time from the beginning of treatment to the last contact with the patient and for alive patients, as the time from the beginning of treatment to the end of follow-up (October 2017).

OS and PFS curves were estimated by using Kaplan-Meier method and log-rank test. Chi-square test was used to compare distribution of discrete variable values between the two arms. Mann-Whitney U test was used to compare continuous variables. Z-test for the equality between two proportions was used to evaluate the difference between proportions of patients between arms. A p-value less than 0.05 was considered statistically significant.

Results

Patient characteristics

A total of 102 patients treated between September 2005 and November 2010 were included in this analysis. Patients at median age of 57 were mostly men (78.4%). More than half of patients (56.4%) had tumours in stage IIIA and squamous histology (57.8%). Detailed patient demographics according to PD-L1 expression are listed in Table 1.

Treatment delivery

Of all, only 49% of patients completed all three planned cycles of induction ChT and 45.1% of patients received 2 cycles of induction ChT. The dose intensity, measured as mean value of percentage of drug administered, was for cisplatin 87% and for gemcitabine 86.8%. After induction ChT, one patient had pulmectomy. Radical RT was completed in 85.3% of patients with doses of ≥ 60 Gy. Both therapy was completed in 52% of patients and 5.9% of patients received no concurrent ChT. The main reasons for omitting concurrent ChT were haematological toxicity and esophagitis.

Toxicity

Treatment-related acute toxicities of the induction ChT were generally well tolerated and are listed in Table 2. The most common grade 3 or 4 adverse event was neutropenia with 23.5%. No patient with febrile neutropenia was observed. Other grade 3 or 4 adverse events were rare with appearance less than 5%. One patient had grade 4 acute peripheral ischemia leading to amputation. With regard to PD-L1 status there were less thrombocytopenia grade 1,2 in PD-L1 positive patients; however, there was more acute kidney injury among them.

Treatment-related acute toxicities of CCRT were more pronounced and are listed in Table 3. The most common grade 1 and 2 adverse events were anaemia in 95.1% and esophagitis in 66.3% of patients. Most expressed grade 3 and 4 adverse events were neutropenia in 28.4% and esophagitis in 13.9%. With regard to PD-L1 status there was no anaemia grade 3,4 in PD-L1 positive patients. Significantly, more nausea and vomiting grade 3,4 were noticed among patients with PD-L1 expression.

Response and survival

The median OS of all patients was 24.8 months (95% CI 18.7–31.0) with 10 year-survival rate of 11.2% and 1,2,3,5 year-survival rate were 76.5%, 52.0%, 38.2%, 22.5%, respectively. At the time of last evaluation in October 2017, fourteen patients were still alive with the median follow-up of 117.5 months, but none with PD-L1 expression (Table 4).

The median OS of patients with PD-L1 expression was 12.1 months (95% CI 0.1–31.6; p = 0.005). OS data are shown in Figure 1.

The median PFS of all patients was 16.4 months (95% CI 13.0 to 19.9). PFS of patients with PD-L1

TABLE 1. Patients characteristics according to PD-L1 expression

	PD-L1 negative or unknown (N = 95)	PD-L1 expression (N = 7)	Total (N = 102)
Gender			
Male	74	6	80
Female	21	1	22
Age			
Median	57	59	57
Range	30–77	54–64	30–77
ECOG PS			
0	82	7	89
1	13	0	13
Histology			
Squamous	53	6	59
Adeno	23	0	23
Large cell	6	0	6
Other & unspecified	13	1	14
Stage			
IIIA	54	4	58
IIIB	41	3	44
Inoperable due to			
Extent	93	7	100
Functional	1	0	1
Refuse	1	0	1

ECOG PS = Eastern Cooperative Oncology Group performance status; PD-L1 = programmed cell death ligand 1

TABLE 2. Treatment-related toxicities of induction chemotherapy with regard to PD-L1 status

	PD-L1 negative or unknown N = 95 (%)	PD-L1 expression N = 7 (%)	p
Anaemia			
Grade 1, 2	87 (91.6)	6 (85.7)	0.780
Grade 3, 4	1 (1.1)	0	
Neutropenia			
Grade 1, 2	24 (25.5)	0	0.168
Grade 3, 4	23 (24.2)	1 (14.3)	
Thrombocytopenia			
Grade 1, 2	23 (24.5)	1 (14.3)	0.001
Grade 3, 4	0	1 (14.3)	
Acute kidney injury			
Grade 1, 2	30 (31.6)	5 (71.4)	0.045
Grade 3, 4	0	0	
Nausea/vomiting			
Grade 1, 2	34 (35.8)	5 (71.4)	0.167
Grade 3, 4	4 (4.3)	0	

PD-L1 = programmed cell death ligand 1

TABLE 3. Treatment-related toxicities of concurrent chemoradiotherapy (CCRT) with regard to PD-L1 status

		PD-L1 negative or unknown N = 94 (%)	PD-L1 expression N = 7 (%)	p
Anemia	Grade 1, 2	91 (95.8)	6 (85.7)	0.001
	Grade 3, 4	4 (4.3)	0	
Neutropenia	Grade 1, 2	27 (28.7)	2 (28.6)	0.171
	Grade 3, 4	29 (30.5)	0	
Thrombocytopenia	Grade 1, 2	48 (50.5)	2 (28.6)	0.357
	Grade 3, 4	5 (5.3)	0	
Acute kidney injury	Grade 1, 2	35 (36.8)	4 (57.1)	0.250
	Grade 3, 4	0	0	
Nausea/vomiting	Grade 1, 2	16 (17.0)	0	0.041
	Grade 3, 4	5 (5.3)	2 (28.6)	
Esophagitis	Grade 1, 2	63 (67.0)	4 (57.1)	0.500
	Grade 3, 4	12 (12.8)	2 (28.6)	
Pneumonitis	Grade 1, 2	5 (5.3)	0	0.294
	Grade 3, 4	3 (3.2)	1 (14.3)	

PD-L1 = programmed cell death ligand 1

expression was 10.1 months (95% CI 0.1–20.4) and in patients with negative or unknown PD-L1 status was 17.9 months (95% CI 14.2–21.7; p = 0.003) (Figure 2).

Discussion

This retrospective analysis in LA-NSCLC patients treated with induction ChT and CCRT resulted in median survival of 24.8 months and 10-year overall survival rate of 11.2%. Survival data are excellent and comparable even to reported data from studies with trimodality treatment that include surgery.[15] Since in Slovenia at the time of the study duration only one radiotherapy centre was active and all candidates for radical treatment were included, the present results represent 10-year national survival data of treatment in locally advanced inoperable NSCLC.

Patients with Stage III NSCLC represent the most diverse group in terms of treatment. Multimodality treatment options include combination of systemic treatment with ChT, RT and surgery.[16] For inoperable patients, combination of ChT and RT represent the best treatment options. Sequential approach has been proven inferior for survival to concurrent one in meta-analysis.[2,17] CCRT survival benefit of 4.5% at 5 years derived from 6.5% improved local control while the number of distant metastasis was the same with CCRT and sequential ChT. Therefore, further improvement of overall survival could only be achieved through better control of distant metastasis. Adding ChT, either as induction treatment before RT or as consolidation treatment after RT, has not resulted in desired clinically important improvement of overall survival.[18,19] Results with novel agents such as thyrosin kinase inhibitors of epidermal growth factor receptor and vascular endothelial growth factor monoclonal antibodies were disappointing.[5,20,21] New systemic therapies, including immunotherapy, are hoped to bring brake through results to improve treatment results.

Recently, in the study of consolidation therapy with new PD-L1 monoclonal antibody durvalumab, 11-month improvement of PFS compared to placebo was reported after definitive CCRT in LA-NSCLC.[10] This improvement was associated with better local and systemic control. PFS benefit resulted from significantly higher local objective tumour response as well as from significantly better systemic control with improved time to distant metastases and lower frequency of new lesions, including brain metastases. The benefit was observed irrespective of PD-L1 expression before treatment.

The results of improved PFS in patient treated with combination of RT and immunotherapy are not surprising. Many preclinical studies reported synergistic effects and substantial increases in local and systemic tumour control when radiation was combined with checkpoint blockade immunotherapy. Results of a preclinical study by Zeng *et al*. that observed long-term survival of the mice with intracranial glioma treated with anti-PD-1 monoclonal antibodies plus RT, showed local response as well as systemic immunologic memory in the surviving mice, as they were able to reject a secondary challenge of glioma cells.[22] Although neither PD-1 blockade nor local RT alone eradicated intracranial gliomas, the combination of both therapies generated durable responses. In a test of immunologic memory, naïve and long-term surviving mice were injected with glioma cells. All naïve mice died from the growth of the challenged glioma cells, whereas mice that received prior treatment with combined regimen rejected the glioma challenge. In this study, the combination therapy induced increased tumour infiltration by CD8+ CTLs and decreased the number of CD4+ Tregs. Similarly, many other investigators reported significantly improved local tumour control when radiotherapy was com-

TABLE 4. Median overall survival (OS) according to PD-L1 status

	PD-L1 negative or unknown N = 95	PD-L1 expression N = 7
Median OS (months)	25.2	12.1
1-year OS (%)	77.9	57.1
2-year OS (%)	54.7	14.3
3-year OS (%)	40.0	14.3
4-year OS (%)	28.4	14.3
5-year OS (%)	24.2	0
10-year OS (%)	12.1	0

PD-L1 = programmed cell death ligand 1

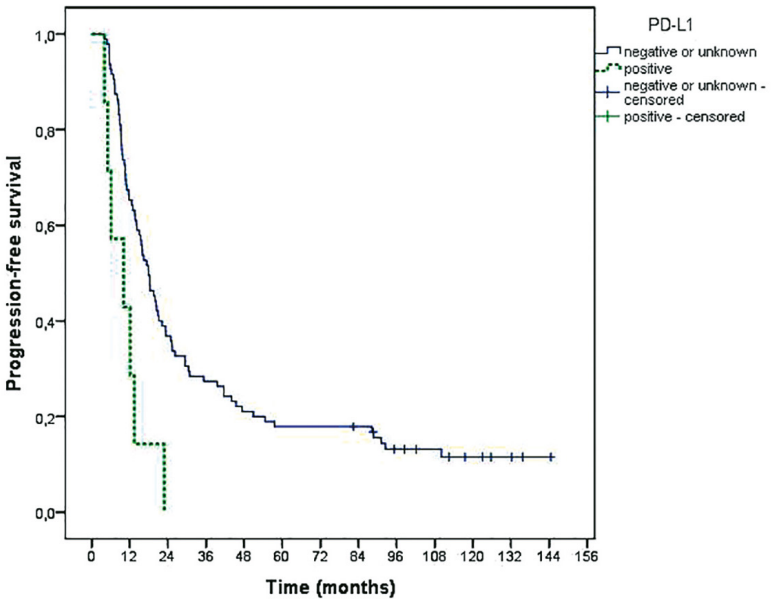

FIGURE 1. Median overall survival (OS) according to PD-L1 status.

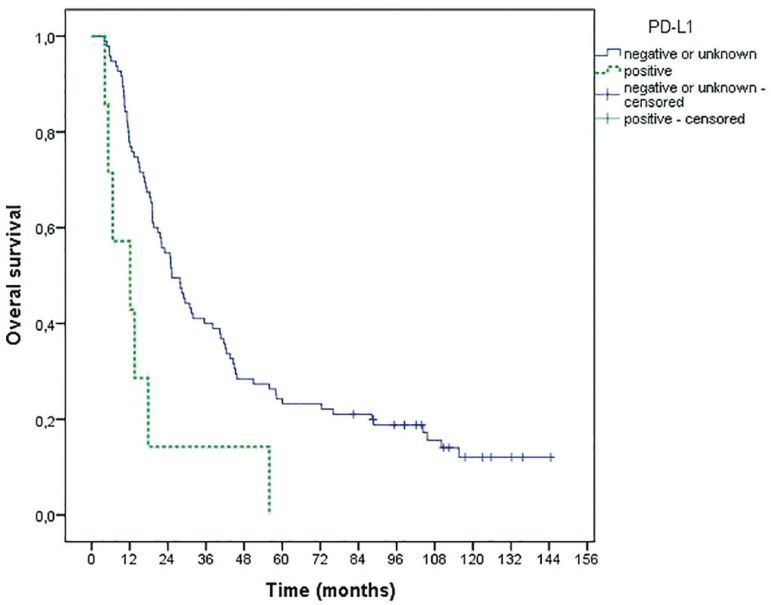

FIGURE 2. Median progression-free survival (PFS) according to PD-L1 status.

bined with anti PD-L1 in different animal models. Improved local control and long term survival was associated with increased CD8+T cells.[23,24] Sharabi *et al*. also noted enhanced proliferation and activation of endogenous antigen-specific CD8+T cells and effector memory cells in the draining lymph node.[25] These findings raise the question about the meaning of elective nodal irradiation since it might compromise the development of radiation-induced immune response. Park and colleagues noticed in models of melanoma and renal cell carcinoma that irradiation of one tumour type (renal cell carcinoma) induced protective immune responses that did not cross over to other tumour types (melanoma) in the same host.[26]

Radiation alone as a form of local therapy induce tumour cell death by direct DNA damage but also induce immunogenic cancer cell death as a consequence of modulation of multiple molecular signals in the tumour microenvironment that leads to enhanced local and systemic immune response. Radiation has both immunostimulatory and immunosuppressive effects.[27] The first step in immune response to tumour cells death from radiation is uptake and cross-presentation of tumour-derived antigens by dendritic cells (DCs). Besides enhancing the release of autologous neoantigens to the immune system, radiation also affect others mediators and mechanisms that contribute to immune cell death, such as production of type I interferon which is necessary for DC activation, calreticullin translocation, release of nuclear protein high-mobility group box-1 (HMGB1) and adenosine triphosphate (ATP).[28] Other mediators of immune response enhanced by radiation are major histocompatibility complex (MHC) class I and Fas surface expression that induces programmed cell death.[29] Radiation also increases the density of tumour-infiltrating lymphocytes. The mechanism is probable multifactorial, two main are proposed: changes in vascular endothelium that increase immune cell extravasation and enhanced expression of chemokine that affect immune cell migration and invasion.[30,31] On the contrary, radiation can also suppress the immune system by increasing the infiltration of Treg and myeloid-derived suppres-

sor cells (MDSCs) into the tumour microenvironment.[32,33] Those are responsible for down regulation of immune response. There are some other factors and pre-existing barriers that are important for tumour rejection and can be modified by radiation such as limited availability of antigen-presenting cells (like DCs). An important barrier for tumour rejection is also the poor homing of effector T cells in tumours and dysfunctional tumour vasculature which can result in low infiltration by T cells. Furthermore, number of fractions and dose per fraction also influence the immunogenic response. There are some data to suggest that traditional 2 Gy per fraction has lower impact on immune response than hypofractionation.[34]

One of the important radiation mediated response is also induced expression of PD-L1 in cancer cells and infiltrating myeloid cells.[23,24,35] PD-L1 expression is being investigated extensively in preclinical and clinical trials but so far results are not consistent since some of them indicate poor prognosis in patients with pretreatment PD-L1 expression and others reported better prognosis than in PD-L1 negative patients.[36-39] It is not clear if PD-L1 expression is prognostic or predictive factor of tumour response to treatment including the PD-1/PD-L1 pathway blockade. In most preclinical studies an increase in PD-L1 expression after radiation was reported.[23,24] Changes in expression of PD-L1 also were observed after treatment with anti-PD-L1 agents. In a study of Herbst *et al*. the PD-L1 expression increased during immunotherapy, however the levels of pretreatment tumour PD-L1 expression did not correlate with radiographic response.[40] In recent publication, Fujimoto *et al*. investigated impact of CCRT on PD-L1 expression from paired NSCLC specimens of patients that had been treated with CCRT followed by surgery.[30] In this study a total of 35 patients had sufficient material before and after CCRT for matched analysis. Of these, 22 patients had PD-L1 expression on tumour cells in the pre-CCRT specimens, and 21 patients had PD-L1 expression on tumour cells in the post-CCRT specimens. Overall, the percentage of tumour cells with PD-L1 expression significantly decreased between the pre- and post-CCRT specimens ($p = 0.024$). Sixteen patients had decreased, 15 unchanged and 4 increased PD-L1 expression after CCRT compared with that before CCRT. Of the 15 patients with unchanged PD-L1 expression, PD-L1 expression was negative in pre- and remained in post-CCRT specimens in 11 patients. PD-L1 expression in pre- and post CCRT tumour material was not significantly associated with OS, however they found significant association between the change in PD-L1 expression and survival time. The median OS of patients with decreased, unchanged, or increased PD-L1 expression was 85.1, 92.8 and 14.6 months, respectively ($p < 0.001$). They also found that the stromal CD8+ lymphocytes density increased after CCRT. They observed that patients with intermediate or high stromal CD8+ lymphocytes density in the pre- or post- CCRT material tended to have longer OS. In other studies, increased PD-L1 expression and increased number of tumour-infiltrating lymphocytes were associated with better response to PD-1/PD-L1 inhibitors. These data could be beneficial in the future for selection of appropriate patients and planning the optimal time for incorporation of immunotherapy in treatment of locally advanced NSCLC, but more data are needed for final conclusions.

All these data suggest that radiation will play an important role in the treatment of LA-NSCLC also in the future, but will be combined with new therapies such as immunotherapy. RT can act as a stimulus of the immune system with the enhanced release of tumour antigens, followed by activation and migration of dendritic cells and cross-presentation of tumour antigens that resulted in tumour specific T-cell activation and proliferation. On the other hand, PD-1/PD-L1 antibodies by blocking inhibitory signalling pathways on infiltrating T cells act as the immune system modulator on the side of subsequent immune response that can synergistically contribute to more definitive and durable both systemic and local anti-tumour action than either approach alone.

Conclusions

Long-term treatment results with CCRT for patients with LA-NSCLC in our analysis showed 10-year survival rate of 11.2%, which are comparable to published data though far from satisfactory. New treatment strategies are investigated to improve these results including treatment with check-point inhibitors. Evaluation of OS with regard to pretreatment PD-L1 status in our analysis showed that patients with PD-L1 expression had significant lower OS. This data suggest that immune system play an important role in the regulation of antitumour response to treatment.

Radiation dose, fractionation schedules and the optimal timing of immunotherapy for optimal synergy between RT and immunotherapy are the field for the future investigation.

References

1. Zadnik V, Primic Zakelj M, Lokar K, Jarm K, Ivanus U, Zagar T, et al. Cancer burden in Slovenia with the time trends analysis. *Radiol Oncol* 2017; **51:** 47-55. doi: 10.1515/raon-2017-0008
2. Aupérin A, Le Péchoux C, Rolland E, Curran WJ, Furuse K, Fournel P, et al. Meta-analysis of concomitant versus sequential radiochemotherapy in locally advanced non–small-cell lung cancer. *J Clin Oncol* 2010; **28:** 2181-90. doi: 10.1200/JCO.2009.26.2543
3. Pless M, Stupp R, Ris H-B, Stahel RA, Weder W, Thiersteinet S, et al. Induction chemoradiation in stage IIIA/N2 non-small-cell lung cancer: a phase 3 randomised trial. *Lancet* 2015; **386:** 1049-56. doi: 10.1016/S0140-6736(15)60294-X
4. Eberhardt WEE, Pöttgen C, Gauler TC, Friedel G, Veit S, Heinrichet V, et al. Phase III study of surgery versus definitive concurrent chemoradiotherapy boost in patients with resectable stage IIIA(N2) and selected IIIB non–small-cell lung cancer after induction chemotherapy and concurrent chemoradiotherapy (ESPATUE). *J Clin Oncol* 2015; **33:** 4194-201. doi: 10.1200/JCO.2015.62.6812
5. Bradley JD, Paulus R, Komaki R, Masters G, Blumenscheinet G, Schild S, et al. Standard-dose versus high-dose conformal radiotherapy with concurrent and consolidation carboplatin plus paclitaxel with or without cetuximab for patients with stage IIIA or IIIB non-small-cell lung cancer (RTOG 0617): a randomised, two-by-two factorial p. *Lancet Oncol* 2015; **16:** 187-99. doi: 10.1016/S1470-2045(14)71207-0
6. Garon EB, Naiyer AR, Hui R, Leighl N, Balmanoukian AS, Eder JP, et al. Pembrolizumab for the treatment of non–small-cell lung cancer. *N Engl J Med* 2015; **372:** 2018-28. doi: 10.1056/NEJMoa1501824
7. Brahmer J, Reckamp KL, Baas P, Crinò L, Eberhardt WEE, Poddubskaya E, et al. Nivolumab versus docetaxel in advanced squamous-cell non–small-cell lung cancer. *N Engl J Med* 2015; **373:** 123-35. doi: 10.1056/NEJMoa1504627
8. Reck M, Rodríguez-Abreu D, Robinson AG, Hui R, Csőszi T, Fülöp A, et al. Pembrolizumab versus chemotherapy for PD-L1–positive non–small-cell lung cancer. *N Engl J Med* 2016; **375:** 1823-33. doi: 10.1056/NEJMoa1606774
9. Shaverdian N, Lisberg AE, Bornazyan K, Veruttipong D, Goldman JW, Formenti SC, et al. Previous radiotherapy and the clinical activity and toxicity of pembrolizumab in the treatment of non-small-cell lung cancer: a secondary analysis of the KEYNOTE-001 phase 1 trial. *Lancet Oncol* 2017; **18:** 895-903. doi: 10.1016/S1470-2045(17)30380-7
10. Antonia SJ, Villegas A, Daniel D, Vicente D, Murakami S, Hui R, et al. Durvalumab after chemoradiotherapy in stage III non–small-cell lung cancer. *N Engl J Med* 2017; **377:** 1919-29. doi: 10.1056/NEJMoa1709937
11. Albain KS, Crowley JJ, Turrisi AT, Gandara DR, Farrar WB, Clark JI, et al. Concurrent cisplatin, etoposide, and chest radiotherapy in pathologic stage IIIB non–small-cell lung cancer: a southwest oncology group phase II study, SWOG 9019. *J Clin Oncol* 2002; **20:** 3454-60. doi: 10.1200/JCO.2002.03.055
12. National Institute of Cancer. Common terminology criteria for adverse events (CTCAE) common terminology criteria for adverse events v3.0 (CTCAE). [cited 2017 Nov 2]. Available at http://ctep.cancer.gov/protocolDevelopment/ electronic_applications/docs/ctcaev3.pdf. *NIH Publ* 2010; **2009:** 0-71. doi: 10.1080/00140139.2010.489653
13. Therasse P, Arbuck SG, Eisenhauer EA, Wanders J, Kaplan RS, Rubinstein L, et al. New guidelines to evaluate the response to treatment in solid tumors. *JNCI* 2000; **92:** 205-16. doi: 10.1093/jnci/92.3.205
14. Vrankar M, Zwitter M, Kern I, Stanic K. PD-L1 expression can be regarded as prognostic factor for survival of non-small cell lung cancer patients after chemoradiotherapy. *Neoplasma* 2018; **59:** 101-6. doi: 10.4149/neo_2018_170206N77
15. Albain KS, Swann RS, Rusch VW, Turrisi AT, Shepherd FA, Smith C, et al. Radiotherapy plus chemotherapy with or without surgical resection for stage III non-small-cell lung cancer: a phase III randomised controlled trial. *Lancet* 2009; **374:** 379-86. doi: 10.1016/S0140-6736(09)60737-6
16. Postmus PE, Kerr KM, Oudkerk M, Senan S, Waller DA, Vansteenkiste J, et al. Early and locally advanced non-small-cell lung cancer (NSCLC): ESMO Clinical Practice Guidelines for diagnosis, treatment and follow-up†. *Ann Oncol* 2017; **28 (Suppl 4):** iv1-21. doi: 10.1093/annonc/mdx222
17. Kovač V, Smrdel U. Meta-analyses of clinical trials in patients with non-small cell lung cancer. *Neoplasma* 2004; **51:** 334-40.
18. Tsujino K, Kurata T, Yamamoto S, Kawaguchi T, Kubo A, Isa S, et al. Is consolidation chemotherapy after concurrent chemo-radiotherapy beneficial for patients with locally advanced non–small-cell lung cancer?: A pooled analysis of the literature. *J Thorac Oncol* 2013; **8:** 1181-9. doi: 10.1097/JTO.0b013e3182988348
19. Luo H, Yu X, Liang N, Xie J, Deng G, Liu Q, et al. The effect of induction chemotherapy in patients with locally advanced nonsmall cell lung cancer who received chemoradiotherapy. *Medicine* 2017; **96:** e6165. doi: 10.1097/MD.0000000000006165
20. Kelly K, Chansky K, Gaspar LE, Albain KS, Jett J, Ung YC, et al. Phase III trial of maintenance gefitinib or placebo after concurrent chemoradiotherapy and docetaxel consolidation in inoperable stage III non-small-cell lung cancer: SWOG S0023. *J Clin Oncol* 2008; **26:** 2450-6. doi: 10.1200/JCO.2007.14.4824
21. Wozniak AJ, Moon J, Thomas CR, Kelly K, Mack PC, Gaspar LE, et al. A pilot trial of cisplatin/etoposide/radiotherapy followed by consolidation docetaxel and the combination of bevacizumab (NSC-704865) in patients with inoperable locally advanced stage III non–small-cell lung cancer: SWOG S0533. *Clin Lung Cancer* 2015; **16:** 340-7. doi: 10.1016/j.cllc.2014.12.014
22. Zeng J, See AP, Phallen J, Jackson CM, Belcaid Z, Ruzevick J, et al. Anti-pd-1 blockade and stereotactic radiation produce long-term survival in mice with intracranial gliomas. *Int J Radiat Oncol* 2013; **86:** 343-9. doi: 10.1016/j.ijrobp.2012.12.025
23. Deng L, Liang H, Burnette B, Beckett M, Darga T, Weichselbaum RR, et al. Irradiation and anti–PD-L1 treatment synergistically promote antitumor immunity in mice. *J Clin Invest* 2014; **124:** 687-95. doi: 10.1172/JCI67313
24. Dovedi SJ, Adlard AL, Lipowska-Bhalla G, McKenna C, Jones S, Cheadle EJ, et al. Acquired resistance to fractionated radiotherapy can be overcome by concurrent PD-L1 blockade. *Cancer Res* 2014; **74:** 5458-68. doi: 10.1158/0008-5472.CAN-14-1258
25. Sharabi AB, Lim M, DeWeese TL, Drake CG. Radiation and checkpoint blockade immunotherapy: Radiosensitisation and potential mechanisms of synergy. *Lancet Oncol* 2015; **16:** e498-509. doi: 10.1016/S1470-2045(15)00007-8
26. Park SS, Dong H, Liu X, Harrington SM, Krco CJ, Grams MP, et al. PD-1 restrains radiotherapy-induced abscopal effect. *Cancer Immunol Res* 2015; **3:** 610-9. doi: 10.1158/2326-6066.CIR-14-0138
27. Lumniczky K, Sáfrány G. The impact of radiation therapy on the antitumor immunity: local effects and systemic consequences. *Cancer Lett* 2015; **356:** 114-25. doi: 10.1016/j.canlet.2013.08.024
28. Demaria S, Golden EB, Formenti SC. Role of local radiation therapy in cancer immunotherapy. *JAMA Oncol* 2015; **1:** 1325. doi: 10.1001/jamaoncol.2015.2756
29. Derer A, Frey B, Fietkau R, Gaipl US. Immune-modulating properties of ionizing radiation: rationale for the treatment of cancer by combination radiotherapy and immune checkpoint inhibitors. *Cancer Immunol Immunother* 2016; **65:** 779-86. doi: 10.1007/s00262-015-1771-8
30. Fujimoto D, Uehara K, Sato Y, Sakanou I, Ito M, Teraoka S, et al. Alteration of PD-L1 expression and its prognostic impact after concurrent chemoradiation therapy in non-small cell lung cancer patients. *Sci Rep* 2017; **7:** 11373. doi: 10.1038/s41598-017-11949-9
31. Hallahan D, Kuchibhotla J, Wyble C. Cell adhesion molecules mediate radiation-induced leukocyte adhesion to the vascular endothelium. *Cancer Res* 1996; **56:** 5150-5.
32. Sharabi AB, Nirschl CJ, Kochel CM, Nirschl TR, Francica BJ, Velarde E, et al. Stereotactic radiation therapy augments antigen-specific PD-1-mediated antitumor immune responses via cross-presentation of tumor antigen. *Cancer Immunol Res* 2015; **3:** 345-55. doi: 10.1158/2326-6066.CIR-14-0196
33. Kachikwu EL, Iwamoto KS, Liao Y-P, DeMarco JJ, Agazaryan N, Economou J, et al. Radiation enhances regulatory T cell representation. *Int J Radiat Oncol* 2011; **81:** 1128-35. doi: 10.1016/j.ijrobp.2010.09.034
34. Reits EA, Hodge JW, Herberts CA, Groothuis TA, Chakraborty M, K.Wansley E, al. Radiation modulates the peptide repertoire, enhances MHC class I expression, and induces successful antitumor immunotherapy. *J Exp Med* 2006; **203:** 1259-71. doi: 10.1084/jem.20052494
35. Vanpouille-Box C, Diamond JM, Pilones KA, Zavadil J, Babb JS, Formenti,SC, et al. TGF is a master regulator of radiation therapy-induced antitumor immunity. *Cancer Res* 2015; **75:** 2232-42. doi: 10.1158/0008-5472.CAN-14-3511

36. Velcheti V, Schalper Ka, Carvajal DE, Anagnostou VK, Syrigos KN, Sznol M, et al. Programmed death ligand-1 expression in non-small cell lung cancer. *Lab Investig* 2014; **94:** 107-16. doi: 10.1038/labinvest.2013.130

37. Cooper WA, Tran T, Vilain RE, Madore J, Selinger CI, Kohonen-Corish M, et al. PD-L1 expression is a favorable prognostic factor in early stage non-small cell carcinoma. *Lung Cancer* 2015; **89:** 181-8. doi: 10.1016/j.lungcan.2015.05.007

38. Wang A, Wang HY, Liu Y, Zhao MC, Zhang HJ, Lu ZY, et al. The prognostic value of PD-L1 expression for non-small cell lung cancer patients: a meta-analysis. *Eur J Surg Oncol* 2015; **41:** 450-6. doi: 10.1016/j.ejso.2015.01.020

39. Zhou Z, Zhan P, Song Y. PD-L1 over-expression and survival in patients with non-small cell lung cancer: a meta-analysis. *Transl Lung Cancer Res* 2015; **4:** 203-2082015; **4:** 203-8. doi: 10.3978/j.issn.2218-6751.2015.03.02

40. Herbst RS, Soria J, Kowanetz M, Fine GD, Hamid O, Gordon MS, et al. Predictive correlates of response to the anti-PD-L1 antibody MPDL3280A in cancer patients. *Nature* 2014; **515:** 563-7. doi: 10.1038/nature14011

research article

Prevalence of BRAF, NRAS and c-KIT mutations in Slovenian patients with advanced melanoma

Maja Ebert Moltara[1], Srdjan Novakovic[2], Marko Boc[1], Marina Bucic[2], Martina Rebersek[1], Vesna Zadnik[3], Janja Ocvirk[1]

[1] Department of Medical Oncology, Institute of Oncology Ljubljana, Ljubljana, Slovenia
[2] Department of Molecular Diagnostics, Institute of Oncology Ljubljana, Ljubljana, Slovenia
[3] Epidemiology and Cancer Registry, Institute of Oncology Ljubljana, Slovenia

Radiol Oncol 2018; 52(3): 289-295.

Received 25 October 2017
Accepted 27 February 2018

Correspondence to: Assoc. Prof. Janja Ocvirk, M.D., Ph.D., Department of Medical Oncology, Institute of Oncology Ljubljana, Ljubljana, Slovenia. Phone: +386 1 5879 285; E-mail: jocvirk@onko-i.si

Disclosure: No potential conflicts of interest were disclosed.

Background. BRAF, NRAS and c-KIT mutations are characteristics of tumour tissues that influence on treatment decisions in metastatic melanoma patients. Mutation frequency and their correlation with histological characteristics in Slovenian population have not been investigated yet.

Patients and methods. In our retrospective analysis we analysed mutational status of BRAF, NRAS and c-KIT in 230 pathological samples of patients who were intended to be treated with systemic therapy due to metastatic disease at the Institute of Oncology Ljubljana between 2013 and 2016. We collected also histological characteristics of primary tumours and clinical data of patients and correlated them with mutational status of tumour samples.

Results. The study population consisted of 230 patients with a mean age 59 years (range 25−85). 141 (61.3%) were males and 89 (38.7%) females. BRAF mutations were identified in 129 (56.1%), NRAS in 31 (13.5%) and c-KIT in 3 (1.3%) tissue samples. Among the 129 patients with BRAF mutations, 114 (88.4%) patients had V600E mutation and 15 (11.6%) had V600K mutation. Patients with BRAF mutations tended to be younger at diagnosis (52 *vs.* 59 years, $p < 0.05$), patients with NRAS mutations older (61 *vs.* 55 years, $p < 0.05$). Number of c-KIT mutations were too low for any statistical correlation, but there was one out of 3 melanoma located in mucus membranes.

Conclusions. The analysis detected high rate of BRAF mutations, low NRAS mutations and low c-KIT mutations compared to previously published studies in Europe and North America. One of the main reasons for this observation is specific characteristics of study population.

Key words: BRAF; NRAS; c-KIT; prevalence

Introduction

Melanoma incidence is on the 6th place among all the cancers in Slovenia and it is constantly rising during last period.[1,2] Although early melanoma has a good prognosis, melanoma with distant metastasis carries a high mortality rate.[3] Until recently there was a lack of successful treatment approach in metastatic melanoma. Nowadays we are experiencing a new era in this field since there are several options available: immunotherapy, target therapy and chemotherapy. Still a proper adjustment of the treatment is needed according to tumour and patient characteristics.[4]

Mechanisms of melanoma development and progression are complex. There are several mutations identified, some are recognized as causative "driver" mutations (BRAF, NRAS, c-KIT, GNAQ/GNA11), others are bystander "passenger" mutations (MET, AKT3, PTEN, ...).[5] In majority of melanoma MAPK (Ras-Raf-MEK/ERK) signalling pathway is constitutively activated due to mutation in BRAF or NRAS.[5]

The most prevalent mutations in melanoma are BRAF mutations with a frequency between 40–70%[6,7], among them BRAF V600E 80–90%, BRAF V600K 5–12% and other less frequent.[6,8,9] Second most common mutations are NRAS mutations with a frequency around 15–30%.[6,9,10] BRAF and NRAS mutations are mutually exclusive. C-KIT mutations present in 5–10%.[11]

BRAF, NRAS and c-KIT mutations were correlated to pathological and clinical characteristics of melanoma.[10,12,13] Melanomas with BRAF mutations are more common in younger patients, in superficial spreading melanoma and on a skin without chronical UV skin damage.[14,15,16,17] NRAS mutations appear more frequent in older patients, in nodular melanoma and on a skin with chronical UV damage.[18,19] Majority of c-KIT mutation are found in acral lentiginous and mucosal melanomas.[11,12]

Several clinical studies confirmed the link between certain mutation status and treatment response, therefor many guidelines already recommend standard testing for BRAF, NRAS and c-KIT muatation.[4]

However, prevalence of mutation and their correlation with pathological and clinical characteristic in Slovenian patients has not been investigated till now.

Patients and methods

In retrospective study we included 230 patients with metastatic melanoma who were planned to be treated with systemic therapy between 2013–2016 at Institute of Oncology Ljubljana, the only cancer centre for treating metastatic melanoma in the country.

Patient characteristics

All data, such as patient demographics (age, gender), details of primary melanoma (date of primary diagnosis, Clark, Breslow, ulceration, mitotic rate, histological subtype, anatomic site, stage) and clinical course were obtained from archived patient medical records at the Institute of Oncology Ljubljana and from the Cancer Registry of Republic of Slovenia.

The primary melanomas were categorised as cutaneous, mucosal, uveal or occult. Anatomical site was coded as: head and neck, trunk, extremities, uveal, mucosal or occult. Histological subtypes of cutaneous melanomas were grouped for analysis as superficial spreading melanoma (SSM), nodular melanoma (NM), lentigo maligna melanomas (LMM), acral lentigo maligna (ALM), other specified and no other specified (NOS).

The study was conducted according to the Declaration of Helsinki and was approved by the medical ethics committee of Institute of Oncology Ljubljana and National Ethics Committee (approval number 46/09/16).

Tumour tissue and molecular testing

The tumour tissues (44.8% from primary and 55.2% from metastatic lesion) were recollected from archived paraffin-embedded samples. Molecular testing was performed using RT-PCR BRAF Mutation Analysis Kit II (EntroGen, Inc.), RT-PCR NRAS Mutation Analysis Kit (EntroGen, Inc.), RT-PCR RAS c.59/117 Mutation Detection Kit (EntroGen, Inc), and c-KIT Mutation Detection Kit (EntroGen, Inc.), according to manufacturer's instructions. Molecular testing for BRAF mutation was completed on all 230 samples, but for NRAS and c-KIT only on 205 samples due to the lack of tissue material.

Statistical analysis

Categorical data are described using absolute numbers and percentages, continuous by mean, minimum and maximum. For all patients, clinical and pathological features were tested for association with BRAF, NRAS and c-KIT mutation using simple cross tabulation and Pearson's χ^2 test. All the statistical analysis was performed using SPSS software, version 22.0. For all analysis, two-tailed $p < 0.05$ was considered statistical significant.

Results

Patient demographic data are shown in Table 1. A total of 230 patients with melanoma were included in the study. Mean age was 59 years (range 25–85). There were 141 (61.3%) males and 89 (38.7%) females. Location of primary melanoma lesion was skin in 167 (72.6%) cases, mucus membranes in 7 (3.0%) and uveal in 11 (4.8%). In 45 (19.6%) cases no primary tumour was found. Most common anatomical primary site of cutaneous melanoma was trunk in 91 (39.6%) cases, extremities in 52 (22.6%) cases, head and neck in 24 (10.4%) cases.

Among primary cutaneous melanomas the most common histological subtype was superficial spreading melanoma in 61 (36.6%) cases, nodular

melanoma in 45 (26.9%) cases, lentigo maligna melanoma in 4 (2.4%) cases and acral lentigo melnoma in 1 (0.6%) case, 2 (1.2%) other rare types. There were 54 (32.3%) cases of unclassified type or not otherwise specified.

The overall mutation frequency in samples analysed for all mutation (N = 205) was 146 (71.2%); for BRAF 129 (54.6%), NRAS 31 (15.1%) and c-KIT 3 (1.5%). Wild type frequency for all tested mutation was 59 (28.8%). In our study population BRAF, NRAS, c-KIT were mutually excluded in all cases.

In 25 cases only analysis of BRAF mutation was carried out, due to lack of appropriate material for additional molecular testing.

BRAF was mutated in 129 samples out of 230; 114 (49.6%) samples had V600E, 15 (6.5%) samples V600K and none had V600D mutation.

Patients with BRAF mutations tended to be younger at diagnosis compared to non-mutated (52 *vs.* 59 years old, $p<0.05$). Among BRAF mutated the oldest were those with V600K mutation compared to patients with V600E mutation (60 *vs.* 51 years old). We didn't find any statistical significant correlation between BRAF mutation and gender, anatomical location or any histological feature. We also didn't find more BRAF mutation in a group with primary metastatic patients (Table 4).

NRAS was mutated in 31 out of 205 samples. NRAS mutated patients were older at diagnosis compared to non-mutated (61 *vs.* 55 years old, $p<0.01$). We didn't find any statistical significant correlation between NRAS mutation and gender, anatomical location or any histological feature. We also didn't find more NRAS mutations in a group with primary metastatic patients (Table 4).

C-KIT was mutated in 3 (1.5%) patients, one was located on mucus membrane and two were nodular melanomas of the skin. The sample was too small to carry out further statistical analysis (Table 4).

TABLE 1. Patient demographic and clinical characteristics of primary melanoma

		Number of patient (N = 230)	% of all patient
Gender			
male		141	61.3
female		89	38.7
Age at the time of diagnosis (years)			
< 50		78	33.9
50 – 59		58	25.2
60 – 69		55	23.9
> 69		39	17.0
Location of primary tumour			
cutaneous			
	trunk	91	39.6
	extremities	52	22.6
	head and neck	24	10.4
uveal		11	4.8
mucusal		7	3.0
occult		45	19.6
Tumour stages at diagnosis			
in situ		1	0.4
localised		67	29.1
regional		116	50.5
distant		46	20.0

Discussion

Prevalence of BRAF, NRAS and c-KIT mutation varies across different regions in the world. There are several studies that have examined the prevalence of BRAF, NRAS and c-KIT and their association with tumour characteristics.[20,21,23] However, until now, we lacked detailed information about the situation in our region.

In a present study, we recorded high prevalence of BRAF mutation (56.1%) compared to majority of studies published.[9-12,16-19,23,25] During interpretation of our results we need to be aware that any direct comparison to a single study is difficult since several differences among studies exists (different study population, methods,…). To overcome some of these barriers two meta-analyses on prevalence of BRAF mutation were performed.[20,21] Their final results estimate the prevalence of BRAF mutation to around 40% in white population and even lower 19.5% in Asian.

Our results revealed that our study group does not represent general population of patient with melanoma, as well as not the most common group of patients in the majority of studies. Our cohort consists of patients with advanced melanoma, with their own characteristics (mixed clinical subgroup, all M stages) and specific tumour features (higher rate of nodular melanoma (26.9%), worse histopathological features of primary melanoma) that had led to metastatic spread.

The evidences of a higher BRAF mutation rates in a metastatic disease already exist.[9,10,18,21,23] In a

TABLE 2. Histopathological characteristic of cutaneous melanoma (N = 167)

	Number of patient (N = 167)	% of all patient	Mean	Range
Melanoma subtype				
SSM	61	36.6		
NM	45	26.9		
ALM	1	0.6		
LMM	4	2.4		
NOS	54	32.3		
Other	2	1.2		
Clark			3.8	(2.0–5.0)
Breslow			4.8	(0.2–48.0)
Mitotic index			8.4	(0.0–60.0)
Ulceration	81	48.5		

ALM = acral lentigo maligna; LMM = lentigo maligna melanomas; NOS = not other specified; NM = nodular melanoma; SSM = superficial spreading melanoma

study where researchers were comparing paired samples of primary and metastatic lesion they detected differences between BRAF mutations in metastatic lesion as high as in 53% compared to the primary samples in 43%.[9] The mutation analyses in our analyses were performed from metastatic lesion in more than half of them.

We also need to be aware of the impact of various diagnostic methods used in distinct studies, their detection limit and the influence of DNA quality in formalin-fixed paraffin embedded samples.[22] The detection limit of the methods used in our study ranges from 0.25 – 3.0% of mutated DNA in the background of wild type DNA.

Among all BRAF mutations (N = 129) we observed similar distribution of V600E mutation in 88.4% and V600K mutation in 11.6% compared to results published in other studies.[18,23]

However according to higher prevalence of BRAF mutation, we have detected low frequency of NRAS (15.1%) mutation and c-KIT (1.5%) mutation compared to similar studies. All of tested mutations were mutually excluding in our study group.

In order to demonstrate the association between mutational status (BRAF, NRAS and c-KIT) and clinico-pathological characteristics we completed a correlation analysis between several data, but only association between BRAF and NRAS mutation and age reached the statistical significance of $p<0.05$. Patients with BRAF mutation were statistically significantly younger than those without BRAF mutation, patients with NRAS mutation were older than those without NRAS mutation at the time of diagnosis. This association was reported already in previously published data[23,24], but was not confirmed by metaanalysis.[20]

We have found no statistically significant association between BRAF or NRAS mutations and gender or pathological features (Breslow thickness, ulceration, regression, mitotic index).

According to anatomical tumour location, the prevalence of BRAF mutation was highest in a trunk (48.8%), followed by other locations and

TABLE 3. Mutation of BRAF, NRAS and c-KIT

	Number of wild type (%)	Number of mutation (%)	Type
BRAF (N = 230)	101 (43.9%)	129 (56.1%)	
		114 (49.6%)	V600E: Val600Glu (c.1799T>A)
		15 (6.5%)	V600K: Val600Lys (c.1798_1799GT>AA)
NRAS* (N = 205)	174 (84.9%)	31 (15.1%)	
		10 (4.9%)	c.181C>A p.(Gln61Lys)
		14 (6.7%)	c.182A>G p.(Gln61Arg)
		2 (1.0%)	c.182A>T p.(Gln61Leu)
		1 (0.5%)	c.34G>T p.(Gly12Cys)
		3 (1.5%)	c.37G>C p.(Gly13Arg)
		1 (0.5%)	c.183A>C p.(Gln61His)
c-KIT* (N = 205)	202 (98.5%)	3 (1.5%)	
	2 (1.0%)	c.1676T>C p.(Val559Ala)	
	1 (0.5%)	c.1727T>C p.(Leu576Pro)	

* in 25 cases NRAS and c-KIT analysis was not completed due to inadequact tissue samples

TABLE 4. Correlation of BRAF, NRAS, c-KIT mutation and clinico-pathological features of melanoma, all patients (N = 230)

		BRAF			NRAS			c-KIT		
		mutation	wild type	P	mutation	wild type	P	mutation	wild type	P
		129 (56.1%)	101 (43.9%)		31 (15.1%)	174 (84.9%)		3 (1.5%)	202 (98.5%)	
Age (years; mean)		52.3	59.3	**< 0.05**	61.4	54.7	**< 0.05**	63.4	54.9	**N.A.**
Gender	male	82 (63.6%)	59 (58.4%)	**0.43**	19 (61.3%)	113 (64.9%)	**0.62**	2 (66.7%)	130 (64.4%)	**N.A.**
	female	47 (36.4%)	42 (41.6%)		12 (38.7%)	61 (35.1%)		1 (33.3%)	72 (35.6%)	
Histological subtypes*										
	SSM	40 (31.0%)	21 (20.8%)	**< 0.05***	6 (19.3%)	46 (26.4%)	**0.59***	0 (0.0%)	52 (25.7%)	**N.A.**
	NM	22 (17.1%)	23 (22.8%)		10 (32.3%)	33 (19.0%)		2 (66.7%)	41 (20.3%)	
	ALM	0 (0.0%)	1 (1.0%)		0 (0.0%)	1 (0.6%)		0 (0.0%)	1 (0.5%)	
	LMM	1 (0.8%)	3 (3.0%)		0 (0.0%)	3 (1.7%)		0 (0.0%)	3 (1.5%)	
	other	3 (2.3%)	11 (10.9%)		2 (6.5%)	9 (5.1%)		1 (33.3%)	10 (5.0%)	
	NOS	63 (48.8%)	42 (41.5%)		13 (41.9%)	82 (47.2%)		0 (0.0%)	95 (47.0%)	
Site of primary										
	head and neck	12 (9.3%)	12 (11.9%)	**0.46**	1 (3.2%)	21 (12.1%)	**0.56**	0 (0.0%)	22 (10.9%)	**N.A.**
	trunk	63 (48.8%)	28 (27.8%)		10 (32.2%)	70 (40.2%)		1 (33.3%)	79 (39.1%)	
	extremities	25 (19.4%)	27 (26.7%)		12 (38.8%)	33 (19.0%)		1 (33.3%)	44 (21.7%)	
	unknown	27 (20.9%)	18 (17.8%)		8 (25.8%)	35 (20.1%)		0 (0.0%)	43 (21.3%)	
	mucosal	0 (0.0%)	7 (6.9%)		0 (0.0%)	7 (4.0%)		1 (33.3%)	6 (3.0%)	
	uveal	2 (1.6%)	9 (8.9%)		0 (0.0%)	8 (4.6%)		0 (0.0%)	8 (4.0%)	
Initially metastatic disease										
	Yes	36 (27.9%)	25 (24.8%)	**0.59**	10 (32.2%)	47 (27.0%)	**0.73**	1 (33.3%)	56 (27.7%)	**N.A.**
	No	93 (72.1%)	76 (75.2%)		21 (67.8%)	127 (73.0%)		2 (66.7%)	146 (72.3%)	

* due to low number of specified groups results should be interpreted carefully

ALM = acral lentigo maligna; LMM = lentigo maligna melanomas; N.A. = not applicable, NOS = not other specified; NM = nodular melanoma; SSM = superficial spreading melanoma

NRAS on extremities (38.8%). Associations we have observed between anatomical location and histological subtypes with mutations have been described before and are consistent with meta-analysis results.[20,21,23]

In our study group we could also notice a trend to a higher frequency of BRAF mutation in superficial spreading melanoma and higher frequency of NRAS mutation in nodular melanoma (Figure 1), but results of statistical analysis were weak due to low sample number in some of the subgroups.

Correlations of clinical-pathological features with c-KIT mutation were not performed because of a small number of cases.

Conclusions

Today we are aware, that there are distinct sets of melanoma, with several genetic alterations that lead to molecular pathways dysregulation and influence the cell growth, proliferation and differentiation. Discovery of the drugs that target those mutations significantly changed every day clinical practise. Testing for BRAF mutation is today already recommended as a standard diagnostic test before starting systemic treatment in advanced melanoma. In patients without BRAF mutation some cancer centres perform additional testing, for other less frequent mutation as NRAS and c-KIT,

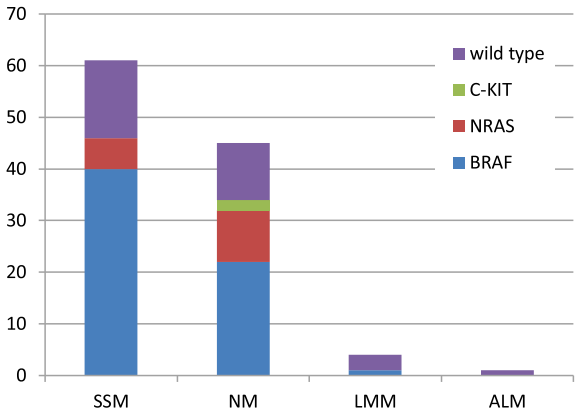

FIGURE 1. Distributions of BRAF, NRAS and c-KIT mutation according to common histological subtypes in cutaneous melanoma.

ALM = acral lentigo maligna; LMM = lentigo maligna melanomas; NOS = not other specified; NM = nodular melanoma; SSM = superficial spreading melanoma

that can further assist at how to individually adjust most appropriate systemic treatment.[25,26]

The main purpose of our study was to determine the frequency of most common mutations in melanoma and their correlation with histological characteristics in the Slovenian population. Our analysis detected higher rate of BRAF mutation, lower rate of NRAS and c-KIT mutation compared to previously published studies in Europe and North America. Explanation for such results is complex, mostly due to specific characteristic of our study group. The main consequence of high rate of BRAF mutation in our population will be a higher consumption of BRAF inhibitors. At the same time low c-KIT mutation among our population raise a question about the role and cost-benefit of implementation a c-KIT as a standard testing in our region.

Our study has limitations and results should be interpreted carefully. Our study group consist of patient with specific clinical and tumour tissue characteristics and do not represent general population. We have had also relatively small sample size and therefore some planned statistical analyses were not applicable. Therefore, the results may not be applicable for the general population of patients with melanoma in Slovenia.

Acknowledgment

The reaserch was funded by Slovenian Reaserch Agency (ARRS), grant number P3-0321.

References

1. *Cancer in Slovenia 2013.* Ljubljana: Institute of Oncology Ljubljana, Epidemiology and Cancer Registry, Cancer Registry of Republic of Slovenia; 2016.
2. Zadnik V, Primic Zakelj M, Lokar K, Jarm K, Ivanus U, Zagar T. Cancer burden in slovenia with the time trends analysis. *Radiol Oncol* 2017; **51:** 47-55. doi: 10.1515/raon-2017-0008
3. Ferlay J, Steliarova-Foucher E, Lortet-Tieulent J, Rosso S, Coebergh JWW, Comber H, et al. Cancer incidence and mortality patterns in Europe: estimates for 40 countries in 2012. *Eur J Cancer* 2013; **49:** 1374-403. doi: 10.1016/j.ejca.2012.12.027
4. Dummer R, Hauschild A, Lindenblatt N, Pentheroudakis G, Keilholz U. Cutaneous melanoma: ESMO Clinical Practice Guidelines for diagnosis, treatment and follow-up. *Ann Oncol* 2010; **21(Suppl 5):** v194-7. doi: 10.1093/annonc/mdv297
5. Shtivelman E, Davies MQ, Hwu P, Yang J, Lotem M, Oren M, et al. Pathways and therapeutic targets in melanoma. *Oncotarget* 2014; **5:** 1701-52. doi: 10.18632/oncotarget.1892
6. COSMIC, Catalogue of Somatic Mutations in Cancer. [citated 2017 Oct 10]. Available at http://cancer.sanger.ac.uk/cosmic
7. Mandalà M, Voit C. Targeting BRAF in melanoma: biological and clinical challenges. *Crit Rev Oncol Hematol* 2013; **87:** 239-55. doi: 10.1016/j.critrevonc.2013.01.003
8. McArthur GA, Chapman PB, Robert C, Larkin J, Haanen JB, Dummer R, et al. Safety and efficacy of vemurafenib in $BRAF^{V600E}$ and $BRAF^{V600K}$ mutation-positive melanoma (BRIM-3): extended follow-up of a phase 3, randomised, open-label study. *Lancet Oncol* 2014; **15:** 323-32. doi: 10.1016/S1470-2045(14)70012-9
9. Colombino M, Capone M, Lissia A, Cossu A, Rubino C, De Giorgi V, et al. BRAF/NRAS mutation frequencies among primary tumors and metastases in patients with melanoma. *J Clin Oncol* 2012; **30:** 2522-9. doi: 10.1200/JCO.2011.41.2452
10. Jakob JA, Bassett RL Jr, Ng CS, Curry JL, Joseph RW, Alvarado GC, et al. NRAS mutation status is an independent prognostic factor in metastatic melanoma. *Cancer* 2012; **118:** 4014-23. doi: 10.1002/cncr.26724
11. Curtin JA, Busam K, Pinkel D, Bastian BC. Curtin JA, et al. Somatic activation of KIT in distinct subtypes of melanoma. *J Clin Oncol* 2006; **24:** 4340-6. doi: 10.1200/JCO.2006.06.2984
12. Pracht M, Mogha A, Lespagnol A, Fautrel A, Mouchet N, Le Gall F, et al. Prognostic and predictive values of oncogenic BRAF, NRAS, c-KIT and MITF in cutaneous and mucous melanoma. *J Eur Acad Dermatol Venereol* 2015; **29:** 1530-8. doi: 10.1111/jdv.12910
13. Curtin JA, Fridlyand J, Kageshita T, Patel HN, Busam KJ, Kutzner H, et al. Distinct sets of genetic alterations in melanoma. *N Engl J Med* 2005; **353:** 2135-47. doi: 10.1056/NEJMoa050092
14. Kim SY, Kim HJ, Hahn HJ, Lee YW, Choe YB, Ahn KJ. Meanalysis of BRAF mutations and clinical-pathologiy characteistics in primary melanoma. *J Am Acad Dermatol* 2015; **72:** 1036-46.e2. doi: 10.1016/j.jaad.2015.02.1113
15. Yamazaki N, Tanaka R, Tsutsumida A, Namikawa K, Eguchi H, Omata W, et al. BRAF V600 mutations and pathological features in Japanese melanoma patients. *Melanoma Res* 2015; **25:** 9-14. doi: 10.1097/CMR.0000000000000091
16. Menzies AM, Haydu LE, Visintin L, Carlino MS, Howle JR, Thompson JF, et al. Distinguishing clinical-pathologic features of patients with V600E and V600K BRAF-mutant metastatic melanoma. *Clin Cancer Res* 2012; **18:** 3242-9. doi: 10.1158/1078-0432.CCR-12-0052
17. Bauer J, Büttner P, Murali R, Okamoto I, Kolaitis NA, Landi MT, et al. BRAF mutations in cutaneous melanoma are independently associated with age, anatomic site of the primary tumor, and the degree of solar elastosis at the primary tumor site. *Pigment Cell Melanoma Res* 2011; **24:** 345-51. doi: 10.1111/j.1755-148X.2011.00837.x
18. Carlino MS, Haydu LE, Kakavand H, Menzies AM, Hamilton AL, Yu B, et al. Correlation of BRAF and NRAS mutation status with outcome, site of distant metastasis and response to chemotherapy in metastatic melanoma. *Br J Cancer* 2014; **111:** 292-9. doi: 10.1038/bjc.2014.287

19. Devitt B, Liu W, Salemi R, Wolfe R, Kelly J, Tzen CY, et al. Clinical outcome and pathological features associated with NRAS mutation in cutaneous melanoma. *Pigment Cell Melanoma Res* 2011; **24:** 666-72. doi: 10.1111/j.1755-148X.2011.00873.x

20. Lee JH, Choi JW, Kim YS. Frequencies of BRAF and NRAS mutations are different in histological types and sites of origin of cutaneous melanoma: a meta-analysis. *Br J Dermatol* 2011; **164:** 776-84. doi: 10.1111/j.1365-2133.2010.10185.x

21. Hodis E, Watson IR, Kryukov GV, Arold ST, Imielinski M, Theurillat JP, et al. A landscape of driver mutations in melanoma. *Cell* 2012; **150:** 251-63. doi: 10.1016/j.cell.2012.06.024

22. Valachis A, Ullenhag GJ. Discrepancy in BRAF status among patients with metastatic malignant melanoma: A meta-analysis. *Eur J Cancer* 2017; **81:** 106-15. doi: 10.1016/j.ejca.2017.05.015

23. Long GV, Menzies AM, Nagrial AM, Haydu LE, Hamilton AL, Mann GJ, et al. Prognostic and clinical-pathologic associations of oncogenic BRAF in metastatic melanoma. *J Clin Oncol* 2011; **29:** 1239-46. doi: 10.1200/JCO.2010.32.4327

24. Edlundh-Rose E, Egyházi S, Omholt K, Månsson-Brahme E, Platz A, Hansson J, et al. NRAS and BRAF mutations in melanoma tumours in relation to clinical characteristics: a study based on mutation screening by pyrosequencing. *Melanoma Res* 2006; **16:** 471-8. doi: 10.1097/01.cmr.0000232300.22032.86

25. Johnson DB, Lovly CM, Flavin M, Panageas KS, Ayers GD, Zhao Z, et al. Impact of NRAS mutations for patients with advanced melanoma treated with immune therapies. *Cancer Immunol Res* 2015; **3:** 288-95. doi: 10.1158/2326-6066.CIR-14-0207.

26. Carvajal RD, Antonescu CR, Wolchok JD, Chapman PB, Roman RA, Teitcher J, et al. KIT as a therapeutic target in metastatic melanoma. *JAMA* 2011; **305:** 2327-34. doi: 10.1001/jama.2011.746

research article

Pharmacogenomic markers of glucocorticoid response in the initial phase of remission induction therapy in childhood acute lymphoblastic leukemia

Vladimir Gasic[1], Branka Zukic[1], Biljana Stankovic[1], Dragana Janic[2], Lidija Dokmanovic[2], Jelena Lazic[2], Nada Krstovski[2], Vita Dolzan[3], Janez Jazbec[4], Sonja Pavlovic[1], Nikola Kotur[1]

[1] Laboratory for Molecular Biomedicine, Institute of Molecular Genetics and Genetic Engineering, University of Belgrade, Belgrade, Serbia

[2] Department of Hematology and Oncology, University Children's Hospital, University of Belgrade, Belgrade, Serbia

[3] Pharmacogenetics Laboratory, Institute of Biochemistry, Faculty of Medicine, University of Ljubljana, Ljubljana, Slovenia

[4] Department of Oncology and Haematology, University Children's Hospital, University Medical Centre Ljubljana, Ljubljana, Slovenia

Radiol Oncol 2018; 52(3): 296-306.

Received 19 February 2018
Accepted 24 April 2018

Correspondence to: Nikola Kotur, Ph.D., Institute of Molecular Genetics and Genetic Engineering, University of Belgrade, Vojvode Stepe 444a, 11010 Belgrade, Serbia. Phone: +381 11 39 76 445; Fax: +381 11 39 75 808; E-mail: nikola.kotur@imgge.bg.ac.rs

Disclosure: No potential conflict of interest were disclosed.

Background. Response to glucocorticoid (GC) monotherapy in the initial phase of remission induction treatment in childhood acute lymphoblastic leukemia (ALL) represents important biomarker of prognosis and outcome. We aimed to study variants in several pharmacogenes (*NR3C1*, *GSTs* and *ABCB1*) that could contribute to improvement of GC response through personalization of GC therapy.

Methods. Retrospective study enrolling 122 ALL patients was carried out to analyze variants of *NR3C1* (rs33389, rs33388 and rs6198), *GSTT1* (null genotype), *GSTM1* (null genotype), *GSTP1* (rs1695 and rs1138272) and *ABCB1* (rs1128503, rs2032582 and rs1045642) genes using PCR-based methodology. The marker of GC response was blast count per microliter of peripheral blood on treatment day 8. We carried out analysis in which cut-off value for GC response was 1000 (according to Berlin-Frankfurt-Munster [BFM] protocol), as well as 100 or 0 blasts per microliter.

Results. Carriers of rare *NR3C1* rs6198 GG genotype were more likely to have blast count over 1000, than the non-carriers ($p = 0.030$). *NR3C1* CAA (rs33389-rs33388-rs6198) haplotype was associated with blast number below 1000 ($p = 0.030$). *GSTP1* GC haplotype carriers were more likely to have blast number below 1000 ($p = 0.036$), below 100 ($p = 0.028$) and to be blast negative ($p = 0.054$), while *GSTP1* GT haplotype and rs1138272 T allele carriers were more likely to be blasts positive ($p = 0.034$ and $p = 0.024$, respectively). *ABCB1* CGT (rs1128503-rs2032582-rs1045642) haplotype carriers were more likely to be blast positive ($p = 0.018$).

Conclusions. Our results have shown that *NR3C1* rs6198 variant and *GSTP1* rs1695-rs1138272 haplotype are the most promising pharmacogenomic markers of GC response in ALL patients.

Key words: pharmacogenomics; childhood ALL; glucocorticoids; glucocorticoid receptor gene; glutathione S-transferase genes; multidrug resistance 1 gene

Introduction

Acute lymphoblastic leukemia (ALL) is the most common hematological and overall malignancy in pediatrics, accounting for around 30% of all childhood cancers and around 80% of all childhood leukemias. It is one of the pediatric malignancies with the highest cure rate, exceeding 80%, when treated

with standardized protocols like the European standard, the Berlin-Frankfurt-Munster (BFM) protocol.[1-3] However, there is still more than 10% of patients with unfavorable outcome. The treatment of childhood ALL is based on risk stratification. Patients can be classified into groups according to the features that have been shown to affect prognosis and risk of treatment failure. In time, more elements are considered in order to modulate the treatment protocols and make them more efficient. Implementation of pharmacogenomics in the childhood ALL therapeutic strategy is the most promising approach to improve the outcome of childhood ALL.[4]

The four main components of ALL therapy are remission induction, consolidation, maintenance, and central nervous system-directed therapy. According to the BFM protocol, in the initial phase of the remission induction treatment of childhood ALL, glucocorticoid (GC) monotherapy is administered during the first 8 days. Its goal is to lower the number of lymphoblasts since GC have the ability to induce apoptosis in leukemic cells mediated through the glucocorticoid receptor (GR).[5] The lymphoblast count on the day 8 is one of the stratification criteria important for therapy regime and survival.[6] If the blast count in blood is below 1000/microL, the patient is declared as a GC sensitive patient or a prednisone good responder (PGR). If the peripheral blast count of a patient remains over 1000/microL, the patient is declared as GC resistant patient or a prednisone poor responder (PPR) and this is associated with a poor prognosis.

The mechanism of GC resistance in childhood ALL is still poorly understood, but genetic factors might play an important role.[7-9] Therefore, it is of great importance for better treatment of childhood ALL to investigate, understand and overcome the problems related to pharmacogenomics profile of patients with a poor response to the initial GC treatment.

The glucocorticoid receptor gene (*NR3C1*) codes the GR, which is essential for the effects of glucocorticoids to manifest. Several *NR3C1* variants, leading to altered sensibility of GR to glucocorticoids have been studied in pediatric diseases. Most frequently studied variants, like rs6189/rs6190 (ER22/23EK) and rs56149945 (N363S) have not shown significant association with the response on the day 8, when it comes to the therapeutic response to glucocorticoids in ALL.[10,11] One extensively studied variant, rs41423247 (*BclI* polymorphism), has shown association with the therapeutic response.[12]

Three variants in the *NR3C1* gene, rs33389 (c.1185-6766C>T), rs33388 (c.1185-3562A>T) and rs6198 (c.*3833A>G) have not been widely studied as pharmacogenomics markers in childhood ALL. The first two variants are located in intron 2, where they can alter consensus recognition sites for RNA splicing factors.[13] If the minor rs33389 T allele and the major rs33388 A allele are present, alternate splicing occurs and an isoform of GR with lower affinity for glucocorticoids is expressed in a higher degree.[14] In the pediatric nephrotic syndrome, the steroid response was affected by the presence of these two alleles in intron 2.[15] The rs6198 variant is located in the 3′ UTR region exon 9β, in the "ATTTA" motif of an isoform of GR with drastically lower affinity for glucocorticoids.[16] If the minor rs6198 G allele is present, the mRNA becomes more stable and it leads up to greater translation of the isoform of GR with lower affinity for glucocorticoids.[17]

Three glutathione S-transferase (GST) genes (*GSTP1*, *GSTT1*, and *GSTM1*) code the GST proteins, which are essential for GC elimination by making its first step, conjugation, possible.[18,19] Null-allele variants of *GSTM1* and *GSTT1* caused by a deletion of the gene, result in the absence of activity of these enzymes. Additionally, it was reported that *GSTP1* gene variants rs1695 (c.313A>G, p.Ile105Val) and rs1138272 (c.341C>T, p.Ala114Val) influence the activity and the structure of GSTP1 and alter the efficiency of GC conjugation, if the minor alleles are present.[20] An association between the rs1695 variant and GC response was found in ALL.[21]

The multidrug resistance 1 gene (*MDR1*, also known as *ABCB1),* encodes for a membrane transporter P-glycoprotein (P-gp), responsible for the efflux of chemotherapeutic agents used in leukemia therapy.[22] Glucocorticoids are substrates of P-gp, which transports glucocorticoids out of cells. Overexpression of P-gp could mediate GC resistance.[23] When considering *ABCB1*, three variants were often analyzed as pharmacogenomics markers for GC response (rs1128503 (c.1236C>T, p.Gly412=), rs2032582 (c.2677G>A/T, p.Ser893Ala) and rs1045642 (c.3435TC>T, p.Ile1145=)). The rs2032582 variant is a missense mutation, while rs1045642 is a synonymous mutation which leads to decreased expression of *ABCB1* gene on the intestinal cell membranes.[24] It was found that the steroid response in children with nephrotic syndrome varied based on the expression of *ABCB1* gene.[25]

There have been a few reports which dealt with the topic of pharmacogenomics of GC resistance

in adult leukemias, but they lacked conclusive evidence of a single contributing mechanism.[26] The topic of pharmacogenomics of GC resistance in ALL, when it comes to the pediatric population, has not been sufficiently studied. In the reported results, only tendencies towards association with GC response for certain genotypes[27] have been found, while most of the genetic variants, shown to be relevant for GC response, have never been studied in childhood ALL.

The aim of this study is to investigate the association between variants in *NR3C1*, *GSTP1*, *GSTT1*, *GSTM1* and *ABCB1* genes and GC therapeutic response in the initial phase of remission induction therapy of pediatric ALL patients. Also, we aimed to investigate if the analyzed pharmacogenomics markers could be helpful to achieve improved personalization of GC therapy, leading to more individualized approach. Namely, other values than 1000 of blast number on day 8 might be potentially used as a marker of therapy efficacy. For example, it has been reported that childhood ALL patients who has zero blasts on day 8 (blast negative), have longer disease-free survival than patients with detectable blasts (blast positive).[28] In order to better characterize GC response on day 8 related to analyzed genetic variants, we carried out additional analysis in which cut-off value for GC response was 100 or 0 blasts in peripheral blood. By understanding the factors which contribute to GC resistance or good response, predictions could be made for an individual patient before the initial treatment, in order to use the adequate treatment regime and increase the chances of more efficient GC response.

Patients and methods

Patients

Peripheral blood samples (n = 122) have been collected from unselected patients with the diagnosis of childhood ALL from the University Children's Hospital in Belgrade. The samples for genetic analyses were collected on the day of the diagnosis. Childhood ALL patients were diagnosed, stratified in risk groups and treated according to Berlin-Frankfurt-Munster protocols: BFM ALL IC-2002 and BFM ALL IC-2009. All patients received induction therapy with prednisone. This study was approved by the Ethics Committee of the University Children's Hospital, University of Belgrade. The study was conducted according to the principles of Declaration of Helsinki.

DNA isolation

Genomic DNA was extracted from peripheral blood samples of the participants' using a QIAamp DNA Blood Mini Kit (Qiagen, Hilden, Germany) and stored at - 20 °C until analysis.

GSTM1 and GSTT1 deletion detection

The detection of *GSTM1* and *GSTT1* homozygous deletions was performed using multiplex polymerase chain reaction (PCR), as previously described with modifications.[29] In the final reaction volume of 20 microL, 1x buffer were added, 3.875 mM of $MgCl_2$, 0.5 mM of dNTP, 0.3 microM of the forward and reverse primer for *GSTT1*, 0.25 microM of the forward and the reverse primer for *GSTM1*, 0.25 microM of forward and reverse primer for β globin gene segment (control PCR product), 1U of Taq polymerase (Hot Star polymerase, Qiagen, Hilden, Germany) and 60ng of DNA. After the initial denaturation at 95 C for 15', followed 35 cycles of 95 °C / 53 °C / 72 °C, lasting 30'', 45'' and 60'' respectively, ending with a final extension step at 72 °C lasting for 7'.

Genotyping of *ABCB1* variants

The variant rs2032582 of *ABCB1* gene was genotyped using the amplification-refractory mutation system polymerase chain reaction (ARMS PCR). A forward primer was designed for each allele specifically in order to pinpoint the exact genotype. The protocol was adapted from Kuzawski and coworkers.[30] For each patient's sample, 3 separate PCR mixes were prepared, each containing different allele specific primer. In the final reaction volume of 15 microL, 1x buffer were added, 3 mM of $MgCl_2$, 0.67 mM of dNTP, 0.3 microM of the forward (allele specific) and reverse primer, 1U of Taq polymerase (Hot Star polymerase, Qiagen, Hilden, Germany) and 60ng of DNA. The PCR program started with a 95 °C initial denaturation which lasted for 15', followed by 10 cycles of 95 °C / 60 °C / 72 °C lasting 30'', 30'' and 40'' respectively, followed by 30 cycles of 95 °C / 56 °C / 72 °C, lasting 30'', 30'' and 40'' respectively and the final step was an extension at 72 °C which endured for 5'.

Variants rs1045642 and rs1128503 of *ABCB1* were genotyped using the Kompetitive Allele Specific PCR genotyping system (KASP) (LGC, Teddington, Middlesex, UK), according to manufacturer's instructions.

Genotyping of *NR3C1* variants

Variants rs33389, rs33388 and rs6198 of *NR3C1* were genotyped using TaqMan® SNP Genotyping Assays (Thermo Fisher Scientific) according to manufacturer's instructions. The fluorofore VIC was used to detect the wild type allele, while FAM was used to detect the variant allele. For genotyping of rs33389, rs33388 and rs6198 variants, C___1032036_10, C___1046426_10 and C___8951023_10 assays were used, respectively.

Genotyping of *GSTP1* variants

Variants rs1695 and rs1138272 of *GSTP1* were detected using the KASP genotyping system according to manufacturer's instructions (LGC, Teddington, Middlesex, UK).

Statistical analysis

Hardy-Weinberg equilibrium conformance was examined using χ^2 test. Haplotype phases and frequencies were estimated using Arlequin software.[31] The associations between carrier status of specific allele or haplotype and the number of blasts at the day 8 have been analyzed in 2x2 contingency tables using the χ^2 test or the Fisher's exact test, when appropriate. Both dominant and recessive genetic model were applied when we considered single variant at the time, and stronger association with GC response was reported. Carriers of a specific haplotype were compared to all other patients with any other haplotype for each haplotype. Odds ratio with 95% confidence interval was used to assess the impact of clinical or genetic variable on GC drug response. The cut-off for statistical significance has been chosen at the value of $p = 0.05$, while the cut-off value for borderline significance has been chosen at the value of $p = 0.07$. To control for demographic and clinical difference between groups, multivariate analysis was performed using logistic regression. Correlation between continuous variables were estimated using Spearman's correlation coefficient (rs). The SPSS software package (IBM SPSS Statistics v.21) was used for statistical analyses.

Results

Demographic and clinical characteristics of childhood ALL patients on diagnosis

Out of 122 childhood ALL patients, there were 66 boys (54.1%) and the median age was 5.2 (interquartile range: 3.3–10.2) years. B-cell leukemia was represented with 108 (88.5%) cases and the rest of patients were diagnosed with T-cell leukemia. About 47% of patients had initially over 20,000 white blood cells (WBC) per microliter of blood, which is considered as unfavorable factor according to both BFM ALL IC-2002 and BFM ALL IC-2009 protocols (Table 1).

GC response on day 8

In our study, blast count per microliter of blood on day 8 was used as surrogate marker of GC response. There were thirteen patients (11%) with more than 1000 blasts/microL on day 8 of GC treatment in our cohort of patients. We have analyzed the correlation of clinical and demographic characteristics of patients with prednisone response. Namely, leukocyte count on diagnosis was positively correlated with absolute blast count on day 8 ($rs = 0.44$, $p = 0.000001$). In addition, patients suffering from T-cell leukemia were in greater risk to respond poorly to initiation GC treatment (≥ 1000 blasts/microL on day 8) (Fisher's exact test, $p = 0.043$) than B-cell leukemia patients. Furthermore, age and gender of childhood ALL patients showed borderline association with prednisone response (Table 1).

Association of gene variants with PGR and PPR according to BFM protocol

Two homozygous deletions in *GSTM1* and *GSTP1* genes were studied as well as 8 single nucleotide variants (SNV) in *NR3C1* (rs33389, rs33388 and rs6198), *GSTP1* (rs1695 and rs1138272) and *ABCB1* (rs1128503, rs2032582 and rs1045642) genes. Genotype frequencies of all analyzed SNVs conformed to HW equilibrium for the ALL cohort.

When we carried out analysis in which 1000 blasts/microL set the limit of PGR and PPR, we found some positive correlation of pharmacogenomic markers with GC response. Regarding *NR3C1* gene, our results have shown that *NR3C1* variants were associated with glucocorticoid response on day 8. Namely, rare *NR3C1* rs6198 GG genotype was associated with PPR (Fisher's exact test; $p = 0.030$) (Table 2). When estimated haplotypes of *NR3C1* gene were considered, it was found that CAA (rs33389-rs33388-rs6198) haplotype was associated with PGR (< 1000 blasts/microL) (Fisher's exact test; $p = 0.030$) (Table 3). Both associations remained significant or borderline significant when controlled for age, gender and ini-

TABLE 1. Clinical and demografic characteristics and their association with glucocorticoid (GC) response . The GC response is assesed by absolute number of blasts per mm3 of blood on day 8. Statistically significant associations (p < 0.05) were bolded

Patients characteristics	Group	Entire group	≥1000 blasts	100≤ blasts <1000	1≤ blasts <100	blast negative patients	GC response (cutoff=1000 blasts)[0]	GC response (cutoff=100 blasts)[1]	GC response (cutoff=0 blasts)[2]
		n (%)	n (%)	n (%)	n (%)	n (%)	OR [95%CI], p[0]	OR [95%CI], p[1]	OR [95%CI], p[2]
Age	≥1 and <6 (non-risk)	65 (53.3)	4 (30.8)	17 (54.8)	21 (55.3)	23 (57.5)	reference	reference	reference
	<1 or ≥6 (risk)	57 (46.7)	9 (69.2)	14 (45.2)	17 (44.7)	17 (42.5)	2.86 [0.83-9.85], 0.085	1.42 [0.68-2.98], 0.356	1.29 [0.60-2.76], 0.514
Gender	male	66 (54.1)	10 (76.9)	13 (41.9)	20 (52.6)	23 (57.5)	reference	reference	reference
	female	56 (45.9)	3 (23.1)	18 (58.1)	18 (47.4)	17 (42.5)	0.32 [0.083-1.26], 0.081	1.12 [0.54-2.35], 0.761	1.28 [0.57-2.63], 0.598
Initial WBC count*	<20,000/microL	64 (53.3)	1 (8.3)	13 (43.3)	21 (55.3)	29 (72.5)	reference	reference	reference
	≥20,000/microL	56 (46.7)	11 (91.7)	17 (56.7)	17 (44.7)	11 (27.5)	15.40 [1.92-123.6], **0.001**	3.57 [1.62-7.88], **0.001**	3.39 [1.49-7.72], **0.003**
Immunophenotype	B	108 (88.5)	9 (69.2)	27 (87.1)	35 (92.1)	37 (92.5)	reference	reference	reference
	T	14 (11.5)	4 (30.8)	4 (12.9)	3 (7.9)	3 (7.5)	4.40 [1.15-16.90], **0.043**[F]	2.67 [0.86-8.27], 0.081	1.91 [0.50-7.28], 0.546

[0] Association with prednosine response on day 8 according to Berlin-Frankfurt-Munster (BFM) protocol: prednisone poor responder (PPR) group (≥1000 blasts) vs. prednisone good responder (PGR) group (<1000 blasts)
[1] Association with number of blasts on day 8 with cut-off value of 100: higher (≥ 100 blasts) vs lower (< 100 blasts) number of blasts
[2] Association with blast status on day 8: blast positive vs blast negative patients.
[F] Fisher exact test
OR = Odds ratio between a group with higher number of blasts in comparison with a group with lower number of blasts. The group with lower number of blasts represents reference group.
CI = Confidence interval

tial WBC count (logistic regression, p = 0.036 and p = 0.052, respectively) (Tables 2 and 3).

When variants in *ABCB1* and *GST* genes were considered in relation to GC response, no significant association was found. However, when estimated haplotypes were considered, *GSTP1* GC (rs1695-rs1138272) haplotype was associated with PGR (χ^2 test, p = 0.036) (Table 3).

Additional analyses of GC response on day 8 in regard to genetic variants

Besides cut-off value of 1000 blasts/microL on day 8, used to delimit patients with good or poor GC response according to BFM protocol, other values of blast count on day 8 might be potentially used as a marker of GC response. In order to confirm importance of analyzed genetic variants to GC response, we carried out additional analyses in which cut-off value for prednisone response was 0 (blast negative) or 100 blasts in peripheral blood. In our group of childhood ALL patients, 40 (32.8%) were blast negative, while 38 (31.1%) patients had between 1 and 99 blasts/microL after 8 days of GC treatment. Initial WBC count was correlated with blast positive status and higher number of blasts (≥ 100 blasts/microL) (Table 1).

Regarding *NR3C1* gene, our results have shown that carriers of minor rs33389 T allele tended towards higher blast count (≥ 100 blasts/microL) (χ^2 test; p = 0.095), while carriers of minor rs33388 T allele tended towards lower blast count (< 100 blasts/microL) (χ^2 test; p = 0.098), but the results didn't reach statistical significance. When estimated haplotypes were considered, identical associations were obtained, because rs33389 T allele defines relatively rare TAA (rs33389-rs33388-rs6198) haplotype, while rs33388 T allele defines the most frequent CTA haplotype (Tables 2 and 3).

Additional analysis regarding *GSTP1* gene showed that carriers of minor *GSTP1* rs1138272 T allele were about 5 times more likely to be blast positive on day 8, when compared to carriers of CC genotype (χ^2 test; p = 0.024). Next, we analyzed estimated haplotypes of *GSTP1* gene consisting of rs1695 and rs1138272 variants. We found that *GSTP1* GC haplotype is associated not only with PGR, but also with lower blast count on day 8. Namely, this haplotype was associated with blast count below 100 (< 100 blasts/microL, χ^2 test; p = 0.028) and borderline associated with blast negative status (χ^2 test; p = 0.054). Also, it was shown that *GSTP1* GT haplotype is borderline associated with higher blast count (≥ 100 blasts/microL, χ^2 test; p = 0.062) and significantly associated with blast positive status (χ^2 test; p = 0.034). The majority of those associations remained significant or borderline significant when controlled for age, gender and initial WBC count employing logistic regression. Taken together, our results regarding *GSTP1* variants indicate that carriers of GC haplotype have better response to prednisone treat-

TABLE 2. Genotype frequencies and association with glucocorticoid (GC) response. The GC response is assesed taking into account absolute number of blasts per mm3 of blood on day 8. For univariate analysis, chi square test was used, unless differently stated. Dominant model was used unless differently stated. Statistically significant associations ($p < 0.05$) were bolded

Genotype	≥ 1000 blasts	100 ≤ blasts < 1000	1 ≤ blasts < 100	blast negative patients	GC response (cutoff=1000 blasts)[0]	GC response (cutoff=1000 blasts)[0, ADJ]	GC response (cutoff=100 blasts)[1]	GC response (cutoff=100 blasts)[1, ADJ]	GC response (cutoff=0 blasts)[2]	GC response (cutoff=0 blasts)[2, ADJ]
	n (%)	n (%)	n (%)	n (%)	OR[95%CI] P value	OR[95%CI] P value	OR[95%CI] P value	OR[95%CI] P value	OR[95%CI] P value	OR[95%CI] P value
NR3C1 rs33389										
CC	10 (76.9)	21 (67.7)	33 (86.8)	32 (80.0)	reference	reference	reference	reference	reference	reference
CT	3 (23.1)	9 (29.0)	4 (10.5)	6 (15.0)	1.12[0.29-4.41] 1[F]	1.10[0.21-5.92] 0.910	2.1[0.87-5.05] 0.095	1.85[0.73-4.71] 0.195	1.12[0.44-2.86] 0.805	0.89[0.32-2.44] 0.826
TT	0 (0.0)	1 (3.2)	1 (2.6)	2 (5.0)						
NR3C1 rs33388										
AA	4 (30.8)	11 (35.5)	7 (18.4)	9 (22.5)	reference	reference	reference	reference	reference	reference
AT	4 (30.8)	15 (48.4)	19 (50.0)	19 (47.5)	0.74[0.21-2.60] 0.737[F]	0.71[0.16-3.13] 0.658	0.5[0.22-1.15] 0.098	0.53[0.28-1.26] 0.148	0.79[0.32-1.92] 0.606	0.83[0.32-2.11] 0.699
TT	5 (38.5)	5 (16.1)	12 (31.6)	12 (30.0)						
NR3C1 6198										
AA	7 (53.8)	21 (67.7)	28 (73.7)	30 (75.0)	reference	reference	reference	reference	reference	reference
AG	4 (30.8)	10 (32.3)	9 (23.7)	10 (25.0)						
GG	2 (15.4)	0 (0.0)	1 (2.6)	0 (0.0)	19.64[1.65-234.32] **0.030**[R,F]	16.76[1.20-234.27] **0.036**[R]	1.66[0.75-3.68] 0.222[R]	4.01[0.34-47.4] 0.27[R]	1.04[0.99-1.08] 0.22[R]	- 1[R]
GSTP1 rs1695										
AA	7 (53.8)	15 (48.4)	16 (42.1)	16 (40.0)	reference	reference	reference	reference	reference	reference
AG	5 (38.5)	13 (41.9)	18 (47.4)	19 (47.5)	0.65[0.21-2.06] 0.46	0.91[0.26-3.25] 0.885	0.70[0.33-1.46] 0.338	0.73[0.34-1.58] 0.423	0.77[0.36-1.66] 0.508	0.84[0.37-1.9] 0.682
GG	1 (7.7)	3 (9.7)	4 (10.5)	5 (12.5)						
GSTP1 rs1138272										
CC	9 (69.2)	25 (80.6)	31 (81.6)	38 (95.0)	reference	reference	reference	reference	reference	reference
CT	3 (23.1)	6 (19.4)	7 (18.4)	2 (5.0)	2.79[0.76-10.20] 0.119[F]	3.17[0.76-13.28] 0.115	2.26[0.84-6.07] 0.122	2.23[0.81-6.15] 0.121	4.97[1.09-22.69] **0.024**	4.44[0.9-21.08] 0.060
TT	1 (7.7)	0 (0.0)	0 (0.0)	0 (0.0)						
GSTM1 homozygous deletion										
WT	6 (46.2)	13 (41.9)	18 (47.4)	19 (47.5)	reference	reference	reference	reference	reference	reference
DEL	7 (53.8)	18 (58.1)	20 (52.6)	21 (52.5)	0.99[0.31-3.13] 0.99	0.96[0.25-3.70] 0.953	1.19[0.56-2.50] 0.707	1.03[0.47-2.27] 0.941	1.0[0.51-2.38] 0.805	0.96[0.43-2.18] 0.935
GSTT1 homozygous deletion										
WT	8 (61.5)	23 (74.2)	31 (81.6)	35 (87.5)	reference	reference	reference	reference	reference	reference
DEL	5 (38.5)	8 (25.8)	7 (18.4)	5 (12.5)	2.78[0.82-9.09] 0.138[F]	3.70[0.95-14.08] 0.058	2.33[0.94-5.56] 0.063	2.39[1.03-6.25] **0.044**	2.27[0.78-6.67] 0.127	2.06[0.67-6.29] 0.202
ABCB1 rs1128503										
CC	5 (38.5)	10 (32.3)	13 (34.2)	13 (32.5)	reference	reference	reference	reference	reference	reference
CT	6 (46.2)	16 (51.6)	21 (55.3)	17 (42.5)	0.79[0.24-2.59] 0.759[F]	0.74[0.20-2.76] 0.651	0.97[0.44-2.11] 0.932	0.89[0.40-1.99] 0.773	0.92[0.41-2.07] 0.857	0.84[0.36-1.97] 0.691
TT	2 (15.4)	5 (16.1)	4 (10.5)	10 (25.0)						
ABCB1 rs2032582										
GG	5 (31.3)	9 (24.3)	15 (30.6)	14 (27.5)	reference	reference	reference	reference	reference	reference
GT	4 (25.0)	16 (43.2)	17 (34.7)	16 (31.4)	0.86[0.26-2.80] 0.769[F]	1.08[0.29-4.05] 0.908	1.27[0.58-2.78] 0.693	1.27[0.56-2.88] 0.57	0.98[0.44-2.17] 0.968	0.9[0.39-2.1] 0.813
TT	3 (18.8)	5 (13.5)	6 (12.2)	9 (17.6)						
GA	1 (6.3)	1 (2.7)	0 (0.0)	1 (2.0)						
ABCB1 rs1045642										
CC	3 (23.1)	6 (19.4)	11 (28.9)	11 (27.5)	reference	reference	reference	reference	reference	reference
CT	7 (53.8)	16 (51.6)	19 (50.0)	18 (45.0)	1.15[0.30-4.49] 1[F]	1.47[0.31-6.35] 0.657	1.53[0.63-3.70] 0.393	1.92[0.74-4.98] 0.18	1.17[0.5-2.77] 0.711	1.31[0.52-3.28] 0.559
TT	3 (23.1)	9 (29.0)	8 (21.1)	11 (27.5)						

[0] Association with prednosine response on day 8 according to Berlin-Frankfurt-Munster (BFM) protocol: prednisone poor responder (PPR) group (≥1000 blasts) vs. prednisone good responder (PGR) group (< 1000 blasts)
[1] Association with number of blasts on day 8 with cut-off value of 100: higher (≥ 100 blasts) vs lower (< 100 blasts) number of blasts
[2] Association with blast status on day 8: blast positive vs blast negative patients.
[F] Fisher exact test
[R] Recessive model
[ADJ] Adjusted for age, gender and initial white blood cells (WBC) count using logistic regression
OR = Odds ratio between a group with higher number of blasts in comparison with a group with lower number of blasts. The group with lower number of blasts represents reference group.
CI = Confidence interval

TABELE 3. Haplotype carring status and association with glucocorticoid (GC) response. The GC response is assesed taking into account absolute number of blasts per mm3 of blood on day 8. For univariate analysis, chi square test was used, unless differently stated. Statistically significant associations ($p < 0.05$) were bolded

Haplotype (estimated frequency)	Carrier status*	≥ 1000 blasts	100 ≤ blasts < 1000	1 ≤ blasts < 100	blast negative patients	GC response (cutoff=1000 blasts)[2]	GC response (cutoff=1000 blasts)[2, ADJ]	GC response (cutoff=100 blasts)[1]	GC response (cutoff=100 blasts)[1, ADJ]	GC response (cutoff=0 blasts)[0]	GC response (cutoff=0 blasts)[0, ADJ]
		n (%)	n (%)	n (%)	n (%)	OR [95%CI] p value	OR [95%CI] p value	OR [95%CI] p value	OR [95%CI] p value	OR [95%CI] p value	OR [95%CI] p value
NR3C1 (rs33389-rs33388-rs6198) haplotypes											
CTA (51.2%)	absent	4 (30.8)	11 (35.5)	7 (18.4)	9 (22.5)	reference	reference	reference	reference	reference	reference
	present	9 (69.2)	20 (64.5)	31 (81.6)	31 (77.5)	0.71[0.21-2.60] 0.737[F]	0.72[0.16-3.13] 0.658	0.50[0.22-1.15] 0.098	0.53[0.22-1.26] 0.148	0.79[0.32-1.92] 0.606	0.83[0.32-2.11] 0.699
CAA (20.5%)	absent	12 (92.3)	15 (48.4)	25 (65.8)	25 (62.5)	reference	reference	reference	reference	reference	reference
	present	1 (7.7)	16 (51.6)	13 (34.2)	15 (37.5)	0.12[0.015-0.98] **0.030**[F]	0.12[0.013-1.02] 0.052	1.12[0.52-2.41] 0.763	1.27[0.57-2.80] 0.561	0.96[0.44-2.1] 0.922	1.22[0.53-2.80] 0.643
CAG (16.0%)	absent	7 (53.8)	20 (64.5)	28 (73.7)	29 (72.5)	reference	reference	reference	reference	reference	reference
	present	6 (46.2)	11 (35.5)	10 (26.3)	11 (27.5)	2.06[0.64-6.62] 0.222[F]	1.82[0.49-6.74] 0.372	1.71[0.78-3.75] 0.18	1.60[0.70-3.65] 0.262	1.29[0.56-2.97] 0.543	1.28[0.53-3.1],0.576
TAA (12.3%)	absent	10 (76.9)	21 (67.7)	33 (86.8)	32 (80.0)	reference	reference	reference	reference	reference	reference
	present	3 (23.1)	10 (32.3)	5 (13.2)	8 (20.0)	1.12[0.29-4.41] 1.000[F]	1.10[0.21-5.92] 0.91	2.10[0.87-5.05] 0.095	1.85[0.73-4.71] 0.195	1.12[0.44-2.86] 0.805	0.89[0.32-2.44] 0.826
GSTP1 (rs1695-rs1138272) haplotypes											
AC (66.4%)	absent	1 (7.7)	3 (9.7)	4 (10.5)	5 (12.5)	reference	reference	reference	reference	reference	reference
	present	12 (92.3)	28 (90.3)	34 (89.5)	35 (87.5)	1.49[0.18-12.45] 1.000[F]	0.99[0.11-9.21] 0.993	1.30[0.38-4.51] 0.768[F]	1.18[0.33-4.19] 0.797	1.32[0.4-4.33] 0.756	1.15[0.33-3.93] 0.825
GC (25.4%)	absent	11 (84.6)	20 (64.5)	21 (55.3)	18 (45.0)	reference	reference	reference	reference	reference	reference
	present	2 (15.4)	11 (35.5)	17 (44.7)	22 (55.0)	0.22[0.045-1.01] **0.036**	0.27[0.054-1.38] 0.117	0.42[0.19-9.20] **0.028**	0.42[0.19-0.96] **0.041**	0.47[0.22-1.02] 0.054	0.55[0.24-1.23] 0.149
GT (7.8%)	absent	9 (69.2)	25 (80.6)	32 (84.2)	38 (95.0)	reference	reference	reference	reference	reference	reference
	present	4 (30.8)	6 (19.4)	6 (15.8)	2 (5.0)	3.02[0.82-11.12] 0.101[F]	3.41[0.81-14.34] 0.094	2.57[0.93-7.11] 0.062	2.61[0.93-7.37] 0.069	4.6[1.00-21.12] **0.034**	4.33[0.91-20.62] 0.065
ABCB1 (rs1128503-rs2032582-rs1045642) haplotypes											
CGC (45.9%)	absent	4 (30.8)	10 (32.3)	8 (21.1)	12 (30.0)	reference	reference	reference	reference	reference	reference
	present	9 (69.2)	21 (67.7)	30 (78.9)	28 (70.0)	0.85[0.25-2.98] 0.754[F]	0.74[0.19-2.81] 0.654	0.74[0.33-1.67] 0.465	0.73[0.32-1.69] 0.461	1.17[0.5-2.7] 0.714	1.43[0.58-3.53] 0.432
TTT (36.9%)	absent	6 (46.2)	12 (38.7)	17 (44.7)	16 (40.0)	reference	reference	reference	reference	reference	reference
	present	7 (53.8)	19 (61.3)	21 (55.3)	24 (60.0)	0.82[0.26-2.60] 0.772	0.85[0.24-3.08] 0.805	1.06[0.50-2.24 0.88	1.13[0.52-2.47] 0.76	0.89[0.41-1.93] 0.778	0.91[0.4-2.05] 0.821
CGT (8.6%)	absent	10 (76.9)	24 (77.4)	30 (78.9)	38 (95.0)	reference	reference	reference	reference	reference	reference
	present	3 (23.1)	7 (22.6)	8 (21.1)	2 (5.0)	1.62[0.40-6.52] 0.446[F]	2.29[0.50-10.59] 0.289	2.00[0.76-5.27] 0.156	2.34[0.86-6.33] 0.095	5.34[1.17-24.31] **0.018**	7.56[1.6-35.82] **0.011**

[0] Association with prednosine response on day 8 according to Berlin-Frankfurt-Munster (BFM) protocol: prednisone poor responder (PPR) group (≥ 1000 blasts) *vs.* prednisone good responder (PGR) group (< 1000 blasts)
[1] Association with number of blasts on day 8 with cut-off value of 100: higher (≥ 100 blasts) vs lower (< 100 blasts) number of blasts
[2] Association with blast status on day 8: blast positive vs blast negative patients.
[F] Fisher exact test
[ADJ] Adjusted for age, gender and initial white blood cells (WBC) count using logistic regression
OR = Odds ratio between a group with higher number of blasts in comparison with a group with lower number of blasts. The group with lower number of blasts represents reference group.
CI = Confidence interval

ment, while carriers of GT haplotype have poorer response to prednisone treatment.

Regarding *GSTT1* gene, our results have shown that carriers of null genotype are more likely to have blast count over 100 (≥ 100 blasts/microL) (χ^2 test; $p = 0.063$), in comparison with carriers of at least one functional *GSTT1* gene copy. Interestingly, when controlled for age, gender and initial WBC count, this association turned out to be statistically significant (Logistic regression, $p = 0.044$)

Regarding *ABCB1* gene variants in relation to blast count, no association was found. However, when estimated haplotypes were considered, it was found that carriers of relatively rare CGT (rs1128503-rs2032582-rs1045642) haplotype had been 5 times more likely to be blast positive (χ^2

test; p = 0.018), than the non-carriers. This association remained significant when controlled for age, gender and initial WBC count employing logistic regression.

Discussion

Pharmacogenomics is dealing with the fact that the efficacy of the drug depends on the patient's ability to absorb and metabolize the drug, which influences the effectiveness of the treatment. Furthermore, the toxicity of drug depends on the patient's genome. Pharmacogenomics testing is already incorporated as a dosage-calibrating tool in the maintenance phase of childhood ALL treatment in order to minimize the occurrence of serious toxicities during 6-MP treatment.[4, 32]

Glucocorticoids are an essential component to induction remission phase of childhood ALL therapy. A poor response to the standard initial GC treatment and the persistence of blast count over 1000 per microliter on the day 8, puts a patient in a higher risk group with a poor prognosis. The following phases of treatment are dependent on risk-directed stratification of patients. However, many children experience severe toxicity associated with treatment with dangerous side effects, while some of them are not cured.[33] So, it could be argued that these groupings are not yet comprehensive enough.[34] As for induction remission phase of ALL treatment, it is essential to find as many potential markers of GC resistance as possible. By analyzing the associations between the pharmacogenetic variants and GC resistance or good response, this study was meant to contribute to individualization of GC treatment, so that the patients could be in future adequately treated according to their genetic background.

A few studies dealt with variants in *NR3C1*, *GST*s and *ABCB1* gene in relation with GC toxicity or disease-free survival in childhood ALL patients, often with conflicting results.[10, 35-38] Although toxicity and survival are the most important therapy outcome signifiers, still, they cannot be associated solely with GC response. On the contrary, we believe that GC response on day 8 assessed by blast count in blood is probably the best measure of GC efficacy in childhood ALL, because no other chemotherapeutic drug is given systemically beforehand. Low blast count (< 100 blasts/microL) or blast negative status could also be important to reveal patients with particularly good response to GC therapy. Those patients might require adjustment of GC dose to achieve remission.

In this study we focused on variants in non-coding region of *NR3C1* gene, rather than on the most extensively studied variants of *NR3C1* gene that were earlier analyzed in regard to GC response on day 8 in childhood ALL. One of those studies found only *BclI* variant to be associated with GC response in relatively small Chinese cohort of ALL patients.[12] However, other studies did not find significant association with GC response on day 8.[10, 11]

Concerning the variant rs6198 in the *N3RC1* gene, we have found an increased risk of PPR (> 1000 blasts/microL) in the initial stage when the carrier has the rare GG genotype. This variant is important for GRβ mRNA stabilization. Moreover, the GG genotype leads to greater expression of the GRβ isoform.[17] And the increased level of GRβ isoform leads to the dominant negative inhibition of the GRα isoform.[39] The GRβ isoform provides enhanced resistance to the biological and pharmacological effects of glucocorticoids.[14, 16, 40, 41] The level of isoform GRβ was shown to influence glucocorticoid response in childhood ALL. Namely, glucocorticoid sensitivity was negatively correlated with GRβ/GRα ratio in leukemic blast cells.[42] Our study is the first to report any result concerning association between rs6198 variant and response to GC treatment on day 8. The association of this variant and glucocorticoid response was shown in patients suffering from other diseases. In the pediatric nephrotic syndrome, it was found that carriers of the GG genotype had a worse treatment outcome,[43] which is in line with our findings. Also, in the major depressive disorder, a haplotype (rs10482605-rs6198) containing the G allele of rs6198 was associated with GRβ mRNA stability. This haplotype contributed to the hyperactivity of the hypothalamus-pituitary-adrenal axis.[44]

Our results have shown that carriers of minor *NR3C1* rs33389 T allele tended towards higher blast count (≥ 100 blasts/microL), while carriers of *NR3C1* rs33388 T allele tended towards lower blast count (< 100 blasts/microL) at day 8 of GC treatment. It has been shown that the variants rs33389 and rs33388, T and A alleles respectively, are located in intron 2 of *NR3C1*, in a region where alternate splicing occurs, resulting in increased expression of isoform GRγ.[14] GRγ has an affinity for the ligand similar to the standard isoform GRα, but it lacks the stability of GRα in binding to the glucocorticoid response element.[45] On the other hand, rs33389 C allele and rs33388 T allele are

parts of ACT (rs41423247-rs33389-rs33388) haplotype which is strongly associated with glucocorticoid sensitivity.[46] Also, in the pediatric nephrotic syndrome, a significant association was shown between this haplotype and a good response to GC treatment.[15] Moreover, CTA (rs33389-rs33388-rs6198) haplotype consisting of alleles found to be favorable for GC response on day 8 in our study, was associated with longer survival time in acute leukemia patients who underwent hematopoietic stem cell transplantation.[47] Interestingly however, in our cohort, CAA haplotype was associated with PGR. This result further points out favorable association of rs33389 C and rs6198 A alleles with lower blast count.

Carriers of *GSTP1* GC (rs1695-rs1138272) haplotype had decreased risk of PPR, were more likely to have low blast count (< 100 blasts/microL) and to be blast negative on day 8 of GC treatment. It was shown, while investigating the activity and the structure of GSTP1, that this haplotype codes the substrate binding region, H-site, of the GSTP1 protein, turning it into a protein with a much smaller Michaelis constant, leading to less efficient conjugation of agents.[20] Consequently, glucocorticoid agents are capable of acting for a longer period of time. Our results have also associated *GSTP1* rs1138272 T allele carriers and *GSTP1* GT haplotype with blast positive status. Two studies that dealt with variants in *GSTP1* gene and GC response on day 8 of ALL treatment, did not find significant association, but they enrolled relatively small number of patients.[21, 48]

Carriers of the *GSTT1* null-genotype were more likely to have higher blast count on day 8 in our childhood ALL cohort. In contrast to our result, one study did not find any association,[21] while the other observed statistical trend towards a PGR in childhood ALL.[48] Also, Meissner and coworkers found that in subgroup of childhood ALL patients who were in higher risk for PPR, *GSTT1* null allele is correlated with decreased risk of PPR.[27] When it comes to risk of relapse and outcome in relation with *GSTT1* null genotype, conflicting results were noted in two studies that enrolled large number of childhood ALL patients.[36, 38]

Regarding *ABCB1* gene, we found that carriers of rare CGT (rs1128503-rs2032582-rs1045642) haplotype are more likely to be blast positive. Higher expression of *ABCB1* was associated with steroid resistance.[25, 49] Mayor alleles were found to lead to higher *ABCB1* expression or higher ABCB1 activity,[50] making them more likely to be associated with poor GC response.[51] Our study is the first to deal with GC response on GC treatment day 8 of childhood ALL patients regarding *ABCB1* haplotypes. In a large cohort of idiopathic thrombocytopenic purpura patients, various haplotype combinations of the same variants we analyzed were associated with GC response.[51] However, no association was found in regard to CGT haplotype.

Despite the promising results, the limitations of the study need to be affirmed. The sample size is not big, since this is a single centric study enrolling patients suffering from a rare disease. Moreover, certain alleles of genetic variants we studied are not frequent, meaning that in some cases there are only a few carriers of certain genotypes. As a consequence, conclusions drawn analyzing such small groups of patients need to be taken with caution. Considering the shortcomings mentioned, it would be of great benefit to validate the results gained in this study on a larger sample preferably using prospective approach.

Association studies on the pharmacogenomic profile of patients and data on the toxicity of drugs are the most promising directions on the road to personalized medicine. The ultimate goal of the ongoing multicentric clinical trials is to optimize the use of known antileukemic drugs in the context of individual pharmacogenomic profile of each patient and molecular markers of the leukemic cells and modulate the treatment resulting in less toxicity and adverse reactions, and a higher survival rates.[52] Personalized medicine approach of tailoring treatment to the individual characteristics of each patient has been a great success in several diseases. One thing that we have learnt from those successful examples is that a personalized childhood ALL approach implementation may be difficult. Our study pointed out the association between several variants in *NR3C1, GSTP1, GSTT1, GSTM1* and *ABCB1* genes and GC therapeutic response in the initial phase of remission induction therapy of pediatric ALL patients. We have shown that *NR3C1* rs6198 variant and *GSTP1* rs1695-rs1138272 haplotype are the most promising pharmacogenetic markers of GC response in ALL patients. However, studies including more childhood ALL patients, as well as more comprehensive analysis of personal "pharmacomics" profiles are needed for discovery of novel potential genetic markers for targeted therapy[53] and for a design of modulations of the existing treatment protocols, leading to more individualized and more successful childhood ALL treatment.

Acknowledgement

This work was supported by Ministry of Education, Science and Technological Development, Republic of Serbia (Grant No. III41004).

References

1. Schrappe M, Reiter A, Zimmermann M, Harbott J, Ludwig WD, Henze G, et al. Long-term results of four consecutive trials in childhood ALL performed by the ALL-BFM study group from 1981 to 1995. *Leukemia* 2000; **14:** 2205-22. doi: 10.1038/sj.leu.2401973
2. Pui C-H, Robison LL, Look AT. Acute lymphoblastic leukaemia. *Lancet (London, England)* 2008; **371:** 1030-43. doi: 10.1016/S0140-6736(08)60457-2
3. Stary J, Zimmermann M, Campbell M, Castillo L, Dibar E, Donska S, et al. Intensive chemotherapy for childhood acute lymphoblastic leukemia: results of the randomized intercontinental trial ALL IC-BFM 2002. *J Clin Oncol* 2014; **32:** 174-84. doi: 10.1200/JCO.2013.48.6522
4. Rudin S, Marable M, Huang RS. The promise of pharmacogenomics in reducing toxicity during acute lymphoblastic leukemia maintenance treatment. *Genomics, Proteomics, Bioinformatics* 2017; **15:** 82-93. doi: 10.1016/j.gpb.2016.11.003
5. Helmberg A, Auphan N, Caelles C, Karin M. Glucocorticoid-induced apoptosis of human leukemic cells is caused by the repressive function of the glucocorticoid receptor. *EMBO J* 1995; **14:** 452-60.
6. Campbell M. ALL IC-BFM 2009 a randomized trial of the I-BFM-SG for the management of childhood non-B acute lymphoblastic leukemia. 2009; 178.
7. Schmidt S, Rainer J, Ploner C, Presul E, Riml S, Kofler R. Glucocorticoid-induced apoptosis and glucocorticoid resistance: molecular mechanisms and clinical relevance. *Cell Death Differ* 2004; **11:** S45-55. doi: 10.1038/sj.cdd.4401456
8. Koper JW, Van Rossum EFC, Van Den Akker ELT. Glucocorticoid receptor polymorphisms and haplotypes and their expression in health and disease. *Steroids* 2014; **92:** 62-73. doi: 10.1016/j.steroids.2014.07.015
9. DeRijk RH, Schaaf M, De Kloet ER. Glucocorticoid receptor variants**:** clinical implications. *J Steroid Biochem Mol Biol* 2002; **81:** 103-22. doi: 10.1016/S0960-0760(02)00062-6
10. Eipel OT, Németh K, Török D, Csordás K, Hegyi M, Ponyi A, et al. The glucocorticoid receptor gene polymorphism N363S predisposes to more severe toxic side effects during pediatric acute lymphoblastic leukemia (ALL) therapy. *Int J Hematol* 2013; **97:** 216-22. doi: 10.1007/s12185-012-1236-1
11. Tissing WJE. Genetic variations in the glucocorticoid receptor gene are not related to glucocorticoid resistance in childhood acute lymphoblastic leukemia. *Clin Cancer Res* 2005; **11:** 6050-56. doi: 10.1158/1078-0432.CCR-04-2097
12. Xue L, Li C, Wang Y, Sun W, Ma C, He Y, et al. Single nucleotide polymorphisms in non-coding region of the glucocorticoid receptor gene and prednisone response in childhood acute lymphoblastic leukemia. *Leuk Lymphoma* 2015; **56:** 1704-09. doi: 10.3109/10428194.2014.951848
13. Cartegni L, Chew SL, Krainer AR. Listening to silence and understanding nonsense: Exonic mutations that affect splicing. *Nat Rev Genet* 2002; **3:** 285-98. doi: 10.1038/nrg775
14. Gross KL, Lu NZ, Cidlowski JA. Molecular mechanisms regulating glucocorticoid sensitivity and resistance. *Mol Cell Endocrinol* 2009; **300:** 7-16. doi: 10.1016/j.mce.2008.10.001.Molecular
15. Zalewski G, Wasilewska A, Zoch-Zwierz W, Chyczewski L. Response to prednisone in relation to NR3C1 intron B polymorphisms in childhood nephrotic syndrome. *Pediatr Nephrol* 2008; **23:** 1073-8. doi: 10.1007/s00467-008-0772-7
16. Schaaf MJM, Cidlowski JA. Molecular mechanisms of glucocorticoid action and resistance. *J Steroid Biochem Mol Biol* 2002; **83:** 37-48. doi: 10.1016/S0960-0760(02)00263-7
17. Derijk RH, Schaaf MJ, Turner G, Datson Na, Vreugdenhil E, Cidlowski J, et al. A human glucocorticoid receptor gene variant that increases the stability of the glucocorticoid receptor beta-isoform mRNA is associated with rheumatoid arthritis. *J Rheumatol* 2001; **28:** 2383-8.
18. Vega L. 3. Role of glutathione S-transferase enzymes in toxicology, pharmacology and human disease. *Pharmacological and Toxicological Aspects* 2010; **661:** 45-66.
19. Homma H, Listowsky I. Identification of Yb-glutathione-S-transferase as a major rat liver protein labeled with dexamethasone 21-methanesulfonate. *Proc Natl Acad Sci U S A* 1985; **82:** 7165-69. doi: 10.2307/26329
20. Johansson AS, Stenberg G, Widersten M, Mannervik B. Structure-activity relationships and thermal stability of human glutathione transferase P1-1 governed by the H-site residue 105. *J Mol Biol* 1998; **278:** 687-98. doi: 10.1006/jmbi.1998.1708
21. Zubowska M, Zielińska E, Zmysłowska A, Bodalski J. [Increased frequency of A-G transition at exon 5 of GSTP1 as a genetic risk factor for acute childhood leukaemia]. [Polish]. *Med Wieku Rozwoj* 2004; **8:** 245-57.
22. Farrell RJ, Menconi MJ, Keates AC, Kelly CP. P-glycoprotein-170 inhibition significantly reduces cortisol and ciclosporin efflux from human intestinal epithelial cells and T lymphocytes. *Aliment Pharmacol Ther* 2002; **16:** 1021-31. doi: 10.1046/j.1365-2036.2002.01238.x
23. Hoffmeyer S, Burk O, von Richter O, Arnold HP, Brockmöller J, Johne A, et al. Functional polymorphisms of the human multidrug-resistance gene: multiple sequence variations and correlation of one allele with P-glycoprotein expression and activity in vivo. *Proc Natl Acad Sci U S A* 2000; **97:** 3473-8. doi: 10.1073/pnas.050585397
24. Ambudkar SV, Dey S, Hrycyna CA, Ramachandra M, Pastan I, Gottesman MM. Biochemical, cellular, and pharmacological aspects of the multidrug transporter. *Annu Rev Pharmacol Toxicol* 1999; **39:** 361-98. doi: 10.1146/annurev.pharmtox.39.1.361
25. Wasilewska A, Zoch-Zwierz W, Pietruczuk M, Zalewski G. Expression of P-glycoprotein in lymphocytes from children with nephrotic syndrome, depending on their steroid response. *Pediatr Nephrol* 2006; **21:** 1274-80. doi: 10.1007/s00467-006-0187-2
26. Smith LK, Cidlowski JA. Glucocorticoid-induced apoptosis of healthy and malignant lymphocytes. *Prog Brain Res* 2010; **182:** 1-30. doi: 10.1016/S0079-6123(10)82001-1
27. Meissner B, Stanulla M, Ludwig W-D, Harbott J, Möricke a, Welte K, et al. The GSTT1 deletion polymorphism is associated with initial response to glucocorticoids in childhood acute lymphoblastic leukemia. *Leukemia* 2004; **18:** 1920-3. doi: 10.1038/sj.leu.2403521
28. Vaghela N, Anand IS, Trivedi DH, Jani M. Prognostic value of peripheral blood blast percentage on day 8 in long term cure in patients with ALL. *World J Pharmacy Pharm Sci* 2014; **3:** 1839-47.
29. Chen CL, Liu Q, Relling MV. Simultaneous characterization of glutathione S-transferase M1 and T1 polymorphisms by polymerase chain reaction in American whites and blacks. *Pharmacogenetics* 1996; **6:** 187-91.
30. Kurzawski M, Pawlik A, Górnik W, Droździk M. Frequency of common MDR1 gene variants in a Polish population. *Pharmacol Rep* 2006; **58:** 35-40.
31. Excoffier L, Lischer HEL. Arlequin suite ver 3.5: a new series of programs to perform population genetics analyses under Linux and Windows. *Mol Ecol Resour* 2010; **10:** 564-67. doi: 10.1111/j.1755-0998.2010.02847.x
32. Dokmanovic L, Urosevic J, Janic D, Jovanovic N, Petrucev B, Tosic N, et al. Analysis of thiopurine S-methyltransferase polymorphism in the population of Serbia and Montenegro and mercaptopurine therapy tolerance in childhood acute lymphoblastic leukemia. *Ther Drug Monit* 2006; **28:** 800-06. doi: 10.1097/01.ftd.0000249947.17676.92
33. Jackson RK, Irving JAE, Veal GJ. Personalization of dexamethasone therapy in childhood acute lymphoblastic leukaemia. *Br J Haematol* 2016; **173:** 13-24. doi: 10.1111/bjh.13924
34. Asselin BL. The right dose for the right patient. *Blood* 2012; **119:** 1617-8. doi: 10.1182/blood-2011-12-395855
35. Labuda M, Gahier A, Gagné V, Moghrabi A, Sinnett D, Krajinovic M. Polymorphisms in glucocorticoid receptor gene and the outcome of childhood acute lymphoblastic leukemia (ALL). *Leuk Res* 2010; **34:** 492-97. doi: 10.1016/j.leukres.2009.08.007

36. Stanulla M, Schrappe M, Brechlin AM, Zimmermann M, Welte K. Polymorphisms within glutathione S-transferase genes (GSTM1, GSTT1, GSTP1) and risk of relapse in childhood B-cell precursor acute lymphoblastic leukemia: a case-control study. *Blood* 2000; **95:** 1222-8.

37. Stanulla M, Schäffeler E, Arens S, Rathmann A, Schrauder A, Welte K, et al. GSTP1 and MDR1 genotypes and central nervous system relapse in childhood acute lymphoblastic leukemia. *Int J Hematol* 2005; **81:** 39-44.

38. Franca R, Rebora P, Basso G, Biondi A, Cazzaniga G, Crovella S, et al. Glutathione S-transferase homozygous deletions and relapse in childhood acute lymphoblastic leukemia: a novel study design in a large Italian AIEOP cohort. *Pharmacogenomics* 2012; **13:** 1905-16. doi: 10.2217/pgs.12.169

39. Longui CA, Vottero A, Adamson PC, Cole DE, Chrousos GP. Low glucocorticoid receptor alpha/beta ratio in T-celI lymphoblastic leukemia. *Horm Metab Res* 2000; **32:** 401-6. doi: 10.1055/s-2007-978661

40. Turner JD, Schote AB, Macedo JA, Pelascini LPL, Muller CP. Tissue specific glucocorticoid receptor expression, a role for alternative first exon usage? *Biochem Pharmacol* 2006; **72:** 1529-37. doi: 10.1016/j.bcp.2006.07.005

41. Bamberger CM, Bamberger AM, De Castro M, Chrousos GP. Glucocorticoid receptor B, a potential endogenous inhibitor of glucocorticoid action in humans. *J Clin Invest* 1995; **95:** 2435-41. doi: 10.1172/JCI117943

42. Koga Y, Matsuzaki A, Suminoe A, Hattori H, Kanemitsu S, Hara T. Differential mRNA expression of glucocorticoid receptor α and β is associated with glucocorticoid sensitivity of acute lymphoblastic leukemia in children. *Pediatr Blood Cancer* 2005; **45:** 121-27. doi: 10.1002/pbc.20308

43. Teeninga N, Kist-Van Holthe JE, Van Den Akker ELT, Kersten MC, Boersma E, Krabbe HG, et al. Genetic and in vivo determinants of glucocorticoid sensitivity in relation to clinical outcome of childhood nephrotic syndrome. *Kidney Int* 2014; **85:** 1444-53. doi: 10.1038/ki.2013.531

44. Kumsta R, Moser D, Streit F, Koper JW, Meyer J, Wüst S. Characterization of a glucocorticoid receptor gene (GR, NR3C1) promoter polymorphism reveals functionality and extends a haplotype with putative clinical relevance. *Am J Med Genet B Neuropsychiatr Genet* 2009; **150:** 476-82. doi: 10.1002/ajmg.b.30837

45. Beger C, Gerdes K, Lauten M, Tissing WJE, Fernandez-Munoz I, Schrappe M, et al. Expression and structural analysis of glucocorticoid receptor isoform gamma in human leukaemia cells using an isoform-specific real-time polymerase chain reaction approach. *Br J Haematol* 2003; **122:** 245-52. doi: 10.1046/j.1365-2141.2003.04426.x

46. Stevens A, Ray DW, Zeggini E, John S, Richards HL, Griffiths CEM, et al. Glucocorticoid sensitivity is determined by a specific glucocorticoid receptor haplotype. *J Clin Endocrinol Metab* 2004; **89:** 892-97. doi: 10.1210/jc.2003-031235

47. Pearce KF, Balavarca Y, Norden J, Jackson G, Holler E, Dressel R, et al. Impact of genomic risk factors on survival after haematopoietic stem cell transplantation for patients with acute leukaemia. *Int J Immunogenet* 2016; **43:** 404-12. doi: 10.1111/iji.12295

48. Anderer G, Schrappe M, Brechlin AM, Lauten M, Muti P, Welte K, et al. Polymorphisms within glutathione S-transferase genes and initial response to glucocorticoids in childhood acute lymphoblastic leukaemia. *Pharmacogenetics* 2000; **10:** 715-26. doi: 10.1097/00008571-200011000-00006

49. Jafar T, Prasad N, Agarwal V, Mahdi A, Gupta A, Sharma RK, et al. MDR-1 gene polymorphisms in steroid-responsive versus steroid-resistant nephrotic syndrome in children. *Nephro Dial Transplant* 2011; **26:** 3968-74. doi: 10.1093/ndt/gfr150

50. Wang D, Johnson AD, Papp AC, Kroetz DL, Sadée W. Multidrug resistance polypeptide 1 (MDR1, ABCB1) variant 3435C>T affects mRNA stability. *Pharmacogenet Genomics* 2005; **15:** 693-704. doi: 10.1097/01.fpc.0000178311.02878.83

51. Xuan M, Li H, Fu R, Yang Y, Zhang D, Zhang X, et al. Association of ABCB1 gene polymorphisms and haplotypes with therapeutic efficacy of glucocorticoids in Chinese patients with immune thrombocytopenia. *Hum Immunol* 2014; **75:** 317-21. doi: 10.1016/j.humimm.2014.01.013

52. Hunger SP, Mullighan CG. Acute lymphoblastic leukemia in children. *N Engl J Med* 2015; **373:** 1541-52. doi: 10.1056/NEJMra1400972

53. Dokmanovic L, Milosevic G, Peric J, Tosic N, Krstovski N, Janic D, et al. Next generation sequencing as a tool for pharmacogenomic profiling: Nine novel potential genetic markers for targeted therapy in childhood acute lymphoblastic leukemia. *Srp Arh Celok Lek* 2017; **145:** 194-94. doi: 10.2298/SARH171003194D

research article

Primary debulking surgery versus primary neoadjuvant chemotherapy for high grade advanced stage ovarian cancer: comparison of survivals

Borut Kobal[1], Marco Noventa[2], Branko Cvjeticanin[1], Matija Barbic[1], Leon Meglic[1], Marusa Herzog[1], Giulia Bordi[3], Amerigo Vitagliano[2], Carlo Saccardi[2], Erik Skof[4]

[1] Division of Gynaecology and Obstetrics, University Medical Centre Ljubljana, Ljubljana, Slovenia
[2] Department of Woman and Child Health, University of Padua, Padua, Italy
[3] Department of Gynecology and Obstetrics, University of Insubria, Varese, Italy
[4] Department of Medical Oncology, Institute of Oncology Ljubljana, Ljubljana, Slovenia

Radiol Oncol 2018; 52(3): 307-319.

Received 28 March 2018
Accepted 23 July 2018

Correspondence to: Assist. Prof. Erik Škof, M.D., Ph.D., Institute of Oncology Ljubljana, Zaloška 2, SI-1000 Ljubljana, Slovenia.
Phone: +386 1 5879 282; Fax: +386 1 5879 305; E-mail: eskof@onko-i.si

Disclosure: No potential conflicts of interest were disclosed.

Background. The aim of the study was to analyze the overall survival (OS) and progression free survival (PFS) of patients with high grade and advanced stage epithelial ovarian cancer (EOC) with at least 60 months of follow-up treated in a single gynecologic oncology institute. We compared primary debulking surgery (PDS) versus neoadjuvant chemotherapy plus interval debulking surgery (NACT + IDS) stratifying data based on residual disease with the intent to identify the rationale for therapeutic option decision and the role of laparoscopic evaluation of resectability for that intention.

Patients and methods. This is observational retrospective study on consecutive patients with diagnosis of high grade and International Federation of Gynecology and Obstetrics (FIGO) stage III/IV EOC referred to our center between January 2008 and May 2012. We selected only patients with a follow-up of at least 60 months. Primary endpoint was to compare PDS versus NACT + IDS in term of progression free survival (PFS) and overall survival (OS). Secondary endpoints were PFS and OS stratifying data according to residual disease after surgery in patients receiving PDS versus NACT + IDS. Finally, through Cox hazards models, we tested the prognostic value of different variables (patient age at diagnosis, residual disease after debulking, American Society of Anesthesiologists (ASA) stage, number of adjuvant-chemotherapy cycles) for predicting OS.

Results. A total number of 157 patients were included in data analysis. Comparing PDS arm (108 patients) and NACT + IDS arm (49 patients) we found no significant differences in term of OS (41.3 versus 34.5 months, respectively) and PFS (17.3 versus 18.3 months, respectively). According to residual disease we found no significant differences in term of OS between NACT + IDS patients with residual disease = 0 and PDS patients with residual disease = 0 or residual disease = 1, as well as no significant differences in PFS were found comparing NACT + IDS patients with residual disease = 0 and PDS patients with residual disease = 0; contrarily, median PFS resulted significantly lower in PDS patients receiving optimal debulking (residual disease = 1) in comparison to NACT + IDS patients receiving complete debulking (residual disease = 0). PDS arm was affected by a significant higher rate of severe post-operative complications (grade 3 and 4). Diagnostic laparoscopy before surgery was significantly associated with complete debulking.

Conclusions. We confirm previous findings concerning the non-superiority of NACT + IDS compared to PDS for the treatment of EOC, even if NACT + IDS treatment was associated with significant lower rate of post-operative complications. On the other hand, selecting patients for NACT + IDS, based on laparoscopic evaluation of resectabilty prolongs the PFS and does not worse the OS compared to the patients not completely debulked with PDS.

Key words: epithelial ovarian cancer; advanced stage; primary debulking surgery; interval debulking surgery; neoadjuvant chemotherapy; adjuvant chemotherapy; overall survival; progression free survival

Introduction

Epithelial ovarian cancer (EOC) is the major cause of gynecological cancer-related mortality in developed countries, with annual incidence of more than 200,000 new cases and responsible of 150,000 deaths worldwide.[1] Due to its subtle symptomatology and the lack of specific screening methods, about 70% of EOCs are diagnosed in advanced stage, specifically International Federation of Gynecology and Obstetrics (FIGO) stage III and IV.[2]

Except for patients not eligible for surgery due to severe comorbidities or extensive tumor spread, the standard treatment for advanced stage EOC is primary debulking surgery (PDS), with the goal of optimal cytoreduction followed by adjuvant chemotherapy with paclitaxel plus platinum based agents.[2,3] Survival in patients affected by EOC is strongly related to the residual disease after surgical treatment.[2] Patients without macroscopic residual tumor (complete debulking) showed a better survival than patients with minimal residual disease < 1cm (optimal debulking) and patients with residual disease > 1 cm (suboptimal debulking).[4] The possibility to attain complete cytoreduction depends on several factors like the spread of the disease, the molecular features of the tumor, its microenvironment and the skill of gynecologic oncology surgeon.[5,6]

Current evidence suggest that PDS should only be attempted if at least tumor resection to less than 1 cm seems to be achievable.[2] This concept leads to an unsolved key problem in EOC care, due to lack of worldwide accepted pre-operative strategies able to predict the chances of successful primary debulking.[7] Great progresses have been made concerning the role of pre-operative laparoscopy in evaluating the feasibility of a successful PDS; at this regard recent prospective studies demonstrated a good accuracy of laparoscopic score in predicting residual disease after PDS.[7] However, randomized trials are mandatory to confirm these encouraging results.

For patients in whom a complete cytoreduction during primary surgery is not expected, neoadjuvant chemotherapy (NACT) followed by interval debulking surgery (IDS) is considered the most appropriate therapeutic option.[2,8] Recent studies demonstrated that such strategy allows higher rate of residual disease = 0 in comparison to primary surgery.[9-11] Consequently, an approach based on NACT + IDS as first line treatment in all patients suffering by advanced stage EOC has been recently proposed and two randomized controlled studies have been published in order to compare survivals of PDS versus NACT + IDS strategy.[12,13] Both EORTC and the most recent CHORUS trial showed no differences in overall survival (OS) and progression free survival (PFS) in the two treatments arms.[12,13] However, concerns about the degree of evidence from these two studies have been raised, especially due to possible bias related with poor surgical radicality, low median operating time and the poor OS reported in entire study population.[14] Due to these drawbacks, and considering that other recent prospective and retrospective series reached opposite conclusions in favor to PDS approach, a definitive answer on the role of NACT + IDS in the treatment of advanced stage EOC has not been given yet.[9-11,15,16]

Another fundamental aspect in choosing the two treatments option regards the quality of life of patients. Poor evidence is available concerning QoL (Quality of Life) after PDS or NACT + IDS, mainly supporting higher rate of aggressive surgery and surgery-related complications in patients underwent PDS treatment.[9,10,12,17,18] However, such observations need further clinical confirmations.

Starting from such uncertainties about the optimal primary treatment of advanced stage EOC, we analyzed the OS and PFS of patients with at least 60 months of follow-up in a single gynecologic oncology institute. We compared PDS versus NACT + IDS stratifying data based on residual disease after surgery with the intent to identify the rationale for therapeutic option decision and the role of laparoscopic evaluation of resectability for that intention.

Patients and methods

Study design

We conducted an observational retrospective study on patients with diagnosis of high grade and advanced stage (FIGO stage III or IV) EOC that underwent primary-debulking surgery (PDS) or neoadjuvant chemotherapy (NACT) plus interval debulking surgery (IDS) at our institution (Division of Gynecology and Obstetrics, University Medical Centre Ljubljana, Slovenia) from January 2008 to May 2012. The institutional review board approved this retrospective analysis (IRB: 178/05/09).

Inclusion and exclusion criteria

We included all newly diagnosed patients who referred at our institution with stage III or IV disease according to 1988 FIGO staging criteria.[2] We

considered as inclusion criteria: diagnosis of high grade epithelial ovarian cancer with FIGO stage III or IV, all histological type, patients treated by PDS or NACT + IDS, follow-up with at least 60 months duration, absence of concomitant malignant neoplasms. We excluded all patients that underwent PDS at an outside facility, FIGO stage I–II, non-epithelial histologic type and low grade.

Data collection

Patients were identified through our institution computer database initiated to collect surgical information at point of care. For each patient the investigators (G.B and M.N) reviewed the electronic hospital records and pathology reports to determine study eligibility, patients general features, FIGO stage, tumor grading and histologic type. Vital status was determined by analysis of electronic chart; in case of missing information, investigators contacted directly the patient or family by telephone or email to complete the data collection.

We collected data about patients' age, body mass index (BMI), menopausal status, parity, pre-operative CA-125, documented comorbidities, prior surgeries, number of neoadjuvant or adjuvant chemotherapy cycles, type of chemotherapy, response after NACT, blood loss at surgery and need for transfusions, intraoperative complications (PDS or IDS), post-operative complications (PDS or IDS) based on Clavien Dindo classification system, hospitalization length and residual disease after surgery.[19]

Patients and treatments

Patients included in the study were subsequently divided in two groups for comparison estimates: (1) *PDS group* included patients that underwent primary debulking surgery followed by adjuvant chemotherapy; (2) *NACT + IDS group* included patients that underwent neoadjuvant chemotherapy plus interval debulking surgery followed by adjuvant chemotherapy.

All patients in *PDS group* underwent PDS with the intent to perform a debulking procedure. A Multidisciplinary Group (including a panel of experts in gynecologic oncology, medical oncology, radiology and pathology) established case by case all treatments decisions through consensus. The decision was based on clinical features of each patient (extent of disease, co-morbidity, performance status), on results of imaging techniques (trans-vaginal/trans-abdominal ultrasonography, computerized tomography, magnetic resonance imaging) and for the great majority of cases was based on laparoscopic direct visualization of pelvic and abdominal cavity with the purpose of evaluation for resectability. When the possibility to perform an optimal surgical cytoreduction (residual disease ≤ 1 cm) was considered low, patients were deemed eligible for NACT.

At that time, the selection of patients for PDS or NACT was not based on a formal laparoscopic scoring system but on gynecologic oncologist surgeons expertise. However, a patient was considered candidate for NACT in case of wide spread of the disease in the abdominal and pelvic cavity (unresectable massive peritoneal involvement, widespread infiltrating carcinomatosis of diaphragm, mesenteral retraction, miliary carcinomatosis of the bowel, liver and stomach metastases). Chemotherapy in the adjuvant and neoadjuvant setting included platinum and taxane or doxorubicin regimes according to the standard treatment protocols for the time period. Debulking surgery involved hysterectomy, bilateral oophorectomy, complete omentectomy, selective lymphadenectomy plus if necessary bowel or recto-sigmoid resection, and radical upper abdominal procedures (like diaphragm resection, splenectomy, distal pancreatectomy, and liver resection) to achieve optimal cytoreduction.

The goal at that time period was to obtain at least an optimal (≤ 1 cm residual disease - residual disease = 1) or complete cytoreduction (residual disease = 0). Patients were considered suboptimally debulked if they had any residual disease larger than 1 cm in greatest dimension after surgery (residual disease = 2).

Endpoints of the study

The primary endpoint in this analysis was to compare the two treatments arms in term of progression free survival (PFS) and overall survival (OS).

The secondary endpoint was to compare the progression free survival (PFS) and overall survival (OS) in patients that underwent NACT + IDS with complete cytoreduction (residual disease = 0) versus patients that underwent PDS with optimal (residual disease = 1) or complete (residual disease = 0) cytoreduction.

Tertiary endpoint was to test (using Cox proportional hazards models) the following prognostic factors for OR: type of treatment (PDS versus NACT + IDS), patient age at diagnosis (< 60 versus ≥ 60 years), residual disease after surgical debulking (residual disease = 0 versus residual disease =

TABLE 1. Patient characteristics by treatment arm: primary debulking surgery (PDS) (N = 108) versus neoadjuvant chemotherapy (NACT) (N = 49)

Patients Characteristic	PDS (108 patients)	NACT + IDS (49 patients)	*p value*
Age (years)	59,3 (28 - 85)	61,2 (34 – 80)	0,197
BMI	23,8 (18,6 – 34,6)	23,8 (17 – 42,9)	0,424
Parity (number)	2 (0 – 8)	2 (0 – 5)	0,125
Age at last period (years)	50 (40 – 60)	50 (42 – 58)	0,210
preop CA125 (units/mL)	435,0 (14,0 - 21156,0)	770,0 (68,0 - 36130,0)	0,059
Menopausal status			
Yes No	74,1 (80) 25,9 (28)	89,8 (44) 10,2 (5)	0,033
ASA			
1 2 3 4	16,7 (18) 53,7 (58) 28,7 (31) 0,9 (1)	10,2 (5) 61,2 (30) 26,5 (13) 2,0 (1)	0,559
Histology			
serous endometriod mucinous clear cells	66,7 (72) 25,0 (27) 4,6 (5) 3,7 (4)	85,7 (42) 12,2 (6) 0 (0) 2,0 (1)	0,071
FIGO STAGE			
III IIIa IIIb IIIc IV	95.4 (103) (8) (25) (70) 4.6 (5)	87.7 (43) (1) (0) (42) 12.3 (6)	0,08
Residual disease			
0 mm (RD = 0) 1-10 mm (RD = 1) > 10 mm (RD = 2)	53,7 (58) 17,6 (19) 28,7 (31)	77,6 (38) 8,2 (4) 14,3 (7)	0,020
Recurrence			
Yes No	79,6 (86) 20,4 (22)	87,8 (43) 12,2 (6)	0,265
Vital Status			
Alive Death	35,2 (38) 64,8 (70)	22,4 (11) 77,6 (38)	0,575
Length of follow-up (months)	41,7 (1,4 - 100,0)	34,5 (7,6 – 91,0)	0,21

Continuous variables are expressed as median (range); categorical variables are expressed as percentage (absolute number). IDS = interval-debulking surgery; NACT = neoadjuvant chemotherapy; PDS = primary debulking surgery

1 versus residual disease = 2) ASA stage (I–II versus III–IV) and number of adjuvant chemotherapy (ACHT) cycles.

Statistical analysis

Statistical analysis was performed by SPSS software (Chicago, IL, US) for Windows version 19, applying parametric and non-parametric tests when appropriate. We test the approximately normal distribution of sample through the Shapiro-Wilk's test and the visual inspection of the histograms. Due to the non-normal distribution of continuous variables, we analyzed them by U test of Mann-Whitney; we expressed them as absolute numbers and median (range). Categorical variables have been expressed as percentages and analyzed through the $\chi 2$ test or the Fisher's exact test, when appropriate. Statistically significant differences between treatment arms were defined as p value less than 0.05.

PFS was defined as the time interval from the date of diagnosis (surgery date for PDS and laparoscopy date for NACT) to the date of the documented first recurrence or progression of disease. If there was no documented recurrence, PFS was calculated from the date of surgery to the date of last follow-up or death, which ever occurred first. Date of progression was determined by serum CA-125 levels and/or computed tomography (CT) scan. OS was defined from the diagnosis date to the death date or last follow-up date.

The Kaplan-Meier method was used to estimate survival curves; for each analysis, the significance of the difference in the unadjusted survival curves was assessed using the log-rank test.

We calculated hazard ratios (HRs) for survival over the entire follow-up period using a Cox proportional hazards model and 95% confidence intervals (CIs). We entered the following prognostic factors in the multivariable model: type of treatment (PDS versus NACT + IDS), patient age at diagnosis (< 60 versus ≥ 60 years), residual disease after surgical debulking (residual disease = 0 versus residual disease = 1 versus residual disease = 2), ASA stage (I–II versus III–IV) and number of ACHT cycles.

Results

Patients' characteristics

Over the study period we collected data about 173 patients affected by EOC stage III and IV. We excluded from the analysis a total of 16 patients that after NACT (range 1–8 cycles) did not underwent IDS due to low performance status and progression of the disease. Of the remaining 157 patients, a total of 108 women were included in the PDS group while 49 patients were included in NACT + IDS group. Median age of PDS group was 59.3 years (28–85) versus 61.2 years (34–80) for NACT + IDS group (p = ns); median BMI was 23.8 kg/m^2 (18.6–34.6) for PDS and 23.8 kg/m^2 (17–42.9) for NACT + IDS (p = ns); median preoperative CA-125 was 435 IU/mL in the PDS group compared with 770 IU/mL in the NACT group (p = ns). Parity, age at last period and ASA classification did not differ signifi-

cantly between treatment arms (p = ns). The 95.4% (103 women) of patients included in PDS group presented with FIGO stage III and the remaining 4.6% (5 women) had FIGO stage IV. Similarly, in NACT group 87.7% of the sample (43 women) was diagnosed as FIGO stage III and only 12.3% (6 women) had FIGO stage IV. Histologic subtypes differed between groups; endometriod and mucinous were more represented in PDS group; in particular 25.0% and 4.6% of patients in PDS versus 12.6 and 0% in NACT group. Serous subtype was diagnosed in 66.7% of PDS group and 85.7% of NACT; clear cell carcinoma was diagnosed in 3.7% of PDS group versus 2.0% of NACT group. Patient characteristics grouped by treatment arms are listed in Table 1.

Intraoperative and post-operative data

In the PDS group a total of 51 (47.2%) patients underwent diagnostic laparoscopy before debulking surgery. On the contrary, all 49 patients of NACT + IDS group underwent diagnostic laparoscopy before starting NACT. Blood loss, need for transfusion and total number of EC units were significantly higher for PDS group compared to IDS. Median blood loss during surgery was 500ml (100–5000) for PDS group versus 400ml (50–2000) in NACT + IDS patients (p = 0.0001). As consequence the 40.7% of patients in PDS arm received blood transfusion compared to 24.5% of NACT arm (p = 0.035). Also hospitalization length after PDS was significantly higher, with a median of 15 (7–62) days, compared to NACT + IDS, median of 12 (5–38) days (p = 0.003).

On the contrary, the number of post-operative complications, according to Clavien-Dindo classification system resulted comparable between groups (p = 0.174). However, the rate of grade II, III and IV complications was higher in PDS group than in NACT + IDS group.

Finally, the re-operation rate for cancer recurrence did not differ significantly between arms; 24.2% for PDS group versus 23.8% for NACT + IDS group (p = 0.174). Intraoperative and post-operative data by treatment arm are listed in Table 2.

Neo-adjuvant and adjuvant chemotherapy data

Considering NACT + IDS group, the median interval time between diagnostic laparoscopy and the start of NACT was 3 weeks (2–5) and the median interval time between the end of NACT and the IDS was 3 weeks (2–8).

TABLE 2. Patient intra-operative and post-operative data by treatment arm: primary debulking surgery (PDS) (N = 108) versus neoadjuvant chemotherapy (NACT) (N = 49)

Variables	PDS (108 patients)	NACT + IDS (49 patients)	*p value*
LPS explorative	47,2 (51)	100 (49)	
Blood Loss (ml)	500,0 (100 - 5000)	400,0 (50 – 2000)	0,0001
EC units	2 (1 – 23) 44 patients	2 (2-3) 12 patients	0,019
Transfusion			
Yes No	40,7 (44) 59,3 (64)	24,5 (12) 75,5 (37)	0,035
Hospitalization Lenght	15 (7 - 62)	12 (5 -38)	0,003
Post-op complications			
No/Grade I-II Grade III-IV	77,8 (84) 22,2 (24)	93,9 (46) 6,1 (3)	0,009
Reoperation for recurrence			
Yes No	18,6 (16) 81,4 (70)	25,6 (11) 74,4 (32)	0,174

Continuous variables are expressed as median (range); categorical variables are expressed as percentage (absolute number). IDS = interval-debulking surgery; NACT = neoadjuvant chemotherapy; PDS = primary debulking surgery

The interval time between surgery and ACHT starting did not differ significantly between treatment arms: median of 4 (3–10) weeks for PDS versus 4 (2–7) weeks for NACT, (p = ns); in the same way also the need for a second line ACHT treatment did not differ between groups (p = ns).

Concerning the type of ACHT administered the great majority of patients received a combination of carboplatin and paclitaxel (84.8% in PDS group, 81.3% in NACT + IDS) followed by carboplatin alone (8.7% in PDS group, 8.3% in NACT + IDS), carboplatin plus doxorubicin (5.4% in PDS group, 8.3% in NACT + IDS) and finally carboplatin plus gemcitabine (1.1% in PDS group, 2.1% in NACT + IDS). All data about neo-adjuvant and adjuvant chemotherapy are listed in Table 3.

Residual disease by treatment group

Patients who received NACT were more likely to have no residual disease compared to patients who underwent PDS (p = 0.02). In particular, in PDS group, the 53.7% of patients resulted completely debulked; the 17.6% were optimally debulked (for a total of 71.3% of patients with residual disease = 0 and residual disease = 1 after PDS) and the 28.7 resulted suboptimally debulked. On the contrary in NACT + IDS group the 77.6% of the sample resulted completely debulked; the 8.2% were optimally debulked (for a total of 85.8% of patients with residual disease = 0 and residual disease = 1

after IDS) and only 14.3% resulted suboptimally debulked. All data about residual disease by treatment arm are listed in Table 1.

TABLE 3. Patient data about type of chemotherapy (neoadjuvant chemotherapy [NACT] and adjuvant chemotherapy [ACHT]) and interval time from surgery: primary debulking surgery (PDS) (N = 108) versus NACT (N = 49)

NACT + IDS group			
Cycles of NACT	5 (3 – 6)		
Type of NACT			
Carboplatin Carboplatin and Paclitaxel Carboplatin and Doxorubicin	8,2 (4) 87,8 (43) 4,1 (2)		
Response to NACT			
Complete Partial	20,4 (10) 79,6 (39)		
Interval LPS to NACT (weeks)	3 (2 – 5)		
Interval NACT to IDS (weeks)	3 (2 - 8)		
All Groups	**PDS (108 patients)**	**NACT + IDS (49 patients)**	***p value***
Cycles of ACHT	6 (2 - 9)	3 (2 – 9)	0,000
Type of ACHT			
Carboplatin Carboplatin and Paclitaxel Carboplatin and Doxorubicin	7,4 (8) 88,0 (95) 4,6 (5)	8,2 (4) 87,8 (43) 4,1 (2)	1,000
Interval PDS to ACTH and IDS to ACTH	4 (3 - 10)	4 (2 - 7)	0,147
Second line ACHT			
Yes No	78,9 (56) 21,1 (15)	79,1 (34) 20,9 (9)	0,588

Continuous variables are expressed as median (range); categorical variables are expressed as percentage (absolute number). ACHT = adjuvant chemotherapy; IDS = interval-debulking surgery; NACT = neoadjuvant chemotherapy; PDS = primary debulking surgery

TABLE 4. Overall survival and progression free survival in patients who underwent primary debulking surgery (PDS) (N = 108) and neoadjuvant chemotherapy (NACT) + interval debulking surgery (IDS) (N = 49); NACT stratified by residual disease (all sample)

	PFS		**OS**	
	Median (months)	**95% CI (months)**	**Median (months)**	**95% CI (months)**
PDS				
0 mm (RD = 0) 1-9 mm (RD = 1) > 10 mm (RD = 2)	20,7 11,2 13,3	13,2 - 28,3 10,2 - 12,2 10,0 - 16,5	54,7 34,7 31,3	40,6 - 68,7 0,00 - 71,1 15,6 - 47,0
General	17,3	15,0- 19,5	41,3	31,2 - 51,3
NACT + IDS				
0 mm (RD = 0) 1-9 mm (RD = 1) > 10 mm (RD = 2)	19,9 14,5 8,0	16,1 - 23,7 2,7 - 26,3 6,0 - 9,9	36,3 25,6 16,1	27,7 - 44,8 3,9 - 47,2 8,1 – 24,0
General	18,3	14,9- 21,8	34,5	26,6 - 42,4

Continuous variables are expressed as median (range); categorical variables are expressed as percentage (absolute number). IDS = interval-debulking surgery; NACT = neoadjuvant chemotherapy; OS = overall survival; PDS = primary debulking surgery; PFS = progression free survival

It is important to underline the fundamental role of explorative laparoscopy (LPS) in predicting the resectability of the tumor. Considering the whole sample (both PDS and NACT + IDS), the 71% (71 women) of patients who underwent explorative LPS resulted completely debulked (residual disease = 0) compared to the 43.9% (25 women) of patients who did not perform LPS. On the contrary only 13% (13 women) and 16% (16 women) of patients who underwent LPS before surgery resulted optimally (residual disease = 1) and sub-optimally debulked (residual disease = 2) respectively, compared to the 17.5% (10 women) and 38.6% (22 women) of patients that did not underwent LPS (p = 0,002). Also considering only PDS patients diagnostic laparoscopy was able to predict significantly the resectability of the tumor. The 64.7% of patients who underwent diagnostic laparoscopy (33 women) in PDS group resulted completely debulked (residual disease = 0) versus the 43.9% (25 women) who did not receive LPS. Moreover only 17.6% (9 women) and 17.6% (9 women) of patients who underwent LPS before surgery resulted optimally (residual disease = 1) and sub-optimally debulked (residual disease = 2) respectively, compared to the 17.5% (10 women) and 38.6% (22 women) of patients that did not underwent LPS (p = 0.046).

Overall survival and progression free survival

Considering both treatment arms the median PFS was 17.7 (16.0–19.4; 95% CI) months for all patients and the median OS was 37.9 (32.6–43.2; 95% CI) months for all patients.

The median PFS for patients who underwent PDS was 17.3 (15.0–19.5; 95% CI) months, the median OS was 41.3 (31.2–51.3 95% CI) months. The median PFS and OS for patients selected for NACT was 18.3 (14.9–21.8; 95% CI) and 34.5 (26.6–42.4; 95% CI) months, respectively.

Differences in PFS and OS between groups were not statistically significant (p = 0.737 and p = 0.184 respectively). The 5-years OS resulted 36.1% in PDS group versus 26.5% in NACT + IDS group. All data are presented in Table 4 and Kaplan-Meier curves in Figures 1A and 1B.

Stratifying our arms according to residual disease, we found that patients who underwent NACT + IDS completely debulked (residual disease = 0) experienced a worse median OS (36.3 months; 27.7–44.8; 95% CI), even if not statistically significant, when compared to PDS patients completely debulked (residual disease = 0) (OS 54.7

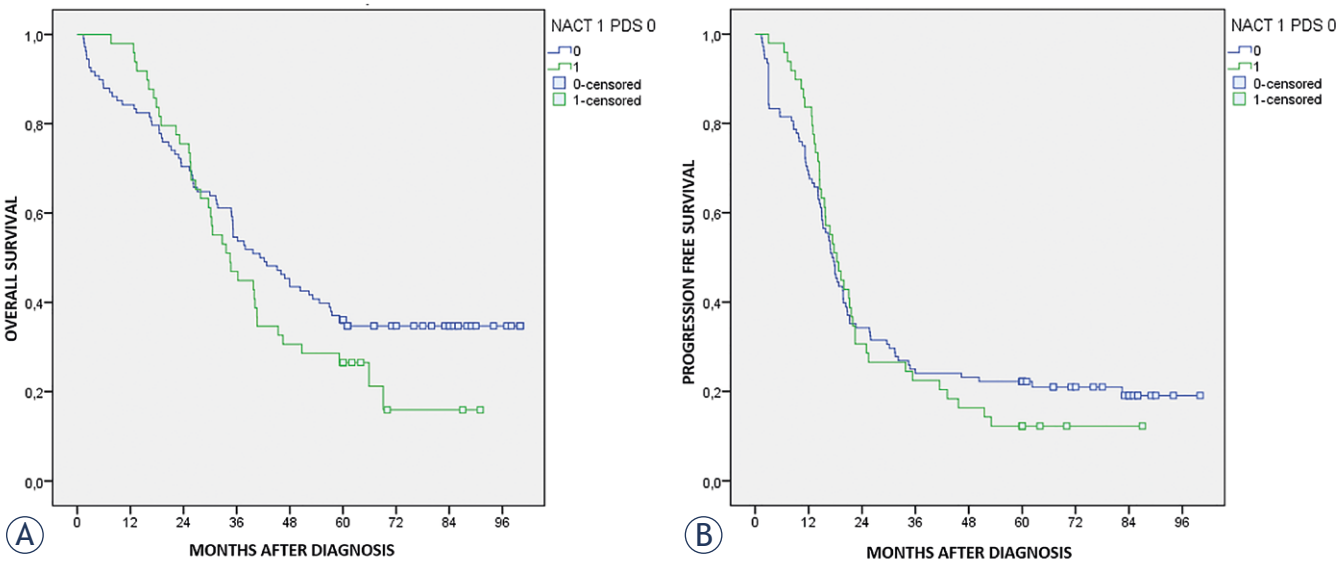

FIGURE 1. (A) Overall survival by treatment arm: primary debulking surgery (PDS) (N = 108) versus neoadjuvant chemotherapy (NACT) (N = 49). **(B)** Progression free survival by treatment arm: primary debulking surgery (PDS) (N = 108) versus neoadjuvant chemotherapy (NACT) (N = 49).

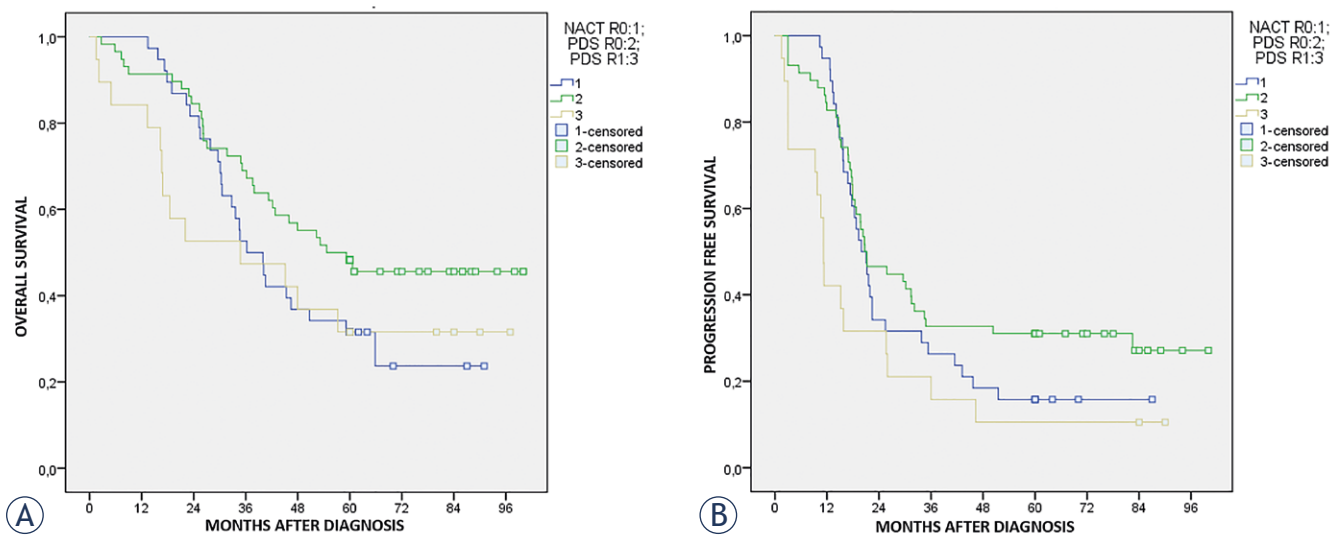

FIGURE 2. (A) Overall survival according the neoadjuvant chemotherapy (NACT) + interval debulking surgery (IDS) with residual disease = 0 versus primary debulking surgery (PDS) with residual disease = 0 and PDS with residual disease = 1. **(B)** Progression free survival according the neoadjuvant chemotherapy (NACT) + interval debulking surgery (IDS) with residual disease = 0 versus primary debulking surgery (PDS) with residual disease = 0 and primary debulking surgery PDS with residual disease = 1.

months; 40.6–68.7; 95% CI) (p = 0.12). The OS between NACT + IDS patients with residual disease = 0 and PDS patients optimally debulked (residual disease = 1) (OS 34.7 months; 0.00–71.1; 95% CI) were comparable (p = 0.73).

Considering PFS we found that patients who underwent NACT + IDS completely debulked (residual disease = 0) experienced comparable median PFS (19.9 months; 16.1–23.7; 95% CI) when compared to PDS patients completely debulked (residual disease = 0) (20.7 months; 13.2–28.3; 95% CI) (p = 0.251). The median PFS of PDS patients optimally debulked (residual disease = 1) (11.2 months; 10.2–12.2; 95% CI) resulted significantly worse than PFS of NACT + IDS patients completely debulked (residual disease = 0) (p = 0.005).

The 5 years OS for NACT + IDS patients residual disease = 0 was 32.6%, for PDS patients residual

TABLE 5. Univariate and multivariate hazard ratios (HRs) and 95% confidence intervals (CIs) associated with selected variables, all sample and stratified by treatment group

Variables	Univariate HR (95% CI)	p	Multivariate HR (95% CI)	p
All sample (157)				
Treatment group				
PDS	1.00 (reference)			
NACT + IDS	1,34 (0,90 – 1,99)	0,14	1,45 (0,87 – 2,42)	0,14
Residual Disease				
0 mm (RD = 0)	1.00 (reference)			
1-9 mm (RD = 1)	1,51 (0,88 - 2,60)	0,13	1,66 (0,96 – 2,82)	0,06
> 10 mm (RD = 2)	2,29 (1,49- 3,53)	0,0001	2,82 (1,79 – 4,46)	0,0001
Age				
< 60	1.00 (reference)			
≥ 60	1,33 (0,91 - 1,95)	0,13	0,91 (0,61 – 1,38)	0,68
ASA				
I - II	1.00 (reference)			
III - IV	2,29 (1,53 – 3,41)	0,0001	2,21 (1,44 – 3,40)	0,0001
ACHT cycles	0,94 (0,82 – 1,08)	0,42	0,99 (0,85 – 1,16)	0,96
PDS group				
Residual Disease				
0 mm (RD = 0)	1.00 (reference)			
1-9 mm (RD = 1)	1,70 (0,89 – 3,26)	0,10	2,12 (1,08 – 4,15)	0,028
> 10 mm (RD = 2)	2,37 (1,40 – 4,0)	0,001	3,12 (1,80 – 5,41)	0,00005
Age				
< 60	1.00 (reference)			
≥ 60	1,49 (0,93 – 2,39)	0,09	0,81 (0,48 – 1,37)	0,44
ASA				
I - II	1.00 (reference)			
III - IV	3,44 (2,08 – 5,68)	0,001	4,40 (2,50 – 7,75)	0,0001
ACHT cycles	0,77 (0,51 – 1,16)	0,22	0,70 (0,53 – 0,93)	0,015
NACT + IDS group				
Residual Disease				
0 mm (RD = 0)	1.00 (reference)			
1-9 mm (RD = 1)	1,38 (0,47 – 3,98)	0,55	1,53 (0,52 – 4,52)	0,43
> 10 mm (RD = 2)	4,92 (2,04 – 11, 88)	0,0001	6,67 (2,43 -18,33)	0,0001
Age				
< 60				
≥ 60	0,95 (0,50 – 1,81)	0,88	0,71 (0,35 – 1,47)	0,36
ASA				
I - II				
III - IV	0,99 (0,48 – 2,01)	0,97	0,77 (0,35 – 1,69)	0,52
ACHT cycles	1,01 (0,85 – 1,19)	0,89	1,03 (0,86 – 1,23)	0,70

Residual disease, age class, ASA score were included in the multivariate analysis. ACHT = adjuvant chemotherapy; ASA = American Society of Anesthesiologists; IDS = interval-debulking surgery; NACT = neoadjuvant chemotherapy; PDS = primary debulking surgery

disease = 0 was 48.3% and finally for PDS patients residual disease = 1 was 31.6%. The 5 years PFS for NACT + IDS patients residual disease = 0 was 15.8%, for PDS patients residual disease = 0 was 31.0% and finally for PDS patients residual disease = 1 was 10.5%. See Kaplan-Meier curves in Figures 2A and 2B. All data about OS and PFS stratified by residual disease are summarized in Table 4.

In our sample there were differences between groups in the distribution of histological type (the great majority of endometriod and all mucinous were included in PDS arm), even if we considered only high grade tumor, this fact could be a potential source of bias. Due to this fact, we decided to repeat vital analysis excluding endometriod and mucinous subtypes.

As expected, also excluding these subtype, the median PFS and OS resulted comparable between groups (p = 0.634 and p = 0.541 respectively). The median PFS and OS for patients selected for PDS was 16.8 (14.6–19.0; 95% CI) and 39.6 (28.9–50.3; 95% CI) months respectively. The median PFS and OS for patients selected for NACT + IDS was 19.3 (15.0–23.5; 95% CI) and 36.3 (27.0–45.5; 95% CI) months respectively. See Kaplan–Meier curves in Figures 3A and 3C.

Also in this case stratifying our arms according to residual disease, we found that NACT + IDS patients completely debulked (residual disease = 0) showed a worse median OS (39.9 months; 31.3–48.6; 95% CI), although not significant, compared to PDS patients completely debulked (residual disease = 0) (47.9 months; 34.5–61.3; 95% CI) (p = 0.434). On the contrary, median OS of NACT + IDS completely debulked (residual disease = 0) was better than median OS of PDS patients optimally debulked (residual disease = 1) (34.7 months; 0.00–76.9; 95% CI), but still not significant (p = 0.656).

In the same way, median PFS of NACT + IDS patients completely debulked (residual disease = 0) resulted comparable (21.0 months, 17.7–24.3; 95% CI) to PDS patients with no residual disease (residual disease = 0) (19.7 months, 16.3–23.1; 95% CI) (p = 0.904). On the contrary, median PFS in PDS patients optimally debulked (residual disease = 1) (10.6 months; 7.8–13.3; 95% CI) resulted significantly worse than NACT + IDS patients completely debulked (residual disease = 0) (p = 0.012). See Kaplan-Meier curves in Figures 4A and 4B. While the 5 years OS for NACT + IDS patients residual disease = 0 was 35.3%, for PDS patients residual disease = 0 was 38.5% OS.

We conducted a multivariate survival analysis for the whole sample and according to treatment

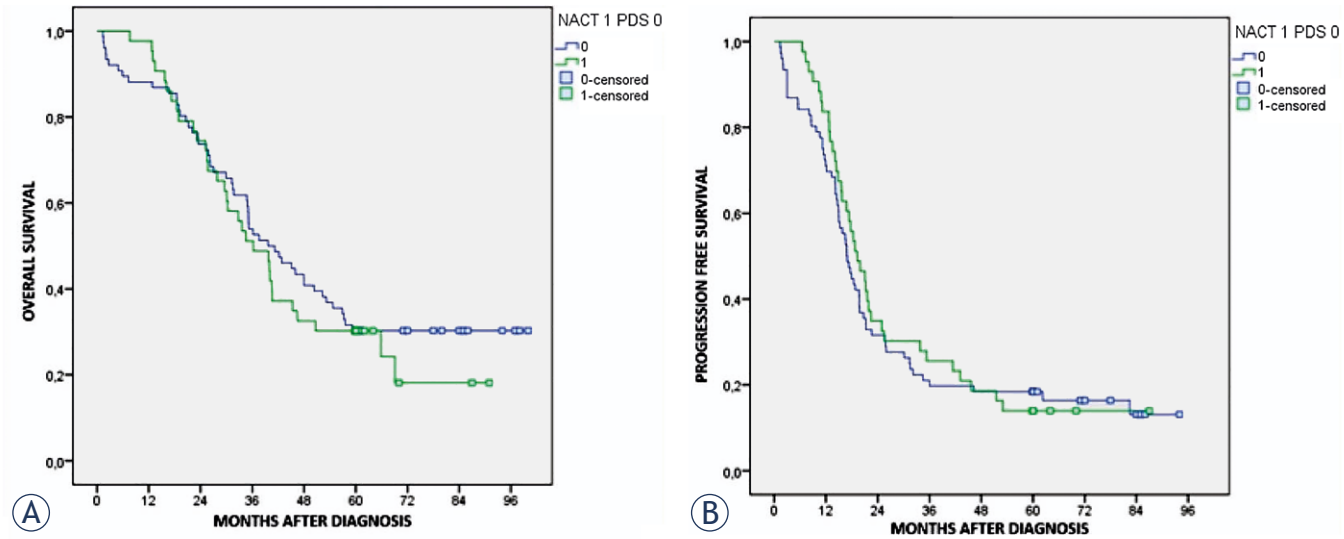

FIGURE 3. (A) Overall survival by treatment excluding endometriod and mucinous histotype. **(B)** Progression free survival by treatment excluding endometriod and mucinous histotype.

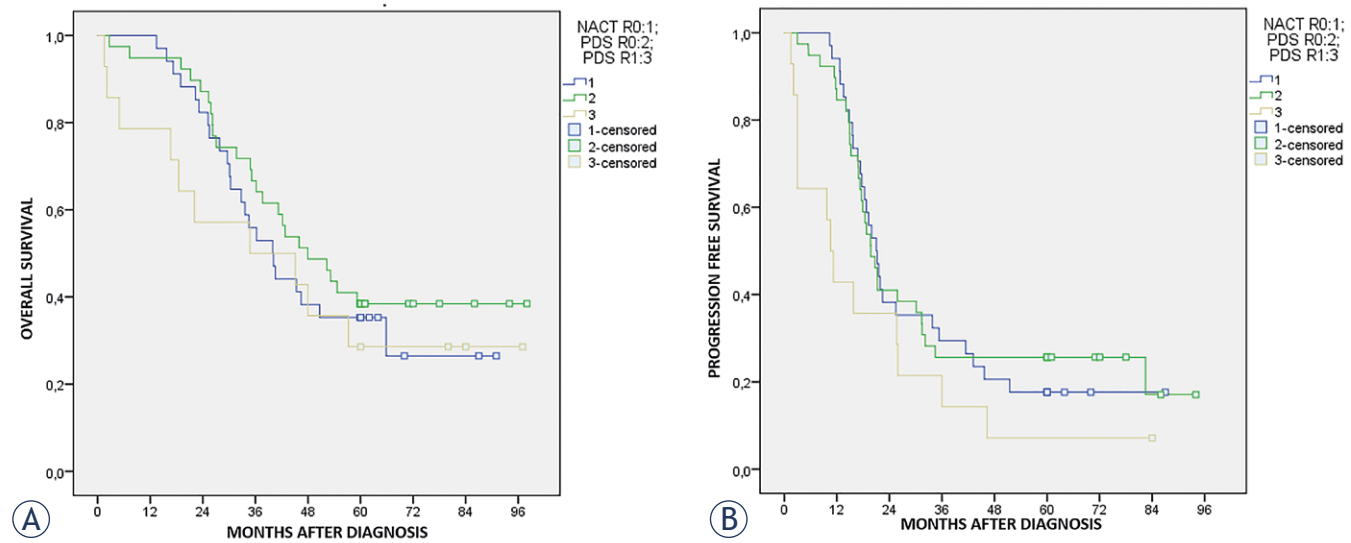

FIGURE 4. (A) Overall survival according the neoadjuvant chemotherapy (NACT) + interval debulking surgery (IDS) with residual disease = 0 versus primary debulking surgery (PDS) with residual disease = 0 and PDS with residual disease = 1 (excluding endometriod and mucinous histotype). **(B)** Progression free survival according the neoadjuvant chemotherapy (NACT) + interval debulking surgery (IDS) with residual disease = 0 versus primary debulking surgery (PDS) with residual disease = 0 and PDS with residual disease = 1 (excluding endometriod and mucinous histotype).

arms. Considering both the whole sample and treatments arms, the presence of residual disease after debulking surgery and pre-operative ASA score > II were significant predictors of survival. On the contrary, age lower than 60 years did not relate with better OS. The number of cycles of ACHT was significantly associated with survival only for PDS arm in multivariate model. Univariate and multivariate analysis are presented in Table 5.

Discussion

General considerations

It is widely confirmed that the amount of residual disease at the time of surgery is the pivotal determinant of outcome in patients affected by advanced stage EOC.[20] Du Bois *et al.*, analyzing the results of three randomized trials, demonstrated that patients with no residual disease showed a

significant better OS and PFS when compared both to optimally and sub-optimally debulked patients.[4] Therefore, it is now accepted that the goal of cytoreductive surgery changed from a residual disease of 1–2 cm to the complete resection of macroscopically visible tumor.[20, 21]

However, in advanced stage EOC the rate of complete debulking is generally estimated lower than 50%.[9-11] The reasons for suboptimal debulking may be related to large intra-abdominal extension of the tumor, localization in critical anatomical site, medical comorbidities, advanced age and poor oncological experience of surgeons.[4,22,23] All such variables are of crucial importance to understand the reasons that led the paradigm shift, in selected cases, from standard PDS approach to alternative therapeutic options like NACT + IDS treatment.[10,15,16]

The rationale of administering NACT before dubulking surgery is to reduce disease spread in abdominal pelvic cavity, in order to increase the probability to perform a subsequent complete debulking with less aggressive surgery and lower post-operative complications.[20]

In our series we found that the 77.6% of patients in NACT + IDS arm showed no macroscopic residual disease after surgery versus the 53.7% of PDS arm. These data certainly confirmed the principle that after NACT administration the rate of complete or optimal debulking is strongly higher. Recent series are in line with our results; in the recent paper by Mueller *et al.* a 47% of PDS and 55% of NACT patients underwent complete gross resection.[10] Also May *et al*. described a residual disease = 0 in 35.2% of PDS patients versus 42.4% of NACT group.[9,10] In addition, also the CHORUS randomized trial described a better rate of residual disease = 0 after IDS than after PDS, even if the 17% of complete debulking after PDS and of 39% after IDS is drastically lower if compared to our results but also to other series.[9,10,11]

Concerning the post-operative complications rate, we confirmed data by previous trials; we found a significant higher rate of grade 3 and 4 complications in PDS group compared to NACT. Both two published randomized trials reported higher rate of severe post-operative complications and mortality in primary surgery group when compared to NACT + IDS arm.[12,13]

However, it is interesting to highlight that higher rate of complete debulking (R = 0), as well as the lower rate of surgery-related complications in NACT + IDS group, did not result in increased OS in large majority of studies; differently, OS was equally comparable or even inferior to PDS arm. In the first published randomized trial Vergote *et al.* analyzing 632 patients treated by PDS or NACT + IDS found no differences in OS (29 months in PDS and 30 months in NACT) between the treatments groups.[13] Similarly, in experience by Kehoe *et al*, the comparison between 276 patients assigned to primary surgery versus 274 assigned to primary chemotherapy showed no differences in term of OS (22.6 months in PDS and 24.1 months in NACT) and PFS (10.7 months in PDS and 12.0 months in NACT).[12]

Stating these data, both Authors concluded that giving primary chemotherapy before surgery is an acceptable standard of care for women with advanced stage EOC. However, different concerns have been raised regarding the reproducibility of these results.[14] Drawbacks include the above mentioned poor rate of surgical radicality compared to other studies; the low-median operating time (120–165 minutes) and finally, most importantly, the very low OS and PFS reported.[9,10] Starting from these limitations of evidence quality from RCTs, the debate on the ideal management of advanced EOC is still open and a comprehensive evaluation of literature should take in account also data from lowly powered studies; at this regard, different authors published some retrospective analysis that reached opposite results in comparison to RCTs. In a recent paper May *et al*. described a better five-years OS in primary surgery group (39%) compared to NACT + IDS arm (27%).[9] Also Mulller *et al.* in their analysis of a cohort of 586 patients demonstrated that PDS patients had significantly higher median OS and PFS (71.7 and 21.7 months respectively) in comparison to NACT patients (42.9 and 13.9 months respectively).[10] From the data analysis of American National Cancer Database, including women with primary EOC with less than 70 years and without comorbidities, Rauh-Hain *et al.* described a median OS of 37.3 months in the PDS group and 32.1 months in the NACT group ($p < 0.001$).[24] Finally, also Rosen *et al.* and Kessous *et al.* reached similar results.[11,12] These different findings in comparison to RCTs may be related to several factors, such as the retrospective design of the studies and the selection bias related to patients included in NACT group, who may be affected by greater spread of disease and lower performance status at the time of study inclusion.

Moreover, another important factor to be considered is that the poor outcome of NACT patients (also with lower residual disease) could be related to own tumor biology, potentially related with

lower chemosensitivity in comparison to patients in which a complete primary debulking can be obtained. In particular, different retrospective series suggested a strong association between tumor volume, suboptimal cytoreduction and NACT + IDS with platinum resistance.[24-26] The most widely accepted hypothesis implicates the outgrowth of resistant clones, which are usually present at low rates before initial treatment and are greater in large tumor volumes treated with platinum compounds.[27]

Main findings

In our series, considering the whole sample, although the higher rate of no residual disease in NACT + IDS arm and of surgical complications of PDS arm, we found a lower OS, but not statistically significant, in NACT + IDS arm (34.4 months) compared to PDS arm (41.3 months). PFS resulted comparable between groups (17.3 months in PDS versus 18.3 months in NACT arm). Also excluding endometrioid and mucinous subtype, in order to decrease as much as possible the selection bias, the trend resulted comparable (OS of 39.6 months in PDS versus 36.3 in NACT arm; PFS of 16.8 months in PDS versus 19.3 months in NACT arm). Our results are in line with retrospective series by Lim *et al.* and Bian *et al.* but also with ERTOC and CHORUS randomized trials.[12,13,28,29]

Considering that the pivotal factor that drives surgical action is the possibility to obtain a complete/optimal cytoreduction, we compared the survival in both arms stratifying data according to residual disease (Table 4). We found better OS, even if not statistically significant, in patients with no residual disease included in PDS arm compared to NACT + IDS arm. Median OS of patients of PDS arm optimally debulked was comparable to NACT + IDS with no residual disease. The PFS of patients with no residual disease was comparable in both groups; however, PDS patients optimally debulked experienced a significant lower PFS of about 9 months if compared to NACT + IDS patients completely debulked.

As in our sample endometrioid and mucinous subtypes were mostly represented in PDS arm, we decided to repeat the analysis excluding these subgroups. We took this decision basing both on statistical reasons, in order to eliminate selection bias between groups, and on biological reasons. Indeed endometrioid cancer is generally associated with better outcome compared to other histology due to its intrinsic biological behavior and to its association with lower grading and staging.[30] Similarly, mucinous subtypes are associated to a good prognosis in case of lower stage, but to worst prognosis (due to its intrinsic biological features of chemo-resistance) if compared to other histological types in case of advanced stage.[31] Interestingly, also excluding these cases we found no change in trends of OS and PFS previously reported.

Therefore, from our analysis, we confirm a non-superiority of NACT + IDS in term of median OS and PFS when compared to standard PDS approach. However, stratifying data based on residual disease after surgery we found that benefits of PDS approach are maximized when residual disease = 0 was attained. The benefit of PDS resulted comparable between optimal debulked PDS patients and complete dubulked NACT patients in term of OS. The median PFS was comparable between treatment arms in case of residual disease = 0; on the contrary benefit of a PDS approach with residual disease = 1 was drastically lower, when compared to NACT + IDS with residual disease = 0.

This data is of crucial importance for patients because a less aggressive surgery and the interval time without disease could be considered surrogate measurement of patient's quality of life. Certainly, also in case of NACT administration maximum efforts must be made to obtain no residual disease after IDS; in a recent report by Marchetti *et al.*, patients who did not undergo IDS after NACT showed a median OS of 18 months that is similar to median OS of our patients with residual disease = 2 after IDS.[32] Therefore, the selection of patients suitable for IDS was a fundamental step to improve survivals and to avoid unnecessary surgery that can only result in a decrease of patient's quality of life.

Different approach has been tested to predict the resectability of tumor like CT, MR and positron emission tomography imaging. However, recent studies point a highly valuable role for laparoscopic Fagotti score to assess the feasibility of complete/optimal cytoreduction.[7] In our sample, all NACT patients received laparoscopy before starting chemotherapy; the decision was not based on a defined laparoscopic score but on experience of gynecologic oncologist surgeon. In our series we confirmed the value of diagnostic laparoscopy for resectability assessment; patients of PDS arm who underwent laparoscopy before surgery showed a significant higher rate of complete debulking compared to patients who did not undergo laparoscopy. In our opinion, laparoscopic assessment before PDS or IDS should became one of the fundamental diagnostic steps to drive treatment decision.

According to different papers we found in univariate and multivariate model that both in PDS and NACT + IDS arms the most important predictor of survival was represented by the residual disease after cytoreductive surgery.[9,10] Moreover, according to Gill *et al*. experience we found also that an ASA score > 2 was strongly associated with survival in both univariate and multivariate model.[33] Concerning adjuvant chemotherapy cycles we found no differences in both univariate and multivariate models in NACT arm, but we found an association with better survival in multivariate analysis in PDS arm.

Limits of the study

Our study is affected by different limitations; the main potential source of bias is related to patients' selection, as primary treatment choice (between PDS and NACT) was based on the spread of the disease and patients' health status; the retrospective design of the study did not allow overcoming this bias.

Secondly, the pre-operative laparoscopic assessment of abdominal cavity was not based on a pre-defined score but on single operator experience; however, the choice of primary treatment was made by a Multidisciplinary Group (including gynecologic oncologists, medical oncologists, radiologists and pathologists) basing on criteria that are similar to other studies. Finally, we included in the analysis only patients who underwent IDS after chemotherapy, excluding 16 patients that did not undergo surgery due to disease progression or medical conditions, potentially leading to an overstatement of NACT + IDS patient's survivals.

Main points of strength of our study are related to rigorous data collection methodology and strict inclusion criteria; all information were collected from our electronic hospital records, which are compiled by clinicians at each step of patient's treatment, representing certainly a guarantee of the completeness and correctness of the data reported. We included exclusively patients referred from diagnosis to treatment to our oncological institute, excluding any sources of bias related to heterogeneous surgical choices and procedures.

Moreover, we selected only high grade and advanced stage EOC, minimizing the heterogeneity related to variable disease spread and stage-related prognosis; additionally, all patients received adjuvant chemotherapy based on platinum agents. A sensitivity analysis was also performed in order to exclude any sources of selection bias potentially related to different outcomes of specific histological subtypes of ovarian cancer. Finally, both study groups resulted comparable in term of general features and length of follow-up (at least 60 months). Despite the different limitations of our study, all these points of strength seemingly confer adequate accuracy to our survival estimates.

Conclusions

In conclusion, according to recent literature, we reaffirm the non-superiority of NACT + IDS compared to PDS approach for the treatment of EOC, even if NACT + IDS treatment is associated with significant lower post-operative complications. In order to maximize survival and to ensure a good quality of life, it is mandatory to define the most effective treatment for advanced EOC based on pre-operative conditions, and most importantly according to potential resectability of tumor. Stating that the goal of advanced stage EOC surgery is to reach complete cytoreduction, more efforts are needed to allow an adequate selection of patients that can benefit from PDS or IDS surgery, avoiding unfavorable procedures. In this light, the laparoscopic primary assessment of tumor extension seems to be reliable in estimating tumor resectability and may potentially represent a valuable strategy for the decision making between primary and interval debulking surgery. However, further studies are needed to confirm the rationale of the use of primary diagnostic laparoscopy as the standard of care in all oncological institutions.

We confirmed the value of primary PDS approach for the treatment of high grade, advanced stage EOC, even if OS is maximized only if no residual disease is attained. If the chances to reach a complete debulking at PDS are low, NACT + IDS approach (with the goal of subsequent residual disease = 0) must be considered because even if we did not evidence benefits in term of OS we found benefits in term of PFS (if compared to PDS with residual disease = 1) that could be related to an increase quality of life. However, if the chances to obtain a complete or at least optimal debulking after standard cycles of NACT are still low, probably subsequent IDS will not be useful to increase patient's survival.

References

1. Siegel RL, Miller KD, Jemal A. Cancer statistics, 2017. *CA Cancer J Clin* 2017; **67:** 7-30. doi: 10.3322/caac.21387
2. Ataseven B, Chiva LM, Harter P, Gonzalez-Martin A, du Bois A. FIGO stage IV epithelial ovarian, fallopian tube and peritoneal cancer revisited. *Gynecol Oncol* 2016; **142:** 597-607. doi: 10.1016/j.ygyno.2016.06.013
3. Kumar L, Pramanik R, Kumar S, Bhatla N, Malik S. Neoadjuvant chemotherapy in gynaecological cancers - Implications for staging. *Best Pract Res Clin Obstet Gynaecol* 2015; **29:** 790-801. doi: 10.1016/j.bpobgyn.2015.02.008
4. du Bois A, Reuss A, Pujade-Lauraine E, Harter P, Ray-Coquard I, Pfisterer J. Role of surgical outcome as prognostic factor in advanced epithelial ovarian cancer: a combined exploratory analysis of 3 prospectively randomized phase 3 multicenter trials: by the Arbeitsgemeinschaft Gynaekologische Onkologie Studiengruppe Ovarialkarzinom (AGO-OVAR) and the Groupe d'Investigateurs Nationaux Pour les Etudes des Cancers de l'Ovaire (GINECO). *Cancer* 2009 15; **115:** 1234-44. doi: 10.1002/cncr.24149
5. Kessous R, Laskov I, Abitbol J, Bitharas J, Yasmeen A, Salvador S, et al. Clinical outcome of neoadjuvant chemotherapy for advanced ovarian cancer. *Gynecol Oncol* 2017; **144:** 474-9. doi: 10.1016/j.ygyno.2016.12.017
6. Liu Z, Beach JA, Agadjanian H, Jia D, Aspuria PJ, Karlan BY, et al. Suboptimal cytoreduction in ovarian carcinoma is associated with molecular pathways characteristic of increased stromal activation. *Gynecol Oncol* 2015; **139:** 394-400. doi: 10.1016/j.ygyno.2015.08.026
7. Gómez-Hidalgo NR, Martinez-Cannon BA, Nick AM, Lu KH, Sood AK, Coleman RL, et al. Predictors of optimal cytoreduction in patients with newly diagnosed advanced-stage epithelial ovarian cancer: Time to incorporate laparoscopic assessment into the standard of care. *Gynecol Oncol* 2015; **137:** 553-8. doi: 10.1016/j.ygyno.2015.03.049
8. Melamed A, Hinchcliff EM, Clemmer JT, Bregar AJ, Uppal S, Bostock I, et al. Trends in the use of neoadjuvant chemotherapy for advanced ovarian cancer in the United States. *Gynecol Oncol* 2016; **143:** 236-40. doi: 10.1016/j.ygyno.2016.09.002
9. May T, Comeau R, Sun P, Kotsopoulos J, Narod SA, Rosen B, et al. A Comparison of Survival Outcomes in Advanced Serous Ovarian Cancer Patients Treated With Primary Debulking Surgery Versus Neoadjuvant Chemotherapy. *Int J Gynecol Cancer* 2017; **27:** 668-74. doi: 10.1097/IGC.0000000000000946
10. Mueller JJ, Zhou QC, Iasonos A, O'Cearbhaill RE, Alvi FA, El Haraki A, et al. Neoadjuvant chemotherapy and primary debulking surgery utilization for advanced-stage ovarian cancer at a comprehensive cancer center. *Gynecol Oncol* 2016; **140:** 436-42. doi: 10.1016/j.ygyno.2016.01.008
11. Rosen B, Laframboise S, Ferguson S, Dodge J, Bernardini M, Murphy J, et al. The impacts of neoadjuvant chemotherapy and of debulking surgery on survival from advanced ovarian cancer. *Gynecol Oncol* 2014; **134:** 462-7. doi: 10.1016/j.ygyno.2014.07.004
12. Kehoe S, Hook J, Nankivell M, Jayson GC, Kitchener H, Lopes T, et al. Primary chemotherapy versus primary surgery for newly diagnosed advanced ovarian cancer (CHORUS): an open-label, randomised, controlled, non-inferiority trial. *Lancet* 2015; **386:** 249-57. doi: 10.1016/S0140-6736(14)62223-6
13. Vergote I, Tropé CG, Amant F, Kristensen GB, Ehlen T, Johnson N, et al. European Organization for Research and Treatment of Cancer-Gynaecological Cancer Group; NCIC Clinical Trials Group. Neoadjuvant chemotherapy or primary surgery in stage IIIC or IV ovarian cancer. *N Engl J Med* 2010; **363:** 943-53. doi: 10.1056/NEJMoa0908806
14. Mahner S, Trillsch F, Chi D, Harter P, Pfisterer J, Hilpert F, et al. Neoadjuvant chemotherapy in ovarian cancer revisited. *Ann Oncol* 2016; **27 (Suppl 1):** i30-2. doi: 10.1093/annonc/mdw092
15. Cornelis S, Van Calster B, Amant F, Leunen K, van der Zee AG, Vergote I. Role of neoadjuvant chemotherapy in the management of stage IIIC-IV ovarian cancer: survey results from the members of the European Society of Gynecological Oncology. *Int J Gynecol Cancer* 2012; **22:** 407-16. doi: 10.1097/IGC.0b013e31823ea1d8
16. Dewdney SB, Rimel BJ, Reinhart AJ, Kizer NT, Brooks RA, Massad LS, et al. The role of neoadjuvant chemotherapy in the management of patients with advanced stage ovarian cancer: survey results from members of the Society of Gynecologic Oncologists. *Gynecol Oncol* 2010; **119:** 18-21. doi: 10.1016/j.ygyno.2010.06.021
17. Chan YM, Ng TY, Ngan HY, Wong LC. Quality of life in women treated with neoadjuvant chemotherapy for advanced ovarian cancer: a prospective longitudinal study. *Gynecol Oncol* 2003; **88:** 9-16. doi:10.1006/gyno.2002.6849
18. Greimel E, Kristensen GB, van der Burg ME, Coronado P, Rustin G, del Rio AS, et al. European Organization for Research and Treatment of Cancer - Gynaecological Cancer Group and NCIC Clinical Trials Group. Quality of life of advanced ovarian cancer patients in the randomized phase III study comparing primary debulking surgery versus neo-adjuvant chemotherapy. *Gynecol Oncol* 2013; **131:** 437-44. doi: 10.1016/j.ygyno.2013.08.014
19. Clavien PA, Barkun J, de Oliveira ML, Vauthey JN, Dindo D, Schulick RD, et al. The Clavien-Dindo classification of surgical complications: five-year experience. *Ann Surg* 2009; **250:** 187-96. doi: 10.1097/SLA.0b013e3181b13ca2
20. Karam A, Ledermann JA, Kim JW, Sehouli J, Lu K, Gourley C, et al. Fifth Ovarian Cancer Consensus Conference of the Gynecologic Cancer InterGroup: first-line interventions. *Ann Oncol* 2017; **28:** 711-7. doi: 10.1093/annonc/mdx011
21. Chang SJ, Hodeib M, Chang J, Bristow RE. Survival impact of complete cytoreduction to no gross residual disease for advanced-stage ovarian cancer: a meta-analysis. *Gynecol Oncol* 2013; **130:** 493-8. doi: 10.1016/j.ygyno.2013.05.040
22. Brand AH. Ovarian cancer debulking surgery: a survey of practice in Australia and New Zealand. *Int J Gynecol Cancer* 2011; **21:** 30-5. doi: 10.1097/IGC.0b013e318205fb4f
23. Dahm-Kähler P, Palmqvist C, Staf C, Holmberg E, Johannesson L. Centralized primary care of advanced ovarian cancer improves complete cytoreduction and survival - A population-based cohort study. *Gynecol Oncol* 2016; **142:** 211-6. doi: 10.1016/j.ygyno.2016.05.025
24. Rauh-Hain JA, Melamed A, Wright A, Gockley A, Clemmer JT, Schorge JO, et al. Overall Survival Following Neoadjuvant Chemotherapy vs Primary Cytoreductive Surgery in Women With Epithelial Ovarian Cancer: Analysis of the National Cancer Database. *JAMA Oncol* 2017; **3:** 76-82. doi: 10.1001/jamaoncol.2016.4411
25. Petrillo M, Ferrandina G, Fagotti A, Vizzielli G, Margariti PA, Pedone AL, et al. Timing and pattern of recurrence in ovarian cancer patients with high tumor dissemination treated with primary debulking surgery versus neoadjuvant chemotherapy. *Ann Surg Oncol* 2013; **20:** 3955-60. doi: 10.1245/s10434-013-3091-6
26. da Costa AA, Valadares CV, Baiocchi G, Mantoan H, Saito A, Sanches S, et al. Neoadjuvant Chemotherapy Followed by Interval Debulking Surgery and the Risk of Platinum Resistance in Epithelial Ovarian Cancer. *Ann Surg Oncol* 2015; **22 (Suppl 3):** S971-8. doi: 10.1245/s10434-015-4623-z
27. Cooke SL, Brenton JD. Evolution of platinum resistance in high-grade serous ovarian cancer. *Lancet Oncol* 2011; **12:** 1169-74. doi: 10.1016/S1470-2045(11)70123-1
28. Bian C, Yao K, Li L, Yi T, Zhao X. Primary debulking surgery vs. neoadjuvant chemotherapy followed by interval debulking surgery for patients with advanced ovarian cancer. *Arch Gynecol Obstet* 2016; **293:** 63-8. doi: 10.1007/s00404-015-3813-z
29. Lim MC, Yoo HJ, Song YJ, Seo SS, Kang S, Kim SH, et al. Survival outcomes after extensive cytoreductive surgery and selective neoadjuvant chemotherapy according to institutional criteria in bulky stage IIIC and IV epithelial ovarian cancer. *J Gynecol Oncol* 2017; **28:** e48. doi: 10.3802/jgo.2017.28.e48
30. Cress RD, Chen YS, Morris CR, Petersen M, Leiserowitz GS. Characteristics of long-term survivors of epithelial ovarian cancer. *Obstet Gynecol* 2015; **126:** 491-7. doi: 10.1097/AOG.0000000000000981
31. Brown J, Frumovitz M. Mucinous tumors of the ovary: current thoughts on diagnosis and management. *Curr Oncol Rep* 2014; **16:** 389. doi: 10.1007/s11912-014-0389-x
32. Marchetti C, Kristeleit R, McCormack M, Mould T, Olaitan A, Widschwendter M, et al. Outcome of patients with advanced ovarian cancer who do not undergo debulking surgery: A single institution retrospective review. *Gynecol Oncol* 2017; **144:** 57-60. doi: 10.1016/j.ygyno.2016.11.001
33. Gill SE, McGree ME, Weaver AL, Cliby WA, Langstraat CL. Optimizing the treatment of ovarian cancer: Neoadjuvant chemotherapy and interval debulking versus primary debulking surgery for epithelial ovarian cancers likely to have suboptimal resection. *Gynecol Oncol* 2017; **144:** 266-73. doi: 10.1016/j.ygyno.2016.11.021

research article

Percutaneous parametrial dose escalation in women with advanced cervical cancer: feasibility and efficacy in relation to long-term quality of life

Sati Akbaba[1,2], Jan Tobias Oelmann-Avendano[1,2], Tilman Bostel[1,2], Harald Rief[1,2,3], Nils Henrik Nicolay[1,2,4,5], Juergen Debus[1,2,4], Katja Lindel[1,2,6], Robert Foerster[1,2,7]

[1] Department of Radiation Oncology, University Hospital Heidelberg, Heidelberg, Germany
[2] National Center for Radiation Research in Oncology (NCRO), Heidelberg Institute for Radiation Oncology (HIRO), Heidelberg, Germany
[3] Gemeinschaftspraxis Strahlentherapie Bonn-Rhein-Sieg, Bonn, Germany
[4] Clinical Cooperation Unit Radiation Oncology, German Cancer Research Center (DKFZ), Heidelberg, Germany
[5] Department of Radiation Oncology, University Hospital Freiburg, Freiburg, Germany
[6] Department of Radiation Oncology, Staedtisches Klinikum Karlsruhe, Karlsruhe, Germany
[7] Department of Radiation Oncology, University Hospital Zurich, Zurich, Switzerland

Radiol Oncol 2018; 52(3): 320-328.

Received 14 February 2018
Accepted 09 May 2018

Correspondence to: Robert Foerster, M.D., Department of Radiation Oncology, University Hospital Zurich, Raemistrasse 100, 8091 Zurich, Switzerland. Phone: +41 44 255 9959; Fax: +41 44 255 4547; E-mail: robert.foerster@usz.ch

Disclosure: No potential conflict of interest were disclosed.

Background. We analyzed long-term quality of life (QoL) and prognostic factors for QoL as well as clinical outcome in patients with advanced cervical cancer (ACC) treated with primary radiochemotherapy (RChT) consisting of external beam radiotherapy (EBRT) with or without sequential or simultaneous integrated boost (SIB) to the parametria, intracavitary brachytherapy and concomitant chemotherapy (ChT).

Patients and methods. Eighty-three women were treated with primary RChT between 2008 and 2014. Survival of all patients was calculated and prognostic factors for survival were assessed in univariate and multivariate analysis. In 31 patients QoL was assessed in median 3 years (range 2–8 years) after treatment. QoL was compared to published normative data and the influence of age, tumour stage, treatment and observed acute toxicities was analyzed.

Results. Thirty-six patients (43.4%) died, 18 (21.7%) had a local recurrence and 24 (28.9%) had a distant progression. Parametrial boost ($p = 0.027$) and ChT ($p = 0.041$) were independent prognostic factors for overall survival in multivariate analysis. Specifically, a parametrial equivalent doses in 2-Gy fractions (EQD2) > 50 Gy was associated with an improved overall survival (OS) ($p = 0.020$), but an EQD2 > 53 Gy did not further improve OS ($p = 0.194$). Tumour size was the only independent prognostic factor for local control ($p = 0.034$). Lymph node status ($p = 0.038$) and distant metastases other than in paraaortic lymph nodes ($p = 0.002$) were independent prognostic factors for distant progression-free survival. QoL was generally inferior to the reference population. Age only correlated with menopausal symptoms ($p = 0.003$). The degree of acute gastrointestinal ($p = 0.038$) and genitourinary ($p = 0.041$) toxicities correlated with the extent of chronic symptom experience. Sexual/vaginal functioning was reduced in patients with larger tumours ($p = 0.012$). Parametrial EQD2 > 53 Gy correlated with reduced sexual/vaginal functioning ($p = 0.009$) and increased sexual worry ($p = 0.009$). Whether parametrial dose escalation was achieved by sequential boost or SIB, did not affect survival or QoL.

Conclusions. Primary RChT is an effective treatment, but long-term QoL is reduced. The degree of acute side effects of RChT correlates with the extent of chronic symptoms. Patients benefit from parametrial SIB or sequential boost, but an EQD2 > 53 Gy does not further improve survival and negatively affects QoL.

Key words: cervical cancer; parametrial boost; quality of life; radiotherapy

Introduction

Primary radiochemotherapy (RChT) with external beam radiotherapy (EBRT), intracavitary brachytherapy (ICBT), and concomitant chemotherapy (ChT) remains a frequently used treatment for advanced cervical cancer (ACC). However, local tumour control requires comparatively large doses, which in turn may lead to relevant treatment-related morbidity.[1,2] In recent years, image guided adaptive brachytherapy (IGABT), based on magnetic resonance imaging (MRI) and combined interstitial / intracavitary brachytherapy (IBT/ICBT), has been successfully implemented as the new standard of care for local dose escalation and substantial reduction of therapy-related morbidity.[3-5]

However, access to IGABT is limited at many brachytherapy facilities. Therefore, despite evidence of the inferiority of percutaneous boosting in terms of organ sparing and target coverage, another approach has been to combine ICBT with modern radiotherapy (RT) techniques, such as intensity-modulated radiotherapy (IMRT) with simultaneous integrated boost (SIB) to the parametria, for percutaneous local dose escalation.[6,7] There is a low incidence of acute toxicities after SIB, but clinical outcome and QoL of these patients have not been investigated so far.[7] Due to limited access to IGABT at many brachytherapy facilities and the unknown effects of SIB in terms of chronic morbidity, IMRT with sequential boost remains a widely used method for parametrial dose escalation. Given the comparatively young age of patients with cervical cancer and improving prognosis, long-term quality of life (QoL) and extent of chronic morbidity become increasingly important issues.

Therefore, we conducted this study to analyze feasibility and efficacy of a percutaneous parametrial boost in relation to long-term QoL as well as to assess tumour- and treatment-related prognostic factors for long-term QoL and outcome in women with ACC.

Patients and methods

Between 2008 and 2014, eighty-three women with ACC underwent primary treatment at our department. Patients' data were acquired from the institutional electronic patient charts and the institutional follow-up database. Median age at first diagnosis was 57 years (range 32–90 years; Table 1). Due to the substantially differing fractionation schedules, all reported doses were recalculated as equivalent doses in 2-Gy fractions with $\alpha/\beta = 10$ ($EQD2_{10}$) for the tumour and $\alpha/\beta = 3$ ($EQD2_3$) for the organs at risk (OARs). OAR doses were documented for volumes of 0.1 cm^3 (D0.1cc), 1 cm^3 (D1cc) and 2 cm^3 (D2cc). They were calculated as the sum of the individual doses received from all brachytherapy fractions and the EBRT plan.[8]

Survival was plotted according to Kaplan and Meier. Overall survival (OS) was defined as the time between first diagnosis and death. Local progression-free survival (LPFS) was defined as the time between first diagnosis and occurrence of any local progression. Since patients with distant metastases (cM1a and cM1c) at first diagnosis were in-

TABLE 1. Patients' characteristics

Age		
Median	57 years	
Range	32–90 years	
	n	**%**
Histology		
Squamous cell carcinoma	67	80.7%
Adenocarcinoma	14	16.9%
Adenosquamous carcinoma	2	2.4%
Grading		
G1	8	9.6%
G2	24	28.9%
G3	35	42.2%
GX	16	19.3%
FIGO stage		
I	2	2.4%
II	40	48.2%
III	15	18.1%
IV	26	31.3%
Tumour size		
T1	3	3.6%
T2	46	55.4%
T3	25	30.1%
T4	9	10.8%
Lymph node status		
N0	28	33.7%
N1	55	66.3%
Distant metastases		
M0	64	77.1%
M1a	12	14.5%
M1c	7	8.4%

TABLE 2. Treatment and toxicity

Radiotherapy dose in EQD2 (α/β = 10)		
Median EBRT	44 Gy	
Range EBRT	35–51 Gy	
Median parametria	53 Gy	
Range parametria	38–67 Gy	
Median HDR-BT	40 Gy	
Range HDR-BT	10–50 Gy	
	n	**%**
Radiotherapy technique		
IMRT	58	69.9%
3D-conformal	25	30.1%
Parametrial boost		
No boost	36	43.4%
Sequential	31	37.3%
SIB	16	19.3%
Parametrial dose in EQD2 (α/β = 10)		
≤ 53 Gy	56	67.5%
> 53 Gy	27	32.5%
Simultanous chemotherapy		
Cisplatin 40 mg/m²	71	85.5%
None	12	14.5%
Total treatment duration		
< 6 weeks	9	10.8%
6-8 weeks	52	62.7%
≥ 9 weeks	22	26.5%
Anemia during therapy		
min. Hb < 10 g/dl	38	45.8%
min. Hb ≥ 10 g/dl	45	54.2%
Transfusions		
≤ 2 ECs	69	83.1%
> 2 ECs	14	16.9%
Observed acute GI toxicity		
Grade 0	33	39.8%
Grade I	15	18.1%
Grade II	20	24.1%
Grade III	12	14.5%
Grade IV	3	3.6%
Observed acute GU toxicity		
Grade 0	15	18.1%
Grade I	34	41.0%
Grade II	28	33.7%
Grade III	6	7.2%

EBRT = external beam radiotherapy; ECs = erythrocyte concentrates; EQD2 = equivalent doses in 2-Gy fractions; GI = gastrointestinal; GU = genitourinary; Hb = haemoglobin; HDR-BT = high-dose-rate brachytherapy; IMRT = intensity-modulated radiotherapy; SIB = simultaneous integrated boost

cluded in this study, distant progression-free survival (DPFS) was defined as the interval between first diagnosis of cervical cancer and occurrence of new distant metastases. Prognostic factors for survival were analyzed with the log-rank test (univariate analysis) and a Cox proportional hazards model (multivariate analysis).

Three years (median; range 2–8 years) after treatment, patients were approached during clinical follow-up examinations and asked to fill-in the European Organization for Research and Treatment of Cancer (EORTC) Quality of Life Questionnaire for Cancer Patients 30 (QLQ-C30) and the Cervical Cancer Module (QLQ-CX24). Thirty-one women agreed to participate. The difference between patients' QoL items scores and published German reference values was analyzed with the t-test (9). Possible prognostic factors for QoL (age, stage, tumour size, lymph node status, distant metastases status, histological grading, histology, RT techniques, applied RT doses, OAR doses, ChT, treatment duration, observed acute toxicities, anemia during RChT, number of transfusions during RChT) were investigated with an analysis of variances and the t-test. Age was used as a covariate. A p-value ≤ 0.05 was considered statistically significant. All statistical analyses were performed with IBM SPSS version 24.0.

This study was conducted in accordance with the declaration of Helsinki and was approved by the responsible independent ethics committee on 22 October 2012 (#S-513/2012). The requirement of informed consent was waived by the ethics committee, due to the retrospective nature of the study.

Results

Treatment and dose-volume histogram analysis

RT was conducted as EBRT (69.9% IMRT, 30.1% 3D-conformal RT), with or without sequential boost / SIB to parametria and involved pelvic / paraaortic lymph nodes (43.4% no boost, 37.3% sequential boost, 19.3% SIB), and high-dose-rate (HDR) ICBT boost (tandem and ring applicator). Median EBRT $EQD2_{10}$ to the whole pelvic (and paraaortic) planning target volume (PTV) was 44 Gy (range 35–51 Gy) and median parametrial $EQD2_{10}$ was 53 Gy (range 38–67 Gy). Including ICBT boost, as prescribed to point A, with a median $EQD2_{10}$ of 40 Gy (range 10–50 Gy), the median prescribed primary tumour $EQD2_{10}$ was 84 Gy (range 54–95 Gy). Seventy-one patients (85.5%) received con-

comitant ChT with 4–6 cycles of cisplatin 40 mg/m^2 weekly (Table 2).

Mean bladder D0.1cc, D1cc and D2cc were 130.2 Gy (± SD 31.7 Gy), 105.6 Gy (± SD 14.2 Gy) and 97.1 Gy (± SD 9.9 Gy), respectively. Mean sigmoid D0.1cc, D1cc and D2cc were 71.9 Gy (± SD 10.6 Gy), 64.1 Gy (± SD 7.9 Gy) and 61.1 Gy (± SD 6.9 Gy), respectively. Mean rectum D0.1cc, D1cc and D2cc were 89.8 Gy (± SD 23.1 Gy), 74.3 Gy (± SD 12.8 Gy) and 68.8 Gy (± SD 9.4 Gy), respectively.

Survival analysis

Thirty-six patients (43.4%) died, 18 (21.7%) had a local progression and 24 (28.9%) developed new distant metastases during follow-up. Calculated 3- / 5-year LPFS, DPFS and OS were 80.5% / 73.2%, 76.7% / 65.3% and 66.5% / 53.2%, respectively.

In univariate analysis (Table 3), Fédération Internationale de Gynécologie et d'Obstétrique (FIGO) stage (I/II *vs.* III/IV; p = 0.015), tumour size (T1/2 *vs.* T3/4; p = 0.036), parametrial boost (yes *vs.* no; p = 0.037), parametrial dose ($EQD2_{10}$ ≤ 50 Gy *vs.* > 50 Gy; p = 0.020 and $EQD2_{10}$ < 53 Gy *vs.* 53 Gy vs. > 53 Gy; p = 0.017), simultaneous ChT (yes *vs.* no; p = 0.004), total treatment duration (6–8 weeks *vs.* ≥ 9 weeks; p = 0.027), anemia during therapy (minimal hemoglobin < 10 g/dl *vs.* ≥ 10 g/dl; p = 0.039) and number of erythrocyte concentrate transfusions (≤ 2 *vs.* > 2; p = 0.007) were prognostic factors for OS. Histological grading showed a tendency towards statistical significance (G1/2 *vs.* G3; p = 0.053). Importantly, a percutaneous dose escalation in the parametria beyond an $EQD2_{10}$ of 53 Gy did not further improve survival (p = 0.194; Figure 1). For DPFS, only tumour size (T1/2 *vs.* T3/4; p = 0.034) was a prognostic factor. Lower FIGO stage (FIGO I/II *vs.* III/IV; p = 0.072) and conductance of a parametrial boost (yes *vs.* no; p = 0.095) showed a tendency towards improved LPFS. DPFS was prolonged in patients without lymph node metastases (N0 *vs.* N1; p = 0.038) and in patients without distant metastases other than in paraaortic lymph nodes (M0/M1a *vs.* M1c; p = 0.002) as well as in patients with low or intermediate histological grading (G1/2 *vs.* G3; p = 0.037). In none of three endpoints we found any difference in outcome between patients receiving SIB or sequential boost.

In multivariate analysis (Table 3), parametrial boost (yes *vs.* no, HR 0.417 [95%CI 0.192–0.900], p = 0.027) and simultaneous ChT (yes *vs.* no, HR 0.382 [95%CI 0.152–0.961], p = 0.041) remained as independent prognostic factors for OS. Advanced tumour size was the only independent prognostic factor for LPFS (T3/4 *vs.* T1/2, HR 2.668 [95%CI 1.032–6.896], p = 0.043). Regarding freedom from distant progression (DPFS), presence of pelvic lymph node metastases (N1 *vs.* N0, HR 4.383 [95%CI 1.003–19.154], p = 0.05) as well as distant metastases other than in the paraaortic lymph nodes at initial diagnosis (M1c *vs.* M0/M1a, HR 4.646 [95%CI 1.466–14.719], p = 0.009) were independent prognostic factors.

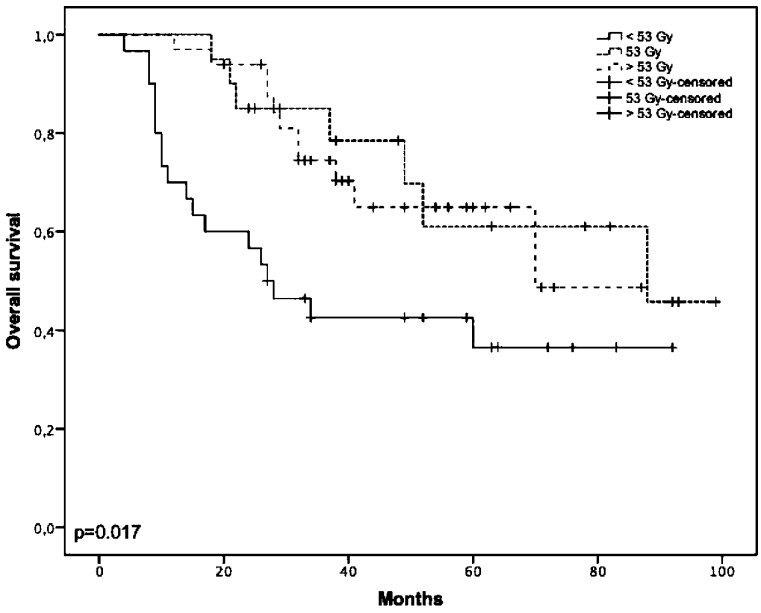

FIGURE 1. Overall survival dependent on parametrial equivalent dose in 2-Gy fractions (EQD2) with α/β = 10.

Quality of life analysis

We found the values of the functioning and symptoms scores in our cohort to be significantly worse comparison those from the normative population (Table 4). Generally, age must be considered when looking at quality of life and we used age as a covariate for our analyses, however age only correlated with menopausal symptoms (p = 0.003) in our analysis and did not affect global health status or any of the other functioning or symptom items scores from the QLQ-C30 or QLQ-CX24 questionnaires in our cohort.

The doses to bladder, sigmoid and rectum did not correlate with any of the QoL item scores. However, we found a statistically significant correlation between the degree of observed acute gastrointestinal (GI) and genitourinary (GU) toxicities with chronic symptom experience (p = 0.038 and p = 0.041), which can be considered an indicator for the known dose-volume dependence of

TABLE 3. Prognostic factors for survival

OS	Univariate analysis (log-rank test)	
	Mean (months)	p-value
FIGO stage		
FIGO I/II	72.6	*0.015*
FIGO III/IV	50.8	
Tumour size		
T1/2	69.2	*0.036*
T3/4	50.4	
Grading		
G1/2	72.4	0.053
G3	50.5	
Parametrial boost		
yes	69.9	*0.037*
no	51.2	
Parametrial dose in EQD2 (α/β = 10)		
≤ 50 Gy	50.7	*0.020*
> 50 Gy	71.5	
≤ 53 Gy	59.5	0.194
> 53 Gy	64.1	
Chemotherapy		
yes	67.4	*0.004*
no	32.1	
Total treatment duration		
6–8 weeks	71.6	*0.027*
≥ 9 weeks	44.7	
Anemia during therapy		
min. Hb < 10 g/dl	52.1	*0.039*
min. Hb ≥ 10 g/dl	70.3	
Transfusions		
≤ 2 ECs	67.6	*0.007*
> 2 ECs	41.6	
LPFS	**Mean (months)**	**p-value**
FIGO stage		
FIGO I/II	85.9	0.072
FIGO III/IV	66.7	
Tumour size		
T1/2	85.7	*0.034*
T3/4	64.1	
Parametrial boost		
yes	84.1	0.095
no	56.1	
DPFS	**Mean (months)**	**p-value**
Lymph node status		
N0	85.6	*0.038*
N1	61.0	
Distant metastases		
M0/M1a	75.2	*0.002*
M1c	37.1	
Grading		
G1/2	84.6	*0.037*
G3	59.8	
Multivariate analysis (Cox regression)		
OS	**HR**	**95% CI**	**p-value**
Parametrial boost			
yes	0.417	0.192-0.900	*0.027*
no	Reference		
Chemotherapy			
yes	0.382	0.152-0.961	*0.041*
no	Reference		
LPFS	**HR**	**95% CI**	**p-value**
Tumour size			
T1/2	Reference		
T3/4	2.668	1.032-6.896	0.043
DPFS	**HR**	**95% CI**	**p-value**
Lymph node status			
N0	Reference		
N1	4.383	1.003-19.154	*0.05*
Distant metastases			
M0/M1a	Reference		
M1c	4.646	1.466-14.719	*0.009*

DPFS = Distant progression-free survival; ECs = erythrocyte concentrates; EQD2 = equivalent doses in 2-Gy fractions; FIGO = Fédération Internationale de Gynécologie et d'Obstétrique; Hb = haemoglobin; LPFS = Local progression-free survival OS = overall survival

chronic morbidity. Patients with higher degree of observed acute GI toxicity also complained more about chronic diarrhea (p = 0.053). Since most of our patients underwent IMRT and all of them received HDR ICBT, we found no difference in QoL between RT techniques. Importantly, we could show, that a parametrial $EQD2_{10}$ > 53 Gy statistically significantly correlated with reduced sexual/vaginal functioning (p = 0.009) and increased sexual worry (p = 0.009). Additionally, these patients also suffered more from chronic constipation (p =

0.057). Whether parametrial dose escalation was achieved by sequential boost or SIB did not affect QoL. Sexual/vaginal functioning was statistically significantly worse in patients with T3/4 tumours compared to those with T1/2 tumours (p = 0.012). Details are shown in Table 5.

Discussion

The objective of this study was to analyze the feasibility and efficacy of a parametrial boost in relation to long-term QoL of patients with ACC. Secondly, we aimed to assess tumour- and treatment-related prognostic factors for long-term QoL and clinical outcome.

Currently, for the QLQ-CX24 items, there are only reference populations from 2 Korean studies available and possible social or cultural differences prevent these cohorts from being reference populations for European studies.[10,11] Therefore, we were unable to compare the QLQ-CX24 items scores of our patients and we can only report on the comparison between our patients' QLQ-C30 items scores and German normative data.[9] Compared to the reference population, the patients in our cohort had significantly worse functioning and symptoms item scores. Similar results have been reported in a large population-based study from the United States. They found health-related QoL in survivors of cervical cancer to be worse than in the normal population as well.[12] In women treated with IGABT within the "European and international study on MRI-guided brachytherapy in locally advanced cervical cancer" (EMBRACE), after a median follow-up of 21 months, functioning and general QoL returned to levels of the reference population, but several clearly treatment-related symptoms, e.g. diarrhea and sexual dysfunction, did develop or persist in those patients during follow-up as well.[13]

While we, probably due to the small cohort, were unable to show a significant correlation between the doses received by the OARs and any of the QoL item scores, others have found a significant dose-volume effect relationship for late rectal and urinary morbidity. Particularly, patients with bladder D2cc > 95 Gy and rectum D2cc ≥ 75 Gy are at risk for severe late toxicities.[14,15] It has been shown that chronic bladder and rectal morbidity can be further reduced by IGABT.[3] Therefore, in the ongoing EMBRACE-2 trial, the planning aims / limits for the prescribed $EQD2_3$ to rectum (D2cc < 65 / < 75 Gy) and bladder (D2cc < 80 / < 90 Gy) are substantially lower than the mean dose values achieved in

TABLE 4. Quality of life of patients compared to reference populations (EORTC QLQ-C30)

	n	mean	SD	p-value
Global health status				
Reference	1309	74.5	15.5	0.001
Patients	30	60.3	21.7	
Physical functioning				
Reference	1309	91.5	15.5	< 0.001
Patients	30	73.6	19.6	
Role functioning				
Reference	1309	89.9	20.6	< 0.001
Patients	31	58.1	33.0	
Emotional functioning				
Reference	1309	83.2	19.3	0.001
Patients	31	65.1	26.7	
Cognitive functioning				
Reference	1309	93.4	14.6	< 0.001
Patients	31	73.2	28.4	
Social functioning				
Reference	1309	93.3	17.1	< 0.001
Patients	31	69.9	29.0	
Fatigue				
Reference	1309	16.4	21.4	< 0.001
Patients	31	51.6	28.0	
Nausea / Vomiting				
Reference	1309	2.4	9.6	0.030
Patients	31	11.3	21.7	
Pain				
Reference	1309	17.0	24.2	0.025
Patients	31	26.9	24.2	
Dyspnea				
Reference	1309	7.2	18.7	0.020
Patients	30	18.9	25.8	
Insomnia				
Reference	1309	13.0	23.6	< 0.001
Patients	31	40.9	36.2	
Appetite loss				
Reference	1309	4.2	13.9	0.002
Patients	31	21.5	27.7	
Constipation				
Reference	1309	3.1	12.1	< 0.001
Patients	31	22.6	27.7	
Diarrhea				
Reference	1309	2.9	12.7	< 0.001
Patients	31	29.0	30.7	
Financial difficulties				
Reference	1309	4.8	16.3	< 0.001
Patients	31	29.0	29.5	

EORTC = European Organization for Research and Treatment of Cancer; QLQ-C30 = quality of life questionnaire for cancer patients 30

TABLE 5. Prognostic factors for patients' long-term quality of life (EORTC QLQ-C30, QLQ-CX24)

	n	mean	SD	p-value
Diarrhea				
Acute GI 0	11	12.1	16.8	0.053
Acute GI I/II	15	35.6	32.0	
Acute GI III/IV	5	46.7	38.0	
Constipation				
Parametria ≤ 53 Gy*	19	14.0	23.1	0.057
Parametria > 53 Gy*	11	33.3	29.8	
Symptom experience				
Acute GI toxicity 0	11	9.4	8.6	*0.038*
Acute GI toxicity I/II	14	20.6	15.9	
Acute GI toxicity III/IV	5	30.3	22.7	
Acute GU toxicity 0	5	14.3	12.9	*0.041*
Acute GU toxicity I/II	22	22.4	9.7	
Acute GU toxicity III/IV	3	38.4	33.5	
Menopausal symptoms				
≤ 49 years	7	57.1	25.2	*0.033*
50–59 years	12	36.1	36.1	
60–69 years	7	14.3	26.2	
≥ 70 years	4	8.3	16.7	
Sexual / vaginal functioning				
T1/2	9	93.5	11.6	*0.012*
T3/4	3	41.7	52.0	
Parametria ≤ 53 Gy*	8	96.9	6.2	*0.009*
Parametria > 53 Gy*	4	47.9	44.2	
Sexual worry				
Parametria ≤ 53 Gy*	17	15.7	26.6	*0.009*
Parametria > 53 Gy*	9	51.8	37.7	

EORTC = European Organization for Research and Treatment of Cancer; GI = gastrointestinal; GU = genitourinary; QLQ-C30 = quality of life questionnaire for cancer patients 30; QLQ-CX24 = quality of life questionnaire cervical cancer module

*expressed as equivalent dose in 2-Gy fractions (EQD2) with α/β = 10

our cohort.[5] Consequently, the QLQ-CX24 symptom experience score was higher in our patients compared to those treated within the EMBRACE study (18.1 ± SD 16.4 *vs*. 12.1 ± SD 11.9; p = 0.063) after 36 months of follow-up.[13] As a further indicator for the dose-volume dependence of chronic morbidity, we found the degree of RT-related acute GI und GU toxicities in patients with ACC to statistically significantly correlate with the extent of chronic symptoms and we have already shown this correlation in a previous study from our institution on women with endometrial cancer.[16] In that study we also demonstrated an improved global health status and fewer chronic GI symptoms by reduction of acute toxicities with IMRT.[16] Since most of the patients in our current analysis were treated with IMRT, we were unable to demonstrate such a benefit in terms of long-term QoL. Apart from the dose-volume-relationship found in both, acute and late toxicities, chronic toxicities may be consequential to acute damage, thus amelioration of the acute response to irradiation may be a useful approach to minimize late side effects.[17]

Our analysis showed a significant impairment of sexual/vaginal functioning, significantly increased sexual worry, and a trend towards more chronic constipation in patients exceeding an $EQD2_{10}$ of 53 Gy in the parametria. This was equally true for patients with SIB or sequential boost. The required dose to the parametria for adequate local tumour control has not been established and dose prescriptions vary greatly among radiation oncologists.[2,18] In patients with traditional midline-shielding, parametrial boost resulted in a significantly higher incidence of radiation proctitis and enterocolitis when > 54 Gy were applied.[19,20] and this technique has been described to substantially contribute to rectum, sigmoid and bladder doses.[21] In the times of IMRT and SIB to the parametria, studies have shown, that local dose escalation can be achieved with a relevantly reduced incidence of acute toxicities.[7,22] So far, no study has ever looked at percutaneous parametrial dose escalation regarding QoL and chronic morbidity. Particularly, chronic vaginal morbidity after EBRT boost has not been the focus of research so far. The Vienna group has provided important evidence, that IGABT delivers superior outcome.[3,23] and can reduce vaginal morbidity significantly, but sexual dysfunction remained a problem in patients treated within the EMBRACE trial as well.[13,24] It is assumed that vaginal toxicity may be further reduced with IGABT by decreasing dwell times in the ovoid/ring and increasing dwell times in tandem/needles.[25,26] In this context it is important to state that the ongoing EMBRACE-2 trial limits percutaneous IMRT boost as SIB to involved lymph nodes and does not allow a parametrial IMRT boost.[5] At our institution, MRI-guided IGABT with combined IBT/ICBT was recently implemented and we are currently planning a study with longitudinal QoL assessment in these patients. Certainly, it should be the ultimate goal to enable access to IGABT at all brachytherapy facilities. Nevertheless, at the moment, availability of IBT and MRI-guidance is low at most brachytherapy centers and EBRT boost remains a widely

used method for parametrial dose escalation. This underlines the importance of our investigation.

While survival rates were generally adequate in our study and in line with previously published data from randomized controlled trials on RChT in patients with ACC, a comparison of our results to data on IGABT is quite challenging because our cohort consists of mostly advanced stage patients.[27,28] The RetroEMBRACE study, a multicenter retrospective observational study, found substantially better 5-year pelvic control and overall survival rates (84% *vs.* 73.2% and 65% *vs.* 53.2%), but their cohort contained much more stage I and far less stage IV patients than our study (16.8% *vs.* 2.4% and 3.1% *vs.* 31.3%) (23). A Dutch retrospective analysis on 46 patients treated with IGABT found a 3-year regional control rate of 86% and a 3-year overall survival rate of 65%.[29] Similarly, Pötter et al. found pelvic control and overall survival to be 91% and 68% after 3-years, respectively.[3] The patient cohorts in these two studies were very similar to the collective of the RetroEMBRACE study. Therefore, our results, despite the large proportion of stage IV patients and the negligible amount of stage I patients, are not inferior in terms of overall survival and seem comparable with respect to local pelvic control. However, primary tumour control was remarkably high with 93% after 3 years in the Vienna series.[3] Furthermore, an analysis from the RetroEMBRACE study comparing IGABT with IBT/ICBT to ICBT only showed the feasibility of local dose escalation without an increase in dose to organs at risk as well as a 10% higher 3-year local control rate with IBT.[30] These results clearly demonstrate the advantage of MRI-based IGABT with combined IBT/ICBT for local dose escalation.

Nevertheless, our analysis showed a statistically significant overall survival benefit from a parametrial boost and this was equally true for patients with SIB or sequential boost. Alongside with simultaneous ChT, parametrial boost was as an independent prognostic factor for OS in the multivariate analysis. Local control was also improved in patients with parametrial boost, but, probably due to the comparatively few events, this did not reach statistical significance. However, the survival benefit was dependent on the applied dose. In particular, overall survival was statistically significantly prolonged in patients with a parametrial $EQD2_{10}$ > 50 Gy, but a dose escalation beyond an $EQD2_{10}$ of 53 Gy did not further improve survival. Thus, we believe IMRT with 25 x 1.8 Gy to the whole pelvic PTV including a SIB with 25 x 2.1 Gy to the parametria to be a feasible and overall efficient EBRT concept for centers without access to IGABT.

We acknowledge that our study is substantially limited by its retrospective nature, the comparatively small sample size and the conductance of multiple subgroup analyses, but we believe our results on parametrial dose and chronic morbidity to be of importance for all brachytherapy centers without access to MRI-guidance and IBT.

Primary RChT is an effective treatment for ACC, but long-term QoL of survivors is inferior compared to normative data. The degree of acute side effects of RChT correlates with the extent of chronic symptoms. For patients treated with EBRT boost and ICBT, we have shown a significant survival benefit from parametrial dose escalation as SIB or sequential boost, but exceeding an $EQD2_{10}$ of 53 Gy with this technique does not further improve survival and has a negative impact on QoL. Therefore, the conductance of a percutaneous parametrial boost has to be seen very critically with respect to local tumour control and long-term QoL. MRI-guided IGABT with combined IBT/ICBT certainly is the gold standard for local dose escalation in ACC.

References

1. Haie-Meder C, Potter R, Van Limbergen E, Briot E, De Brabandere M, Dimopoulos J, et al. Recommendations from Gynaecological (GYN) GEC-ESTRO Working Group (I): concepts and terms in 3D image based 3D treatment planning in cervix cancer brachytherapy with emphasis on MRI assessment of GTV and CTV. *Radiother Oncol* 2005; **74:** 235-45. doi: 10.1016/j.radonc.2004.12.015
2. Viswanathan AN, Creutzberg CL, Craighead P, McCormack M, Toita T, Narayan K, et al. International brachytherapy practice patterns: a survey of the Gynecologic Cancer Intergroup (GCIG). *Int J Radiat Oncol Biol Phys* 2012; **82:** 250-5. doi: 10.1016/j.ijrobp.2010.10.030
3. Potter R, Georg P, Dimopoulos JC, Grimm M, Berger D, Nesvacil N, et al. Clinical outcome of protocol based image (MRI) guided adaptive brachytherapy combined with 3D conformal radiotherapy with or without chemotherapy in patients with locally advanced cervical cancer. *Radiother Oncol* 2011; **100:** 116-23. doi: 10.1016/j.radonc.2011.07.012
4. Rijkmans EC, Nout RA, Rutten IH, Ketelaars M, Neelis KJ, Laman MS, et al. Improved survival of patients with cervical cancer treated with image-guided brachytherapy compared with conventional brachytherapy. *Gynecol Oncol* 2014; **135:** 231-8. doi: 10.1016/j.ygyno.2014.08.027
5. Potter R, Tanderup K, Kirisits C, de Leeuw A, Kirchheiner K, Nout R, et al. The EMBRACE II study: the outcome and prospect of two decades of evolution within the GEC-ESTRO GYN working group and the EMBRACE studies. *Clin Transl Radiat Oncol* 2018; **9:** 48-60. doi: 10.1016/j.ctro.2018.01.001
6. Mohamed S, Kallehauge J, Fokdal L, Lindegaard JC, Tanderup K. Parametrial boosting in locally advanced cervical cancer: combined intracavitary/interstitial brachytherapy vs. intracavitary brachytherapy plus external beam radiotherapy. *Brachytherapy* 2015; **14:** 23-8. doi: 10.1016/j.brachy.2014.09.010
7. Marnitz S, Kohler C, Burova E, Wlodarczyk W, Jahn U, Grun A, et al. Helical tomotherapy with simultaneous integrated boost after laparoscopic staging in patients with cervical cancer: analysis of feasibility and early toxicity. *Int J Radiat Oncol Biol Phys* 2012; **82:** e137-43. doi: 10.1016/j.ijrobp.2010.10.066

8. Potter R, Haie-Meder C, Van Limbergen E, Barillot I, De Brabandere M, Dimopoulos J, et al. Recommendations from gynaecological (GYN) GEC ESTRO working group (II): concepts and terms in 3D image-based treatment planning in cervix cancer brachytherapy-3D dose volume parameters and aspects of 3D image-based anatomy, radiation physics, radiobiology. *Radiother Oncol* 2006; **78:** 67-77. doi: 10.1016/j.radonc.2005.11.014

9. Hinz A, Singer S, Brahler E. European reference values for the quality of life questionnaire EORTC QLQ-C30: results of a German investigation and a summarizing analysis of six European general population normative studies. *Acta Oncol* 2014; **53:** 958-65. doi: 10.3109/0284186x.2013.879998

10. Lee Y, Lim MC, Kim SI, Joo J, Lee DO, Park SY. Comparison of quality of life and sexuality between cervical cancer survivors and healthy women. *Cancer Res Treat* 2016; **48:** 1321-9. doi: 10.4143/crt.2015.425

11. Park SY, Bae DS, Nam JH, Park CT, Cho CH, Lee JM, et al. Quality of life and sexual problems in disease-free survivors of cervical cancer compared with the general population. *Cancer* 2007; **110:** 2716-25. doi: 10.1002/cncr.23094

12. Weaver KE, Forsythe LP, Reeve BB, Alfano CM, Rodriguez JL, Sabatino SA, et al. Mental and physical health-related quality of life among U.S. cancer survivors: population estimates from the 2010 National Health Interview Survey. *Cancer Epidemiol Biomarkers Pre* 2012; **21:** 2108-17. doi: 10.1158/1055-9965.EPI-12-0740

13. Kirchheiner K, Potter R, Tanderup K, Lindegaard JC, Haie-Meder C, Petric P, et al. Health-related quality of life in locally advanced cervical cancer patients after definitive chemoradiation therapy including image guided adaptive brachytherapy: an analysis from the EMBRACE study. *Int J Radiat Oncol Biol Phys* 2016; **94:** 1088-98. doi: 10.1016/j.ijrobp.2015.12.363

14. Kim Y, Kim YJ, Kim JY, Lim YK, Jeong C, Jeong J, et al. Toxicities and dose-volume histogram parameters of MRI-based brachytherapy for cervical cancer. *Brachytherapy* 2017; **16:** 116-25. doi: 10.1016/j.brachy.2016.10.005

15. Mazeron R, Maroun P, Castelnau-Marchand P, Dumas I, del Campo ER, Cao K, et al. Pulsed-dose rate image-guided adaptive brachytherapy in cervical cancer: dose-volume effect relationships for the rectum and bladder. *Radiother Oncol* 2015; **116:** 226-32. doi: 10.1016/j.radonc.2015.06.027

16. Foerster R, Schnetzke L, Bruckner T, Arians N, Rief H, Debus J, et al. Prognostic factors for long-term quality of life after adjuvant radiotherapy in women with endometrial cancer. *Strahlenther Onkol* 2016; **192:** 895-904. doi: 10.1007/s00066-016-1037-1

17. Dorr W, Hendry JH. Consequential late effects in normal tissues. *Radiother Oncol* 2001; **61:** 223-31. doi: 10.1016/S0167-8140(01)00429-7

18. Rajasooriyar C, Van Dyk S, Lindawati M, Bernshaw D, Kondalsamy-Chennakesavan S, Narayan K. Reviewing the role of parametrial boost in patients with cervical cancer with clinically involved parametria and staged with positron emission tomography. *Int J Gynecol Cancer* 2012; **22:** 1532-7. doi: 10.1097/IGC.0b013e31826c4dee

19. Huang EY, Lin H, Hsu HC, Wang CJ, Chen HC, Sun LM, et al. High external parametrial dose can increase the probability of radiation proctitis in patients with uterine cervix cancer. *Gynecol Oncol* 2000; **79:** 406-10. doi: 10.1006/gyno.2000.5997

20. Huang EY, Wang CJ, Hsu HC, Hao L, Chen HC, Sun LM. Dosimetric factors predicting severe radiation-induced bowel complications in patients with cervical cancer: combined effect of external parametrial dose and cumulative rectal dose. *Gynecol Oncol* 2004; **95:** 101-8. doi: 10.1016/j.ygyno.2004.06.043

21. Fenkell L, Assenholt M, Nielsen SK, Haie-Meder C, Potter R, Lindegaard J, et al. Parametrial boost using midline shielding results in an unpredictable dose to tumor and organs at risk in combined external beam radiotherapy and brachytherapy for locally advanced cervical cancer. *Int J Radiat Oncol Biol Phys* 2011; **79:** 1572-9. doi: 10.1016/j.ijrobp.2010.05.031

22. Boyle J, Craciunescu O, Steffey B, Cai J, Chino J. Methods, safety, and early clinical outcomes of dose escalation using simultaneous integrated and sequential boosts in patients with locally advanced gynecologic malignancies. *Gynecol Oncol* 2014; **135:** 239-43. doi: 10.1016/j.ygyno.2014.08.037

23. Sturdza A, Potter R, Fokdal LU, Haie-Meder C, Tan LT, Mazeron R, et al. Image guided brachytherapy in locally advanced cervical cancer: improved pelvic control and survival in RetroEMBRACE, a multicenter cohort study. *Radiother Oncol* 2016; **120:** 428-33. doi: 10.1016/j.radonc.2016.03.011

24. Kirchheiner K, Nout RA, Tanderup K, Lindegaard JC, Westerveld H, Haie-Meder C, et al. Manifestation pattern of early-late vaginal morbidity after definitive radiation (chemo)therapy and image-guided adaptive brachytherapy for locally advanced cervical cancer: an analysis from the EMBRACE study. *Int J Radiat Oncol Biol Phys* 2014; **89:** 88-95. doi: 10.1016/j.ijrobp.2014.01.032

25. Kirchheiner K, Nout RA, Lindegaard JC, Haie-Meder C, Mahantshetty U, Segedin B, et al. Dose-effect relationship and risk factors for vaginal stenosis after definitive radio(chemo)therapy with image-guided brachytherapy for locally advanced cervical cancer in the EMBRACE study. *Radiother Oncol* 2016; **118:** 160-6. doi: 10.1016/j.radonc.2015.12.025

26. Mohamed S, Lindegaard JC, de Leeuw AA, Jurgenliemk-Schulz I, Kirchheiner K, Kirisits C, et al. Vaginal dose de-escalation in image guided adaptive brachytherapy for locally advanced cervical cancer. *Radiother Oncol* 2016; **120:** 480-5. doi: 10.1016/j.radonc.2016.05.020

27. Morris M, Eifel PJ, Lu J, Grigsby PW, Levenback C, Stevens RE, et al. Pelvic radiation with concurrent chemotherapy compared with pelvic and para-aortic radiation for high-risk cervical cancer. *N Engl J Med* 1999; **340:** 1137-43. doi: 10.1056/nejm199904153401501

28. Rose PG, Bundy BN, Watkins EB, Thigpen JT, Deppe G, Maiman MA, et al. Concurrent cisplatin-based radiotherapy and chemotherapy for locally advanced cervical cancer. *N Engl J Med* 1999; **340:** 1144-53. doi: 10.1056/nejm199904153401502

29. Nomden CN, de Leeuw AA, Roesink JM, Tersteeg RJ, Moerland MA, Witteveen PO, et al. Clinical outcome and dosimetric parameters of chemoradiation including MRI guided adaptive brachytherapy with tandem-ovoid applicators for cervical cancer patients: a single institution experience. *Radiother Oncol* 2013; **107:** 69-74. doi: 10.1016/j.radonc.2013.04.006

30. Fokdal L, Sturdza A, Mazeron R, Haie-Meder C, Tan LT, Gillham C, et al. Image guided adaptive brachytherapy with combined intracavitary and interstitial technique improves the therapeutic ratio in locally advanced cervical cancer: Analysis from the retroEMBRACE study. *Radiother Oncol* 2016; **120:** 434-40. doi: 10.1016/j.radonc.2016.03.020

research article

A proposal for a quality control protocol in breast CT with synchrotron radiation

Adriano Contillo[1], Anna Veronese[2], Luca Brombal[2], Sandro Donato[2], Luigi Rigon[2], Angelo Taibi[1], Giuliana Tromba[3], Renata Longo[2], Fulvia Arfelli[2]

[1] University of Ferrara and INFN section of Ferrara, Italy
[2] University of Trieste and INFN section of Trieste, Italy
[3] Elettra-Sincrotrone Trieste S.C.p.A., Italy

Radiol Oncol 2018; 52(3): 329-336.

Received: 4 December 2017
Accepted: 12 December 2017

Correspondence to: Dr. Adriano Contillo, Università degli Studi di Ferrara, Dipartimento di Fisica e Scienze della Terra, Via Saragat 1, 44122 Ferrara, Italy. Phone: +390532974235; Fax: +390532974210; E-mail: contillo@fe.infn.it

Disclosure: No potential conflicts of interest were disclosed.

Background. The SYRMA-3D collaboration is setting up the first clinical trial of phase-contrast breast CT with synchrotron radiation at the Elettra synchrotron facility in Trieste, Italy. In this communication, a quality control protocol for breast CT is proposed, and a first test of image quality measurements is performed by means of a custom-made radiographic phantom.

Materials and methods. A set of projections is acquired and used to perform a CT reconstruction of two selected portions of the phantom. Such portions contain a uniform layer of water and a set of radiographic inserts, respectively. Together, they allow to perform several image quality measurements, namely CT number linearity, reconstruction accuracy, uniformity, noise, and low contrast resolution. All measurements are repeated at different beam energies in the range of interest, and at two different dose values.

Results. Measurements show a good linearity in the soft tissue range, paired to a high accuracy of the CT number reconstruction. Uniformity and noise measurements show that reconstruction inhomogeneities are bound to a few percent of the average pixel values. However, low contrast detectability is limited to the higher portion of the explored energy range.

Conclusions. The results of the measurements are satisfactory in terms of their quality, feasibility and reproducibility. With minimal modifications, the phantom is promising to allow a set of image quality measurements to be used in the upcoming clinical trial.

Key words: breast CT; quality control; radiographic phantom; synchrotron radiation

Introduction

Breast cancer is among the most frequently diagnosed cancers and one of the leading causes of death for women worldwide. Unfortunately, the complex pattern of structures composing the breast parenchyma can significantly reduce the visibility of interesting details, especially in dense breasts. Such effect can hinder early detection, which is a key factor in treating and defeating breast tumors. For this reason, researchers in the field carried out a significant effort during the last decades in investigating 3D imaging modalities, in particular breast computed tomography (CT). In fact, thanks to its intrinsic decoupling of overlapping structures into parallel planes, CT imaging is the most natural answer to any issue related to anatomical noise, although it is worth mentioning other imaging techniques, like ultrasound and magnetic resonance, as valuable complementary techniques routinely used for breast cancer detection.

The design of breast CT, which allows a complete 3D reconstruction of the uncompressed organ, was theorized several decades ago.[1] However, recent technological advances favored a strong revival of the field, starting from a feasibility study[2] which

revealed the potential for high signal-to-noise ratio images with low anatomic noise, obtainable at dose levels comparable to those for mammography. Several research groups worldwide are developing breast CT prototypes. Among these groups it is worth mentioning the Friedrich-Alexander University of Erlangen-Nürnberg (Germany)[3] and the Rochester Medical Center (USA), that promoted a startup company to manufacture and commercialize their prototype.[4] The SYRMA-3D (synchrotron radiation for mammography) collaboration is in the process of setting up the first clinical trial of phase-contrast breast CT with synchrotron radiation at the SYRMEP (synchrotron radiation for medical physics) beamline of the Elettra synchrotron facility in Trieste.[5-8] One of the most peculiar features of a synchrotron facility is the high coherence of the X-ray beam, which allows to access the diagnostic information encrypted in its phase profile.[9] Radiation-matter interaction phenomena involving phase shift are most sensitive to a certain range of imaging details, and such range is distinct from the one of the phenomena involving attenuation. Therefore, accessing the phase profile information is likely to improve the diagnostic potential of the device. Moreover, being tunable to a highly monochromatic beam, synchrotron radiation delivers a lower radiation dose to the imaged organ with respect to conventional X-ray sources, as showed for example in[10,11]. These properties concur in making the SYRMA-3D a unique set up for clinical breast CT examinations.

In order to open a clinical trial, it is first necessary to develop and implement a complete Quality Control (QC) protocol. The enforcement of a QC protocol is paramount to provide the best image quality and the highest patient safety, and to guarantee that said characteristics are preserved over the lifetime of the imaging device. A complete protocol proposal was elaborated by the SYRMA-3D collaboration.[12] It consists of a list of pre-patient tests, alignment checks, dose and image quality measurements, supplemented with precise directions to the associated measuring procedures. Due to the unique nature of the considered set up, the protocol had to be tailored to it, inspired by both mammography[13] and CT[14] protocols, and taking into account the coherent and monochromatic nature of the imaging beam. The protocol for the only existing commercial breast CT system[15] was used as a starting point, including the structure of the dedicated phantom for image quality tests. For this purpose, a custom-made QC phantom was designed and built by the SYRMA-3D collaboration at the laboratories of the University of Ferrara, Italy. The present discussion will focus on the measurements regarding image quality, to be performed on a set of radiographic details embedded in the QC phantom, with the aim of validating the phantom as a viable tool for QC during the standard clinical practice.

Materials and methods

The radiation source of the SYRMEP beamline at Elettra is one of the storage ring bending magnets of the synchrotron machine. The beam is monochromatic in the energy range 8.5–40 keV and the beam cross section in the patient examination room is about 220 mm (horizontal) × 3.4 mm (vertical). The patient support was designed to perform breast CT, by rotating the breast in a pendant geometry through an ergonomically designed aperture at the rotation axis. Concerning the tomographic set up of the SYRMA-3D project, the patient lays in prone position, with the breast hanging without compression from a hole in the patient support, placed at 30 m from the synchrotron source. Due to the peculiar laminar geometry of the beam, full breasts can only be imaged in steps equal to the vertical beam height, moving the patient support vertically after the acquisition of each slab is complete. The value of the air kerma rate is provided by a dosimetric system developed for the clinical mammography trial[16] and based on two ionization chambers, placed 27 m downstream from the source and 3 m upstream from the breast. The dose monitor system of the beamline is based on two identical ionization chambers working in air, at atmospheric pressure. They were calibrated with respect to the air kerma primary standard chamber for low energy X-rays by the Department of Ionizing Radiation Metrology of ENEA (the National Agency for new Technologies, Energy and Sustainable Development). A check on the response of these monitors with respect to a calibrated secondary ionization chamber is performed annually. From the air kerma, the mean glandular dose (MGD) delivered to the scanned slice is evaluated from a custom-made Monte Carlo simulation based on a GEANT4 code optimized for breast dosimetry[17,18], here assuming a 50%-50% breast composition. The images are acquired with PIXIRAD 8, a high efficiency, photon counting, direct conversion CdTe detector.[19] This detector has a pixel size of 60 μm and it is composed of 8 modules, for a global active area of 250 mm × 25 mm. The detec-

tor is placed at about 2 m from the organ, in order to implement the free propagation phase-contrast technique.

The custom-made QC phantom was designed in such a way to mimic the geometrical appearance of a pendant human breast undergoing a CT examination, while including a set of details of radiographic interest for image quality tests. It is composed by a polymethyl methacrylate (PMMA) cylinder of 12 cm diameter and 10 cm height, filled with demineralized water to provide a uniform layer with attenuation properties similar to those of an actual breast. In particular, the cylinder diameter roughly corresponds to 13 cm of breast tissue in the energy range of interest. The uniform layer is useful to measure the uniformity of the CT reconstruction, and to ensure the absence of reconstruction artifacts. The phantom can be suspended from a PMMA disk of 35 cm diameter that is laid on the patient support, so as to hang it through the breast aperture, similarly to an actual breast CT examination. The depth of the suspension system can be adjusted to fit slight design modifications. This hanging configuration is depicted in Figure 1.

Several radiographic details are clung to the bottom of the cylinder: five rods of 1.2 cm diameter, made of different plastic materials, whose attenuation coefficients span the whole range of soft materials composing the breast; and a PMMA cylinder of 4.5 cm diameter, hereafter referred to as *snail*, with five holes of different diameters carved in it. The hole diameters span linearly the interval from 0.2 cm to 1.0 cm. The height of both the rods and the snail is 3 cm. The purpose of the plastic rods is to explore the linearity of the CT number reconstruction in the material range of interest: the reconstructed values are compared to the attenuation coefficients tabulated in[20], in order to verify the linear relationship between them and to calibrate the conversion factor. The snail is designed to explore the device sensitivity to low contrast details: as the rest of the phantom, the holes are filled with water, whose attenuation properties are quite similar to those of PMMA in the selected energy range. The contrasts between the holes and the surrounding background serve as a measurement of the low contrast resolution of the imaging system. The distribution of the inserts is visible in Figure 1, which also lists the plastic materials composing the rods.

To summarize, the present version of the QC phantom allows to perform the following tests of physical image quality:

– CT number linearity;
– Accuracy of reconstructed attenuation coefficients;

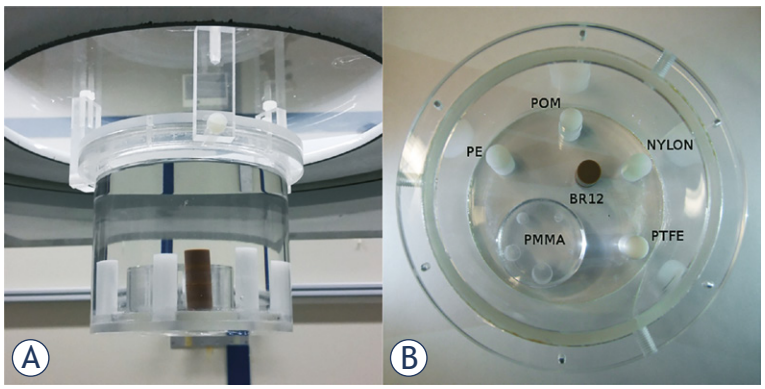

FIGURE 1. (A) QC phantom fixed at the breast position on the patient support. The upper portion is uniformly filled with water, while the radiographic details are visible in the lower portion. **(B)** Arrangement of the details at the bottom of the QC phantom. The rods are made of polyethylene (PE), nylon, polyoxymethylene (POM), polytetrafluoroethylene (PTFE), and BR12, a plastic material mimicking the attenuation properties of breast tissue. The structure of the low contrast PMMA insert, exhibiting the five holes of varying diameter, is clearly perceivable.

– Accuracy of the attenuation coefficient for water;
– Spatial uniformity in water;
– Noise fluctuations in water;
– Low contrast resolution.

Images were taken at four different energies, namely 32, 35, 38, and 40 keV. Each energy was imparted at two different dose levels, about 5 mGy (*low dose*) and 20 mGy (*high dose)*. The phantom was scanned at two different heights, one in its upper portion and the other in its lower portion. As a result, two slabs of 3.4 mm thickness were reconstructed, the first reproducing a uniform layer of water, the second depicting the radiographic details. Regarding the former slab, only the central slice was considered in the analysis. On the contrary, an averaging over the ten central slices of the latter slab was performed. Clearly, due to the averaging procedure, the resulting image quality will not match the one of the actual diagnostic images. Nonetheless, the aim of the protocol is to provide reference values to be compared with the results of the periodic measurements. The choice of performing a slice average suppresses the relative contribution of stochastic fluctuations to the measure, thus enhancing the contribution of systematic effects that may decrease the image quality.

The images resulting from the reconstructions listed above will be hereafter referred to as *water* and *detail* images, respectively. All image quality tests are repeated on each one of the exposure conditions described above.

The images of the QC phantom were generated by rotating the phantom at a constant speed of 4.5

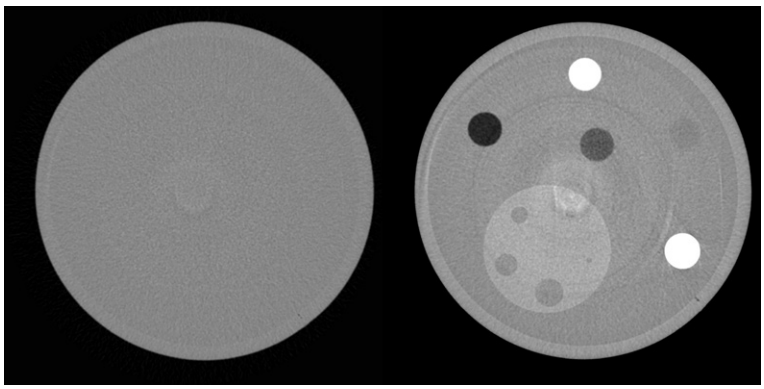

FIGURE 2. Example of reconstructed water image (left panel) and detail image (right panel), acquired at 38 keV and high dose.

deg/s, acquiring 1200 projections over a 180° angle, for a total exposure time of 40 s. The frame rate of the acquisition was equal to 30 frame/s. The CT reconstruction was performed using a filtered back-projection algorithm with a Shepp-Logan filter. The reconstructed image has a slightly anisotropic voxel of 60×60×52 μm and is a 32-bit real, grayscale image. A subsequent 2× binning is applied to the image, with a resulting voxel of 120×120×104 μm. Finally, a smoothing filter is applied to the binned image. Exemplary reconstructed images, acquired at 38 keV and high dose, are shown in Figure 2.

It should be noted that, due to the monochromaticity of the X-ray beam, the output of the CT reconstruction is a map of attenuation coefficients μ. Therefore, it appears natural to express the results in terms of μ units, typically cm^{-1}. However, the unit of measurement that is most widely used in clinical practice is the Hounsfield unit (HU), defined as

$$HU = 1000 \cdot \frac{\mu - \mu_{water}}{\mu_{water} - \mu_{air}}. \quad [1]$$

This is the preferred definition for CT scanners that are calibrated with reference to water. Being the attenuation coefficient of air nearly zero, one HU corresponds to an attenuation coefficient that is 0.1% higher than the one of water.

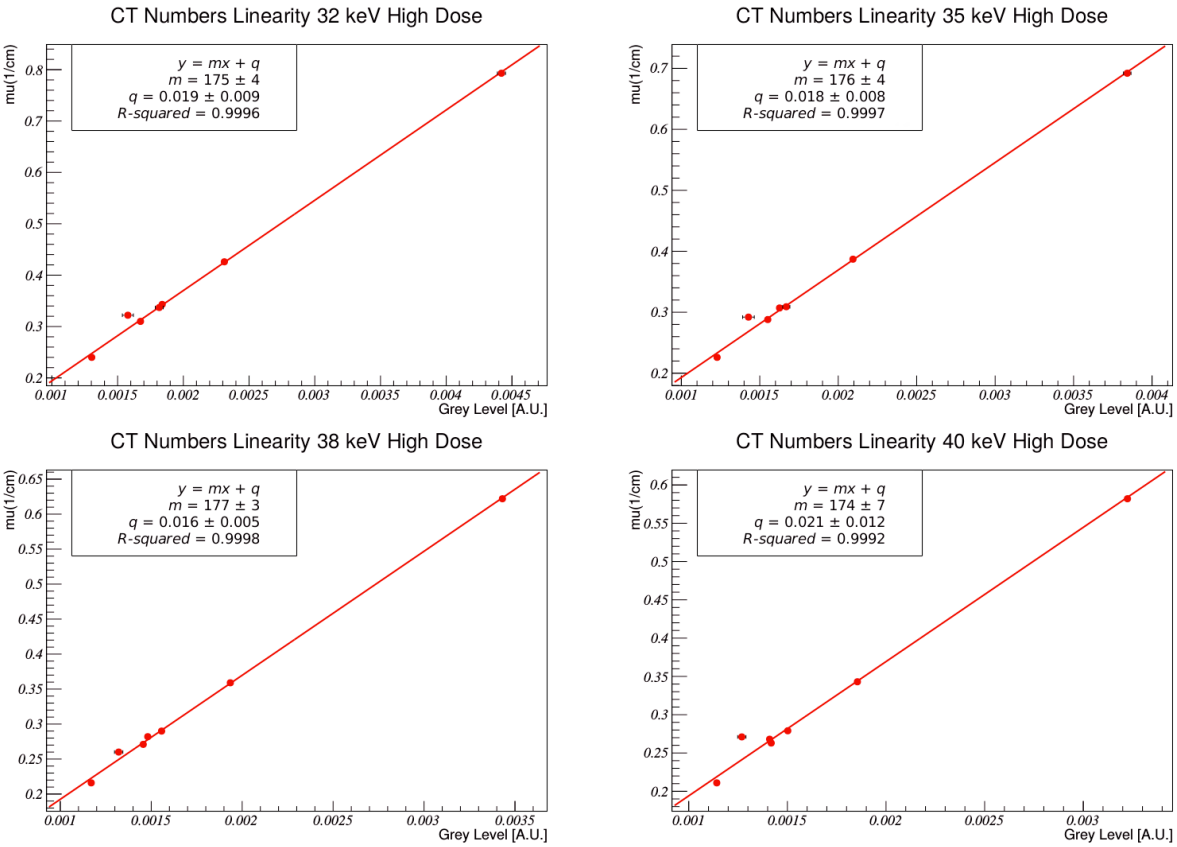

FIGURE 3. Examples of linear regressions, performed on high dose images acquired at 32, 35, 38 and 40 keV, from top left panel to bottom right panel. R^2 coefficients, slopes and intercepts are given as well.

Results

The first measurement to be performed is the CT number linearity. In the detail image, a circular region of about 80 pixel diameter is selected in the center of each rod. Average pixel values are computed, and compared to the tabulated attenuation coefficients. A linear fit allows to determine the CT number linearity (through the R^2 coefficient), the conversion factor (slope of the regression line), and the absence of a nonzero threshold (comparability of the intercept with a zero value). The parameters of the linear regressions are given in Table 1, while some examples of linear regressions are shown in Figure 3. Both the fit parameters and the graphic representation demonstrate a good linearity for all energies.

Once the conversion factor is extracted, it is possible to evaluate the accuracy of the reconstructed attenuation coefficients of the plastic materials. Said accuracy is here defined as the relative percentual discrepancy between measured and expected values

$$accuracy_{\mu} = 100 \cdot \frac{|\mu_{meas} - \mu_{exp}|}{\mu_{exp}}. \quad [2]$$

Moreover, the HU deviation is also computed as the absolute difference between the corresponding HU values

$$accuracy_{HU} = |HU_{meas} - HU_{exp}|. \quad [3]$$

Exemplary results, taken at 38 keV and high dose, are shown in Table 2. All accuracies lie within a few percent.

Accuracy must also be tested on water. This is performed on a set of three nonoverlapping regions in the center of the water image. Such regions are circular, with 80 pixel diameters. Averaged CT numbers are converted to a μ coefficient and compared with the expected value. As for the plastic materials, the result is given as a relative percentual difference. The HU deviation is also computed as before, the expected value in this case being identically zero. This particular measurement is the most natural candidate to be applied in a calibration procedure. Exemplary results, taken at 38 keV and high dose, are also given in Table 2.

As already said, the water image is supposed to be spatially uniform. However, reconstruction artifacts and X-ray beam disuniformities can lead to an uneven CT number distribution across different regions of the image. Therefore, an average is taken over a set of three nonoverlapping regions in the center of the water image, as for the accuracy measurement. Afterwards, equivalent measurements are performed on similar regions close to the edge at the four cardinal points, and μ uniformity is defined as the largest absolute value among the relative percentual differences between the central and the peripheral averages

TABLE 1. Parameters of the linear regressions between measured CT numbers and tabulated attenuation coefficients

Energy (keV)	Dose	R^2	slope (cm^{-1})	intercept (cm^{-1})
32	high	0.9996	175 ± 4	0.019 ± 0.009
	low	0.9996	170 ± 4	0.025 ± 0.009
35	high	0.9997	176 ± 4	0.018 ± 0.008
	low	0.9996	173 ± 4	0.017 ± 0.009
38	high	0.9998	177 ± 3	0.016 ± 0.005
	low	0.9992	175 ± 3	0.013 ± 0.006
40	high	0.9992	174 ± 7	0.021 ± 0.012
	low	0.9991	172 ± 7	0.019 ± 0.012

TABLE 2. Accuracies of reconstructed attenuation coefficients for the plastic materials and water, acquired at 38 keV and high dose. Expected values, measured values and relative percentual differences are given for μ coefficients, absolute differences for the corresponding HU deviations

Material	expected μ (cm^{-1})	measured μ (cm^{-1})	$accuracy_{\mu}$ (%)	$accuracy_{HU}$
PE	0.216	0.221 ± 0.002	3.1 ± 1.3	24 ± 10
BR12	0.260	0.249 ± 0.004	4.0 ± 1.6	37 ± 14
Nylon	0.271	0.273 ± 0.003	0.9 ± 1.0	8 ± 9
PMMA	0.290	0.291 ± 0.003	0.4 ± 1.2	4 ± 12
POM	0.359	0.360 ± 0.003	0.2 ± 0.8	3 ± 11
PTFE	0.622	0.633 ± 0.003	0.1 ± 0.5	3 ± 11
Water	0.282	0.278 ± 0.003	1.5 ± 0.9	14 ± 9

BR12 = breast-tissue equivalent material; PE = polyethylene; PMMA = polymethyl methacrylate; POM = polyoxymethylene; PTFE = polytetrafluoroethylene

TABLE 3. Uniformity of reconstructed attenuation coefficient for water. Relative percentual values are given for μ coefficients, absolute values for the corresponding HU deviations

Energy (keV)	Dose	$uniformity_{\mu}$ (%)	$uniformity_{HU}$
32	high	1.79	17
	low	3.19	32
35	high	1.45	12
	low	1.47	13
38	high	2.58	26
	low	1.35	13
40	high	2.54	24
	low	1.07	10

TABLE 4. Noise measurement of the reconstructed attenuation coefficient for water. Relative percentual results are given for μ coefficients, absolute results for the corresponding HU values

Energy (keV)	Dose	$noise_{\mu}$ (%)	$noise_{HU}$
32	high	4.4	60
	low	8.5	103
35	high	3.8	83
	low	7.3	114
38	high	3.7	66
	low	6.5	109
40	high	3.5	66
	low	6.2	111

TABLE 5. Low contrast measurements. Relative percentual contrasts are given for μ coefficients, absolute contrasts for the corresponding Hounsfield unit (HU)

Energy (keV)	Detail (mm)	μ contrast (%)		HU contrast	
		high dose	low dose	high dose	low dose
32	10	0.81	0.71	7	5
	8	0.96	0.87	9	7
	6	1.10	0.53	10	4
	4	1.08	1.12	10	10
	2	0.52	0.93	5	8
35	10	1.80	1.85	15	15
	8	1.68	1.73	14	14
	6	1.56	1.64	13	13
	4	1.21	0.87	10	8
	2	0.90	0.91	8	8
38	10	4.14	3.86	41	39
	8	3.99	3.41	40	34
	6	3.66	4.02	36	41
	4	3.91	3.45	39	35
	2	3.17	3.79	31	38
40	10	5.35	5.49	54	55
	8	5.09	5.43	52	55
	6	5.12	4.85	52	49
	4	5.31	3.41	54	34
	2	5.73	3.79	59	38

$$uniformity_{\mu} = 100 \cdot max\left\{\frac{|\mu_{center} - \mu_i|}{\mu_{center}}\right\} \quad [4]$$

$$i = north, west, south, east.$$

Alongside the previous measurements, the absolute difference between the corresponding HU values is measured as well

$$uniformity_{HU} = max\{|HU_{center} - HU_i|\} \quad [5]$$

$$i = north, west, south, east.$$

Results are given in Table 3, showing that uniformity lies within a few percent for all energies.

Even in the case of a globally uniform water image, image quality could be spoiled by local fluctuations. As a result, a noise measurement is also necessary. Standard deviations σ are computed over the three central regions defined in the accuracy measurement, and then averaged. The corresponding percentual μ noise is defined as the ratio between such σ average and the globally averaged μ coefficient

$$noise_{\mu} = 100 \cdot \frac{\sigma_{\mu}}{\mu_{averaged}}, \quad [6]$$

while the HU noise is defined as the average of the three standard deviations expressed in HU

$$noise_{HU} = \frac{\sigma_{HU}}{HU_{averaged}}. \quad [7]$$

Results are given in Table 4. Noise values are distributed around an average of about 5%.

The last image quality assessment is performed on the low contrast details of the snail. First, CT number averages are computed over five regions of interest, strictly included in the corresponding holes (concentric to the holes and 4/5 of the hole diameters). These are used as *signals*. Then, CT number averages and standard deviations are computed over five annuli, each concentric to a hole and with inner and outer diameters of 6/5 and 7/5 of the hole diameter, respectively. These are used instead as *backgrounds*. The contrasts between the signals and the backgrounds, percentual relative contrasts for the μ coefficients and absolute contrasts for the corresponding HU values, are given in Table 5. The numerical values exhibited by the contrasts are low, yet in agreement with the expected ones.

Discussion

As already stated, the main goal of the present analysis is to assess the viability of the phantom as a QC tool for the upcoming breast CT imaging device. Nonetheless, secondary evaluations related to the quality of the CT reconstruction and the exposure parameters are possible as well.

Starting from the CT number linearity measurements, the plastic materials were selected in such a way to span the range of attenuation coefficients typical of a breast (both healthy and tumor tissues), thus guaranteeing the linearity of the re-

construction within the attenuation range of breast tissues. As long as the linearity is guaranteed in that range, and the noise is kept below acceptable levels, the reconstruction will be able to capture both tissue contrasts and morphological features. It can be seen from Table 1 that all regressions exhibit a very high linearity ($1-R^2$ is always less than 10^{-3}), while the slopes are extremely stable against exposure parameters variations. All slopes are compatible with each other within uncertainty intervals, as reported in Table 1. A slight systematic offset is noticeable in the intercept values, probably due to the data point corresponding to the breast-tissue equivalent BR12 material, whose chemical composition (and therefore attenuation coefficient) is known with lower accuracy than the other materials. Weighted average values for intercept and slope are 0.018 ± 0.003 cm^{-1} and 174.4 ± 1.6 cm^{-1}, respectively. Such linearity assessment represents a validation of the reconstruction algorithm, a quality check that will prove particularly useful if the filtered back-projection is replaced by more complex algorithms.

CT number accuracy is another important quality of a CT imaging system. Table 2 shows that the accuracies are comparable with zero within two standard deviations. Measurements at other exposure conditions exhibit similar accuracies. Such result guarantees that the soft tissues composing the imaged breasts will be correctly reproduced by the imaging system, and that the measurement provides a stable reference for CT number calibration.

Regarding the uniformity of the water image, it can be seen from Table 3 that disuniformities lie within few percent for all exposure conditions. The water image noise measurements give slightly higher values, probably due to the voxel size, which is smaller than the typical CT system. Moreover, it can be seen that noise values approximately double from high to low doses, as one would expect from the behavior of stochastic fluctuations.

Finally, low contrast details analysis allows to draw two important conclusions. First of all, although the μ contrasts are comparable with the expected ones, as one would assume from an accurate CT imaging system, it is clear from Table 5 that some of the corresponding HU contrasts do not match the ones typically suggested by QC protocols for CT, e.g. Koning.[15] The main issue here is the composition of the snail: the attenuation coefficients of PMMA and water are too similar in the selected energy range to provide a reliable reference, especially for what regards the lower portion of the range. Therefore, it will either be necessary to fill the holes with a material other than water, or to change the composition of the snail, or to select another energy range for the examinations. However, since the optimal imaging energy is mainly determined by the quality of the CT reconstruction, the final choice of materials for the snail will stem from an energy optimization procedure that is still ongoing.

There is one last point worth mentioning, concerning the detectability assessment of high contrast details. A rod made of a more attenuating material like polyvinyl chloride (PVC), originally included in the phantom to mimic the attenuation properties of microcalcifications, was discarded to be replaced by a high contrast insert. This is because such an isolated data point would skew the output of the linear regression, partially hiding the information about the actual linearity in the soft tissues range. On the other hand, linearity is a much looser requirement in the imaging of small details like microcalcifications. This high contrast insert is not included in the present version of the QC phantom, but will be present in the final version. A 2 cm thick disk, supposedly made of synthetic resin, will be suspended in the upper portion of the phantom, above the plastic inserts. Such disk will contain several clusters of specks made of a highly absorbing material, mimicking the attenuation properties of microcalcifications, and a straight tungsten wire tilted at a given angle with respect to the vertical direction. Such details will allow measurements of the system response to small, high contrast details, of its modulation transfer function and of the thickness of the reconstructed slice. These measures will become part of the QC protocol.

Having reviewed in detail the results of each measurement, there are a few general remarks that are worth making. First of all, with the sole exception of the low contrast one, the phantom inserts proved able to allow precise image quality measurements. Moreover, the morphology of the phantom turned out adequate to fit the geometrical set up of the examination. Therefore, once complemented with the high contrast insert and the upgraded snail, the QC phantom will be ready to be used as a QC tool in standard clinical practice. Finally, it is worth stressing that the measurement procedures included in the final version of the protocol will be complemented with the corresponding reference values obtained in optimal experimental conditions, which are essential components of a QC protocol.

Acknowledgements

The SYRMA-3D project is funded by INFN (the National Institute for Nuclear Physics), and we wish to thank all the members of the SYRMA-3D collaboration. Author SD was partially funded by "Fondazione per la Fisica - Trieste".

References

1. Chang CH, Sibala JL, Fritz SL, Gallagher JH, Dwyer 3rd SJ, Templeton AW. Computed tomographic evaluation of the breast. *Am J Roentgenol* 1978; **131:** 459-64. doi: 10.2214/ajr.131.3.459
2. Boone JM, Nelson TR, Lindfors KK, Seibert JA. Dedicated breast CT: radiation dose and image quality evaluation. *Radiol* 2001; **221:** 657-67. doi: 10.1148/radiol.2213010334
3. Kalender, WA, Kolditz D, Steiding C, Ruth V, Lück F, Rößler AC, et al. Technical feasibility proof for high-resolution low-dose photon-counting CT of the breast. *Eur Radiol* 2017; **27:** 1081-6. doi: 10.1007/s00330-016-4459-3
4. New York Koning Corporation, West Henrietta, NY. Koning breast CT. [cited 2017 Aug 14]. Available at http://koninghealth.com/en/kbct
5. Longo R, Arfelli F, Bellazzini R, Bottigli U, Brez A, Brun F, et al. Towards breast tomography with synchrotron radiation at Elettra: first images. *Phys Med Biol* 2016; **61:** 1634-49. doi: 10.1088/0031-9155/61/4/1634
6. Sarno A, Mettivier G, Golosio B, Oliva P, Spandre G, Di Lillo F, et al. Imaging performance of phase-contrast breast computed tomography with synchrotron radiation and a CdTe photon-counting detector. *Phys Med* 2016; **32:** 681-90. doi: 10.1016/j.ejmp.2016.04.011
7. Delogu P, Oliva P, Bellazzini R, Brez A, De Ruvo PL, Minuti M, et al. Characterization of Pixirad-1 photon counting detector for X-ray imaging. *J Instrum* 2016; **11:** P01015. doi: 10.1088/1748-0221/11/01/P01015
8. Longo R. Current studies and future perspectives of synchrotron radiation imaging trials in human patients. *Nucl Instr Meth Phys Res A* 2016; **809:** 13-22. doi: 10.1016/j.nima.2015.10.110A
9. Rigon L. x-Ray Imaging with Coherent Sources. In: Brahme A, editor. *Comprehensive Biomedical Physics.* Vol. 2. Amsterdam: Elsevier; 2014. p. 193-220.
10. Moeckli R, Verdun FR, Fiedler S, Pachoud M, Schnyder P, Valley JF. Objective comparison of image quality and dose between conventional and synchrotron radiation mammography. *Phys Med Biol* 2000; **45:** 3509-23. doi: 10.1088/0031-9155/45/12/301
11. Baldelli P, Taibi A, Tuffanelli A, Gambaccini M. Dose comparison between conventional and quasi-monochromatic systems for diagnostic radiology. *Phys Med Biol* 2004; **49:** 4135-46. doi: 10.1088/0031-9155/49/17/021
12. Veronese A. *A proposal for a quality control protocol in breast CT with synchrotron radiation*. [Master Thesis]. Trieste: Universita degli Studi di Trieste, Dipartimento di Fisica; 2017.
13. European Reference Organization for Quality Assured Breast Screening EUREF and Diagnostic Services. European protocol for the quality control of the physical and technical aspects of mammography screening. In: *European guidelines for quality assurance in breast cancer screening and diagnosis.* Fourth edition. Perry N, Broeders M, de Wolf C, Törnberg S, Holland R, von Karsa L, editors. Luxembourg: Office for Official Publications of the European Communities; 2006. p. 57-166.
14. Edyvean S, Jones A. Computed tomography x-ray scanners. In: *Measurement of the performance characteristics of the diagnostic x-ray systems used in medicine.* IPEM Report n. 32 Part III. York: IPEM; 2003.
15. Koning. *User's manual for Koning breast CT system*. West Henrietta, New York: Koning Corporation. [cited 2017 Aug 14]. Available at www.accessdata.fda.gov/cdrh_docs/pdf13/P130025c.pdf
16. Castelli E, Tonutti M, Arfelli F, Longo R, Quaia E, Rigon L, et al. Mammography with synchrotron radiation: first clinical experience with phase-detection technique. *Radiol* 2011; **259:** 684-94. doi: 10.1148/radiol.11100745
17. Fedon C, Longo F, Mettivier G, Longo R. GEANT4 for breast dosimetry: parameters optimization study. *Phys Med Biol* 2015; **60:** 311-23. doi: 10.1088/0031-9155/60/16/N311
18. Mettivier G, Fedon C, Di Lillo F, Longo R, Sarno A, Tromba G, et al. Glandular dose in breast computed tomography with synchrotron radiation. *Phys Med Biol* 2016; **61:** 569-87. doi: 10.1088/0031-9155/61/2/569
19. Bellazzini R, Spandre G, Brez A, Minuti M, Pinchera M, Mozzo P. Chromatic X-ray imaging with a fine pitch CdTe sensor coupled to a large area photon counting pixel ASIC. *J Instrum* 2013; **8:** C02028. doi: 10.1088/1748-0221/8/02/C02028
20. Boone JM, Chavez AE. Comparison of x-ray cross sections for diagnostic and therapeutic medical physics. *Med Phys* 1996; **23:** 1997–2005. doi:10.1118/1.597899

research article

Singular value decomposition analysis of back projection operator of maximum likelihood expectation maximization PET image reconstruction

Vencel Somai, David Legrady, Gabor Tolnai

Institute of Nuclear Techniques, Budapest University of Technology and Economics, Budapest, Hungary

Radiol Oncol 2018; 52(3): 337-345.

Received 28 August 2017
Accepted 22 February 2018

Correspondence to: Vencel Somai, Budapest University of Technology and Economics, Műegyetem rkp. 3-9. H-1111 Budapest, Hungary.
E-mail: vencel.somai@gmail.com

Disclosure: No potential conflicts of interest were disclosed.

Background. In emission tomography maximum likelihood expectation maximization reconstruction technique has replaced the analytical approaches in several applications. The most important drawback of this iterative method is its linear rate of convergence and the corresponding computational burden. Therefore, simplifications are usually required in the Monte Carlo simulation of the back projection step. In order to overcome these problems, a reconstruction code has been developed with graphical processing unit based Monte Carlo engine which enabled full physical modelling in the back projection.

Materials and methods. Code performance was evaluated with simulations on two geometries. One is a sophisticated scanner geometry which consists of a dodecagon with inscribed circle radius of 8.7 cm, packed on each side with an array of 39 x 81 LYSO detector pixels of 1.17 mm sided squares, similar to a Mediso nanoScan PET/CT scanner. The other, simplified geometry contains a 38,4mm long interval as a voxel space, detector pixels are assigned in two parallel sections each containing 81 crystals of a size 1.17x1.17 mm.

Results. We have demonstrated that full Monte Carlo modelling in the back projection step leads to material dependent inhomogeneities in the reconstructed image. The reasons behind this apparently anomalous behaviour was analysed in the simplified system by means of singular value decomposition and explained by different speed of convergence.

Conclusions. To still take advantage of the higher noise stability of the full physical modelling, a new filtering technique is proposed for convergence acceleration. Some theoretical considerations for the practical implementation and for further development are also presented.

Key words: PET; maximum likelihood expectation maximization reconstruction; positron range; singular value decomposition; convergence speed; transport Monte Carlo,

Introduction

In emission tomography maximum likelihood expectation maximization (ML-EM) image reconstruction technique[1,2] has replaced the analytical approaches (*e.g.* the widely used filtered back projection) in several applications, since ML-EM offers improvements in spatial resolution and stability due to the more accurate modelling of the system and to the ability of accounting for noise structure.[3] In exchange ML-EM has only a linear rate of convergence[2] and its computational cost is still tedious even with the rapidly increasing processing capacity of current computers. Thus a significant part of recent research activities aims at accelerating the algorithm.[3-5] Another important property partly connected to the low convergence rate is the maximal resolution achievable for a given reconstruc-

tion method given a certain noise level towards which most of the developments are directed.[6-9]

In order to achieve improvement in both convergence rate and spatial resolution an ML-EM positron emission tomography (PET) reconstruction code has been developed with graphical processing unit (GPU) based Monte Carlo engine.[10] GPUs parallel threads allow for running the inherently parallel neutral particle Monte Carlo transport simulations approximately hundred times faster than on a comparably priced CPU thus significantly reducing the time required for the reconstruction. As increased computational capacity allows for better physics modelling the main novelty of this code is the ability of full particle transport modelling as accurate as it is worthwhile in hope of improving image quality.[11]

Contrary to expectations such faithful physics modelling in the back projection step of the algorithm causes strong artefacts: modelling positron range leads to tissue dependent inhomogeneity artefacts in the reconstructed image. Furthermore, these inhomogeneities disappear when simplified Monte Carlo simulations are used without. All the differences between the two cases occur in the system matrix (derived from the Monte Carlo simulations) of the back projection step. These differences were analysed with respect to the convergence properties and stability to noise in a smaller test system by means of singular value decomposition (SVD) which is a powerful when analysing rectangular matrices. We found a significant advantage of the matrix belonging to the simplified simulations in terms of both singular values and vectors that characterized the convergence properties and stability of the algorithm. In other words more accurate physical modelling is less efficient in terms of convergence and these differences explained the perceived artefacts. However, after numerous iterations accurate modelling gives better reconstruction for low noise cases. Taking advantage of these results we created an *a posteriori* filtering matrix applied in each iteration after the back projection step with which we could further amplify these differences for speeding up the convergence, but without spoiling the stability to noise.

This paper is organised as follows: in the first subsection of *Materials and methods* the details of our reconstruction code and a simplified system are described. Second subsection contains the notations. Third subsection gives a short tutorial for SVD including the closely related Picard condition and the corresponding convergence and noise analysis. *Results* section is divided into four subsections, which present the perceived artefact in detail, the use of faithful modelling and our newly developed SVD filtering method with comparison to the original algorithm. Finally, possible solutions for the implementation are offered with theoretical considerations to further research. *Discussion* summarises the impact of the SVD analysis and filter and presents our connecting further research goals.

Materials and methods

A 3D Monte Carlo based ML-EM image reconstruction code named PANNI (PET Aimed Novel Nuclear Imager) has been developed in the framework of the TeraTomo project.[12,13]

PANNI is a Monte Carlo based image reconstruction software written for GPUs using C and CUDA environments surmising roughly 40 000 lines.[11] The key feature of our software is the possibility of faithful Monte Carlo modelling which accounts for positron range, gamma photon-matter interaction and detector response supported by advanced variance reduction methods. Detectors around the object are positioned on a quasi-cylindrical surface with dodecagon cross section. Detector response is either simulated or a pre-generated tabulated response function may be used. Positron range modelling simplifies to the following probability density function.[14]

$$\wp(r) = aA^2re^{-Ar} + bB^2re^{-Br}$$

with r being the positron range distance, a, A, b and B material dependent constants.

As sampling each of the terms is equivalent to sampling the sum of two exponentially distributed random variables x can be obtained by using double exponential sampling.[15] Advanced variance reduction methods are implemented for source angular sampling outgoing direction and energy biasing and for free flight sampling. The Monte Carlo engine has been validated against MCNP5.[16] The code is capable of simulating 10^8 photon pairs per second on a commercially available GPU (NVidia GeForce 690).

Both the forward projection and the back projection steps are carried out via the Monte Carlo method. In the back projection step some of the physics modelling may be turned off.

The code has been tested with two geometries, a sophisticated scanner geometry (*"full system"*) and a simplified smaller system (*"1D model"*). Acquisition geometry for the *full system* can be set as wished, in our current setup it consists of a

dodecagon with inscribed circle radius of 8.7 cm, packed on each side with an array of 39 x 81 LYSO detector pixels of 1.17 mm sided squares comparable to a small animal PET scanner similar to the Mediso nanoScan PET/CT scanner. Coincidence counting is accepted between detector pixels on opposite and next to opposite dodecagon sides (1:3 coincidence). The voxel space of the *full system* is divided into 128x128x128 voxels (0.3 mm sided) and contains a water-cylinder (light grey area in Figure 1 and Figure 2) except for a smaller cylindrical area containing bone material (dark grey area in Figure 1 and Figure 2) Activity phantom for the evaluation is a cylindrical ring of ^{15}O partially located in bone material (the more commonly used ^{18}F gives less conspicuous results). From now on simplified modelling means the neglect of the positron range effect in the back projection Monte Carlo simulations in contrast with faithful modelling which accounts for positron range.

The voxel space of the *1D model* is a 38.4 mm long interval containing 256 voxels half of which is located in bone material the other half in water. Detector pixels are assigned in two parallel sections each containing 81 crystals of a size 1.17.x.1.17 mm. Every pixel is in coincidence with every pixel on the opposite side. Roughly speaking the *1D model* is a cross-section of the *full system* geometry of PANNI (Figure 3).

The *1D model* contains only positron range modelling, neither gamma photon-matter interaction nor detector response modelling is included. Detection is based on the angle of view of the detector from a given voxel. The two analysed settings are: positron

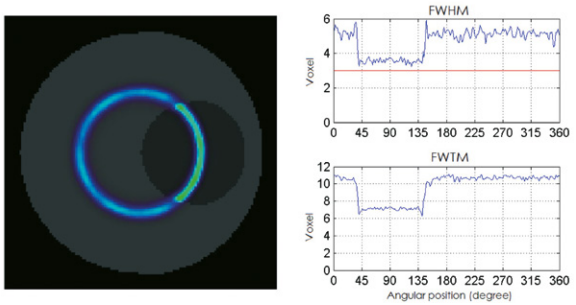

FIGURE 1. Top view of the reconstruction of the cylinder-ring mathematical phantom of the *full system* with faithful modelling in the back projection. Light grey area represents water, dark grey area represents bone material. Underestimated activity and increased full width at half maximum (FWHM) / full width at tenth maximum (FWTM) can be seen for voxels located in water. FWHM and FWTM are calculated along the ring. Red line indicates the phantom ideal FWHM.

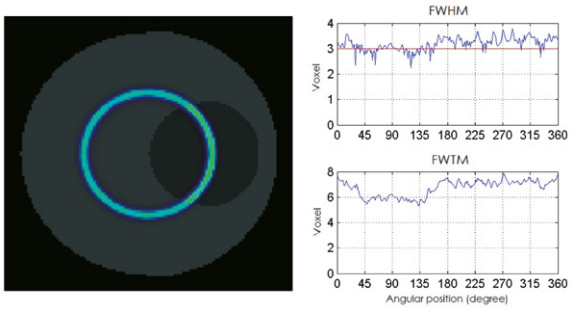

FIGURE 2. Top view of the reconstruction of the cylinder-ring mathematical phantom of the *full system* with simplified modelling in the back projection. Homogeneous activity estimate and full width at half maximum (FWHM) can be seen along the ring, neglect of positron range in theback projection abolished the artefact of Figure 1 and phantom ideal FWHM is reached.

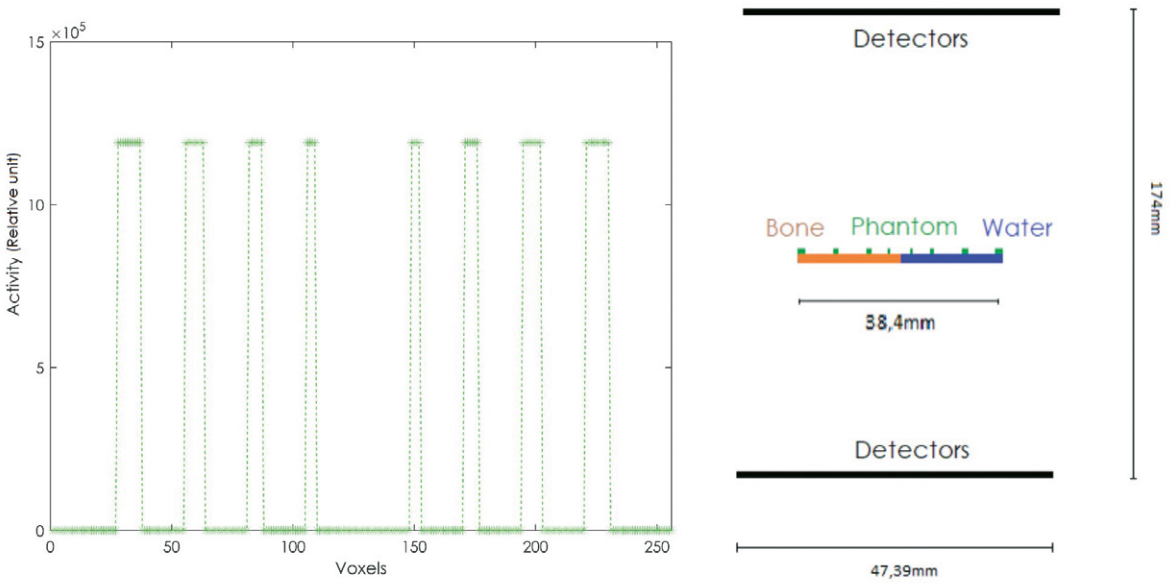

FIGURE 3. Mathematical phantom and system geometry for *1D model*. 1-128 voxels are located in bone material, 129–256 voxels are located in water.

range neglected (back projection posrange OFF) and positron range modelled (back projection posrange ON) in the back projection. Forward projection always accounts for positron range.

Notations

x – vector of activity estimate in the voxels, $x \in \mathbb{R}_{\geq 0}^{Nvoxel}$
y_m – vector of measured data
y – vector of forward-projected data
y_r – pointwise (i.e. Hadamard) ratio vector of measured and forward-projected data $y_r = \frac{y_m}{y}$
v_i – ith singular vector corresponding to voxel space
σ_i – ith singular value
Lor – Line of response
u_i – ith singular vector corresponding to sinogram space
T in superscript means transpose
$\boldsymbol{A}$ – system (response) matrix
$\boldsymbol{A}x$ – forward projection
$\boldsymbol{A}^T y_r$ – back projection
Back projection posrange OFF – simulation neglects positron range in the back projection
Back projection posrange ON – simulation accounts for positron range in the back projection
FWHM – Full Width at Half Maximum
FWTM – Full Width at Tenth Maximum
L_2-norm – Vectorial L_2-norm divided by the L_2-norm of the activity distribution and multiplied by 100:

$$L_2 - norm = 100 * \sqrt{\frac{\sum_{i=1}^{Nvoxel}\left(x_{i,phantom} - x_{i,recon}\right)^2}{\sum_{i=1}^{Nvoxel} x_{i,phantom}^2}}$$

SVD analysis

The effect of positron range modelling and the average positron range is accounted for by the system matrix. As an obvious tool for the analysis of rectangular matrices, the algorithm and the back projection step is examined by means of singular value decomposition. SVD is a factorisation of any $m \times n$ real or complex matrix $\boldsymbol{A}$ of the form $\boldsymbol{A} = \boldsymbol{U}\boldsymbol{D}\boldsymbol{V}^T$. The following notation is used: $\boldsymbol{U}$ is an $m \times n$ matrix, $\boldsymbol{D}$ and $\boldsymbol{V}$ are $n \times n$ square matrices. In general, matrix $\boldsymbol{V}$ has k orthogonal columns where k is the rank of the system matrix $\boldsymbol{A}$. $\boldsymbol{V}$ can be completed to a $n \times n$ dimensional matrix by adding n-k orthogonal vectors from the null space of $\boldsymbol{A}^T$ to form a basis in the voxel space. The first k columns of $\boldsymbol{U}$ are also orthogonal and can also be completed to a basis in the sinogram space by adding m-k orthogonal vectors from the null space of $\boldsymbol{A}$. In this last case, $\boldsymbol{D}$ is zero filled to a $m \times n$ dimensional matrix. In the point of view of our analysis the completion of $\boldsymbol{U}$ is not needed and we chose the nomenclature where $\boldsymbol{U}$ has only n (as $\boldsymbol{A}$ has full rank, thus $k = n$) columns. D and $\boldsymbol{V}$ $n \times n$ in this case.

SVD was used for the analysis of convergence speed of the reconstruction algorithm with respect to the applied back projection. According to Liu *et al*.[17] the speed of convergence of PET ML-EM algorithm particularly depends on the singular values of the back projection system matrix. Singular values represent relative weights for the voxel space basis vectors (*i.e.* corresponding voxel space singular vectors) in the update process of the previous activity estimate in a given iteration.

Sinogram space singular vectors can measure the information content of a given measurement-forward projection Hadamard ratio in the corresponding back projection step by means of Picard condition formalism. For the existence of a square integrable solution to the problem $y = \mathcal{A}x$ the following has to be true ($\mathcal{A}$ is the integral operator the discretization of which is the system matrix $\boldsymbol{A}$).[18]

$$\sum_{i=1}^{\infty}\left(\frac{u_i^T y}{\sigma_i}\right)^2 < \infty$$

In case of matrices instead of integral operators, the discrete Picard condition requires the spectral coefficients $\left|u_i^T y\right|$ to decay faster in average than the singular values.[18] Despite back projection is not a direct inversion from this point of view the faster is the decay of the spectral coefficients $\left|u_i^T y_r\right|$ of the ratio as the index increases the heavier the blurring of the back projection. Higher frequency components level off at a plateau which is dominated by noise and can be regarded as an error-level estimate[18] because these components do not contain information for the corresponding back projection. Even accounting for voxel space effects only (e.g. positron range) sinogram space singular vectors are not the same for the simplified and faithful modelling. The back projection step of the algorithm back projects the Hadamard ratio of the measured and the currently forward-projected data.

$$\boldsymbol{A}^T y_r = \boldsymbol{V}\boldsymbol{D}^T\boldsymbol{U}^T y_r$$

The aforementioned difference in the sinogram space basis affects the $\boldsymbol{U}^T y_r$ product, *i.e.* the spectral coefficients of the Hadamard ratio.

Results

We have compared two reconstruction results for the sophisticated scanner geometry: one with full

physics modelling in the back projection (Figure 1) and one omitting positron range in the back projection (Figure 2). After 80 iterations faithful modelling produced the reconstruction in Figure 1. The cross section of the cylindrical ring phantom in radial direction is originally a box function which is blurred due to gridding and averaging in a given voxel (similarly to partial volume effect). Therefore, it can be well approximated by a gaussian with a Full Width at Half Maximum of 3 voxels which is indicated by the red line in Figure 1 and Figure 2. The Full Width at Half Maximum/Full Width at Tenth Maximum is calculated by fitting a gaussian in radial direction along the ring separately for each angular position with resolution of 1 degree.

Accounting for positron range in the back projection caused systematic inhomogeneity in the reconstructed image in Figure 1. The activity estimation in the bone material is appropriate (FWHM = 3.5 voxel) in contrast with the activity of the voxels located in water which is underestimated (FWHM = 5 voxels). The inhomogeneity reduces with simplified back projection, when positron range is neglected in the Monte Carlo simulation. Also the FWHM is reduced in the water area (Figure 2).

The effect of modelling any physical phenomenon appears in the system matrix, thus our analysis aims at finding the differences in the back projection system matrix caused by positron range. Due to its size the system matrix of the *full system* cannot be stored thus the *1D model* was used for further calculations. For real and valid results a comparison of the test system with the *full system* is needed. Simulations confirmed the analogous behaviour as the perceived artefact appeared in the case of positron range modelling in the back projection while neglecting positron range abolished the problem. Thus, the analysis focuses on the positron range effect, back projection posrange OFF and back projection posrange ON settings are compared. (The positron range free path is sampled with two random variables similarly to the *full system*). As the corresponding system matrix is of a size 6561x256 it can be directly stored and also the numerical SVD calculation may be carried out.

Comparing the back projection posrange OFF and back projection posrange ON case in terms of singular values of the system matrix, Figure 4 shows the positive difference for the first 133 index belonging to the former setting.

In the light of the convergence analysis of Ref.[17] smaller singular values mean that the corresponding frequency components of the solution are later

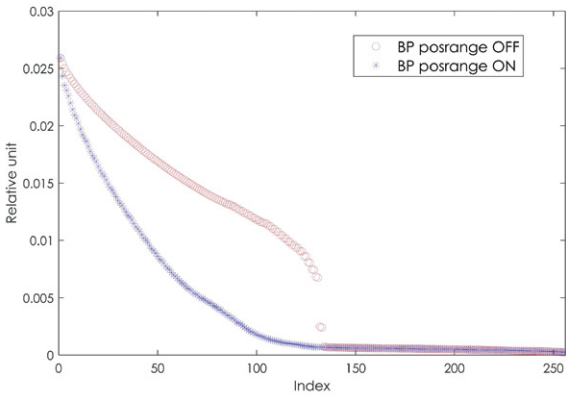

FIGURE 4. Singular values of the system matrix for positron range neglecting and modelling case. Increased values for the former imply the faster convergence of the corresponding (first 133) basis components of the activity estimate.

reconstructed with positron range modelling compared to the positron range neglecting back projection. This space frequency characterises the singular vectors of the voxel space (Figure 5), which is a second but not less significant difference between the two types of system matrices.

Figure 5 on the left accounts only for the symmetries of the system while on the right reflects also the tissue map of the volume. As the average positron free path is much longer in water than in the bone material space frequency of every basis vector is smaller in the area located in the water. Thus the reconstruction of the activity of these voxels is significantly slower and this property is the reason of the obtained artefact resulted from faithful modelling in the back projection and the solution to the perceived anomalous behaviour.

The third and final difference occurs in the sinogram space basis vectors with which the measurement-forward projection Hadamard ratio can be unfolded in a given iteration. The absolute value of the obtained spectral coefficients can be seen in Figure 6 after 15 iterations for the positron range neglecting and modelling case respectively (the spectrum varies slowly through iterations).

Faster decay in the spectral coefficients equals to heavier blurring in the back projection.[18] This means that the positron range modelling gathers less information from the Hadamard ratio in a given iteration than the positron range neglecting back projection. This also implies the faster convergence and higher stability to noise.

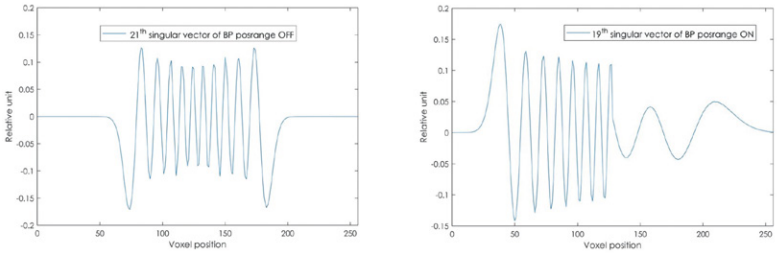

FIGURE 5. One of the voxel space singular vectors of the system matrices corresponding to positron range neglect (left – back projection posrange OFF) and positron range modelling (right – back projection posrange ON). Back projection posrange OFF reflects only the symmetries of the geometry. Back projection posrange ON accounts for the material map as well, increased position uncertainty due to longer average positron free path implies smaller space-frequency in water area.

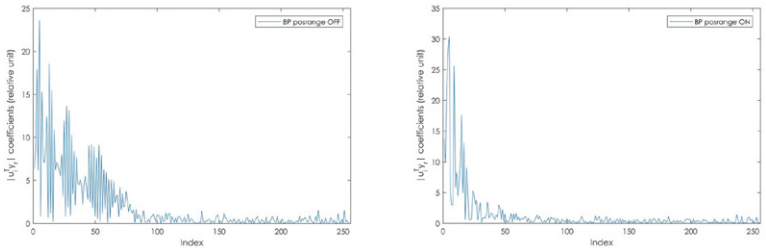

FIGURE 6. Absolute value of the spectral coefficients of the measurement-forward projection Hadamard ratio in the sinogram basis corresponding to positron range neglect (left – back projection posrange OFF) and positron range modelling (right – back projection posrange ON). Faster decay means less information gathered as the coefficients of the horizontal plateau are corrupted by noise thus it represents an error level estimate. Due to one to one correspondence property of SVD between sinogram and voxel space singular (basis) vectors these basis coefficients of the activity are not hoped to be correctly estimated

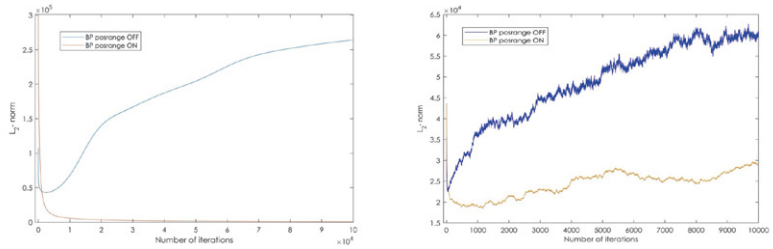

FIGURE 7. The L_2-norm of the difference between the activity distribution and the current estimate after a given number of iterations. Smaller value means better agreement. Subfigure on the left shows the result of the noiseless test case where the convergence of back projection posrange ON setting to the exact solution and the convergence of back projection posrange OFF setting to an other fix point is presented. Subfigure on the right shows the result of a simulated reconstruction with 10^6 positron used for measurement generation and in both forward and back projection Monte Carlo simulations. After slower initial convergence back projection posrange ON reaches much better activity estimate. Back projection posrange OFF converges to a different fix point similarly to noiseless case.

Advantage of faithful modelling

ML-EM with faithful modelling converges to the exact solution.[1,2] Algorithm using simplified back projection converges to different fix point due to unmatched forward-backward projector pair and only approximates the solution.[2,3,5] These statements were verified by test simulations with varying noise level (Figure 7). In presence of high noise semi-convergence property of the algorithm[3,19] is dominant, reaching the optimum estimate as fast as possible is desired which is the advantageous property of the simplified back projection. In low noise case after numerous iterations the faithful modelling outperforms the simplified one reaching much better activity estimate (Figure 7). SVD analysis showed the disadvantage of the former in the term of convergence speed but due to matched forward-backward projector pair it converges to the exact solution[1] in contrast with the simplified modelling.

This result resolves the contradiction as additional information indeed leads to better image reconstruction thus the perceived anomaly was only apparent. Simplification just luckily affects the behaviour of the algorithm from a mathematical point of view. However, this form is not the ideal back projection operator but the one that is easy to implement without much modification to the original algorithm. To obtain a better back projection operator the previously listed advantages can be amplified with a posteriori manipulation and a close to ideal form can be reached. As a possible degree of freedom, singular values of the simplified back projection operator can be further increased similarly to the accompanying effect of the simplified modelling. In this case $\boldsymbol{U}$ and $\boldsymbol{V}$ matrices are unchanged. The possible fix points of the algorithm can be obtained from the next equations (ratio is in a Hadamard sense) as the update process multiplies (also in Hadamard sense) the current estimate by 1 when the following is true:

$$\frac{\boldsymbol{A^T} y_r}{|\boldsymbol{A}|} = \frac{\boldsymbol{A^T} y_r}{\boldsymbol{A^T} * \begin{pmatrix} 1 \\ \vdots \\ 1 \end{pmatrix}_{Lor-space}} = \begin{pmatrix} 1 \\ \vdots \\ 1 \end{pmatrix}_{voxel\ space}$$

Rearranging:

$$\boldsymbol{A^T}\left(y_r - \begin{pmatrix} 1 \\ \vdots \\ 1 \end{pmatrix} \right) = \boldsymbol{A^T}\tilde{y} = 0$$

Using the dyadic definition of SVD:

$$\boldsymbol{A^T}\tilde{y} = \left(\sum_{r=1}^{Rank(\boldsymbol{A})} \sigma_r v_r u_r^T \right) * \tilde{y} = 0$$

v_r and u_r are the columns of matrix $\boldsymbol{V}$ and $\boldsymbol{U}$ respectively. As $\boldsymbol{V}$ is an orthogonal matrix the linear combination above equals to zero precisely when every $\sigma_r u_r^T \tilde{y}$ coefficient equals to zero. The singular values are all nonzero thus the $u_r^T \tilde{y}$ dot product equals to zero for $\forall r$. This implies that $\boldsymbol{U^T}\tilde{y} = 0$. Matrix $\boldsymbol{U}$ remains the same with singular value modification so the possible fix points are unchanged.

SVD filter

The easiest way to modify the singular value spectrum of the back projection system matrix is the application of a matrix of the form:

$$\boldsymbol{B = VD^*V^T}$$

$\boldsymbol{D^*}$ is the matrix with which $\boldsymbol{D^*D}$ has the desired form. In noiseless (test) case, i.e. when there is no noise added to simulations, this form is (the scalar multiple of) the identity matrix, in agreement with the convergence analysis[5,17,20], as the singular values are clustered together as far as possible. The SVD filter fastens the convergence with two orders of magnitude. However, it cannot be applied straightforward for the real, noisy case.

The measurement process equals to $\boldsymbol{Ax = UDV^T}x$ where x stands for the activity distribution. Thus, the measurement attenuates its frequency components according to the singular value spectrum (multiplication with matrix $\boldsymbol{D}$) and adds some noise to the result. As so only those components which fit to the discrete Picard condition (Figure 6) can be amplified.

We performed several reconstructions with such an SVD filter. The best result was obtained when $\boldsymbol{D^*}$ diagonal matrix contains elements of the form (Figure 8):

$$\begin{cases} \frac{1}{\sigma_i^p} \; if \; i < cut-off \\ 0 \; if \; i \geq cut-off \end{cases} \text{ for some } 0 < p = 1 - \varepsilon \text{ and small } \varepsilon.$$

for some and small .

Then $\boldsymbol{D^*D}$ is also diagonal with the following entries: $\begin{cases} \sigma_i^{1-p} & if \; i < cut-off \\ 0 & if \; i \geq cut-off \end{cases}$

which are closer to 1, so the singular value spectrum of the resulted back projection system matrix is contracted.

The conventional ML-EM formula looks like as follows (y_r is the pointwise, *i.e.* Hadamard ratio vector of measured and forward-projected data, $y_r = \frac{y_m}{\boldsymbol{Ax}}$. $\boldsymbol{1}$ is a sinogram space vector containing ones in every coordinate):

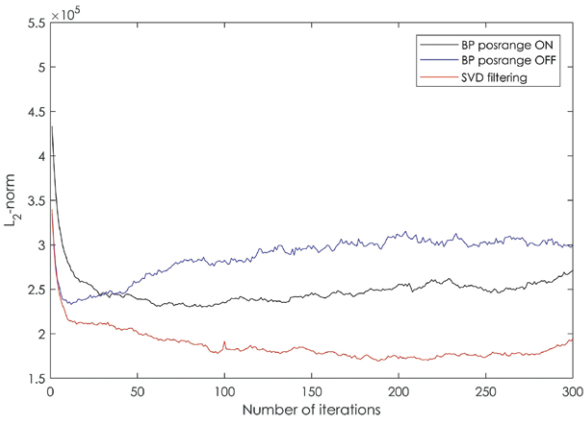

FIGURE 8. The L_2-norm of the difference between the activity distribution and the current estimate after a given number of iterations. Smaller value means better agreement. Reconstruction with SVD filter outperforms the best setting so far in terms of faster initial convergence and the farther starting point of increasing discrepancy due to semi-convergence. Also the faster initial convergence of positron range neglecting back projection can be seen compared to positron range modelling back projection.

$$x^{n+1} = x^n \frac{\boldsymbol{A^T}y_r}{\boldsymbol{A^T1}} = x^n \frac{\boldsymbol{VDU^T}y_r}{\boldsymbol{VD^TU^T1}}$$

Instead, we use the modified iteration formula which looks like as follows ($\boldsymbol{B^T = B}$ as being symmetric and $\boldsymbol{V^TV = I}$ as $\boldsymbol{V}$ is orthogonal. $\boldsymbol{I}$ is the identity matrix. The ratio and the multiplication in the update process of x^n is in Hadamard sense):

$$x^{n+1} = x^n \frac{\boldsymbol{BA^T}y_r}{\boldsymbol{A^TB1}} = x^n \frac{\boldsymbol{VD^*V^TVDU^T}y_r}{\boldsymbol{VD^{*T}V^TVD^TU^T1}} = x^n \frac{\boldsymbol{VD^*DU^T}y_r}{\boldsymbol{VD^{*T}D^TU^T1}}$$

Figure 8 shows the result of the reconstruction compared to regular ML-EM algorithm with both back projection posrange ON and back projection posrange OFF settings (6×10^5 positron used). The L_2-norm of the difference of the activity distribution and the current activity estimate is presented for each setting after a given number of iterations. Smaller L_2-norm means better agreement.

SVD filter outperforms the best setting so far as the initial convergence is faster and better agreement is reached in every iteration. Furthermore, the rise of the discrepancy due to semi-convergence occurs later. Additionally, the faster initial convergence of the positron range neglecting back projection (back projection posrange OFF) can be seen compared to back projection posrange ON.

Implementation of SVD filter for realistic geometries

SVD filter requires the calculation of $\boldsymbol{B} = \boldsymbol{V}\boldsymbol{D}^{*}\boldsymbol{V}^{T}$ matrix, which is of a size Nvoxel×Nvoxel, so impossible to store directly for *full system*. On the other hand, this matrix is diagonally dominant not only in the case of the 1D test system but for a 3D *full system* as well. Consequently it is enough to store the main diagonal and some side-diagonals. Thus, the remaining task is the calculation of the filtering matrix which requires a numerical SVD. As the calculation is still computationally tedious we present an alternative way. The simplified back projection accounts only for the qualities of the imaging system and the material dependent effects in the reconstructed volume are neglected. For the reconstruction, the activity of the voxels is assigned in a finite length vector. A forward projection-back projection operator composition (in matrix terms $\boldsymbol{A}^{T}\boldsymbol{A}$) maps a voxel space vector into another voxel space vector performing a low-pass filtering. In other words, a space-limited signal is low-pass filtered and space-limited again. The eigenfunctions of such an operator are the well-known prolate spheroidal wave functions (PSWF)[21] and per definition these are the voxel space singular functions of the forward projection (and also the back projection) operator for simplified modelling case.

Observing (the square of) the singular value spectra of the system matrix, low-pass filtering is not ideal but PSWFs are good approximation for the singular vectors. Owing to this favourable property, matrix B can be calculated if singular value spectrum has been obtained (*e.g.* by means of inverse iteration). However, for an increased precision, certain generalisation of the functions is needed, as the low-pass filter (characterised by the squares of the singular values) is not ideal. This is done by using special spectral techniques from the theory of Sturm-Liouville operators applied to the Jacobi perturbed differential operator of Karoui *et al*.[22]

$\alpha = \beta = 0$ case in Karoui *et al*.[22] corresponds to regular PSWFs, but $\alpha = \beta > 0$ type generalisation gives a very good approximation for singular value spectrum and the voxel space singular vectors as well.

Discussion

In our paper all of the three SVD matrices from the factorisation of the system matrix were analysed. The results explained the perceived artefact as the convergence speed of the scheme with positron range modelling back projection was material dependent and the further advantage of the simplified back projection in terms of overall convergence speed and stability to noise. The presented SVD filter further amplified these favourable properties so as to fasten the algorithm but preserving its robustness. Additionally the use of faithful modelling was pointed out when high computational capacity is available.

A posteriori filtering is in close relation with such a priori methods when a regularizing term is added to the likelihood function in the problem formulation for decreasing noise sensitivity and accelerate the convergence. The resulted filtering term is then present usually in the nominator of the backprojection in additive form and arises from known constraints about the imaging process. In general, some kind of regularisation is almost always required due to the ill-posed nature of the reconstruction problem. Our SVD filter approaches from a bit different point of view: it does not require any a priori knowledge. The effect of B matrix is not strictly regularisation but rather deconvolution which accelerates the convergence and the deconvolution process itself has to be regularised due to the presence of noise. Thus, the process has a filtering effect as well.

Monte Carlo simulations result slightly different system matrix elements through iterations which imply slightly different SVDs and B matrices. So as to make the most of the presented SVD filtering technique our further aim is to find the connection with conventional deconvolution methods which obtain exactly the same effect but the filtering factors can be recalculated in each iteration tailored to the given back projection system matrix. The special form (PSWF which is strongly connected to Fourier-transform[22,23]) of the singular vectors makes this direction promising.

References

1. Vardi Y, Shepp LA, Kaufman L. A statistical model for positron emission tomography (with discussion). *J Am Stat Assoc* 1985; **80:** 8-20. doi: 10.2307/2288037.1981.389
2. McLachlan G, Krishnan T. *The EM algorithm and extensions*. New York: John Wiley and Sons, Inc; 1997.
3. Zeng GL. *Medical image reconstruction.* Heidelberg: Springer; 2010.
4. Szirmay-Kalos L, Magdics M, Toth B, Bukki T. Averaging and metropolis iterations for positron emission tomography. *IEEE Trans Med Imaging* 2013; **32:** 589-600. doi: 10.1109/TMI.2012.2231693
5. Zeng GL, Gullberg GT. Unmatched projector/backprojector pairs inan iterative reconstruction algorithm. *IEEE Trans Med Imaging* 2000; **19:** 548-55. doi: 10.1109/42.870265

6. Xin F, Hai-Peng W, Ming-Kai Y, Xiao-Li S, Xue-Xiang C, Shuang-Quan L, et al. PET image reconstruction with a system matrix containing point spread function derived from single photon incidence response. *Chinese Phys B* 2015; **24:** 018702. doi: 10.1088/1674-1056/24/1/018702

7. Gong K, Cherry SR, Qi J. On the assessment of spatial resolution of PET systems with iterative image reconstruction. *Phys Med Biol* 2016; **61:** 193-202. doi: 10.1088/0031-9155/61/5/N193

8. Chávez-Rivera LB, Ortega-Máynez L, Mejía J, Mederos B. ML-EM reconstruction model including total variation for low dose PET high resolution data. Nuclear Science Symposium and Medical Imaging Conference (NSS/MIC), 2015 IEEE. doi**:** 10.1109/NSSMIC.2015.7582221

9. Gu XY, Zhou W, Li L, Wei L, Yin PF, Shang LM, et al. High resolution image reconstruction method for a double-plane PET system with changeable spacing. *Chinese Phys C* 2016; **40:** 058201. doi: 10.1088/1674-1137/40/5/058201

10. Cserkaszky A, Légrády D, Wirth A, Bükki T, Patay G. GPU based Monte Carlo for PET image reconstruction: Parameter optimization. International Conference on Mathematics and Computational Methods Applied to Nuclear Science and Engineering (M&C 2011), Rio de Janeiro, RJ, Brazil, May 8-12, 2011.

11. PANNI - PET aimed novel nuclear imager; forward Monte Carlo based image reconstruction software for positron emission tomography corresponding to code revision 664; General description; Coding: Cserkaszky A, Szlávecz Á, Légrády D, Tolnai G. Contact: legrady@reak.bme.hu

12. Wirth A, Cserkaszky A, K*éri* B, Légrády D, Fehér S, Czifrus S, et al. Implementation of 3D Monte Carlo PET reconstruction algorithm on GPU. *IEEE Nuclear Science Symposium Conference Records* 2009; doi: 10.1109/NSSMIC.2009.5402363.

13. Mediso Ltd. Product page of nanoScan. [citated 15 Jul 2017]. Available at http://www.mediso.hu/products.php?fid=2,11&pid=90

14. Derenzo SE. Mathematical removal of positron range blurring in high resolution tomography. *IEEE Nucl Sci* 1986; **33:** 565-9. doi: 10.1109/TNS.1986.4337166

15. Lehnert W, Gregoire MC, Reilhac A, Meikle SR. Analytical positron range modelling in heterogeneous media for PET Monte Carlo simulation. *Phys Med Biol* 2011; **57:** 4075-6. doi: 10.1088/0031-9155/56/11/009

16. Briesmeister JF. MCNP – a General Monte Carlo N-Particle Transport Code. Los Alamos National Laboratory Report LA-13709-M. April 2007

17. Liu Z, Obi T, Yamaguchi M, Ohyama N. An investigation of convergence rates in expectation maximization (EM) iterative reconstruction. *IEEE Nuclear Science Symposium Conference Record* 1999. doi: 10.1109/NSSMIC.1999.842824

18. Hansen PC. Numerical tools for analysis and solution of Fredholm integral equations of the first kind. *Inverse Problems* 1992; **8:** 849-72. doi: https://doi.org/10.1088/0266-5611/8/6/005

19. Magdics M, Szirmay-Kalos L, Toth B, Penzov A. Analysis and control of the accuracy and convergence of the ML-EM iteration. *Lecture notes in computer science*. Berlin: Springer; 2014. p. 147-54.

20. Pyzara A, Bylina B, Bylina J. The influence of a matrix condition number on iterative methods convergence. *IEEE Proceedings of the Federal Conference on Computer Science and Information Systems;* 2011. p. 459-64.

21. Prolate spheroidal wave functions. *Wikipedia*. [cited 15 Jul 2017]. Available at https://en.wikipedia.org/wiki/Prolate_spheroidal_wave_function

22. Karoui A, Souabni A. Generalized prolate spheroidal wave functions: Spectral analysis and approximation of almost band-limited functions. *J Fourier Anal Appl* 2015; **22:** 382-412. doi: 10.1007/s00041-015-9420-3

23. Moore IC, Cada M. Prolate spheroidal wave functions, an introduction to the Slepian series and its properties. *Appl Comput Harmon Anal* 2004; **16:** 208-230. doi: 10.1016/j.acha.2004.03.004

research article

Evaluation of two-dimensional dose distributions for pre-treatment patient-specific IMRT dosimetry

Đeni Smilovic Radojcic[1], David Rajlic[1], Bozidar Casar[2], Manda Svabic Kolacio[1], Nevena Obajdin[1], Dario Faj[3,4], Slaven Jurkovic[1,5*]

[1] University Hospital Rijeka, Medical Physics Department, Rijeka, Croatia
[2] Institute of Oncology LJubljana, Department of Radiation Physics, Ljubljana, Slovenia
[3] Faculty of Medicine, University of Osijek, Osijek, Croatia
[4] Faculty of Dental Medicine and Health, University of Osijek, Osijek, Croatia
[5] Department of Medical Physics and Biophysics, Faculty of Medicine, University of Rijeka, Rijeka, Croatia

Radiol Oncol 2018; 52(3): 346-352.

Received 5 December 2017
Accepted 13 February 2018

Correspondence to: Slaven Jurković, University Hospital Rijeka, Medical Physics Department, Krešimirova 42, Rijeka, Croatia.
E-mail: slaven.jurkovic@medri.uniri.hr

Disclosure: No potential conflicts of interest were disclosed.

Background. The accuracy of dose calculation is crucial for success of the radiotherapy treatment. One of the methods that represent the current standard for patient-specific dosimetry is the evaluation of dose distributions measured with an ionization chamber array inside a homogeneous phantom using gamma method. Nevertheless, this method does not replicate the realistic conditions present when a patient is undergoing therapy. Therefore, to more accurately evaluate the treatment planning system (TPS) capabilities, gamma passing rates were examined for beams of different complexity passing through inhomogeneous phantoms.

Materials and methods. The research was performed using Siemens Oncor Expression linear accelerator, Siemens Somatom Open CT simulator and Elekta Monaco TPS. A 2D detector array was used to evaluate dose distribution accuracy in homogeneous, semi-anthropomorphic and anthropomorphic phantoms. Validation was based on gamma analysis with 3%/3mm and 2%/2mm criteria, respectively.

Results. Passing rates of the complex dose distributions degrade depending on the thickness of non-water equivalent material. They also depend on dose reporting mode used. It is observed that the passing rate decreases with plan complexity. Comparison of the data for all set-ups of semi-anthropomorphic and anthropomorphic phantoms shows that passing rates are higher in the anthropomorphic phantom.

Conclusions. Presented results raise a question of possible limits of dose distribution verification in assessment of plan delivery quality. Consequently, good results obtained using standard patient specific dosimetry methodology do not guarantee the accuracy of delivered dose distribution in real clinical cases.

Key words: IMRT; 2D dose verification; gamma method; anthropomorphic phantom

Introduction

The accuracy of dose calculation and precise dose delivery are crucial factors in the radiotherapy treatment process. There is a common agreement that Monte Carlo (MC) simulation is the most promising method for accurate calculation of absorbed dose.[1,2] In MC based systems the absorbed dose calculated to be delivered by external photon beams can be reported either as dose-to-media (D_m) or dose-to-water (D_w), and there is still no general agreement regarding the choice of the calculation method.[1-3] Hence, experimental verification is essential to validate algorithms before clinical use.[4] These verifications need to be performed using different dosimetric techniques and phan-

toms of different complexity (*e.g.* homogeneous, semi-anthropomorphic, anthropomorphic). The complexity of the phantom is especially important since it has been shown[3,5,6] that performance of algorithms in the heterogeneous medium can differ significantly depending on reporting mode used. Namely, our earlier investigation confirmed previously published results when the calculated values according to respective reporting mode were compared with values measured using ionization chambers in media of various densities. In case of water equivalent media, dose differences were less than 2%.[2,3,7] Similar results were acquired in low-density media.[1,8] However, differences in absorbed dose between two reporting modes were found to be as high as 10–15% when calculated in high-density media[2,3,9] due to their inherent limitations and differences. Compared to the measured values, the differences between D_m and D_w approaches in high-density media (*e.g.* bones) were significant and of opposite sign.[2,3] This problem was of particular interest for our group, and extensive work was performed using a methodology based on absorbed dose measurements with ionization chambers. We found a plausible solution for this problem which can be of practical use when measurements for commissioning of different reporting modes of treatment planning system (TPS) algorithm are performed. Nevertheless, due to the comprehensiveness of this research, the results are prepared to be published as separate research elsewhere.

In addition to these point dose verifications, where ionization chamber was placed in the phantom volumes of different densities, we investigated the performance of the system for the 2D dosimetric verification of dose distributions, which is colloquially known as patient-specific dosimetry. It is well known that this type of verification should be performed before the first fraction of patient's therapy. Patient specific 2D dosimetry can be performed either using film or arrays of ionization chambers or diodes. One of the first 2D detectors was radiographic film, but it is energy dependent[10] and nowadays it is replaced by radiochromic film. Radiochromic film is a detector with a high spatial resolution and it is almost energy independent. Furthermore, it is almost water equivalent, which makes it convenient for measurements of dose distributions produced by high energy photon beams used for radiotherapy.[11] Nevertheless, handling and processing of radiochromic films using flatbed scanners makes its use rather complex for everyday patient specific dosimetry. Consequently, arrays of ionization chambers or diodes are devices of choice for routine patient dose distribution verifications. One of the methods that represent the current standard for patient-specific dosimetry is the evaluation of dose distributions measured with an ionization chamber array inside a homogeneous phantom using gamma method.[12,13] Because beams pass through homogeneous water equivalent media, this does not replicate the realistic conditions present when a patient is undergoing therapy. Therefore, to evaluate the accuracy of the TPS calculations more in detail, gamma methodology was used for verification of resulting dose distribution produced by photon beams passing through inhomogeneous phantoms in different geometries. Calculated dose distributions were obtained using D_m and D_w reporting modes. Also, to better differentiate the underlying reasons for possible discrepancies, a selection of several plans was evaluated, ranging from simple square field to intensity modulated radiation therapy (IMRT) plans of various complexity. The results and analysis of this research will be presented.

Materials and methods

In this study, the research was performed using devices which are in clinical use at Radiotherapy Department of University Hospital Rijeka, Croatia: linear accelerator Siemens Oncor Expression (6 MV photon beam) equipped with multileaf collimator with 160 leaves (leaf width 0.5 cm at isocentre), Somatom Open CT simulator (Siemens Healthineers, Erlangen, Germany) and-Monaco v. 5.11.02 TPS (Elekta, Stockholm, Sweden). Linear accelerator was commissioned and prepared for the clinical implementation of the IMRT according to international standards.[14-17]

A 2D detector array IBA MatriXX (IBA Dosimetry GmbH, Schwarzenbruck, Germany) with 1020 ion chambers spaced at approximately 0.7 cm distance one from another was used to evaluate TPS accuracy in homogeneous MultiCube phantom (IBA Dosimetry GmbH, Schwarzenbruck, Germany) and inhomogeneous phantoms: CIRS Thorax semi-anthropomorphic phantom (Computerized Imaging Reference Systems Inc., Norfolk, USA) and Alderson Radiation Therapy (ART) anthropomorphic phantom (Radiology Support Devices, Long Beach, USA). CIRS semi-anthropomorphic phantoms are well known to all involved in dosimetric verification of TPS performance for point measurements using ionization chambers.[18-21] In

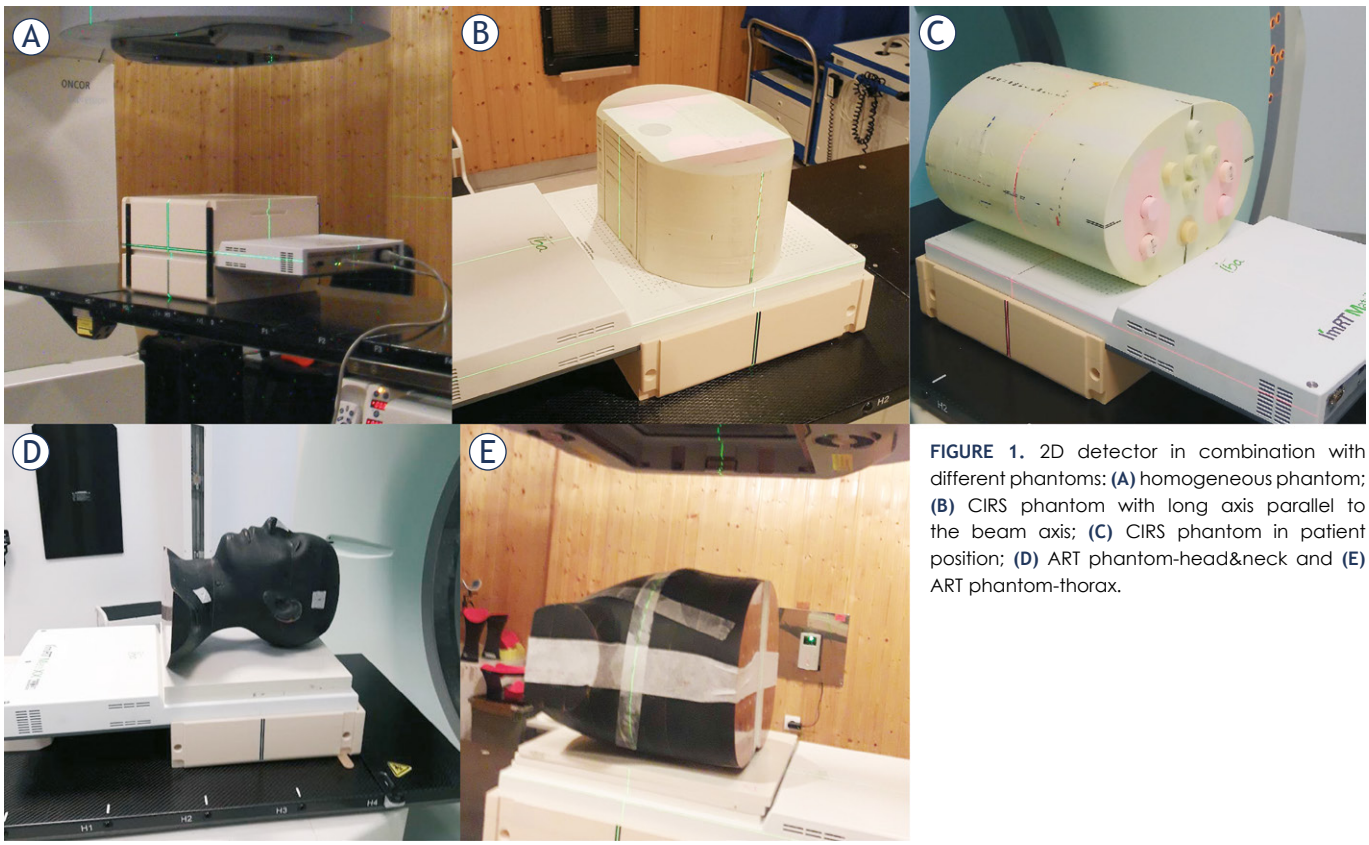

FIGURE 1. 2D detector in combination with different phantoms: **(A)** homogeneous phantom; **(B)** CIRS phantom with long axis parallel to the beam axis; **(C)** CIRS phantom in patient position; **(D)** ART phantom-head&neck and **(E)** ART phantom-thorax.

present study, the CIRS Thorax phantom, where volumes of three different densities (water equivalent, low-density and high-density) are built-in, was used along with a 2D detector for transit dosimetry. For a better resemblance to a realistic situation, the methodology was also verified using three parts of the Alderson phantom; head and neck (H&N), thorax and pelvis.

Gamma analysis was used to quantify the differences between measured and calculated dose distributions using criteria of 3 mm distance-to-agreement (DTA) and 3% relative dose difference (3%/3 mm).[17] To study the effects of more stringent criteria on the passing rate, we also used 2%/2 mm criteria. Gamma analysis was performed using commercial software OmniPro-I'mRT v. 1.7b (IBA Dosimetry GmbH, Schwarzenbruck, Germany). Therefore, measured planar dose distribution was taken as a reference distribution according to which calculated distribution is evaluated. The data were analysed according to following parameters- global gamma normalization, dose maximum to 100%; threshold: 10% of the maximum dose; search distance: 4.5 mm.

Calculated data along with data measured using a 2D detector were used for the evaluation of gamma analysis results considering the dependence on inhomogeneous media, different complexities of radiotherapy plans and different phantom configurations. Phantoms were scanned in all measuring set-ups, and the appropriate relative electron density tables were assigned. To increase the experimental complexity, a 2D detector was placed under different measuring conditions (Figure 1) using above mentioned phantoms. Patient specific dosimetry (PSD) is regularly performed by placing the detector (IBA Matrixx) in the homogeneous phantom MultiCube, which is shown in Figure 1A. This phantom is built of tissue equivalent plastic and 10 cm of it is placed in front of the detector, on the beam path. To increase the experimental complexity, a 2D detector was placed under different measuring conditions (Figure 1). Therefore, various thicknesses of semi-anthropomorphic

TABLE 1. Results of gamma analysis for measured and calculated dose distributions in homogeneous and CIRS thorax phantoms for different levels of plan complexity and different reporting modes

phantom	gamma criteria	15x15		IMRT1		IMRT2		IMRT3		IMRT4	
		% points passing with gamma<1									
		D_w	D_m	D_w	D_m	D_w	D_m	D_w	D_m	D_w	D_m
MultiCube	2mm/2%	93,12	95,62	98,68	96,75	99,53	98,62	97,32	96,01	89,59	84,68
	3mm/3%	98,74	99,97	99,94	99,33	99,99	99,81	99,65	99,31	98,22	95,93
5N CIRS	2mm/2%	90,13	91,51	96,63	94,94	99,03	98,72	93,68	88,49	78,74	70,37
	3mm/3%	97,55	98,71	98,26	98,44	99,94	99,92	98,64	96,19	92,03	84,99
10N CIRS	2mm/2%	88,61	86,14	95,11	92,39	99,14	97,9	93,25	84,54	77,51	70,52
	3mm/3%	97,18	96,15	96,07	97,17	99,98	99,64	97,76	92,57	89,48	84,19
15N CIRS	2mm/2%	85,73	86,06	96,35	94,45	98,42	97,42	89,67	84,66	72,16	64,7
	3mm/3%	96,44	96,46	99,33	98,17	99,99	99,36	96,97	93,32	86,69	79,06
CIRS	2mm/2%	85,05	81,5	91,72	89,16	97,66	97,09	88,25	82,93	67,29	59,28
	3mm/3%	96	95,91	93,98	95,52	99,83	99,27	96,43	92,34	86,72	76,6

phantom CIRS Thorax, with its long axis parallel to the beam central axis (CAX) were placed on top of 3 cm water equivalent RW3 plastic plates (PTW, Freiburg, Germany). The RW3 plates assure that the dose on the detector would not be affected by transitions between different media and potential lack of dose build-up. Different thicknesses of CIRS Thorax phantom, *e.g.* 5, 10 and 15 cm (Figure 1B) respectively, were used to verify the influence of inhomogeneities on measured dose distributions. Dose distribution using CIRS Thorax phantom with long axis of the phantom perpendicular to CAX ('clinical position') was also investigated (Figure 1C). RW3 plates were not used in this measuring arrangement since there was enough tissue equivalent material in front of the detector. Investigation was also performed on three 'anatomical parts' of interest (head&neck, thorax and pelvic) of anthropomorphic phantom in 'clinical position' (Figures 1D, E). Here, build-up material (RW3 plates) was also used due to large 'air gaps' between the phantom and the detector, to ensure consistency of dose measurement.

Dose calculations were performed using Monaco 5.11.02 TPS utilizing D_w and D_m reporting modes. Different dose distributions were calculated for different phantom geometries and configurations (Figure 2), having beams directed vertically to the measuring plane. Beam geometries ranged from simple square (reference) field (15×15 cm^2) to clinical IMRT plans of various complexities considering fluence maps modulation degrees: 1.25, 1.65, 2.25 and 3.65 respectively, which is in accordance with

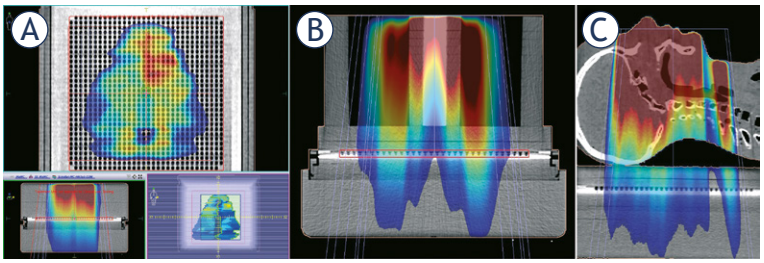

FIGURE 2. Calculated dose distributions for IMRT4 plan on homogeneous **(A)**, CIRS phantom with long axis parallel to the beam axis **(B)** and H&N part of ART phantom **(C)**.

number of segments (23, 40, 76 and 105 segments, respectively). To achieve an appropriate level of dose calculation accuracy and consistency, dose distributions were calculated with 0.2 cm grid size, 0.5% statistical uncertainty, and „per control point" calculation mode. Sequencing parameters were as follows: minimum segment area: 4 cm^2, minimum segment width: 1.5 cm, fluence smoothing: medium, minimum MU/segment: 2, maximum number of segments per plan: 110.

Results

Results of gamma analysis in the homogeneous phantom and different combinations of the semi-anthropomorphic phantom for various levels of plan complexity as well as different reporting modes are presented in Table 1 and Figure 3. The results for 3%/3mm and 2%/2mm criteria are shown in tables. Due to clarity, only the results

TABLE 2. Results of gamma analysis for measured and calculated dose distributions in the thorax, pelvic and head and neck parts of Alderson phantom for different levels of plan complexity and different reporting modes

phantom	gamma criteria	15x15		IMRT1		IMRT2		IMRT3		IMRT4	
		% points passing with gamma<1									
		D_w	D_m	D_w	D_m	D_w	D_m	D_w	D_m	D_w	D_m
Thorax Alderson	2mm/2%	86,39	86,18	97,6	96,79	95,02	94,2	86,3	84,59	75,44	73,62
	3mm/3%	94,24	96,19	99,26	98,89	97,6	97,07	94,07	93,19	93,57	90,8
Pelvic Alderson	2mm/2%	92,05	95,75	99,15	98,16	97,05	94,61	90,85	89,47	78,48	76,33
	3mm/3%	99,19	99,82	99,99	99,65	99,5	98,57	97,85	95,72	93,93	92,99
H&N Alderson	2mm/2%	91,59	91,82	98,14	97,65	95,96	94,83	95,45	94,1	83,51	79,86
	3mm/3%	97,2	98,01	99,65	99,53	99,12	98,14	98,82	98,34	94,73	93,03

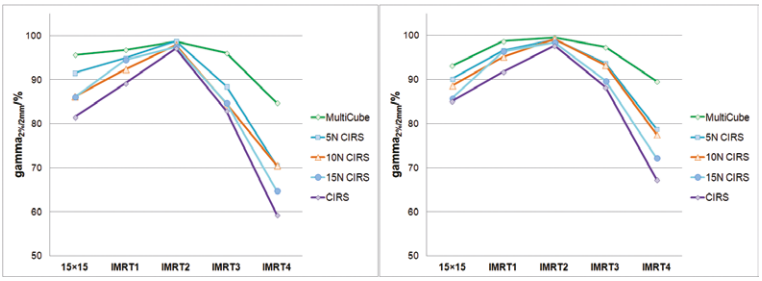

FIGURE 3. Gamma analysis with 2%/2mm criteria for dose-to-media (left) and dose-to-water (right) reporting modes related to the complexity of the particular plan, measured over homogeneous phantom and various set-ups of the semi-anthropomorphic phantom.

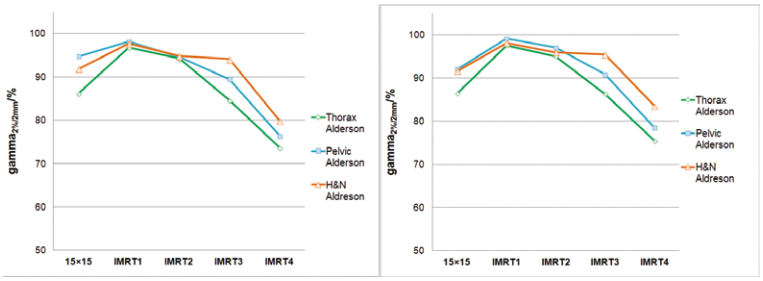

FIGURE 4. Gamma analysis with 2%/2mm criteria for dose-to-media (left) and dose-to-water (right) reporting modes related to plan complexity, measured over different parts of the anthropomorphic phantom.

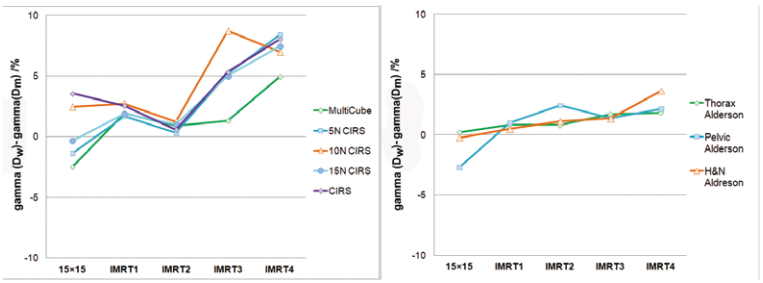

FIGURE 5. Gamma passing rate differences using 2%/2mm criteria between reporting modes related to plan complexity and phantom acquired over homogeneous phantom and different set-ups of the semi-anthropomorphic phantom (left) and different parts of the anthropomorphic phantom (right).

for 2%/2mm criteria were shown graphically. Percentage of points passing with gamma<1 for 3%/3mm criteria of the IMRT plans degrade depending on the thickness of non-water equivalent material up to 12% and up to 19% for dose-to-water and dose-to-media reporting mode, respectively. It also degrades for the most complex IMRT plan.

Percentage of points passing with gamma<1, when using 2%/2mm criteria, degrade depending on the level of complexity of plans, up to 30% for dose-to-water and up to 37% for dose-to-media reporting mode, for CIRS Thorax phantom in the patient position.

Results for anthropomorphic phantom are presented in Table 2 and Figure 4.

Considering more realistic situations in anthropomorphic phantom, gamma passing rates, when using 2%/2mm criteria, degrade depending on the level of complexity of plans, up to 22% for dose-to-water and up to 23% for dose-to-media reporting mode, both in ART Thorax (worst case scenario).

Percentage differences between gamma passing rates using 2%/2mm criteria of dose-to-water and dose-to-media reporting mode for different levels of plan complexity and different phantom set-ups are shown in Figure 5.

Discussion

The motivation for this work was related to a large number of very good gamma analysis results gathered while performing patient-specific dosimetry for IMRT clinical cases in a standard way using homogeneous phantom and 3%/3mm criteria. Obtained results were independent of dose reporting mode used. Thus, we were interested how the above-mentioned patient-specific dosimetry meth-

odology performs in a more realistic clinical situation.

From our results, it is evident that the gamma passing rate decreases with increasing plan complexity. It also depends on the level of inhomogeneity of the analysed region. Data in Table 1 shows that for the simplest case gamma passing rate (reference field and homogeneous phantom) is not as superior as expected in comparison to more complex plans and more complex measuring geometries. Further analysis of dose profiles shows that differences between calculated and measured values are insignificant at the exact positions of ionization chambers in the 2D detector. Nevertheless, in the regions of steep dose gradients, the interpolation between measuring points deteriorates passing rates when 2%/2mm criteria is used. These results, suggest that the resolution of the detector is one of the limiting factors of the analysis. Latter is less pronounced in complex multiple field geometries due to an averaging effect.

Comparing the data for all set-ups of semi-anthropomorphic (Table 1 and Figure 3) and anthropomorphic phantoms (Table 2 and Figure 4) one can conclude that passing rates are higher in the anthropomorphic phantom. Such observation indicates that the TPS calculates real situation more accurately than the extreme ones when different inhomogeneities are separated (Figure 2B). Exceptions are the passing rates for the IMRT2 plan, which are extremely high in all set-ups of the semi-anthropomorphic phantom since all fields that form this plan are small enough to pass through only the homogeneous part of the phantom.

From Figure 5 one can see that gamma passing rate depends on the dose reporting mode used. The magnitude of these differences increases as plan complexity increases. It also depends on the heterogeneity of the region of interest. The influence of heterogeneity on gamma passing rate differences of reporting modes is less pronounced in the anthropomorphic phantom (-2.7% to 3.6%) than in the semi-anthropomorphic phantom (-2.5% to 8.7%). These results raise a question of possible limits of dose distribution verification in the assessment of plan delivery quality. Consequently, one has to bear in mind the fact that good results obtained using standard patient-specific dosimetry methodology do not guarantee the accuracy of delivered dose distribution in real clinical cases.

References

1. Reynaert N, Van der Marck S, Schaart D, Van der Zee W, Van Vliet-Vroegindeweij C, Tomsej M, et. al. Monte Carlo treatment planning for photon and electron beams. *Rad Phys Chem* 2007; **76:** 643-86. doi: 10.1016/j.radphyschem.2006.05.015
2. Andreo P. Dose to 'water-like' media or dose to tissue in MV photons radiotherapy treatment planning: still a matter of debate. *Phys Med Biol* 2015; **60:** 309-37. doi: 10.1088/0031-9155/60/1/309
3. Ma CM, Li J. Dose specification for radiation therapy: dose to water or dose to medium? *Phys Med Biol* 2011; **56:** 3073-89. doi: 10.1088/0031-9155/56/10/012
4. Huq MS, Fraass BA, Dunscombe PB, Gibbons Jr. JP, Ibbott GS, Mundt AJ, et al. The report of Task Group 100 of the AAPM: Application of risk analysis methods to radiation therapy quality management. *Med Phys* 2016; **43:** 4209-62. doi: 10.1118/1.4947547
5. IAEA, International Atomic Energy Agency. *Commissioning of radiotherapy treatment planning systems: testing for typical external beam treatment techniques.* IAEA -TECDOC-1583. Vienna: IAEA; 2008.
6. Kry SF, Alvarez P, Molineu A, Amador C, Galvin J, Followill DS. Algorithms used in heterogeneous dose calculations show systematic differences as measured with the radiological Physics Center's anthropomorphic thorax phantom used for RTOG credentialing. *Int J Radiat Oncol Biol Phys* 2013; **85:** e95-e100. doi: 10.1016/j.ijrobp.2012.08.039
7. Walters BRB, Kramer R and Kawrakow I. Dose to medium versus dose to water as an estimator of dose to sensitive skeletal tissue. *Phys Med Biol* 2010; **55:** 4535-46. doi: 10.1088/0031-9155/55/16/S08
8. Chetty IJ, Curran B, Cygler JE, DeMarco JJ, Ezzell G, Faddegon BA, et al. Report of the AAPM Task Group No. 105: Issues associated with clinical implementation of Monte Carlo-based photon and electron external beam treatment planning. *Med Phys* 2007; **34:** 4818-53. doi: 10.1118/1.2795842
9. Dogan N, Siebers JV and Keall PJ. Clinical comparison of head and neck and prostate IMRT plans using absorbed dose to medium and absorbed dose to water. *Phys Med Biol* 2006; **51:** 4967-80. doi: 10.1088/0031-9155/51/19/015
10. Jurkovic S, Zauhar G, Faj D, Radojcic Smilovic Đ, Svabic M, Kasabasic M, Diklic A. Dosimetric verification of compensated beams using radiographic film. *Radiol Oncol* 2011; **45:** 310-4. doi: 10.2478/v10019-011-0020-9
11. Niroomand-Rad A, Blackwell CR, Coursey BM, Gall KP, Galvin JM, McLaughlin WL, et al. Radiochromic film dosimetry: Recommendations of AAPM Radiation Therapy Committee Task Group 55. *Med Phys* 1998; **25:** 2093-115. doi: 10.1118/1.598407
12. Low DA. Gamma dose distribution evaluation tool. *J Phys Conf Ser* 2010; **250(1):** 012071. doi:10.1088/1742-6596/250/1/012071
13. Son J, Baek T, Lee B, Shin D, Park SY, Park J, et al. Comparison of the quality assurance of four dosimetric tools for intensity modulated radiation therapy. *Radiol Oncol* 2015; **49:** 307-13. doi: 10.1515/raon-2015-0021
14. Code of practice for the quality assurance and control for intensity modulated radiotherapy. Netherlands commission of radiation dosimetry 2013.
15. Low DA, Moran JM, Dempsy JF, Dong L, Oldham M. Dosimetry tools and techniques for IMRT. *Med Phys* 2011; **38:** 1313-38. doi: 10.1118/1.3514120
16. Klein EE, Hanley J, Bayouth J, Yin FF, Simon W, Dresser S, et al. Task Group 142 report: Quality assurance of medical accelerators. *Med Phys* 2009; **36:** 4197-212. doi: 10.1118/1.3190392
17. Ezzell GA, Burmeister JW, Dogan N, LoSasso TJ, Mechalakos JG, Mihailidis D, et al. IMRT commissioning: multiple institution planning and dosimetry comparisons, a report from AAPM Task Group 119. *Med Phys* 2009; **36:** 5359-73. doi: 10.1118/1.3238104
18. Technical report series No. 430: Commissioning and quality assurance of computerised planning system for radiation treatment of cancer. International Atomic Energy Agency: IAEA 2004.
19. Gershkevitsh E, Schmidt R, Velez G, Miller D, Korf E, Yip F, et al. Dosimetric verification of radiotherapy treatment planning systems: Results of IAEA pilot study. *Radiother Oncol* 2008; **89:** 338-46. doi: 10.1016/j.radonc.2008.07.007

20. Gershkevitsh E, Pesznyak C, Petrovic B, Grezdo J, Chelminski K, do Carmo Lopes M, et al. Dosimetric inter-institutional comparison in European radiotherapy centres: Results of IAEA supported treatment planning system audit. *Acta Oncol* 2014; **53:** 628-36. doi: 10.3109/0284186X.2013.840742

21. Jurković S, Švabić M, Diklić A, Smilović Radojčić Đ, Dundara D, Kasabašić M, et al. Reinforcing of QA/QC programs in radiotherapy departments in Croatia: Results of treatment planning system verification. *Med Dosim* 2013; **38:** 100-4. doi: 10.1016/j.meddos.2012.07.008

Radiol Oncol 2018; 52(3): 233-244.
doi: 10.2478/raon-2018-0026

Odvisnost stranskih učinkov dopolnilne radioterapije dojke in obsevalnih načrtov od velikosti tarčnih volumnov

Ratoša I, Jenko A, Oblak I

Izhodišča. Obsevanje je sestavni del zdravljenja po ohranitveni operaciji raka dojk. Eden izmed pomembnih dejavnikov, ki vplivajo na končni izgled dojke po obsevanju, je velikost obsevanega volumna dojke. Namen našega prispevka je pregled raziskav glede neželenih učinkov dopolnilnega obsevanja in ocena obsevalnih načrtov v odvisnosti od velikosti tarčnega volumna.

Zaključki. Višji odstotek takojšnih neželenih učinkov obsevanja in slabši končni izgled dojke je povezan z večjim obsevanim volumnom, neenakomerno prerazporeditvijo predpisane doze in presežkom doze v tarčnem volumnu. Omenjeno ugotavljamo tako pri konvencionalnem obsevanju kot pri hipofrakcionacijskih obsevalnih režimih. Izboljšanje dozne homogenosti lahko dosežemo s tri-dimenzionalno ali intenzitetno modulirano obsevalno tehniko, kar potrjeno vodi v nižje stopnje neželenih učinkov. Raziskovalci predvidevajo, da obstaja povezava med obliko telesa in višjo dozo na prileţna pljuča in srce pri bolnicah z rakom leve doke. Premišljeno predpisovanje doze, delno obsevanje dojke in sodobne tehnike obsevanja, kot so obsevanje v globokem vdihu, obsevanje v bočnem položaju ali na trebuhu ter uporaba termoplastičnega nedrčka lahko pri izbranih bolnicah zmanjša neželene učinke obsevanja.

Radiol Oncol 2018; 52(3): 245-249.
doi: 10.2478/raon-2018-0033

Dinamika z računalniško tomografijo vidnega plevralnega izliva pri bolnikih s pljučnim infarktom

Kocijančič I, Vidmar J, Kastelic M

Izhodišča. Plevralni izliv je pri bolnikih s pljučno embolijo in hkratnim pljučnim infarktom pretežno neraziskano področje. Namen naše raziskave je bil preučiti povezavo med velikostjo pljučnega infarkta in plevralnim izlivom ter opredeliti časovni potek oz. dinamiko izliva pri bolnikih s pljučnim infarktom.

Bolniki in metode. V retrospektivno analizo smo vključili 103 bolnike. Pri analizi smo upoštevali podatke o komorbidnosti, velikosti pljučnega infarkta, prisotnosti in velikosti plevralnega izliva ter podatke o času med začetkom kliničnih simptomov pljučnega infarkta in preiskavo z računalniško tomografijo.

Rezultati. Analiza možnih povezav med velikostjo pljučnega infarkta in starostjo je pokazala statistično značilno negativno korelacijo. Ugotovili smo tudi statistično močno značilno razliko ($p = 0,005$) v povprečni velikosti pljučnega infarkta pri bolnikih z izlivom (34,5 cm^3) v primerjavi s tistimi brez izliva (14,3 cm^3), vendar sama velikost izliva ni korelirala z velikostjo pljučnega infarkta. Velikost izliva je bila največja 4–5 dni po začetku kliničnih simptomov pljučnega infarkta. V prvih 5 dneh po začetku simptomov smo ugotovili statistično značilno korelacijo med časom in velikostjo izliva s pričakovanim povečanjem izliva približno 1,3 mm/12 h.

Zaključki. Podatki raziskave kažejo, da je pri bolnikih s plevralnim izlivom večja verjetnost, da bodo imeli večji pljučni infarkt kot pri tistih brez izliva. Če je izliv prisoten, lahko pričakujemo, da se bo v prvih 5 dneh po začetku kliničnih simptomov pljučnega infarkta relativno počasi in linearno večal.

Radiol Oncol 2018; 52(3): 250-256.
doi: 10.2478/raon-2018-0032

Tridimenzionalno ultrazvočno vrednotenje lege jezika in njen vpliv na artikulacijske motnje pri predšolskih otrocih z odprtim grizom sekalcev

Lah Kravanja S, Hočevar-Boltežar I, Marolt Mušič M, Jarc A, Verdenik I, Ovsenik M

Izhodišča. Lega jezika ima pomembno vlogo v etiologiji odprtega griza sekalcev (AOB) in artikulacijskih motenj ter je ključnega pomena za načrtovanje zdravljenja AOB in stabilnosti po zdravljenju. Klinično vrednotenje lege jezika je pri otrocih nezanesljivo zaradi anatomskih omejitev. Cilj raziskave je bil predstaviti uporabo tridimenzionalnega (3D) ultrazvoka v funkcionalni diagnostiki vrednotenja lege jezike v primerjavi s kliničnim ortodontskim in otorinolaringološkim pregledom ter povezavo med nepravilno lego jezika, otorinolaringološkimi značilnostmi in artikulacijskimi motnjami pri predšolskih otrocih z AOB.

Pacienti in metode. V presečno raziskavo smo vključili 446 otrok, starih od 3–7 let, 236 dečkov in 210 deklic, ki jih je pregledal ortodont, da bi ugotovil pojavnost AOB in artikulacijskih motenj. AOB je imelo 32 otrok. Kontrolno skupino je sestavljalo 43 otrok, naključno izbranih izmed otrok z normalno okluzijo. Funkcionalne in otorinolaringološke odklone, razvade in artikulacijske motnje v skupini z AOB in v kontrolni skupini so ocenile specialistki ortodontije in otorinolaringologije ter logopedinja. Lego jezika je ovrednotila tudi radiologinja s pomočjo 3D ultrazvoka. Primerjali smo 3D ultrazvočno ovrednotenje lege jezika s kliničnim ovrednotenjem specialistk ortodontije in otorinolaringologije.

Rezultati. Pojavnost AOB je bila 7,2%. Skupini AOB in kontrolna skupina sta se značilno razlikovali glede nepravilne lege jezika ($p < 0,001$) in glede motenj artikulacije ($p < 0,001$). Pri otrocih brez artikulacijskih motenj iz obeh skupin je bila nepravilna lega jezika ugotovljena manj pogosto kot pri otrocih z artikulacijskimi motnjami ($p < 0,001$). Po starostni prilagoditvi je statistični regresijski model pokazal, da je pri otrocih z nepravilno lego jezika večja verjetnost za prisotnost AOB (OR 14,63; $p < 0,001$) kot pri drugih. Ko smo artikulacijske motnje vključili v model, je verjetnost za AOB postala neznačilna ($p = 0,177$). Med nepravilno lego jezika in artikulacijskimi motnjami je močna povezanost ($p = 0,002$). 3D ultrazvok je odkril največje število otrok z nepravilno lego jezika, čeprav med 3D ultrazvočnim in kliničnim ovrednotenjem, ki sta ju opravili specialistki ortodontije in otorinolaringologije, ni bilo statistično značilne razlike.

Zaključki. 3D ultrazvok je objektivna, zanesljiva, neinvazivna metoda za vrednotenje lege jezika pri majhnih otrocih v obdobju rasti in razvoja, ki bi lahko v prihodnje postala pomemben sestavni del funkcionalne diagnostike v ortodontiji, otorinolaringologiji in radiologiji.

Radiol Oncol 2018; 52(3): 257-262.
doi: 10.2478/raon-2018-0027

Pojavnost papilarnega raka ščitnice pri bolnikih s subakutnim tiroiditisom je večja kot smo predvidevali. Retrospektivna analiza 137 bolnikov

Gül N, Üzüm AK, Selçukbiricik ÖS, Yegen G, Tanakol R, Aral F

Izhodišča. Pri bolnikih s subakutnim tiroiditisom redko najdemo papilarni rak. V raziskavi smo želeli ugotoviti razširjenost diferenciranega ščitničnega raka v kohorti bolnikov s subakutnim tiroiditisom.

Bolniki in metode. Retrospektivno smo pregledali podatke ambulantnih bolnikov Oddelka za endokrinologije in metabolizma s subakutnim tiroiditisom v zadnjih dvajsetih letih. Iz pregledanih podatkov smo izbrali bolnike s ščitničnimi nodusi in sumljivimi ultrazvočnimi ugotovitvami, pri katerih je bila narejena aspiracijska biopsija s tanko iglo ali pa so bili operirani, ker je obstajal sum za raka ščitnice.

Rezultati. Našli smo 137 bolnikov (100 žensk in 37 moških) z zanesljivimi podatki za potrditev diagnoze subakutni tiroiditis. Povprečna starost bolnic je bila 41,1 ± 9,1 (med 20 in 64 let) in bolnikov 43,0 ± 9,3 (od 20 do 65 let). Na začetku ali med sledenjem bolnikom je bila ena ali več biopsij s tanko iglo narejena pri 23 (16,8 %) bolnikih. Operiranih je bilo 7 bolnikov s sumljivimi ugotovitvami biopsije s tanko iglo, pri šestih bolnikih (4,4 %) je histopatološki pregled ščitničnih nodusov potrdil diagnozo papilarni rak ščitnice.

Zaključki. Ugotovitve kažejo na relativno večjo razširjenost raka ščitnice v majhni seriji bolnikov s subakutnim tiroiditismo, kot smo predvidevali. Potrebne bodo nadaljnje raziskave za ugotavljanje resnične frekvence diferenciranega ščitničnega raka in njegove povezanosti z vnetno patogenezo subakutnega tiroiditisa. Ugotovitve so v skladu z vse večjo pojavnostjo raka ščitnice v svetu. Pri vseh bolnikih s sumljivimi ščitničnimi nodusi ob ustreznih kliničnih in vnetnih parametrih priporočamo ponovitev ultrazvočne analize ter biopsijo s tanko iglo.

Radiol Oncol 2018; 52(3): 263-266.
doi: 10.2478/raon-2018-0031

Epidemiologija ustnih sluzničnih lezij v Sloveniji

Kansky AA, Didanović V, Dovšak T, Lončar Brzak B, Pelivan I, Terlevič D

Izhodišča. Med boleznimi ustne sluznice so maligni tumorji najnevarnejše, vendar ne tudi najpogostejše lezije. Ker je večina raziskav usmerjenih v raka ustne votline, smo se namenili ugotoviti pogostnost benignih sprememb ustne sluznice v Slovenski populaciji. Lezije ustne sluznice so pomemben indikator ustnega zdravja in kakovosti življenja, še posebej v starosti. Prevalenca lezij ustne sluznice, skupaj s podatki o tveganih navadah, povezanih z ustnim zdravjem, kot je uporaba tobaka in alkohola, lahko pomaga pri načrtovanju raziskav na področju ustnega zdravja in presejalnih programov.

Bolniki in metode. V Sloveniji smo v okviru projekta presejanja za raka ustne votline spomladi 2017 izvedli raziskavo o sluzničnih lezijah v ustih, v kateri je sodelovalo preko 50 % zobozdravnikov in smo vanjo vključili 2395 bolnikov (904 moških in 1491 žensk).

Rezultati. Klinični pregled, ki smo ga opravili v skladu s standardi Svetovne zdravstvene organizacije, je pokazal lezije ustne sluznice pri 645 bolnikih (27 %). Deset najpogosteje ugotovljenih lezij so bile: fibromi, gingivitis, Fordyce-jeve pege, obložen jezik, ugrizi sluznice lic, bela črta, stomatitis zaradi proteze, razbrazdan jezik, ponavljajoče se aftozne ulceracije in *lichen planus*.

Zaključki. Zbrani epidemiološki podatki kažejo na potrebo po specifičnih zdravstvenih politikah za preventivo, diagnostiko in zdravljenje sluzničnih lezij v ustih.

Radiol Oncol 2018; 52(3): 267-274.
doi: 10.2478/raon-2018-0028

Uvodna kemoterapija, kemoradioterapija in konsolidacijska kemoterapija pri zdravljenju raka danke. Dolgoročni rezultati zdravljenja v klinični raziskavi *OIGIT-01 raziskava*

Golo D, But-Hadžić J, Anderluh F, Brecelj E, Edhemović I, Jeromen A, Omejc M, Oblak I, Sečerov-Ermenc A, Velenik V

Izhodišča. Namen raziskave je bil izboljšati učinkovitost zdravljenja lokalno napredovalega raka danke z enim krogom uvodne in dvema krogoma konsolidacijske kemoterapije. Primarni cilj raziskave je bil ugotoviti stopnjo popolnega patološkega odgovora na zdravljenje.

Bolniki in metode. Med oktobrom 2011 in aprilom 2013 smo 66 bolnikov z lokalno napredovalim rakom danke zdravili z uvodnim krogom kemoterapije, ki ji je sledila kemoradioterapija (KT/RT), dva konsolidacijska kroga kemoterapije, operacija in 3 krogi adjuvantne kemoterapije s kapecitabinom. Obsevalna doza je bila 50,4 Gy za tumorje T2–3 in 54 Gy za tumorje T4 v dnevnih odmerkih po 1,8 Gy. Odmerek sočasnega kapecitabina je znašal 825 mg/m²/12 ur, neo/adjuvantnega pa 1250 mg/m²/12 ur.

Rezultati. Triinštirideset (65,1 %) bolnikov je prejelo zdravljenje po protokolu. Skladnost z načrtovano uvodno, konsolidacijsko in adjuvantno kemoterapijo je bila 98,5 %, 92 % in 87,3 %. Kemoradioterapijo je zaključilo 65/66 bolnikov z 13.6 % G ≥ 3 ne-hematološko toksičnostjo. Stopnja patološkega popolnega odgovora (17,5 %) sicer ni bila statistično značilno boljša, ugotovili pa smo precejšnje znižanje odstotka prizadetih bezgavk (77,7 %) in celokupnega stadija (79,3 %). V srednjem času sledenja 55 mesecev smo zabeležili en lokalni recidiv (1,6 %). Petletno preživetje brez bolezni je bilo 64,0 % (95 % interval zaupanja [CI] 63,89–64,11), celokupno preživetje pa 69,5 % (95 % CI 69,39–69,61).

Zaključki. Okrepitev predoperativnega zdravljenja lokalno napredovalega raka danke z dodatno kemoterapijo s kapecitabinom pred in po kemoradioterapiji je spremljala sprejemljiva toksičnost, bolniki so jo dobro prenašali in večina je tudi zaključila zdravljenje po protokolu. S takšnim načinom zdravljenja nismo uspeli zvišati odstotek popolnega patološkega odgovora, dosegli pa smo dobro lokalno kontrolo bolezni, preživetje brez bolezni in celokupno preživetje.

Radiol Oncol 2018; 52(3): 275-280.
doi: 10.2478/raon-2018-0012

Ali je obsevanje po mastektomiji res potrebno pri bolnicah z rakom dojk in s številnimi pozitivnimi pazdušnimi bezgavkami?

Marinko T, Stanič K

Izhodišča. Obsevanje po mastektomiji izboljša preživetje z odstranitvijo morebitnih okultnih lezij v steni prsnega koša in limfnega drenažnega področja. Metaanaliza je pokazala, da obsevanje po mastektomiji zmanjšuje smrtnost in lokalno ponovitev bolezni pri bolnicah z rakom dojk, pri katerih smo ugotovili pozitivne pazdušne bezgavke. Nimamo pa podatkov o učinkovitosti obsevanje po mastektomiji v podskupini bolnic z velikim številom pozitivnih pazdušnih bezgavk. Namen raziskave je bil analizirati vpliv števila pozitivnih pazdušnih bezgavk na lokalno ponovitev bolezni ter na oddaljene metastaze, celokupno preživetje in preživetje brez oddaljenih metastaz pri bolnicah, ki smo jih zdravili z obsevanjem po mastektomiji.

Bolniki in metode. Pregledali smo medicinsko dokumentacijo 129 zaporednih bolnic z rakom dojk, ki smo jih zdravili na Onkološkem inštitutu Ljubljana z obsevanjem po mastektomiji med januarjem 2003 in decembrom 2004. Bolnice smo združili v skupine glede na število pozitivnih pazdušnih bezgavk: skupina 1 z manj kot 15 bezgavkami in skupina 2 z več kot 15 bezgavkami. Vse bolnice smo dopolnilno sistemsko zdravili v skladu s kliničnimi smernicami. Analizirali smo število lokoregionalnih ponovitev bolezni, oddaljenih metastaz, celokupno preživetje, preživetje brez napredovanja bolezni in preživetje brez oddaljenih metastaz.

Rezultati. Po srednjem času spremljanja 11,5 let je analiza preživetja po Kaplan-Meier-ju pokazala znatno krajše celokupno preživetje ($p = 0,006$), krajše preživetje brez napredovanja bolezni ($p = 0,002$) in krajše preživetje brez oddaljenih metastaz ($p < 0,001$) v skupini bolnic, ki so imele več kot 15 pozitivnih pazdušnih bezgavk. V skupini bolnic z več kot 15 pozitivnimi pazdušnimi bezgavkami smo ugotovili le eno lokoregionalno ponovitev bolezni. V multivariatni analizi je več kot 15 pozitivnih pazdušnih bezgavk in kemoterapevtsko zdravljenje z antraciklini statistično pomembno vplivalo na celokupno preživetje in preživetje brez oddaljenih metastaz. Prisotnost več kot 15 pozitivnih pazdušnih bezgavk je bil edini neodvisni dejavnik krajšega preživetja brez napredovanja bolezni.

Zaključki. Bolnice z več kot 15 pozitivnimi pazdušnimi bezgavkami imajo krajše preživetje brez oddaljenih metastaz, preživetje brez napredovanja bolezni in celokupno preživetje v primerjavi z bolnicami z manj kot 15 pozitivnimi pazdušnimi bezgavkami, čeprav prejmejo enako lokoregionalno zdravljenje. Za nadaljnje vrednotenje naših ugotovitev je potrebnih več raziskav z večjim številom vključenih bolnikov.

Radiol Oncol 2018; 52(3): 281-288.
doi: 10.2478/raon-2018-0009

Dolgotrajno preživetje bolnikov z lokalno napredovalim nedrobnoceličnim rakom pljuč III. stadija, ki smo jih zdravili s kemoradioterapijo in možnost zdravljenja z imunoterapijo

Vrankar M, Stanič K

Izhodišča. Standardno zdravljenje bolnikov z neoperabilnim lokalno napredovalim nedrobnoceličnim rakom pljuč (NDRP) je sočasna kemoradioterapija. Petletno preživetje je 15–25 %, o rezultatih dolgotrajnega preživetja pa redko poročajo.

Bolniki in metode. V analizo dolgotrajnega preživetja smo vključili 102 bolnikov z nedrobnoceličnim rakom pljuč v III. stadiju, ki smo jih med septembrom 2005 in novembrom 2010 zdravili z uvodno kemoterapijo in sočasno kemoradioterapijo. Vse bolnike smo testirali na status PD-L1 ter primerjali celokupno preživetje, preživetje brez znakov bolezni in toksičnost glede na izraženost PD-L1.

Rezultati. Srednji čas celokupnega preživetja pri vseh bolnikih je bil 24,8 mesecev (95 % interval zaupanja [CI] 18,7–31,0) z 10-letnim preživetjem 11,2 %. Srednji čas celokupnega preživetja pri bolnikih z izraženim PD-L1 je bil 12,1 meseca (95% CI 0,1–26,2), brez izraženosti PD-L1 ali neznanim statusom PD-L1 statusom pa je bilo značilno daljše, 25,2 meseca (95% CI 18,9–31,6), $p = 0,005$. Srednji čas preživetja vseh bolnikov brez znakov bolezni je bil 16,4 meseca (95% CI 13,0–19,9). Srednji čas preživetja brez znakov bolezni pri bolnikih z PD-L1 izraženostjo je bil 10,1 meseca (95% CI 0,1–20,4), pri bolnikih brez izraženosti ali neznanim statusom PD-L1 pa 17,9 meseca (95% CI 14,2–21,7), $p = 0,003$.

Zaključki. 10-letno preživetje bolnikov z nedrobnoceličnim rakom pljuč III. stadija po kemoradioterapiji je 11,2 %. Čas preživetja brez znakov bolezni in celokupno preživetje je različno glede na status PD-L1, značilno krajše je za bolnike z izraženostjo PD-L1. Novo zdravljenje z inhibitorji kontrolnih točk v kombinaciji z obsevanjem se nakazuje kot obetavna strategija za izboljšanje teh rezultatov.

Radiol Oncol 2018; 52(3): 289-295.
doi: 10.2478/raon-2018-0017

Pogostost mutacij BRAF, NRAS in c-KIT med slovenskimi bolniki z napredovalim melanomom

Ebert Moltara M, Novaković S, Boc M, Bučić M, Reberšek M, Zadnik V, Ocvirk J

Izhodišča. Na odločitev o vrsti zdravljenja bolnikov z napredovalim melanomom lahko pomembno vpliva status mutacij v genih za BRAF, NRAS in c-KIT. Pogostost mutacij in njihove medsebojne povezave s histološkimi značilnostmi tumorskih tkiv na slovenski populaciji do sedaj še niso bili raziskani.

Bolniki in metode. Analizo smo izvedli retrospektivno. Mutacije BRAF, NRAS in c-KIT smo določili na 230 patoloških vzorcih bolnikov, ki smo jih nameravali zdraviti s sistemsko terapijo zaradi metastatskega melanoma na Onkološkem Inštitutu Ljubljana med leti 2013 in 2016. Zbrali smo histološke značilnosti primarnih tumorjev in klinične podatke bolnikov ter jih testirali na medsebojno povezanost z mutacijskim statusom.

Rezultati. Povprečna starost 230 bolnikov je bila 59 let (razpon 25–85). Moških je bilo 141 (61,3 %) in žensk 89 (38,7 %). Ugotovili smo 129 (56,1 %) mutacij BRAF, 31 (13,5 %) NRAS in 3 (1,3 %) c-KIT mutacij v tkivnih vzorcih. Med 129 bolniki z mutacijami BRAF je imelo 114 (88,4 %) bolnikov mutacijo V600E in 15 (11,6 %) mutacijo V600K. Bolniki z BRAF mutacijami so bili ob diagnozi mlajši (52 v primerjavi s 59 let, $p < 0,05$), bolniki z NRAS mutacijami starejši (61 v primerjavi s 55 leti, $p < 0,05$). Število mutacij c-KIT je bilo prenizko za smiselno testiranje na medsebojne povezanosti, je pa bil eden izmed treh melanomov s c-KIT mutacijo melanom sluznice.

Zaključki. Rezultati analize so v skupini slovenskih bolnikov z metastatskim melanomom odkrili visok delež mutacij BRAF ter nizek delež mutacij NRAS in c-KIT v primerjavi s predhodno objavljenimi raziskavami v Evropi in Severni Ameriki. Eden od glavnih vzrokov so specifične značilnosti naše študijske populacije, ki niso bile enake kot značilnosti celotne populacije bolnikov z melanomom.

Radiol Oncol 2018; 52(3): 296-306.
doi: 10.2478/raon-2018-0034

Farmakogenomski označevalci odgovora na zdravljenje z glukokortikoidi ob začetku remisije po indukcijskem zdravljenju pri otrocih z akutno limfoblastno levkemijo

Gašić V, Zukić B, Stanković B, Janić D, Dokmanović L, Lazić J, Krstovski N, Dolžan V, Jazbec J, Pavlović S, Kotur N

Izhodišča. Odgovor na monoterapijo z glukokortikoidi ob začetku remisije po indukcijskem zdravljenju pri otrocih z akutno limfoblastno levkemijo (ALL) predstavlja pomemben napovedni dejavnik glede napovedi poteka bolezni in izida zdravljenja. Namen raziskave je bil preučiti genetske spremembe v nekaterih farmakogenih (*NR3C1*, *GST* in *ABCB1*), ki bi lahko prispevali k bolj bolniku prilagojenemu in bolj učinkovitemu zdravljenju z glukokortikoidi.

Bolniki in metode. V retrospektivni raziskavi smo pri 122 otrocih z ALL opravili analizo genetskih sprememb *NR3C1* (rs33389, rs33388 in rs6198), *GSTT1* (nični genotip), *GSTM1* (nični genotip), *GSTP1* (rs1695 in rs1138272) in *ABCB1* (rs1128503, rs2032582 in rs1045642) s postopki, ki temeljijo na polimerazni verižni reakciji (PCR). Pokazatelj odgovora na zdravljenje z glukokortikoidi je bil število blastov na mikroliter periferne krvi osmi dan zdravljenja. Pri analizi smo kot mejne vrednosti za odgovor na glukokortikoide upoštevali 1000 (glede na protokol Berlin-Frankfurt-Münster [BFM]), kot tudi 100 ali 0 blastov na mikroliter.

Rezultati. Nosilci genotipa *NR3C1* rs6198 GG so pogosteje imeli več kot 1000 blastov kot bolniki brez tega genotipa ($p = 0,030$). Haplotip *NR3C1* CAA (rs33389-rs33388-rs6198) je bil značilno povezan s številom blastov pod 1000 ($p = 0,030$). Nosilci haplotipa *GSTP1* GC so imeli pogosteje število blastov pod 1000 ($p = 0,036$), pod 100 ($p = 0,028$) ali pa 0 ($p = 0,054$), medtem ko so nosilci haplotipa *GSTP1* GT in alela rs1138272 T pogosteje imeli prisotne blaste ($p = 0,034$ in $p = 0,024$). Nosilci haplotipa *ABCB1* CGT (rs1128503-rs2032582-rs1045642) so pogosteje imeli prisotne blaste ($p = 0,018$).

Zaključki. Rezultati raziskave kažejo, da sta *NR3C1* rs6198 in haplotip *GSTP1* rs1695-rs1138272 najbolj obetavna farmakogenomska označevalca odgovora na zdravljenje z glukokortikoidi pri otrocih z ALL.

Radiol Oncol 2018; 52(3): 307-319.
doi: 10.2478/raon-2018-0030

Primerjava preživetij primarne razbremenilne operacije proti primarni preoperativni kemoterapiji pri napredovalem epitelijskem raku jajčnikov visoke stopnje malignosti

Kobal B, Noventa M, Cvjetičanin B, Barbič M, Meglič L, Herzog M, Bordi G, Vitagliano A, Saccardi C, Škof E

Izhodišča. Namen raziskave je bil analizirati celokupno preživetje in preživetje brez napredovanja bolezni pri bolnicah z napredovalim, epitelijskim raku ovarijev visoke stopnje malignosti, ki smo jih zdravili v terciarnem ginekološko-onkološkem centru in smo jih sledili najmanj 60 mesecev. Primerjali smo primarno citoredukcijsko operacijo z intervalno citoredukcijsko operacijo po zaključeni neoadjuvantni kemoterapiji. Podatke smo stratificirali glede na pooperativni ostanek bolezni z namenom opredelitve vloge in pomena laparoskopije za oceno operabilnosti.

Bolniki in metode. V to observacijsko, retrospektivno raziskavo smo vključili bolnice, ki so bile zdravljene zaradi napredovalega (FIGO stadij III/IV) epitelijskega raka ovarijev visoke stopnje malignosti med januarjem 2008 in majem 2012. Vključili smo samo bolnice, ki smo jih sledili najmanj 60 mesecev. Primarni cilj raziskave je bila primerjava celokupnega preživetja in preživetja brez napredovanja bolezni med zdravljenjem s primarno citoredukcijsko operacijo in intervalno citoredukcijsko operacijo po zaključeni neoadjuvantni kemoterapiji. Sekundarni cilj je bil primerjava preživetja brez napredovanja bolezni in celokupno preživetje glede na pooperativni ostanek pri primarni citoredukcijski operaciji in pri intervalni citoredukcijski operaciji. S pomočjo Coxovega modela smo testirali napovedno vrednost različnih spremenljivk za napoved celokupnega preživetja: starost bolnic ob diagnozi, pooperativni ostanek bolezni po operaciji, ocena stanja po Ameriškem združenju za anestezijo (ASA), število krogov adjuvante kemoterapije.

Rezultati. Analizirali smo 157 bolnic. Med skupinama s primarno citoredukcijsko operacijo (108 bolnic) in skupino z intervalno citoredukcijsko operacijo po zaključeni neoadjuvantni kemoterapiji (49 bolnic) nismo ugotovili značilne razlike v celokupnemu preživetju (41,3 proti 34,5 mesecev), niti v preživetju brez napredovanja bolezni (17,3 proti 18,3 mesecev). Glede na pooperativni ostanek bolezni ni bilo značilnih razlik v celokupnemu preživetju bolnic med intervalno citoredukcijsko operacijo brez pooperativnega ostanka bolezni in primarno citoredukcijsko operacijo brez oz. z < 1 cm pooperativnega ostanka bolezni. Prav tako ni bilo značilne razlike v preživetju brez napredovanja bolezni med bolnicami, ki so bile zdravljene z intervalno citoredukcijsko operacijo brez pooperativnega ostanka bolezni in primarno citoredukcijsko operacijo brez pooperativnega ostanka bolezni. Preživetje brez napredovanja bolezni pa je bilo značilno krajše pri bolnicah zdravljenih s primarno citoredukcijsko operacijo z <1 cm pooperativnega ostanka bolezni, v primerjavi z bolnicami brez pooperativnega ostanka bolezni po intervalni citoredukcijski operaciji. Skupina bolnic zdravljenih s primarno citoredukcijsko operacijo je imela značilno več resnih pooperativnih zapletov (gradus 3 in 4). Predoperativna diagnostična laparoskopija je bila značilno povezana s popolno citoredukcijo (operacijo brez pooperativnega ostanka bolezni).

Zaključki. Potrdili smo predhodne ugotovitve o ne-superiornosti intervalne citoredukcijske operacije v primerjavi s primarno citoredukcijsko operacijo pri zdravljenju napredovalega epitelijskega raka ovarijev, kljub temu da ima zdravljenje z intervalno citoredukcijsko operacijo značilno manj pooperativnih zapletov. Po drugi strani pa odločitev za intervalno citoredukcijsko operacijo na osnovi laparoskopske ocene operabilnosti podaljša preživetje brez napredovanja bolezni in ne skrajša celokupno preživetje v primerjavi z neoptimalno primarno citoredukcijsko operacijo.

Radiol Oncol 2018; 52(3): 320-328.
doi: 10.2478/raon-2018-0029

Perkutano povečanje doze na parametrije pri ženskah z napredovalim rakom materničnega vratu. Izvedljivost in učinkovitost v povezavi z dolgoročno kakovostjo življenja

Akbaba S, Oelmann-Avendano JT, Bostel T, Rief H, Nicolay NH, Debus J, Lindel K, Foerster R

Izhodišča. Analizirali smo dolgoročno kakovost življenja in napovedne dejavnike za kakovost življenja ter klinični izid pri bolnicah z napredovalim rakom materničnega vratu, ki smo jih zdravili s primarno radiokemoterapijo. Radioterapijo smo izvajali z zunanjim snopom z ali brez zaporednih ali simultano integriranih dodatkov doze na parametre, intrakavitarne brahiterapije in sočasne kemoterapije.

Bolniki in metode. Med leti 2008 in 2014 smo zdravili 83 žensk s primarno kemoradioterapijo. Izračunali smo preživetje vseh bolnic in ocenili napovedne dejavnike za preživetje v univariatni in multivariatni analizi. Kakovost življenja po zdravljenju smo ocenili pri 31 bolnicah po srednjem času treh let (razpon 2–8 let). Primerjali smo jo z objavljenimi normativnimi podatki in analizirali vpliv starosti, stadija tumorja, zdravljenja in opazovane akutne toksičnosti.

Rezultati. 36 bolnic (43,4 %) je umrlo, 18 (21,7 %) je imelo lokalno ponovitev in 24 (28,9 %) je imelo oddaljene zasevke. Dodatek doze na parametrije (p = 0,027) in sočasna kemoterapija (p = 0,041) sta bila v multivariatni analizi neodvisna napovedna dejavnika za celokupno preživetje. Natančneje, parametrični ekvivalent doze ob frakcijah 2-Gy (EQD2) > 50 Gy je bil povezan z izboljšanim celokupnega preživetja (p = 0,020), vendar EQD2 > 53 Gy ni izboljšal celokupnega preživetja (p = 0,194). Velikost tumorja je bil edini neodvisni napovedni dejavnik za lokalni nadzor bolezni (p = 0,034). Bezgavčni status (p = 0,038) in oddaljeni zasevki drugje kot v paraaortnih bezgavkah (p = 0,002) sta bila neodvisna napovedna dejavnika za preživetje brez napredovanja bolezni. Kvaliteta življenja je bila na splošno slabša kot pri referenčni populaciji. Starost je bila sorazmerna s simptomi menopavze (p = 0,003). Stopnji akutne gastrointestinalne (p = 0,038) in genitourinarne (p = 0,041) toksičnosti sta bili sorazmerni z obsegom kroničnih simptomov. Spolno/vaginalno delovanje je bilo zmanjšano pri bolnicah z večjimi tumorji (p = 0,012). Parametri EQD2 > 53 Gy so bili povezani z zmanjšanim spolnim/vaginalnim delovanjem (p = 0,009) in povečano spolno skrbjo (p = 0,009). Povečanje parametričnega odmerka, doseženo z zaporednim povečanjem ali simultano integrirano dodano dozo ni vplivalo na preživetje ali kakovost življenja.

Zaključki. Primarna radiokemoterapija je učinkovito zdravljenje, vendar je dolgoročna kvaliteta življenja zmanjšana. Stopnja akutnih stranskih učinkov kemoradioterapije je sorazmerna z obsegom kroničnih simptomov. Bolniki imajo koristi od parametričnega simultano integriranega dodatka doze ali zaporednega povečanja doze, vendar EQD2 > 53 Gy ne izboljša preživetja in negativno vpliva na kvaliteto življenja.

Radiol Oncol 2018; 52(3): 329-336.
doi: 10.2478/raon-2018-0015

Predlog protokola za preverjanje kakovosti pri CT slikanju dojk z uporabo sinhrotronskega sevanja

Contillo A, Veronese A, Brombal L, Donato S, Rigon L, Taibi A, Tromba G, Longo R, Arfelli F

Izhodišča. Skupina SYRMA-3D načrtuje prvo klinično raziskavo fazno kontrastnega CT slikanj dojk s sinhrotronskim sevanjem na sinhrotronu Elettra v Trstu v Italiji. V članku predlagamo protokol za preverjanje kakovosti CT slikanja dojk, obenem pa smo analizirali prve meritve kakovosti slik z uporabo prilagojenega radiografskega fantoma.

Materiali in metode. Za CT rekonstrukcijo dveh izbranih delov fantoma smo uporabili več projekcij. Izbrana dela fantoma sta bila sestavljena iz homogene plasti vode in iz več radiografskih vložkov. S kombinaciji obeh smo lahko izvedli meritve več parametrov, ki so določali kakovost slik: linearnost CT števila, natančnost rekonstrukcije, uniformnost, šum in ločljivost v področju nižjega kontrasta. Meritve smo ponovili pri različnih žarkovnih energijah za dve različni vrednosti doze.

Rezultati. Ob visoki natančnosti rekonstrukcije CT števil, so meritve pokazale dobro linearnost v področju mehkih tkiv. Negotovosti meritev uniformnosti in šuma so bile v okviru nekaj odstotkov, medtem ko je zaznavanje ločljivosti v področju nižjih kontrastnih vrednosti bilo omejeno zgolj na višje vrednosti uporabljenih energij.

Zaključki. Rezultati meritev so bili zadovoljivi glede na kakovost, uporabnost in ponovljivost. Ob minimalnih dopolnitvah bomo lahko opisan fantom uporabili v načrtovani klinični raziskavi za meritve parametrov, ki določajo kakovost slik.

Radiol Oncol 2018; 52(3): 337-345.
doi: 10.2478/raon-2018-0013

Analiza operatorja povratne projekcije s singularnim razcepom za rekonstrukcijo slike PET z maksimizacijo pričakovanja maksimalne priličnosti

Somai V, Legrady D, Tolnai G

Izhodišča. Rekonstrukcija slike z maksimizacijo pričakovanja maksimalne priličnosti (*angl. Maximum likelihood expectation maximization*, ML-EM) je zamenjala analitične pristope v številnih aplikacijah. Najpomembnejša ovira te iterativne metode je linearna stopnja konvergence in s tem povezano procesorsko breme. Zatorej so potrebne poenostavitve v simulaciji Monte-Carlo pri povratni projekciji. Rešitev je rekonstrukcijski program, temelječ na implementaciji simulacije Monte-Carlo na grafičnem procesorju, ki omogoča popolno simulacijo fizike v povratni projekciji.

Materiali in metode. Uspešnost kode smo ovrednotili s simulacijami v dveh geometrijah. Prva je geometrija prefinjene priprave v obliki dvanajstkotnika s polmerom včrtanega kroga 8,7 cm. Vsaka stranic je bila sestavljena iz matrike 39 x 81 LYSO detektorskih kristalov s stranico 1.17 mm, podobno pripravi PET/CT *Mediso nanoScan*. Drugo, poenostavljeno geometrijo je predstavljal interval dolžine 38,4 mm, detektorski elementi pa so bili razporejeni v dva vzporedna vektorja 81 kvadratnih celic oz. kristalov s stranico 1,17 mm.

Rezultati. Prikazan je dokaz, da popolna simulacija Monte Carlo v povratni projekciji vodi do z materialno sestavo objekta povezanih nehomogonosti v rekonstruirani sliki. Analiza razlogov za to navidezno nepravilno vedenje smo opravili v poenostavljenem linearnem sistemu s pomočjo singularnega razcepa in pojasnili z različno hitrostjo konvergence.

Zaključki. Kljub navideznim nepravilnostim lahko prednost stabilnosti nasproti šumu pri popolnem modeliranju fizike izrabimo s pomočjo predlagane nove metode filtracije, ki omogoča pospešek pri konvergenci. Predstavili smo nekatere teoretične premisleke o praktični implementaciji in nadaljnjem razvoju metode.

Radiol Oncol 2018; 52(3): 346-352.
doi: 10.2478/raon-2018-0018

Ocena dvo-dimenzionalne razporeditve doze za potrebe dozimetričnega preverjanja, specifičnega za bolnika pred IMRT

Smilović Radojčić Đ, Rajlić D, Casar B, Švabić Kolacio M, Obajdin N, Faj D, Jurković S

Izhodišča. Natančnost izračuna doze je ključnega pomembna za uspešno zdravljenje z radioterapijo. Ena izmed metod, ki trenutno predstavlja standard na področju dozimetrije, specifične za bolnika, je ocena razporeditve doze, izmerjene z vrstičnim ionizacijskim detektorjem znotraj homogenega fantoma uporabo metode gamma. Žal ta metoda ne predstavlja dejanskih razmer, ki so prisotne med obsevanjem bolnika. Da bi natančneje ocenili zmožnosti načrtovalnega sistema, smo analizirali stopnje ujemanja gamma za različno kompleksne žarke ob prehajanju skozi nehomogene fantome.

Materiali in metode. Raziskavo smo izvedli na linearnem pospeševalniku Siemens Oncor Expression, CT simulatorju Siemens Somatom Open in načrtovalni postaji Elekta Monaco. Za oceno natančnosti razporeditve doze v homogenem, semi-antropomorfnem in antropomorfnem fantomu smo uporabili dvo-dimenzionalni vrstični detektor (IBA Matrixx). Ocena je temeljila na analizi gamma s kriteriji 3%/3mm in 2%/2mm.

Rezultati. Stopnje ujemanja kompleksnih razporeditev doze so se zmanjševale v odvisnosti od debeline materiala, ki ni bil ekvivalenten vodi. Odvisne so bile tudi od uporabljenega načina poročanja doze. Ugotovili smo, da se stopnja ujemanja zmanjševale s kompleksnostjo obsevalnih načrtov. Primerjava podatkov za vse nastavitve semi-antropomrofnih in antopomorfnih fantomov so pokazale, da so stopnje ujemanja višje v antropomorfnem fantomu.

Zaključki. Predstavljeni rezultati izpostavljajo vprašanje možnih omejitev pri verifikaciji razporeditve doze med ocenjevanjem kakovosti izvedenega obsevalnega načrta. Dobri rezultati, dobljeni s standardno dozimetrično metodologijo, specifično za bolnika, ne zagotavljajo natančnosti v dejanski razporeditvi doze v realnih kliničnih primerih.

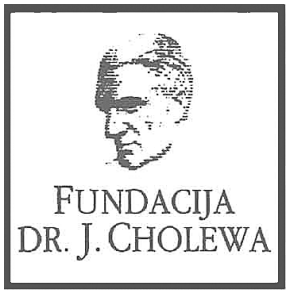

Fundacija "Docent dr. J. Cholewa"
je neprofitno, neinstitucionalno in nestrankarsko
združenje posameznikov, ustanov in organizacij, ki želijo
materialno spodbujati in poglabljati raziskovalno
dejavnost v onkologiji.

Dunajska 106
1000 Ljubljana

IBAN: SI56 0203 3001 7879 431

Activity of "Dr. J. Cholewa" Foundation for Cancer Research and Education – a report for the third quarter of 2018

Dr. Josip Cholewa Foundation for cancer research and education continues with its planned activities in the third quarter of 2018. Its primary focus remains the provision of grants, scholarships, and other forms of financial assistance for basic, clinical and public health research in the field of oncology. In parallel, it also makes efforts to provide financial and other support for the organisation of congresses, symposia and other forms of meetings to spread the knowledge about prevention and treatment of cancer, and finally about rehabilitation for cancer patients. In Foundation's strategy, the spread of knowledge should not be restricted only to the professionals that treat cancer patients, but also to the patients themselves and to the general public.

The Foundation continues to provide support for »Radiology and Oncology«, a quarterly scientific magazine with a respectable impact factor that publishes research and review articles about all aspects of cancer. The magazine is edited and published in Ljubljana, Slovenia. »Radiology and Oncology« is an open access journal available to everyone free of charge. Its long tradition represents a guarantee for the continuity of international exchange of ideas and research results in the field of oncology for all in Slovenia that are interested and involved in helping people affected by many different aspects of cancer.

The Foundation will continue with its activities in the future, especially since the problems associated with cancer affect more and more people in Slovenia and elsewhere. Ever more treatment that is successful reflects in results with longer survival in many patients with previously incurable cancer conditions. Thus adding many new dimensions in life of cancer survivors and their families.

Borut Štabuc, M.D., Ph.D.

Tomaž Benulič, M.D.

Andrej Plesničar, M.D., M.Sc.

Viljem Kovač M.D., Ph.D.

ENA SAMA 30-MINUTNA INFUZIJA ZAGOTOVI CELOVITO ZDRAVLJENJE ABSSSI [1]

Enostavno odmerjanje

Odrasli pacienti z ABSSSI: 1500 mg z enkratnim infundiranjem ali 1000 mg prvi teden, naslednji teden pa 500 mg.

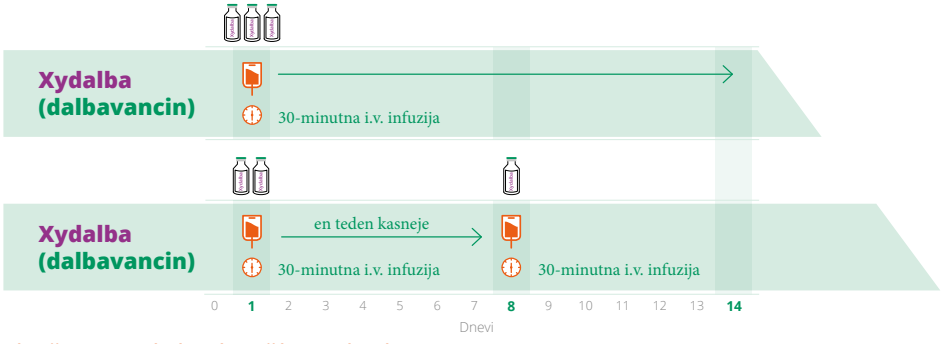

Xydalba™ dalbavancin

ANGELINI

Skrajšan povzetek glavnih značilnosti zdravila

Xydalba™ 500 mg prašek za koncentrat za raztopino za infundiranje

Za to zdravilo se izvaja dodatno spremljanje varnosti. Tako bodo hitreje na voljo nove informacije o njegovi varnosti. Zdravstvene delavce naprošamo, da poročajo o katerem koli domnevnem neželenem učinku zdravila.

Sestava: Ena viala vsebuje dalbavancinijev klorid, kar ustreza 500 mg dalbavancina. Po rekonstituciji en ml vsebuje 20 mg dalbavancina. Razredčena raztopina za infundiranje mora imeti končno koncentracijo od 1 do 5 mg/ml dalbavancina. **Terapevtske indikacije:** Zdravilo Xydalba je indicirano za zdravljenje akutnih bakterijskih infekcij kože in kožnih struktur (ABSSSI) pri odraslih. Pozornost je treba nameniti uradnim navodilom o ustrezni uporabi protibakterijskih zdravil. **Odmerjanje in način uporabe:** Odmerjanje: *Priporočeni odmerek in trajanje zdravljenja pri odraslih:* Priporočeni odmerek dalbavancina pri odraslih pacientih z akutno bakterijsko infekcijo kože in kožnih struktur (ABSSSI) je 1500 mg z enkratnim infundiranjem 1500 mg ali 1000 mg prvi teden, naslednji teden pa 500 mg. *Starejše osebe:* Prilagoditev odmerka ni potrebna. *Okvara delovanja ledvic:* Pri pacientih z blago ali zmerno okvaro delovanja ledvic prilagoditve odmerka niso potrebne (kreatininski očistek ≥ 30 do 79 ml/min). Pri pacientih, ki redno prejemajo hemodializo (3-krat tedensko), prilagoditve odmerka niso potrebne, dalbavancin se lahko uporablja ne glede na čas hemodialize. Pri pacientih s kronično okvaro delovanja ledvic, katerih kreatininski očistek je < 30 ml/min in ki ne prejemajo redno hemodialize, je priporočen odmerek dalbavancina zmanjšan na 1000 mg z enkratnim infundiranjem ali 750 mg, ki mu sledi 375 mg v naslednjem tednu. *Okvara delovanja jeter:* Pri pacientih z blago okvaro delovanja jeter (Child-Pugh A) prilagoditev odmerka dalbavancina ni potrebna. Previdnost je potrebna pri predpisovanju dalbavancina pacientom z zmerno ali hudo okvaro delovanja jeter (Child-Pugh B & C), ker ni ustreznih podatkov za določitev primernega odmerjanja. *Otroci:* Varnost in učinkovitost dalbavancina pri otrocih v starosti od rojstva do < 18 let še nista ugotovljeni. Priporočila o odmerjanju ne moremo podati. Način uporabe: Zdravilo Xydalba mora biti rekonstituirano in potem še razredčeno pred dajanjem intravenske infuzije, ki traja 30 minut. **Kontraindikacije:** Preobčutljivost na zdravilno učinkovino ali katerokoli pomožno snov. **Posebna opozorila in previdnostni ukrepi:** Preobčutljivostne reakcije: Posebej pozorno se mora zdravilo Xydalba uporabljati pri pacientih, za katere je znano, da so preobčutljivi na druge glikopeptide, saj se lahko pojavi navzkrižna preobčutljivost. Če se pojavi alergijska reakcija na zdravilo Xydalba, je treba njegovo uporabo prekiniti in uvesti ustrezno terapijo za alergijsko reakcijo. Driska zaradi bakterije *Clostridium difficile:* Kolitis, povezan s protibakterijskimi zdravili, in psevdomembranski kolitis sta bila zabeležena pri uporabi skoraj vseh antibiotikov in sta lahko blaga pa vse do smrtno ogrožajoča. Zato je pri pacientih z drisko med ali po zdravljenju z dalbavancinom pomembno upoštevati tudi to diagnozo. V takšnih okoliščinah je treba razmisliti o prekinitvi zdravljenja z dalbavancinom in uvesti podporne ukrepe skupaj z jemanjem posebnega zdravila proti bakteriji *Clostridium difficile.* Takih pacientov nikoli ne smemo zdraviti z zdravili, ki zavirajo peristaltiko. Reakcije, povezane z infuzijo: Zdravilo Xydalba se uporablja z intravenskim infundiranjem, ki traja skupaj 30 minut, da se zmanjša tveganje za z infuzijo povezano reakcijo. Hitre intravenske infuzije glikopeptidnih protibakterijskih zdravil lahko povzročijo reakcijo, ki je podobna "sindromu rdečeličneža", z rdečico na zgornjem delu telesa, z urtikarijo, pruritusom in/ali izpuščajem. S prekinitvijo ali upočasnitvijo infundiranja lahko te reakcije izginejo. Okvara delovanja ledvic: Podatki o učinkovitosti in varnosti dalbavancina pri pacientih s kreatininskim očistkom, manjšim od 30 ml/min, so omejeni. Na podlagi simulacij je prilagoditev odmerjanja potrebna pri pacientih s kronično okvaro delovanja ledvic, katerih kreatininski očistek je manjši od 30 ml/min in ki redno ne prejemajo hemodialize. Mešane okužbe: Pri mešanih okužbah, kjer obstaja sum na Gram-negativne bakterije, se morajo pacienti zdraviti tudi z ustreznim protibakterijskim zdravilom oz. zdravili, proti Gram-negativnim bakterijam. Neobčutljivi organizmi: Uporaba antibiotikov lahko pospeši prekomerno rast neobčutljivih mikroorganizmov. Če pride med zdravljenjem do superinfekcije, je treba ustrezno ukrepati. Omejitev kliničnih podatkov: Podatki o varnosti in učinkovitosti dalbavancina pri uporabi več kot dveh odmerkov (v razmiku enega tedna) so omejeni. V večjih preskušanjih pri akutnih bakterijskih infekcijah kože in kožnih struktur (ABSSSI) so bile vrste zdravljenih infekcij omejene samo na celulitis/šen, abscese in okužbe ran. Izkušenj z dalbavancinom pri zdravljenju pacientov s hudo oslabljenim imunskim sistemom ni. **Medsebojno delovanje z drugimi zdravili in druge oblike interakcij:** Dalbavancin se ne presnavlja z encimi CYP in vitro, zato sočasni CYP induktorji ali inhibitorji malo verjetno vplivajo na farmakokinetiko dalbavancina. Ni znano, ali je dalbavancin substrat za prenašalce jetrnega privzema in efluksa. Uporaba skupaj z inhibitorji teh prenašalcev lahko poveča izpostavljenost dalbavancinu. Primeri takšnih inhibitorjev prenašalcev so okrepljeni inhibitorji proteaze, verapamil, kinidin, itrakonazol, klaritromicin in ciklosporin. Pričakovana je majhna verjetnost interakcije dalbavancina z zdravili, ki se presnavljajo z encimi CYP, saj ni niti inhibitor niti induktor encimov CYP *in vitro.* Podatki o dalbavancinu kot inhibitorju CYP2C8 niso na voljo. Ni znano, ali je dalbavancin inhibitor prenašalcev. Povečane izpostavljenosti substratom prenašalcev, občutljivim na inhibicijo aktivnosti prenašalcev, kot so statini in digoksin, ni mogoče izključiti, če so kombinirani z dalbavancinom. **Plodnost, nosečnost in dojenje:** Nosečnost: O uporabi dalbavancina pri nosečnicah ni podatkov. Študije na živalih so pokazale vpliv na sposobnost razmnoževanja. Uporaba zdravila Xydalba med nosečnostjo ni priporočljiva, razen kadar je to nujno. Dojenje: Ni znano, ali se dalbavancin izloča v mleko pri človeku. Potrebno je sprejeti odločitev o nadaljevanju/prekinitvi dojenja ali o nadaljevanju/prekinitvi zdravljenja z zdravilom Xydalba, pri tem pa pretehtati koristi dojenja za otroka in koristi zdravljenja za doječo žensko. Plodnost: Študije na živalih so pokazale zmanjšano plodnost. Potencialno tveganje za ljudi ni znano. **Neželeni učinki:** Pogosti: glavobol, navzea, driska. Občasni: vulvovaginalna glivična okužba, okužba sečil, glivična okužba, kolitis zaradi razrasta *Clostridium difficile,* oralna kandidiaza, anemija, trombocitoza, eozinofilija, levkopenija, nevtropenija, zmanjšan apetit, insomnia, dizgevzija, omotica, vročinski oblivi, flebitis, kašelj, zaprtost, bolečine v trebuhu, dispepsija, neprijeten občutek v trebuhu, bruhanje, pruritus, urtikarija, izpuščaj, vulvovaginalni pruritus, z infuzijo povezana reakcija, zvišana laktat-dehidrogenaza v krvi, zvišana alanin-aminotransferaza, zvišana aspartat-aminotransferaza, zvišana raven sečne kisline v krvi, neobičajni rezultati testa jetrne funkcije, zvišane vrednosti transaminaz, zvišane vrednosti alkalne fosfataze v krvi, zvišano število krvnih ploščic, zvišana telesna temperatura, zvišana raven jetrnih encimov, zvišane vrednosti gama-glutamil transferaze. Redki: anafilaktoidna reakcija, bronhospazem. **Način in režim predpisovanja in izdaje:** H - Zdravilo se izdaja le na recept, uporablja pa se samo v bolnišnicah. **Imetnik dovoljenja za promet:** Allergan Pharmaceuticals International Ltd., Clonshaugh Industrial Estate, Coolock, Dublin 17, Irska. **Datum zadnje revizije besedila:** 01/2017. **Predstavnik imetnika dovoljenja za promet z zdravilom:** Angelini Pharma d.o.o., Koprska ulica 108A, 1000 Ljubljana.

Pred predpisovanjem se seznanite s celotnim Povzetkom glavnih značilnosti zdravila.
Samo za strokovno javnost. Datum priprave informacije: maj 2018

Vir:

1. Xydalba™ (dalbavancin), Povzetek glavnih značilnosti zdravila, 30. 1. 2017

PRVA REGISTRIRANA TERAPIJA V 2. LINIJI ZA ZDRAVLJENJE ADENOKARCINOMA ŽELODCA ALI GASTRO-EZOFAGEALNEGA PREHODA[1]

CYRAMZA®
(ramucirumab)

UKREPAJTE ZDAJ

USPOSOBLJENI ZA SPREMEMBE, ZA NEPRIMERLJIVE IZKUŠNJE

Skrajšan povzetek glavnih značilnosti zdravila

▼ Za to zdravilo se izvaja dodatno spremljanje varnosti. Tako bodo hitreje na voljo nove informacije o njegovi varnosti. Zdravstvene delavce naprošamo, da poročajo o katerem koli domnevnem neželenem učinku zdravila.

Cyramza 10 mg/ml koncentrat za raztopino za infundiranje

En mililiter koncentrata za raztopino za infundiranje vsebuje 10 mg ramucirumaba. Ena 10-mililitrska viala vsebuje 100 mg ramucirumaba. **Terapevtske indikacije** Zdravilo Cyramza je v kombinaciji s paklitakselom indicirano za zdravljenje odraslih bolnikov z napredovalim rakom želodca ali adenokarcinomom gastro-ezofagealnega prehoda z napredovalo boleznijo po predhodni kemoterapiji, ki je vključevala platino in fluoropirimidin. Monoterapija z zdravilom Cyramza je indicirana za zdravljenje odraslih bolnikov z napredovalim rakom želodca ali adenokarcinomom gastro-ezofagealnega prehoda z napredovalo boleznijo po predhodni kemoterapiji s platino ali fluoropirimidinom, za katere zdravljenje v kombinaciji s paklitakselom ni primerno. Zdravilo Cyramza je v kombinaciji s shemo FOLFIRI indicirano za zdravljenje odraslih bolnikov z metastatskim kolorektalnim rakom (mCRC), z napredovanjem bolezni ob ali po predhodnem zdravljenju z bevacizumabom, oksaliplatinom in fluoropirimidinom. Zdravilo Cyramza je v kombinaciji z docetakselom indicirano za zdravljenje odraslih bolnikov z lokalno napredovalim ali metastatskim nedrobnoceličnim pljučnim rakom, z napredovanjem bolezni po kemoterapiji na osnovi platine. **Odmerjanje in način uporabe** Zdravljenje z ramucirumabom morajo uvesti in nadzirati zdravniki z izkušnjami v onkologiji. Odmerjanje *Rak želodca in adenokarcinom gastro-ezofagealnega prehoda* Priporočeni odmerek ramucirumaba je 8 mg/kg 1. in 15. dan 28-dnevnega cikla, pred infuzijo paklitaksela. Priporočeni odmerek paklitaksela je 80 mg/m^2 in se daje z intravenskim infundiranjem, ki traja približno 60 minut, 1., 8. in 15. dan 28-dnevnega cikla. Pred vsakim infundiranjem paklitaksela je treba pri bolnikih pregledati celotno krvno sliko in izvide kemičnih preiskav krvi, da se oceni delovanje jeter. Priporočeni odmerek ramucirumaba kot monoterapije je 8 mg/kg vsaka 2 tedna. *Kolorektalni rak* Priporočeni odmerek ramucirumaba je 8 mg/kg vsaka 2 tedna, dan z intravensko infuzijo pred dajanjem sheme FOLFIRI. Pred kemoterapijo je treba bolnikom odvzeti kri za popolno krvno sliko. *Nedrobnocelični pljučni rak (NSCLC)* Priporočeni odmerek ramucirumaba je 10 mg/kg na 1. dan 21-dnevnega cikla, pred infuzijo docetaksela. Priporočeni odmerek docetaksela je 75 mg/m^2, dan z intravensko infuzijo v približno 60 minutah na 1. dan 21-dnevnega cikla. *Premedikacija* Pred infundiranjem ramucirumaba je priporočljiva premedikacija z antagonistom histaminskih receptorjev H1. Način uporabe Po redčenju se zdravilo Cyramza daje kot intravenska infuzija v približno 60 minutah. Zdravila ne dajajte v obliki intravenskega bolusa ali hitre intravenske injekcije. Da boste dosegli zahtevano trajanje infundiranja približno 60 minut, največja hitrost infundiranja ne sme preseči 25 mg/minuto, saj morate sicer podaljšati trajanje infundiranja. Bolnika je med infundiranjem treba spremljati glede znakov reakcij, povezanih z infuzijo, zagotoviti pa je treba tudi razpoložljivost ustrezne opreme za oživljanje. **Kontraindikacije** Pri bolnikih z NSCLC je ramucirumab kontraindiciran, kjer gre za kavitacijo tumorja ali prepletenost tumorja z glavnimi žilami. **Posebna opozorila in previdnostni ukrepi** Trajno prekinite zdravljenje z ramucirumabom pri bolnikih, pri katerih se pojavijo resni arterijski trombembolični dogodki, gastrointestinalne perforacije, krvavitev stopnje 3 ali 4, če zdravstveno pomembne hipertenzije ni mogoče nadzirati z antihipertenzivnim zdravljenjem ali če se pojavi fistula, raven beljakovin v urinu > 3 g/24 ur ali v primeru nefrotskega sindroma. Pri bolnikih z neuravnano hipertenzijo zdravljenja z ramucirumabom ne smete uvesti, dokler oziroma v kolikor obstoječa hipertenzija ni uravnana. Pri bolnikih s ploščatoceličnо histologijo obstaja večje tveganje za razvoj resnih pljučnih krvavitev. Če se pri bolniku med zdravljenjem razvijejo zapleti v zvezi s celjenjem rane, prekinite zdravljenje z ramucirumabom, dokler rana ni povsem zaceljena. V primeru pojava stomatitisa je treba takoj uvesti simptomatsko zdravljenje. Pri bolnikih, ki so prejemali ramucirumab in docetaksel za zdravljenje napredovalega NSCLC z napredovanjem bolezni po kemoterapiji na osnovi platine, so opazili trend manjše učinkovitosti z naraščajočo starostjo. **Medsebojno delovanje z drugimi zdravili in druge oblike interakcij** Med ramucirumabom in parlitakselom niso opazili medsebojnega delovanja. **Plodnost, nosečnost in dojenje** Ženskam v rodni dobi je treba svetovati, naj se izogn ejo zanositvi med zdravljenjem z zdravilom Cyramza in jih je treba seznaniti z možnim tveganjem za nosečnost in plod. Ni znano, ali se ramucirumab izloča v materino mleko. **Neželeni učinki** *Zelo pogosti (≥ 1/10)* nevtropenija, levkopenija, trombocitopenija, hipoalbuminemija, hipertenzija, epistaksa, gastrointestinalne krvavitve, stomatitis, driska, proteinurija, utrujenost/astenija, periferni edem, bolečina v trebuhu. *Pogosti (≥ 1/100 do < 1/10)* hipokaliemija, hiponatriemija, glavobol. **Rok uporabnosti** 3 leta **Posebna navodila za shranjevanje** Shranjujte v hladilniku (2 °C–8 °C). Ne zamrzujte. Vialo shranjujte v zunanji ovojnini, da zagotovite zaščito pred svetlobo. **Pakiranje** 2 viali z 10 ml **IMETNIK DOVOLJENJA ZA PROMET Z ZDRAVILOM** Eli Lilly Nederland B.V., Papendorpseweg 83, 3528 BJ Utrecht, Nizozemska **DATUM ZADNJE REVIZIJE BESEDILA** 25.01.2016
Režim izdaje: Predpisovanje in izdaja zdravila je le na recept, zdravilo pa se uporablja samo v bolnišnicah.

Pomembno obvestilo:

Pričujoče gradivo je namenjeno **samo za strokovno javnost**. Zdravilo Cyramza se izdaja le na recept, zdravilo pa se uporablja samo v bolnišnicah. Pred predpisovanjem zdravila Cyramza vas vljudno prosimo, da preberete celotni Povzetek glavnih značilnosti zdravila Cyramza. Podrobnejše informacije o zdravilu Cyramza in o zadnji reviziji besedila Povzetka glavnih značilnosti zdravila so na voljo na sedežu podjetja Eli Lilly (naslov podjetja in kontaktni podatki spodaj) in na spletni strani European Medicines Agency (EMA): www.ema.europa.eu. in na spletni strani European Commission http://ec.europa.eu/health/documents/community-register/html/alfregister.htm.

Eli Lilly farmacevtska družba, d.o.o., Dunajska cesta 167, 1000 Ljubljana, telefon: (01) 5800 010, faks: (01) 5691 705

Referenca: 1. https://pharmaphorum.com/news/lilly-s-cyramza-approved-in-eu-for-stomach-cancer/?epoch=1505121044344

PP-RB-SI-0002, 17.11.2017.

Lilly

TECENTRIQ®
atezolizumab

Zdravilo TECENTRIQ® ▼ (atezolizumab) je humanizirano monoklonsko protitelo, ki deluje na ligand za programirano celično smrt 1 (PD-L1).[1]

Zdravilo TECENTRIQ® (atezolizumab) je v monoterapiji indicirano za zdravljenje:

- odraslih bolnikov z lokalno napredovalim ali metastatskim urotelijskim karcinomom, ki so bili predhodno zdravljeni s kemoterapijo na osnovi platine ali niso primerni za zdravljenje s cisplatinom;
- odraslih bolnikov z lokalno napredovalim ali metastatskim nedrobnoceličnim rakom pljuč, ki so bili predhodno zdravljeni s kemoterapijo. Bolniki z EGFR-aktivirajočimi mutacijami ali ALK-pozitivnimi tumorji morajo pred uvedbo zdravila TECENTRIQ® prejeti tudi tarčno zdravljenje.[1]

SKRAJŠAN POVZETEK GLAVNIH ZNAČILNOSTI ZDRAVILA TECENTRIQ

▼Za to zdravilo se izvaja dodatno spremljanje varnosti. Tako bodo hitreje na voljo nove informacije o njegovi varnosti. Zdravstvene delavce naprošamo, da poročajo o katerem koli domnevnem neželenem učinku zdravila. Kako poročati o neželenih učinkih, si poglejte skrajšani povzetek glavnih značilnosti zdravila pod "Poročanje o domnevnih neželenih učinkih".

Ime zdravila: Tecentriq 1200 mg koncentrat za raztopino za infundiranje. **Kakovostna in količinska sestava:** Ena 20-ml viala s koncentratom vsebuje 1200 mg atezolizumaba. Po razredčenju 1 ml raztopine vsebuje približno 4,4 mg atezolizumaba. Atezolizumab je humanizirano monoklonsko protitelo IgG1 z inženirsko obdelano domeno Fc, ki je pridobljeno iz celic jajčnika kitajskega hrčka s tehnologijo rekombinantne DNA in deluje na ligand za programirano celično smrt 1 (PD-L1). **Terapevtske indikacije:** Zdravilo Tecentriq je kot monoterapija indicirano za zdravljenje: odraslih bolnikov z lokalno napredovalim ali metastatskim urotelijskim karcinomom, ki so bili predhodno zdravljeni s kemoterapijo na osnovi platine ali niso primerni za zdravljenje s cisplatinom in odraslih bolnikov z lokalno napredovalim ali metastatskim nedrobnoceličnim rakom pljuč, ki so bili predhodno zdravljeni s kemoterapijo. Bolniki z EGFR-aktivirajočimi mutacijami ali ALK-pozitivnimi tumorji morajo pred uvedbo zdravila Tecentriq prejeti tudi tarčno zdravljenje. **Odmerjanje in način uporabe:** Zdravilo Tecentriq morajo uvesti in nadzorovati zdravniki z izkušnjami pri zdravljenju raka. Odmerjanje: priporočeni odmerek zdravila Tecentriq je 1200 mg intravensko na vsake tri tedne. *Trajanje zdravljenja:* zdravljenje z zdravilom Tecentriq je priporočljivo nadaljevati, dokler je klinično koristno ali dokler se ne pojavijo neobvladljivi neželeni toksični učinki. *Zapozneli ali izpuščeni odmerki:* v primeru izpuščenega načrtovanega odmerka zdravila Tecentriq je treba odmerek dati čim prej; ni priporočljivo čakati do naslednjega načrtovanega odmerka. Urnik dajanja zdravila je treba nato prilagoditi 3-tedenskemu presledku med odmerki. *Prilagoditev odmerka med zdravljenjem:* odmerkov zdravila Tecentriq ni priporočljivo zmanjševati. Bolnikom, ki jih zdravite z zdravilom Tecentriq, morate dati Opozorilno kartico za bolnika in jih poučiti o tveganjih zdravljenja z zdravilom Tecentriq. Posebne populacije bolnikov: *Pediatrična populacija:* varnost in učinkovitost zdravila Tecentriq pri otrocih in mladostnikih, mlajših od 18 let, nista dokazani. Podatkov ni na voljo. Starejši: glede na populacijsko farmakokinetično analizo bolnikom v starosti ≥ 65 let odmerka zdravila Tecentriq ni treba prilagoditi. *Okvara ledvic:* glede na populacijsko farmakokinetično analizo bolnikom z blago ali zmerno okvaro ledvic odmerka ni treba prilagoditi. *Okvara jeter:* glede na populacijsko farmakokinetično analizo bolnikom z blago okvaro jeter odmerka ni treba prilagoditi. Način uporabe: zdravilo Tecentriq je namenjeno za intravensko uporabo. Infuzij se ne sme dajati kot hiter intravenski odmerek ali bolus. Začetni odmerek zdravila Tecentriq je treba dati v 60 minutah. Če bolnik prvo infuzijo dobro prenese, je mogoče vse nadaljnje infuzije dati v 30 minutah. **Kontraindikacije:** Preobčutljivost na atezolizumab ali katero koli pomožno snov. **Posebna opozorila in previdnostni ukrepi:** Za izboljšanje sledljivosti bioloških zdravil je treba lastniško ime in številko serije uporabljenega zdravila jasno zabeležiti (ali navesti) v bolnikovi dokumentaciji. Večina imunsko pogojenih neželenih učinkov, ki so se pojavili med zdravljenjem z atezolizumabom, je bila po prekinitvi atezolizumaba in uvedbi kortikosteroidov in/ali podpornega zdravljenja reverzibilna. Opazili so imunsko pogojene neželene učinke, ki vplivajo na več kot en organski sistem. Imunsko pogojeni neželeni učinki, povezani z atezolizumabom, se lahko pojavijo po zadnjem odmerku atezolizumaba. Pri sumu na imunsko pogojene neželene učinke je treba opraviti temeljito oceno za potrditev etiologije oziroma izključitev drugih vzrokov. Glede na izrazitost neželenega učinka je treba uporabo atezolizumaba odložiti in uvesti kortikosteroide. Atezolizumab je treba trajno prenehati uporabljati pri vseh imunsko pogojenih neželenih učinkih 3. stopnje, ki se ponovijo, in pri vseh imunsko pogojenih neželenih učinkih 4. stopnje, z izjemo endokrinopatij, ki jih je mogoče nadzorovati z nadomestnimi hormoni. Imunsko pogojeni pnevmonitis: v kliničnih preskušanjih atezolizumaba so opažali primere pnevmonitisa, vključno s smrtnimi primeri. Bolnike je treba spremljati glede znakov in simptomov pnevmonitisa. Imunsko pogojeni hepatitis: v kliničnih preskušanjih atezolizumaba so opazili primere hepatitisa, nekatere s smrtnim izidom. Bolnike je treba spremljati glede znakov in simptomov hepatitisa. Vrednosti aspartat-aminotransferaze (AST), alanin-aminotransferaze (ALT) in bilirubina je treba spremljati pred začetkom zdravljenja z atezolizumabom, redno med zdravljenjem in kot je potrebno glede na klinično oceno. Imunsko pogojeni kolitis: v kliničnih preskušanjih atezolizumaba so opažali primere diareje ali kolitisa. Bolnike je treba spremljati glede znakov in simptomov kolitisa. Imunsko pogojene endokrinopatije: v kliničnih preskušanjih atezolizumaba so opažali hipotiroidizem, hipertiroidizem, insuficiencno nadledvičnih žlez, hipofizitis in sladkorno bolezen tipa 1, vključno z diabetično ketoacidozo. Bolnike je treba spremljati glede znakov in simptomov endokrinopatij. Imunsko pogojeni meningoencefalitis: v kliničnih preskušanjih z atezolizumabom so opažali meningoencefalitis. Bolnike je treba spremljati glede znakov in simptomov meningitisa ali encefalitisa. V primeru meningitisa ali encefalitisa je treba zdravljenje z atezolizumabom trajno ukiniti ne glede na njuno stopnjo. Imunsko pogojene nevropatije: pri bolnikih, zdravljenih z atezolizumabom, so opažali miastenijski sindrom/miastenijo gravis ali Guillain-Barréjev sindrom, ki je lahko življenje ogrožujoč. Bolnike je treba spremljati glede znakov in simptomov motorične in senzorične nevropatije. V primeru miastenijskega sindroma/miastenije gravis ali Guillain-Barréjevega sindroma je treba zdravljenje z atezolizumabom trajno prekiniti ne glede na njihovo stopnjo. Imunsko pogojeni pankreatitis: v kliničnih preskušanjih z atezolizumabom so opazili pankreatitis, vključno z zvišanjem amilaze in lipaze v serumu. Bolnike je treba nadzorovati glede znakov in simptomov, ki kažejo na akutni pankreatitis. Imunsko pogojeni miokarditis: v kliničnih preskušanjih z atezolizumabom so opazili miokarditis. Bolnike je treba nadzorovati glede znakov in simptomov, ki kažejo na miokarditis. V primeru miokarditisa 2. stopnje je treba zdravljenje z atezolizumabom odložiti in uvesti zdravljenje s sistemskimi kortikosteroidi. V primeru miokarditisa 3. ali 4. stopnje je treba zdravljenje z atezolizumabom trajno ukiniti. Z infundiranjem povezane reakcije: v kliničnih preskušanjih z atezolizumabom so opažali z infundiranjem povezane reakcije. Pri bolnikih, ki imajo z infundiranjem povezane reakcije 1. ali 2. stopnje, je treba hitrost infundiranja zmanjšati ali zdravljenje prekiniti. Pri bolnikih, ki imajo z infundiranjem povezane reakcije 3. ali 4. stopnje, je treba zdravljenje z atezolizumabom trajno ukiniti. Bolniki, ki imajo z infundiranjem povezane reakcije 1. ali 2. stopnje, lahko še naprej prejemajo atezolizumab pod natančnim nadzorom; v poštev pride premedikacija z antipiretikom in antihistaminikom. Bolniki, ki niso bili vključeni v klinična preskušanja: v klinična preskušanja niso bili vključeni bolniki z naslednjimi stanji: z anamnezo avtoimunske bolezni, anamnezo pnevmonitisa, simptomatskimi možganskimi metastazami, okužbo z virusom HIV, s hepatitisom B ali hepatitisom C. Prav tako v klinična preskušanja niso bili vključeni bolniki, ki so bili v obdobju 28 dni pred vključitvijo v študijo cepljeni z živim oslabljenim cepivom, ki so v obdobju 4 tednov pred vključitvijo v študijo dobili sistemska imunostimulacijska sredstva ali v obdobju 2 tednov sistemska imunosupresivna zdravila. Pri teh skupinah je treba zaradi pomanjkanja podatkov atezolizumab uporabljati previdno in po skrbni oceni razmerja med koristmi in tveganji zdravila za bolnika. Uporaba atezolizumaba pri urotelijskem karcinomu pri predhodno nezdravljenih bolnikih, ki niso primerni za zdravljenje s cisplatinom: izhodiščne in prognostične značilnosti bolezni 1. kohorte študijske populacije IMvigor210 so bile na splošno primerljive z značilnostmi bolnikov, ki niso bili primerni za zdravljenje s cisplatinom, vendar pa bi bili primerni za kombinirano kemoterapijo na osnovi karboplatina. Za podskupino bolnikov, neprimernih za katero koli kemoterapijo, ni dovolj podatkov, zato je treba atezolizumab pri njih uporabljati previdno, po temeljitem pretehtanju razmerja med možnimi tveganji in koristmi za vsakega posameznega bolnika. Opozorilna kartica bolnika: Vsi zdravniki, ki predpisujejo zdravilo Tecentriq, morajo biti dobro seznanjeni z Informacijami za zdravnika in Smernicami za vodenje bolnikov. Zdravnik, ki predpiše zdravilo, se mora z bolnikom pogovoriti o tveganjih zdravljenja z zdravilom Tecentriq. Bolniku je treba dati Opozorilno kartico za bolnika in mu naročiti, naj jo ima vedno pri sebi. **Medsebojno delovanje z drugimi zdravili in druge oblike interakcij:** Formalnih študij farmakokinetičnega medsebojnega delovanja zdravil z atezolizumabom niso izvedli. Ker se atezolizumab odstrani iz obtoka s katabolizmom, ni pričakovati presnovnih medsebojnih delovanj med zdravili. Uporabi sistemskih kortikosteroidov ali imunosupresivov se je pred uvedbo atezolizumaba treba izogibati, ker lahko vplivajo na farmakodinamično aktivnost in učinkovitost atezolizumaba. Vendar pa se sistemske kortikosteroide ali druge imunosupresive lahko uporabi po začetku zdravljenja z atezolizumabom za zdravljenje imunsko pogojenih neželenih učinkov. **Neželeni učinki:** povzetek neželenih učinkov, ki so se v kliničnih preskušanjih pojavili bolnikom, zdravljenim z zdravilom Tecentriq. *Zelo pogosti:* zmanjšan apetit, dispneja, navzea, bruhanje, diareja, izpuščaj, srbenje, artralgija, zvišana telesna temperatura, utrujenost in astenija. *Pogosti:* trombocitopenija, preobčutljivost, hipotiroidizem, hipertiroidizem, hipokaliemija, hiponatriemija, hipotenzija, pnevmonitis, hipoksija, zamašenost nosu, bolečine v trebuhu, kolitis, disfagija, zvišanje AST, zvišanje ALT, mišično-skeletna bolečina, z infundiranjem povezane reakcije, gripi podobna bolezen in mrzlica. Poročanje o domnevnih neželenih učinkih: Poročanje o domnevnih neželenih učinkih zdravila po izdaji dovoljenja za promet je pomembno. Omogoča namreč stalno spremljanje razmerja med koristmi in tveganji zdravila. Od zdravstvenih delavcev se zahteva, da poročajo o katerem koli domnevnem neželenem učinku zdravila na: Javna agencija Republike Slovenije za zdravila in medicinske pripomočke, Sektor za farmakovigilanco, Nacionalni center za farmakovigilanco, Slovenčeva ulica 22, SI-1000 Ljubljana, Tel: +386 (0)8 2000 500, Faks: +386 (0)8 2000 510, e-pošta: h-farmakovigilanca@jazmp.si, spletna stran: www.jazmp.si. Za zagotavljanje sledljivosti zdravila je pomembno, da pri izpolnjevanju obrazca o domnevnih neželenih učinkih zdravila navedete številko serije biološkega zdravila. **Režim izdaje zdravila:** H. **Imetnik dovoljenja za promet:** Roche Registration GmbH, Emil-Barell-Strasse 1, 79639 Grenzach-Wyhlen, Nemčija. **Verzija:** 2.0/18. **Informacija pripravljena:** april 2018.

PM-0009-2018-TCN

Samo za strokovno javnost.

Literatura: 1. Povzetek glavnih značilnosti zdravila TECENTRIQ. Dostopano april 2018 na: http://www.ema.europa.eu/docs/sl_SI/document_library/EPAR_-_Product_Information/human/004143/WC500235778.pdf

DODATNE INFORMACIJE SO NA VOLJO PRI: Roche farmacevtska družba d.o.o., Vodovodna cesta 109, 1000 Ljubljana

Roche

Zdravilo za predhodno že zdravljene bolnike z mKRR

Več časa za trenutke, ki štejejo

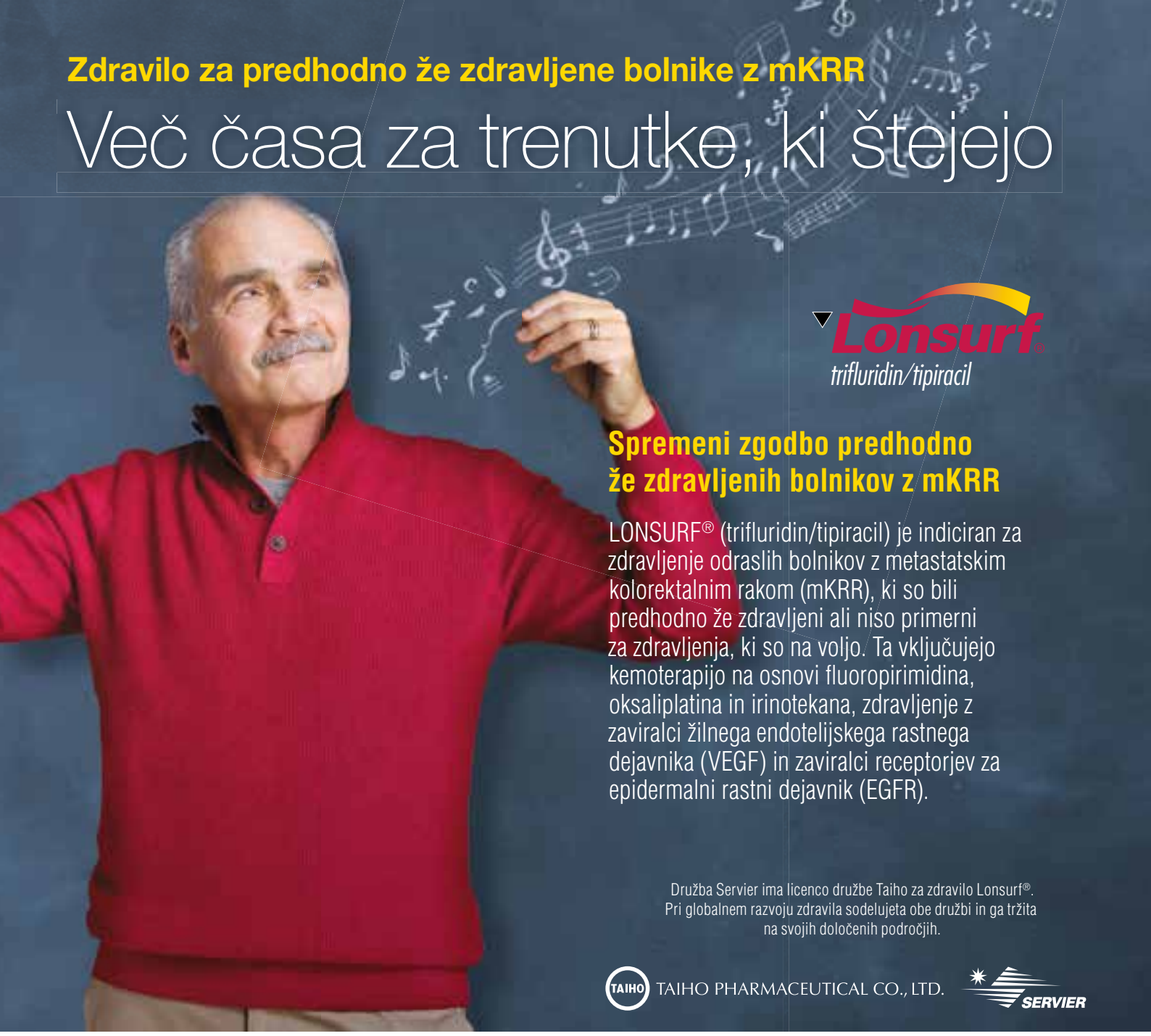

Lonsurf®
trifluridin/tipiracil

Spremeni zgodbo predhodno že zdravljenih bolnikov z mKRR

LONSURF® (trifluridin/tipiracil) je indiciran za zdravljenje odraslih bolnikov z metastatskim kolorektalnim rakom (mKRR), ki so bili predhodno že zdravljeni ali niso primerni za zdravljenja, ki so na voljo. Ta vključujejo kemoterapijo na osnovi fluoropirimidina, oksaliplatina in irinotekana, zdravljenje z zaviralci žilnega endotelijskega rastnega dejavnika (VEGF) in zaviralci receptorjev za epidermalni rastni dejavnik (EGFR).

Družba Servier ima licenco družbe Taiho za zdravilo Lonsurf®. Pri globalnem razvoju zdravila sodelujeta obe družbi in ga tržita na svojih določenih področjih.

TAIHO PHARMACEUTICAL CO., LTD.

SERVIER

Skrajšan povzetek glavnih značilnosti zdravila: Lonsurf 15 mg/6,14 mg filmsko obložene tablete in Lonsurf 20 mg/8,19 mg filmsko obložene tablete

▼ Za to zdravilo se izvaja dodatno spremljanje varnosti. **SESTAVA*: Lonsurf 15 mg/6,14 mg:** Ena filmsko obložena tableta vsebuje 15 mg trifluridina in 6,14 mg tipiracila (v obliki klorida). **Lonsurf 20 mg/8,19 mg:** Ena filmsko obložena tableta vsebuje 20 mg trifluridina in 8,19 mg tipiracila (v obliki klorida). **TERAPEVTSKE INDIKACIJE*:** Zdravilo Lonsurf je indicirano za zdravljenje odraslih bolnikov z metastatskim kolorektalnim rakom, ki so bili predhodno že zdravljeni ali niso primerni za zdravljenja, ki so na voljo. Ta vključujejo kemoterapijo na osnovi fluoropirimidina, oksaliplatina in irinotekana, zdravljenje z zaviralci žilnega endotelijskega rastnega dejavnika (VEGF - Vascular Endothelial Growth Factor) in zaviralci receptorjev za epidermalni rastni dejavnik (EGFR - Epidermal Growth Factor Receptor). **ODMERJANJE IN NAČIN UPORABE*:** Priporočeni začetni odmerek zdravila Lonsurf pri odraslih je 35 mg/m^2/odmerek peroralno dvakrat dnevno na 1. do 5. dan in 8. do 12. dan vsakega 28-dnevnega cikla zdravljenja, najpozneje 1 uro po zaključku jutranjega in večernega obroka. Odmerjanje, izračunano glede na telesno površino, ne sme preseči 80 mg/odmerek. Možne prilagoditve odmerka glede na varnost in prenašanje zdravila: dovoljena so največ 3 zmanjšanja odmerka na najmanjši odmerek 20 mg/m^2 dvakrat dnevno. Potem ko je bil odmerek zmanjšan, povečanje ni dovoljeno. **KONTRAINDIKACIJE*:** Preobčutljivost na zdravilni učinkovini ali katero koli pomožno snov. **OPOZORILA IN PREVIDNOSTNI UKREPI*:** Supresija kostnega mozga: Pred uvedbo zdravljenja, pred vsakim ciklom zdravljenja in po potrebi je treba pregledati celotno krvno sliko. Zdravljenja ne smete začeti, če je absolutno število nevtrofilcev < 1,5 x 10^9/l, če je število trombocitov < 75 x 10^9/l ali če se je pri bolniku zaradi predhodnih zdravljenj pojavila klinično pomembna nehematološka toksičnost 3. ali 4. stopnje, ki še traja. Bolnike je treba skrbno spremljati zaradi morebitnih okužb, uvesti je treba ustrezne ukrepe, kot je klinično indicirano. Toksičnost za prebavila: Potrebna je uporaba antiemetikov, antidiaroikov ter drugih ukrepov, kot je klinično indicirano. Če je potrebno, prilagodite odmerke. Ledvična okvara: Zdravilo Lonsurf ni primerno za uporabo pri bolnikih s hudo ledvično okvaro ali končno stopnjo ledvične okvare. Bolnike z zmerno ledvično okvaro je treba zaradi hematoloških toksičnosti bolj pogosto spremljati. Jetrna okvara: Uporaba zdravila Lonsurf pri bolnikih z obstoječo zmerno ali hudo jetrno okvaro ni priporočljiva. Proteinurija: Pred začetkom zdravljenja in med njim je priporočljivo spremljanje proteinurije z urinskimi testnimi lističi. Pomožne snovi: Zdravilo vsebuje laktozo. **INTERAKCIJE*:** Zdravila, ki medsebojno delujejo z nukleozidnimi prenašalci CNT1, ENT1 in ENT2, zaviralci OCT2 ali MATE1, substrati humane timidin-kinaze (npr. zidovudinom), hormonskimi kontraceptivi. **PLODNOST*, NOSEČNOST IN DOJENJE*:** Ni priporočljivo. **KONTRACEPCIJA*:** Ženske in moški morajo uporabljati učinkovito metodo kontracepcije med zdravljenjem in do 6 mesecev po zaključku zdravljenja. **VPLIV NA SPOSOBNOST VOŽNJE IN UPRAVLJANJA S STROJI*:** Med zdravljenjem se lahko pojavijo utrujenost, omotica ali splošno slabo počutje. **NEŽELENI UČINKI*:** *Zelo pogosti:* nevtropenija, levkopenija, anemija, trombocitopenija, zmanjšan apetit, diareja, navzea, bruhanje, utrujenost. *Pogosti:* okužba spodnjih dihal, okužba zgornjih dihal, febrilna nevtropenija, limfopenija, monocitoza, hipoalbuminemija, nespečnost, disgevzija, periferna nevropatija, omotica, glavobol, vročinski oblivi, dispneja, kašelj, bolečina v trebuhu, zaprtje, stomatitis, bolezni ustne votline, hiperbilirubinemija, sindrom palmarne plantarne eritrodisestezije, izpuščaj, alopecija, pruritus, suha koža, proteinurija, pireksija, edem, vnetje sluznice, splošno slabo počutje, zvišanje jetrnih encimov, zvišanje alkalne fosfataze v krvi, zmanjšanje telesne mase. *Občasni:* septični šok, infekcijski enteritis, pljučnica, okužba žolčevoda, gripa, okužba sečil, vnetje dlesni, herpes zoster, tinea pedis, kandidiaza, bakterijska okužba, okužba, bolečina zaradi raka, pancitopenija, granulocitopenija, monocitopenija, eritropenija, levkocitoza, dehidracija, hiperglikemija, hiperkaliemija, hipokaliemija, hipofosfatemija, hipernatriemija, hiponatriemija, hipokalciemija, protin, anksioznost, nevrotoksičnost, disestezija, hiperestezija, hipoestezija, sinkopa, parestezija, pekoč občutek, letargija, zmanjšana ostrina vida, zamegljen vid, diplopija, kataraka, konjunktivitis, suho oko, vrtoglavica, neugodje v ušesu, angina pektoris, aritmija, palpitacije, embolija, hipertenzija, hipotenzija, pljučna embolija, plevralni izliv, izcedek iz nosu, disfonija, orofaringealna bolečina, epistaksa, hemoragični enterokolitis, krvavitev v prebavilih, akutni pankreatitis, ascites, ileus, subileus, kolitis, gastritis, refluksni gastritis, ezofagitis, moteno praznjenje želodca, abdominalna distenzija, analno vnetje, razjede v ustih, dispepsija, gastroezofagealna refluksna bolezen, proktalgija, bukalni polip, krvavitev dlesni, glositis, parodontalna bolezen, bolezen zob, siljenje na bruhanje, flatulenca, slab zadah, hepatotoksičnost, razširitev žolčnih vodov, luščenje kože, urtikarija, preobčutljivostne reakcije na svetlobo, eritem, akne, hiperhidroza, žulj, bolezni nohtov, otekanje sklepov, artralgija, bolečina v kosteh, mialgija, mišično-skeletna bolečina, mišična oslabelost, mišični krči, bolečina v okončinah, občutek teže, ledvična odpoved, neinfektivni cistitis, motnje mikcije, hematurija, levkociturija, motnje menstruacije, poslabšanje splošnega zdravstvenega stanja, bolečina, občutek spremembe telesne temperature, kseroza, zvišanje kreatinina v krvi, podaljšanje intervala QT na elektrokardiogramu, povečanje mednarodnega umerjenega razmerja (INR), podaljšanje aktiviranega parcialnega tromboplastinskega časa (aPTČ), zvišanje sečnine v krvi, zvišanje laktatne dehidrogenaze v krvi, znižanje celokupnih proteinov, zvišanje C-reaktivnega proteina, zmanjšan hematokrit. *Post-marketinške izkušnje:* pri bolnikih, zdravljenih z zdravilom Lonsurf na Japonskem, so poročali o primerih intersticijske bolezni pljuč. **PREVELIKO ODMERJANJE*:** Neželeni učinki, o katerih so poročali v povezavi s prevelikim odmerjanjem, so bili v skladu z uveljavljenim varnostnim profilom. Glavni pričakovani zaplet prevelikega odmerjanja je supresija kostnega mozga. **FARMAKODINAMIČNE LASTNOSTI*:** *Farmakoterapevtska skupina:* zdravila z delovanjem na novotvorbe, antimetaboliti, oznaka ATC: L01BC59. Zdravilo Lonsurf sestavljata antineoplastični timidinski nukleozidni analog, trifluridin, in zaviralec timidin-fosforilaze (TPaze), tipiracilijev klorid. Po privzemu v rakave celice timidin-kinaza fosforilira trifluridin. Ta se v celicah nato presnovi v substrat deoksiribonukleinske kisline (DNA), ki se vgradi neposredno v DNA ter tako preprečuje celično proliferacijo. TPaza hitro razgradi trifluridin in njegova presnova po peroralni uporabi je hitra zaradi učinka prvega prehoda, zato je v zdravilo vključen zaviralec TPaze, tipiracilijev klorid. **PAKIRANJE*:** 20 filmsko obloženih tablet. **NAČIN PREDPISOVANJA IN IZDAJE ZDRAVILA:** Rp/ Spec. **Imetnik dovoljenja za promet:** Les Laboratoires Servier, 50, rue Carnot, 92284 Suresnes cedex, Francija. **Številka dovoljenja za promet z zdravilom:** EU/1/16/1096/001 (Lonsurf 15 mg/6,14 mg), EU/ 1/16/1096/004 (Lonsurf 20 mg/8,19 mg). **Datum zadnje revizije besedila: avgust 2017. * Pred predpisovanjem preberite celoten povzetek glavnih značilnosti zdravila. Celoten povzetek glavnih značilnosti zdravila in podrobnejše informacije so na voljo pri: Servier Pharma d.o.o., Podmilščakova ulica 24, 1000 Ljubljana, tel: 01 563 48 11, www.servier.si.**

Datum priprave informacije: februar 2018.
LNF17/18C2AD2 Samo za strokovno javnost.

PODOBNA BIOLOŠKA ZDRAVILA DRUŽBE AMGEN

V LETU 2018 ZNOVA PRESTAVLJAMO MEJNIKE

Smo vodilni na področju biotehnologije in med prvimi, ki raziskujemo inovativna biološka zdravila. Naša podobna biološka zdravila označujejo za nas začetek novega obdobja, saj širimo naš nabor zdravil in omogočamo več bolnikom dostop do novih možnosti zdravljenja, ki rešujejo življenja. Za več informacij obiščite: **www.amgenbiosimilars.eu**

Pomembne izkušnje

Družba Amgen je že skoraj štiri desetletja vodilna na področju bioloških in drugih inovativnih zdravil.

Predanost

Predani smo dolgoročnemu zagotavljanju širokega nabora podobnih bioloških in inovativnih zdravil.

Potencial podobnih bioloških zdravil

Podobna biološka zdravila družbe Amgen nudijo bolnikom in zdravnikom dodatne možnosti zdravljenja, kot tudi večjo vzdržnost zdravstvenega sistema.

Dokazano strokovno znanje

Naše dolgoletne izkušnje vlivajo zaupanje bolnikom kot tudi zdravstvenim delavcem pri izbiri zdravljenja.

AMGEN® BIOSIMILARS

Amgen zdravila d.o.o.
Šmartinska cesta 140, 1000 Ljubljana, Slovenija

SLHR-SL-P-BIO-0718-066155

Instructions for authors

The editorial policy

Radiology and Oncology is a multidisciplinary journal devoted to the publishing original and high quality scientific papers and review articles, pertinent to diagnostic and interventional radiology, computerized tomography, magnetic resonance, ultrasound, nuclear medicine, radiotherapy, clinical and experimental oncology, radiobiology, radiophysics and radiation protection. Therefore, the scope of the journal is to cover beside radiology the diagnostic and therapeutic aspects in oncology, which distinguishes it from other journals in the field.

The Editorial Board requires that the paper has not been published or submitted for publication elsewhere; the authors are responsible for all statements in their papers. Accepted articles become the property of the journal and, therefore cannot be published elsewhere without the written permission of the editors.

Submission of the manuscript

The manuscript written in English should be submitted to the journal via online submission system Editorial Manager available for this journal at: **www.radioloncol.com**.

In case of problems, please contact Sašo Trupej at **saso.trupej@computing.si** or the Editor of this journal at **gsersa@onko-i.si**

All articles are subjected to the editorial review and when the articles are appropriated they are reviewed by independent referees. In the cover letter, which must accompany the article, the authors are requested to suggest 3-4 researchers, competent to review their manuscript. However, please note that this will be treated only as a suggestion; the final selection of reviewers is exclusively the Editor's decision. The authors' names are revealed to the referees, but not vice versa.

Manuscripts which do not comply with the technical requirements stated herein will be returned to the authors for the correction before peer-review. The editorial board reserves the right to ask authors to make appropriate changes of the contents as well as grammatical and stylistic corrections when necessary. Page charges will be charged for manuscripts exceeding the recommended length, as well as additional editorial work and requests for printed reprints.

Articles are published printed and on-line as the open access (**https://content.sciendo.com/raon**).

All articles are subject to 700 EUR + VAT publication fee. Exceptionally, waiver of payment may be negotiated with editorial office, upon lack of funds.

Manuscripts submitted under multiple authorship are reviewed on the assumption that all listed authors concur in the submission and are responsible for its content; they must have agreed to its publication and have given the corresponding author the authority to act on their behalf in all matters pertaining to publication. The corresponding author is responsible for informing the coauthors of the manuscript status throughout the submission, review, and production process.

Preparation of manuscripts

Radiology and Oncology will consider manuscripts prepared according to the Uniform Requirements for Manuscripts Submitted to Biomedical Journals by International Committee of Medical Journal Editors (www.icmje.org). The manuscript should be written in grammatically and stylistically correct language. Abbreviations should be avoided. If their use is necessary, they should be explained at the first time mentioned. The technical data should conform to the SI system. The manuscript, excluding the references, tables, figures and figure legends, must not exceed 5000 words, and the number of figures and tables is limited to 8. Organize the text so that it includes: Introduction, Materials and methods, Results and Discussion. Exceptionally, the results and discussion can be combined in a single section. Start each section on a new page, and number each page consecutively with Arabic numerals.

The Title page should include a concise and informative title, followed by the full name(s) of the author(s); the institutional affiliation of each author; the name and address of the corresponding author (including telephone, fax and E-mail), and an abbreviated title (not exceeding 60 characters). This should be followed by the abstract page, summarizing in less than 250 words the reasons for the study, experimental approach, the major findings (with specific data if possible), and the principal conclusions, and providing 3-6 key words for indexing purposes. Structured abstracts are required. Slovene authors are requested to provide title and the abstract in Slovene language in a separate file. The text of the research article should then proceed as follows:

Introduction should summarize the rationale for the study or observation, citing only the essential references and stating the aim of the study.

Materials and methods should provide enough information to enable experiments to be repeated. New methods should be described in details.

Results should be presented clearly and concisely without repeating the data in the figures and tables. Emphasis should be on clear and precise presentation of results and their significance in relation to the aim of the investigation.

Discussion should explain the results rather than simply repeating them and interpret their significance and draw conclusions. It should discuss the results of the study in the light of previously published work.

Charts, Illustrations, Images and Tables

Charts, Illustrations, Images and Tables must be numbered and referred to in the text, with the appropriate location indicated. Charts, Illustrations and Images, provided electronically, should be of appropriate quality for good reproduction. Illustrations and charts must be vector image, created in CMYK color space, preferred font "Century Gothic", and saved as .AI, .EPS or .PDF format. Color charts, illustrations and Images are encouraged, and are published without additional charge. Image size must be 2.000 pixels on the longer side and saved as .JPG (maximum quality) format. In Images, mask the identities of the patients. Tables should be typed double-spaced, with a descriptive title and, if appropriate, units of numerical measurements included in the column heading. The files with the figures and tables can be uploaded as separate files.

References

References must be numbered in the order in which they appear in the text and their corresponding numbers quoted in the text. Authors are responsible for the accuracy of their references. References to the Abstracts and Letters to the Editor must be identified as such. Citation of papers in preparation or submitted for publication, unpublished observations, and personal communications should not be included in the reference list. If essential, such material may be incorporated in the appropriate place in the text. References follow the style of Index Medicus, DOI number (if exists) should be included.

All authors should be listed when their number does not exceed six; when there are seven or more authors, the first six listed are followed by "et al.". The following are some examples of references from articles, books and book chapters:

Dent RAG, Cole P. In vitro maturation of monocytes in squamous carcinoma of the lung. *Br J Cancer* 1981; **43:** 486-95. doi: 10.1038/bjc.1981.71

Chapman S, Nakielny R. *A guide to radiological procedures*. London: Bailliere Tindall; 1986.

Evans R, Alexander P. Mechanisms of extracellular killing of nucleated mammalian cells by macrophages. In: Nelson DS, editor. *Immunobiology of macrophage.* New York: Academic Press; 1976. p. 45-74.

Authorization for the use of human subjects or experimental animals

When reporting experiments on human subjects, authors should state whether the procedures followed the Helsinki Declaration. Patients have the right to privacy; therefore the identifying information (patient's names, hospital unit numbers) should not be published unless it is essential. In such cases the patient's informed consent for publication is needed, and should appear as an appropriate statement in the article. Institutional approval and Clinical Trial registration number is required. Retrospective clinical studies must be approved by the accredited Institutional Review Board/Committee for Medical Ethics or other equivalent body. These statements should appear in the Materials and methods section.

The research using animal subjects should be conducted according to the EU Directive 2010/63/EU and following the Guidelines for the welfare and use of animals in cancer research (Br J Cancer 2010; 102: 1555 – 77). Authors must state the committee approving the experiments, and must confirm that all experiments were performed in accordance with relevant regulations.

These statements should appear in the Materials and methods section (or for contributions without this section, within the main text or in the captions of relevant figures or tables).

Transfer of copyright agreement

For the publication of accepted articles, authors are required to send the License to Publish to the publisher on the address of the editorial office. A properly completed License to Publish, signed by the Corresponding Author on behalf of all the authors, must be provided for each submitted manuscript.

The non-commercial use of each article will be governed by the Creative Commons Attribution-NonCommercial-NoDerivs license.

Conflict of interest

When the manuscript is submitted for publication, the authors are expected to disclose any relationship that might pose real, apparent or potential conflict of interest with respect to the results reported in that manuscript. Potential conflicts of interest include not only financial relationships but also other, non-financial relationships. In the Acknowledgement section the source of funding support should be mentioned. The Editors will make effort to ensure that conflicts of interest will not compromise the evaluation process of the submitted manuscripts; potential editors and reviewers will exempt themselves from review process when such conflict of interest exists. The statement of disclosure must be in the Cover letter accompanying the manuscript or submitted on the form available on **www.icmje.org/coi_disclosure.pdf**

Page proofs

Page proofs will be sent by E-mail to the corresponding author. It is their responsibility to check the proofs carefully and return a list of essential corrections to the editorial office within three days of receipt. Only grammatical corrections are acceptable at that time.

Open access

Papers are published electronically as open access on **https://content.sciendo.com/raon**, also papers accepted for publication as E-ahead of print.